

Electronic Thesis and Dissertation Repository

---

11-20-2020 1:00 PM

## Cyclization of peptide structures by creating metal foldamers using $^{99m}\text{Tc}/\text{Re}(\text{CO})_3$

Dhvani D. Oza, *The University of Western Ontario*

Supervisor: Luyt, Leonard G., *The University of Western Ontario*

A thesis submitted in partial fulfillment of the requirements for the Master of Science degree in Chemistry

© Dhvani D. Oza 2020

Follow this and additional works at: <https://ir.lib.uwo.ca/etd>

 Part of the [Inorganic Chemistry Commons](#), and the [Radiochemistry Commons](#)

---

### Recommended Citation

Oza, Dhvani D., "Cyclization of peptide structures by creating metal foldamers using  $^{99m}\text{Tc}/\text{Re}(\text{CO})_3$ " (2020). *Electronic Thesis and Dissertation Repository*. 7521.  
<https://ir.lib.uwo.ca/etd/7521>

This Dissertation/Thesis is brought to you for free and open access by Scholarship@Western. It has been accepted for inclusion in Electronic Thesis and Dissertation Repository by an authorized administrator of Scholarship@Western. For more information, please contact [wlsadmin@uwo.ca](mailto:wlsadmin@uwo.ca).

## Abstract

Constrained peptides have been successful as therapeutics owing to the rigidity in their framework, allowing them to have enhanced pharmacological properties. Apart from covalent bond-based cyclization, constraints can be induced by cyclization using metal coordination. The metals Re and  $^{99m}\text{Tc}$  are one of the few metals which have not been studied in great detail for their ability to cyclize linear peptides. A tri-alanine sequence was employed in the peptide backbone due to its ability to form stable helices. In addition, another tripeptide sequence RGD, which is recognized by the integrin  $\alpha_v\beta_3$ , was also used. These tripeptide sequences flanked by unnatural amino acid and synthetic chelating agent on the terminal ends, were cyclized using  $[\text{Re}(\text{CO})_3(\text{OH}_2)_3]^+$  to form a 2+1 chelation complex. This involved chelation to the metal through a bidentate ligand, pyridyl triazole acetic acid or 2,2'-bipyridine-4-carboxylic acid (synthetic chelating ligand), and a monodentate ligand 3-Pyridyl alanine (unnatural amino acid) from N- and C- terminal respectively. NMR spectroscopy was used to compare the changes in chemical shift between linear and cyclic peptides. Specific changes in the NMR of cyclic peptide confirmed the formation of 2+1 chelation system. Circular dichroism spectroscopy was able to confirm the formation of a turn into the linear peptide on cyclization. Variable temperature NMR spectroscopy suggested the formation of a secondary structure by detecting intramolecular hydrogen bonding in the cyclic peptide. Lastly, the linear peptide pyta-Ala-Ala-Ala-3Pal was successfully radiolabeled using  $[\text{}^{99m}\text{Tc}(\text{CO})_3(\text{OH}_2)_3]^+$ . Linear peptides were successfully cyclized through  $^{99m}\text{Tc}/\text{Re}(\text{CO})_3$ , thus creating metal foldamers where the metal acts as the central core around which the turn occurs.

Keywords – Rhenium, technetium, cyclic peptides, metal clips, 2+1 chelation.

## Summary for Lay Audience

Peptides have increasingly garnered attention as a targeting component for molecular imaging probes due to cumulative factors such as low molecular weight, small size and their ease to synthesize. They display good tumour to background ratio and showcase the ability of having a variety of bifunctional ligands attached to its C and N terminus. However, there are number of disadvantages associated with having linear peptides as the targeting entity, such as their poor *in vivo* stability and reduced specific binding.

Structural constraints, through cyclization of peptide backbone, can resolve some of the difficulties seen with short linear peptides. Cyclic peptides have improved stability and targeting affinity compared to their linear peptide counterparts. Owing to a locked conformation, cyclic peptides maintain a desirable secondary structure which results in higher binding affinity. Apart from covalent bond-based cyclization, cyclization can also be induced through metal coordination. Metal complexes are known to stabilize peptide sequences. A turn can be induced within a peptide backbone by metal coordination where the metal acts as a central core around which, a turn occurs.

$^{99m}\text{Tc}$  is used in 80 % of all nuclear medicine procedures worldwide. However,  $^{99m}\text{Tc}$  is a short-lived radioisotope which is used in sub-microgram scale. This makes standard spectroscopic characterization quite difficult. Rhenium and technetium belong to the same group of the periodic table and therefore have similar physical and chemical properties. Hence, rhenium is used as a non-radioactive analogue.

The research focuses on cyclization of linear peptides by  $^{99m}\text{Tc}/\text{Re}(\text{CO})_3^+$  coordination through the use of a mono and a bidentate ligand. Pyta and 2,2'-bipyridine-4-carboxylic acid were used as bidentate ligand along with 3-pyridyl alanine as a monodentate ligand. The cyclic and linear peptides were characterised by various spectroscopic methods, which suggested a change in conformation upon cyclization. This was especially observed for peptides with pyta as a ligand, suggesting formation of a secondary structure. Thus, an innovative approach of introducing structural constraints through metal-based cyclization is described. This approach would provide a new direction for creating imaging agents, where a medically relevant metal is incorporated into a peptide structure.

## Co-authorship statement

Project conceptualization and manuscript editing was provided by Dr. Len Luyt.

The raw data for circular dichroism spectroscopy in chapter 3 was obtained by Ms. Lee-Ann Briere, facility manager at Biomolecular Interactions and Conformations (BICF)

## Acknowledgement

I would first like to thank my supervisor Dr. Len Luyt, for the unparalleled support and guidance provided by him throughout the two years of my Master's. Thank you for selecting me to be a part of Luyt lab. The experience and knowledge gained by me in the lab is priceless and I will always be proud to have been a part of it!

Next, I would like to thank my parents Mr. Dharmesh Oza and Mrs. Riddhi Oza for being brave enough to send their only child so far away from home. Thank you for your guidance and firm belief that I can achieve anything I put my mind to. Also, for listening to all my rants about my project and chemistry even when you had no clue what I was talking about!

I would like to extend my gratitude to all my lab mates Tyler, Emily, Marina, Geran, Priyanka, Julia, Peter, Maryam, Arundhasa for always being helpful and supportive. A special thanks to Dr. Carlie Charron, Dr. Mark Milne and Dr. Lihai Yu for teaching me so many things about chemistry.

Last but not the least, thank you to all my friends in Canada and India for always cheering me up. Grad school became fun because of you all.

# Table of Contents

Abstract.....	ii
Summary for lay audience.....	iii
Co-authorship statement .....	iv
Acknowledgement .....	v
Table of Contents.....	vi
List of Tables .....	ix
List of Figures.....	x
List of Schemes.....	xii
List of Appendices .....	xiii
List of abbreviations and symbol.....	xiv
Chapter 1.....	1
1.1 Introduction.....	1
1.2 Targeting entity.....	1
1.3 Solid phase peptide synthesis.....	3
1.4 Structural constraints through cyclization .....	4
1.5 Metal co-ordination.....	7
1.6 Imaging entity .....	8
1.7 Single photon emission computed tomography.....	9
1.8 Technetium-99m as signaling source for SPECT.....	10
1.9 Rhenium Analogues.....	13
1.10 Technetium-99m radiopharmaceuticals.....	15
1.11 Goal of the study.....	15
1.12 References.....	17

Chapter 2.....	21
2 Optimization of cyclization reaction of linear peptides with rhenium tricarbonyl metal core.....	21
2.1 Introduction.....	21
2.2 Results and Discussion .....	23
2.3 Solution phase peptide synthesis .....	24
2.4 Solid phase peptide synthesis of Pyta-AAA-3Pal, <b>3.1</b> .....	25
2.5 Temperature and time optimization.....	26
2.6 Optimization of reaction solvent.....	29
2.7 Optimization using a base.....	29
2.8 Conclusion .....	29
2.9 Experimental data .....	29
2.10 <i>Small molecule synthesis</i> .....	30
a) <i>tert-butyl azido acetate, 1</i> .....	30
b) <i>tert-butyl-2-(4-phenyl-1H-1,2,3-triazol-1-yl) acetate, 2</i> .....	30
c) <i>2-(4-phenyl-1H-1,2,3-triazol-1-yl) acetic acid (Pyta), 3</i> .....	31
d) <i>3-Pyridyl alanine methoxy ester, 4</i> .....	31
e) <i>Tris-aqua tris-carbonyl rhenium (I) triflate, 5</i> .....	31
2.11 <i>General procedure for Peptide synthesis (Solution phase)</i> .....	32
2.11.1 <i>Boc-Ala-3-Pal-OMe, 2.1</i> .....	32
2.11.2 <i>Boc-Ala-Ala-3-Pal-OMe, 2.2</i> .....	33
2.11.3 <i>Boc-Ala-Ala-Ala-3-Pal-OMe, 2.3</i> .....	33
2.11.4 <i>Pyta-Ala-Ala-Ala-3-Pal-OMe, 2.4</i> .....	34
2.12 <i>Peptide synthesis (Solid phase)</i> .....	34
2.12.1 <i>Pyta-Ala-Ala-Ala-3Pal, 3.1</i> .....	35
2.13 <i>Optimization using temperature and time (general procedure)</i> .....	35

2.14	<i>Optimization using change of solvent</i> .....	35
2.15	<i>Optimization by presence of base</i> .....	36
2.16	References .....	36
3	Chapter Three .....	38
3	Cyclization of small linear peptides by creating metal foldamers using <sup>99m</sup> Tc/ Re(CO) <sub>3</sub> core .....	38
3.1	Results and Discussion .....	41
3.1.1	Synthesis of linear peptide .....	42
3.2	Optimization of peptide sequence length .....	52
3.3	Variable temperature NMR studies .....	53
3.4	Circular Dichroism Spectroscopy .....	57
3.5	<sup>99m</sup> Tc labelling of linear peptide pyta-Ala-Ala-Ala-3pal .....	59
3.6	Conclusion .....	60
3.7	Experimental data .....	61
3.7.1	<i>Small molecule synthesis</i> .....	62
3.7.2	<i>4-methyl-2-bromo pyridine carboxylate, 6</i> .....	62
3.7.3	<i>4-Methyl-2,2'-bipyridine carboxylate, 7</i> .....	62
3.7.4	<i>2,2'-bipyridine carboxylic acid, 8</i> .....	63
3.7.5	Peptide synthesis .....	63
3.7.6	Metal coordination .....	67
3.8	Circular Dichroism spectroscopy .....	71
3.9	References .....	71
4	Conclusion .....	75
4.1	References .....	78
	Appendices .....	80
	Curriculum Vitae .....	138



## List of Tables

Table 3.1 Amino acids proton shifts (ppm) of the linear peptide Pyta-AAA-3-Pal-NH <sub>2</sub> , 3.1 and rhenium coordinated peptide, 3.8.....	47
Table 3.2 Chemical shifts for the amino acids in the linear 3.2, and cyclic peptide Pyta-RGD-3Pal, 3.9 .....	49
Table 3.3 Chemical shifts for the amino acids in the linear 3.6, and cyclic peptide Bipyd-Ala-Ala-Ala-3Pal, 3.13 .....	50
Table 3.4 Chemical shifts for the amino acids in the linear 3.7, and cyclic peptide Bipyd-RGD-3Pal, 3.14 .....	51
Table 3.5 The $\Delta\delta/\Delta T$ values obtained from the VT <sup>1</sup> H NMR analysis for each amide proton in peptide 3.8.....	54
Table 3.6 The $\Delta\delta/\Delta T$ values obtained from the VT <sup>1</sup> H NMR analysis for each amide proton in peptide 3.9.....	55
Table 3.7 The $\Delta\delta/\Delta T$ values obtained from the VT <sup>1</sup> H NMR analysis for each amide proton in peptide 3.10.....	55
Table 3.8 The $\Delta\delta/\Delta T$ values obtained from the VT <sup>1</sup> H NMR analysis for each amide proton in peptide 3.13.....	56
Table 3.9 The $\Delta\delta/\Delta T$ values obtained from the VT <sup>1</sup> H NMR analysis for each amide proton in peptide 3.14.....	57

## List of Figures

Figure 1.1 Scheme of a molecular imaging probe .....	1
Figure 1.2 Solid phase peptide synthesis (SPPS) using 9-fluorenylmethoxycarbonyl (Fmoc) strategy .....	4
Figure 1.3 Various types of peptide cyclization .....	5
Figure 1.4 Structural constraints introduced through head to tail cyclization, a) MBP, b) Cyclo (Arg-Gly-Asp-DPhe-Val) .....	6
Figure 1.5 Structure of Ac-[D-Lys <sup>2</sup> ( <sup>125</sup> I-IBA), Arg <sup>11</sup> ]-ReCCMSH .....	8
Figure 1.6 SPECT imaging machine .....	10
Figure 1.7 Decay scheme of <sup>99</sup> Mo to <sup>99</sup> Ru .....	11
Figure 1.8 Schematic of a <sup>99</sup> Mo/ <sup>99m</sup> Tc generator .....	12
Figure 1.9 SAACQ; the metallated derivative fMLF[Re(CO) <sub>3</sub> -SAACQ]G <sup>42</sup> .....	14
Figure 1.10 Rhenium tricarbonyl bearing Ghrelin (1-14) <sup>44</sup> .....	15
Figure 1.11 Pentapeptide Ac-HAAAH synthesized by Simpson et.al <sup>45</sup> .....	16
Figure 1.12 2+1 coordination using an integrated design.....	16
Figure 2.1 a) Rhenium coordination at C-terminal forming 7 or 8 membered ring, b) rhenium coordination at N- terminal forming 6 membered ring.....	22
Figure 2.2 UHPLC of cyclic peptide 3.8, showing dominant (A) and less dominant conformer (B, C).....	27
Figure 2.3 Graph of total coordinated product vs time for the four different temperatures used for synthesis of 3.8 (Scheme 2.4), where total coordinated product % = (cyclic peptide / linear peptide + cyclic peptide) % .....	28

Figure 2.4 Graph of % coordinated peptide vs time for synthesis of 3.8, where % coordinated peptide = $[A \text{ or } (B + C) / \text{linear peptide} + \text{cyclic peptide}] \%$ .....	28
Figure 3.1 a) Pendant design; b-c) Integrated designs .....	39
Figure 3.2 Mixed ligand systems having: a) N, O bidentate donors; b) O, O donors; c) S, S donors; d) N, N donors.....	40
Figure 3.3 a) Rhenium metal complex of isothiocyanate functionalized 4-(2-pyridyl)-1,2,3 triazole and pyridine ligand; b) cyclic cRGDfK conjugate of isothiocyanate functionalized 4-(2-pyridyl)-1,2,3 triazole ligand. ....	41
Figure 3.4 UHPLC chromatogram of the cyclic peptide $\text{Re}(\text{CO})_3[\text{Pyta-Ala-Ala-Ala-3Pal}]$ , 3.8. ....	44
Figure 3.5 Aromatic region from $^1\text{H}$ NMR spectra of cyclic (3.8) and linear peptide (3.1) .....	45
Figure 3.6 COSY NMR spectra of cyclic peptide 3.8, in $\text{DMSO-d}_6$ at 400 MHz.....	46
Figure 3.7 NOESY NMR spectra of cyclic peptide 3.8, in $\text{DMSO-d}_6$ at 400 MHz .....	47
Figure 3.8 VT $^1\text{H}$ NMR spectra of coordinated peptide 3.8 in $\text{DMSO-d}_6$ at $5^\circ\text{C}$ intervals from $25-60^\circ\text{C}$ at 600 MHz.....	54
Figure 3.9 VT $^1\text{H}$ NMR spectra of coordinated peptide 3.13 in $\text{DMSO-d}_6$ at $5^\circ\text{C}$ intervals from $25-60^\circ\text{C}$ at 600 MHz.....	56
Figure 3.10 CD spectroscopy for the linear (3.1, 3.2, 3.3, 3.6, 3.7) and cyclic peptides, (3.8, 3.9, 3.10, 3.13, 3.14) in MilliQ water at a concentration of 0.25 mg/mL.....	58
Figure 3.11 Analytical HPLC traces showing correlations between $\gamma$ trace of crude $^{99\text{m}}\text{Tc}(\text{CO})_3^+$ labelled peptide (A), 3.15 and UV trace of $\text{Re}(\text{CO})_3^+$ coordinated peptide, 3.8 (B) showing less dominant isomers and no correlation with UV trace of dominant peak of 3.8 (C).....	60
Figure 4.1 a) Formation of a 7 membered ring with histidine as a chelator, b), c) 5 membered ring formed by pyridyl triazole acetic acid and 2,2'-bipyridine-4-carboxylic acid.....	76

## List of Schemes

Scheme 2.1 Synthesis of pyridyl triazole acetic acid <sup>9</sup> , 3 .....	23
Scheme 2.2 Esterification of 3-pyridyl alanine, 4.....	24
Scheme 2.3 Synthesis of linear peptide sequence pyta-Ala-Ala-Ala-3Pal-OMe, 2.4 using solution phase peptide synthesis .....	25
Scheme 2.4 Rhenium coordination of peptide sequence pyta-Ala-Ala-Ala-3Pal, 3.1.....	26
Scheme 3.1 Synthesis of 2,2'-bipyridine-4-carboxylic acid <sup>19</sup> , 8 .....	42
Scheme 3.2 Synthesis of linear peptide sequences 3.1, 3.2, 3.6, 3.7 using Fmoc strategy.....	43
Scheme 3.3 Rhenium coordination of linear peptide pyta-Ala-Ala-Ala-3Pal, 3.1 .....	44
Scheme 3.4 Rhenium coordination of linear peptide pyta-RGD-3Pal, 3.2.....	48
Scheme 3.5 Rhenium coordination of linear peptide Bipyd-Ala-Ala-Ala-3Pal, 3.6 .....	50
Scheme 3.6 Rhenium coordination of linear peptide Bipyd-RGD-3Pal, 3.7 .....	51
Scheme 3.7 Cyclization reaction of linear peptide sequences with varying length, (3.3 - 3.5)....	53
Scheme 3.8 <sup>99m</sup> Tc labelling of Pyta-AAA-3Pal, 3.15 .....	59

## List of Appendices

Appendix A Chromatographs of selected compounds.....	80
Appendix B. $^1\text{H}$ and 2D g-COSY, NOESY NMR spectra of linear and cyclic peptides .....	86
Appendix C Variable temperature NMR spectra.....	131

## List of abbreviations and symbol

- 2D:** two-dimensional
- 3-Pal:** 3-pyridylalanine
- Boc:** *tert*-butoxycarbonyl
- CD:** circular dichroism
- CT:** computed tomography
- DCM:** dichloromethane
- DIPEA:** N,N-diisopropylethylamine
- DMF:** N,N-dimethylformamide
- DMSO-d<sub>6</sub>:** deuterated dimethyl sulfoxide
- ESI:** electrospray ionization
- Fmoc:** 9-fluorenylmethoxycarbonyl
- gCOSY:** correlation spectroscopy
- HATU:** (2-(7-aza-1H-benzotriazole-1-yl)-1,1,3,3-tetramethyluronium hexafluorophosphate)
- HCTU:** (2-(6-chloro-1H-benzotriazole-1-yl)-1,1,3,3-tetramethylaminium hexafluorophosphate)
- HPLC:** high performance liquid chromatography
- LC:** liquid chromatography
- M:** molar
- MS:** mass spectroscopy
- NMR:** nuclear magnetic resonance
- OtBu:** *tert*-butyl ester
- OTf:** trifluoromethanesulfonate
- Pbf:** 2,2,4,6,7-Pentamethyldihydrobenzofuran-5-sulfonyl
- PET:** positron emission tomography
- Py:** pyridine
- pyta:** pyridyl-triazole
- RGD:** arginine-glycine-aspartic acid
- RP:** reverse phase
- SPECT:** single photon emission computed tomography
- SPPS:** solid phase peptide synthesis
- TBME:** *tert*-butyl methyl ether

**TIPS:** triisopropylsilane

**TFA:** trifluoroacetic acid

**TSTU:** (O-(N-succinimidyl)-1,1,3,3-tetramethyl uronium tetrafluoroborate)

**US:** ultrasound

**VT:** variable temperature

# Chapter 1

## 1.1 Introduction

Molecular imaging can be broadly defined as the *in vivo* visualization, characterization and measurement of biological processes at the molecular and cellular levels.<sup>1</sup> It is an exciting field of research that has a wide range of applications which includes diagnostics, drug discovery and development, theragnostic and personalized medicine. Based on its enormous potential, it has been viewed as an important means of exploring the inner workings of the body in both normal and disease states.<sup>2</sup>

The technique involves use of a molecular imaging probe to determine the expression of indicative molecular markers at different stages of diseases and disorders. An ideal imaging probe should have high binding affinity and specificity for a particular receptor, rapid clearance from non-target tissue, high target to background ratio, low toxicity and immunogenicity, high *in vivo* stability and easy production.<sup>3</sup> Considering all of these requirements, the design and development of molecular imaging probes is a challenging endeavor. A typical targeted imaging probe consists of a targeting entity which enables site specific delivery of the probe to the diseased tissue, and a labelling moiety which permits external detection of the target (Figure 1.1).

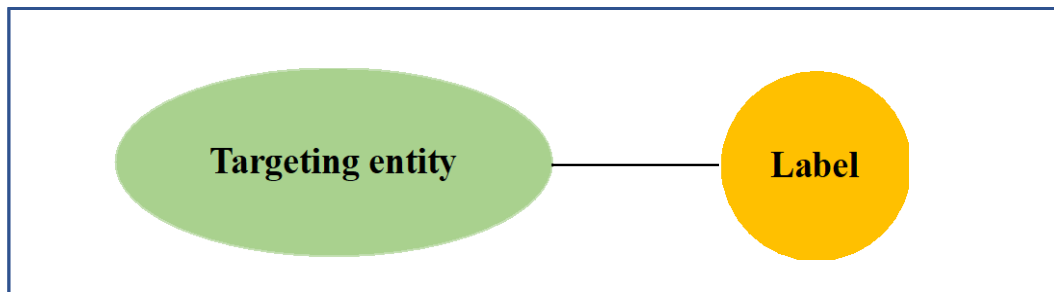


Figure 1.1 Scheme of a molecular imaging probe

## 1.2 Targeting entity

A targeting entity is a component of an imaging probe which has high affinity for the biological target and selectively binds in much higher concentration to the diseased state than the surrounding healthy tissue. It is quite important to select a targeting entity that can enable a high target to non-target ratio, thereby increasing the contrast in the image, as well as the precision and accuracy in



diagnoses.<sup>4</sup> Depending on the desired target, the targeting entity can vary between small molecules, peptides and monoclonal antibodies. Several strategies have been employed to use small molecules and macromolecules like monoclonal antibodies and antibody fragments to accurately diagnose disease, but these efforts have been largely unsuccessful due to their low specificity (small molecules) or limited target permeability (antibodies).

Peptides on the other hand have achieved significant success in their role as a targeting entity due to desirable properties like favorable pharmacokinetics, improved binding affinity and selectivity, better imaging ability as well as biosafety.<sup>4</sup> Peptides are easy to synthesize and can be structurally modified to enhance their pharmacokinetic properties. A variety of bi-functional chelating agents can be attached at the C and N terminal of the peptide. They can also be labelled with radiometals and optical agents, allowing for use with a variety of imaging modalities.<sup>5,6,7</sup> An increasing number of peptides, such as somatostatin (SST) peptide, vasoactive intestinal peptide (VIP), Arg-Gly-Asp (RGD) peptide, and bombesin/gastrin-releasing peptide (BBN/GRP), have been successfully characterized for tumor receptor imaging.<sup>8,9,10,11,12,13</sup> Although peptides have many desirable properties which gives them an edge compared to other targeting entities, they have many disadvantages as well. The main concern over the use of linear peptides is their short biological life due to enzymatic degradation. In addition, linear peptides have high flexibility in their backbone which allows them to bind to multiple binding sites and as a result they have reduced specificity towards the biological target.<sup>14</sup> Therefore, in order to use peptides as targeting entities, optimization is required.

The obstacles faced by linear peptides in terms of their biological stability and reduced specificity, can be overcome by introducing structural constraints or by employing the use of peptidomimetics. Peptidomimetics are molecules designed to mimic peptides in 3D space and retains their binding and biological (agonist/antagonist) activity. This design entails alteration in the peptide backbone or incorporation of an unnatural amino acid which reduces the rate of enzymatic degradation and thereby enhances their *in vivo* stability.<sup>15,16</sup> In addition, alteration of the N- and C- termini and head to tail cyclization are methods used for resisting degradation by exopeptidases, an enzyme known to specifically hydrolyze the N- and C- termini of the linear peptide.<sup>14</sup> Structural constraints can be employed to induce cyclization of small linear peptides, which aids in restricting the flexible

nature of the peptides and enhances *in vivo* stability. The rigid geometry of the cyclic peptide leads to enhanced binding affinity and specificity to the biological target.<sup>17</sup>

### 1.3 Solid phase peptide synthesis

Peptides can be synthesized by either solution phase or solid phase peptide synthesis methods. The solution phase approach is an efficient method and can be used for synthesis of linear peptides in a large scale. However, isolation, purification and characterization steps are required after the addition of each amino acid, which makes it a rather time-consuming technique. Solid phase peptide synthesis is a technique introduced by Merrifield in 1973.<sup>18</sup> It can efficiently synthesize large and more complex peptides. In this technique, peptides are synthesized in a stepwise manner from C to N terminus, where the C terminus is attached to an insoluble resin. This allows the use of excess reagents which ensures the complete addition of each amino acid. The reagents and the by-products formed in this technique are soluble and can be easily removed by excess washing and filtering without affecting the peptide which remains attached to the resin. This eliminates the need of purification after each coupling step.

SPPS uses two strategies depending on the protecting groups 9-fluorenyl methoxycarbonyl (Fmoc) or *tert*-butoxycarbonyl (Boc). Both of these strategies involve orthogonal protecting groups which allow only the N terminal amino acid to be deprotected selectively before the addition of the next protected amino acid, while the other side chain amino acids in the peptide sequence remain protected. The Fmoc group is base labile and can be removed using piperidine whereas the protecting groups on the side chains of the amino acid residues and the resin are acid labile. Once the Fmoc group is removed, the next amino acid in the sequence is added along with the coupling reagent and a base, N, N-diisopropylethylamine (DIPEA) in DMF. This cycle is repeated until the desired peptide sequence is achieved. The peptide is then cleaved from the resin using trifluoroacetic acid (TFA) along with triisopropyl silane (TIPS) which is used as a carbocation scavenger (Figure 1.2) The cleaved peptide is purified using reverse phase high performance liquid chromatography (RP-HPLC) and characterized by mass spectroscopy (MS).

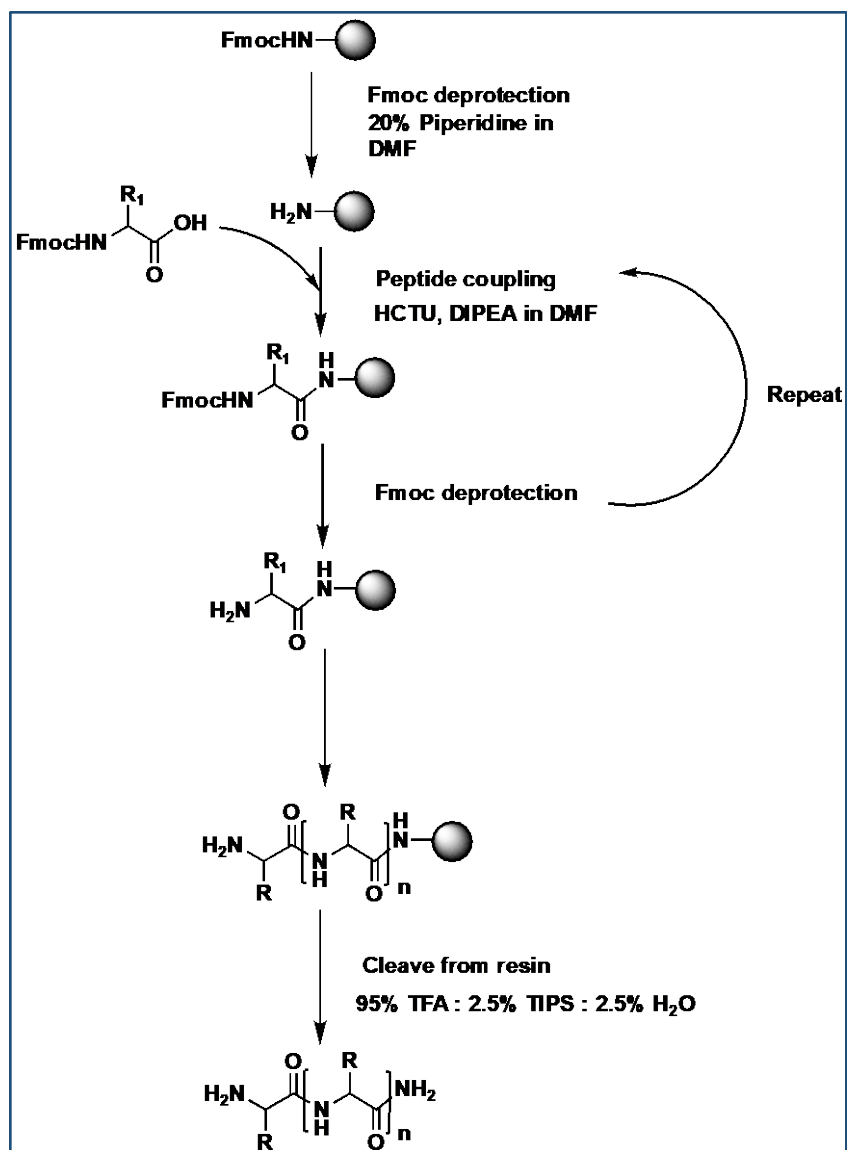


Figure 1.2 Solid phase peptide synthesis (SPPS) using 9-fluorenylmethoxycarbonyl (Fmoc) strategy

#### 1.4 Structural constraints through cyclization

Short peptide sequences often face entropic penalty for folding in their bioactive conformation because of the flexibility in the linear structure. In addition, peptides readily undergo proteolytic degradation, which affects their *in vivo* stability. These two problems can be overcome by a number of structural changes, including the use of D-amino acids, backbone alterations (by N-methylation or use of amide bond isosteres), use of non-native /unnatural amino acids or cyclization strategies.<sup>19</sup> Cyclization limits conformational flexibility of the macrocyclic structure

and thus, improves their favorable binding properties as well reduces the entropic penalty upon binding.<sup>20</sup> Cyclization can be introduced through various strategies like head to tail cyclization, side chain to side chain cyclization or through formation of a disulfide bond between side chains of amino acid (Figure 1.3).

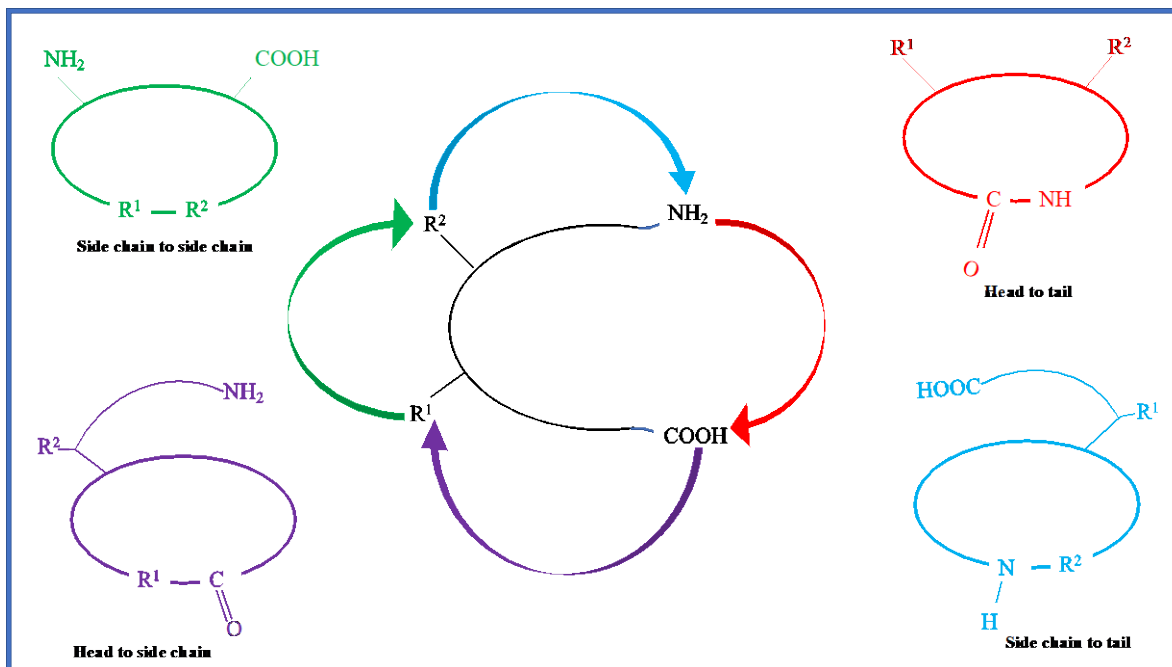


Figure 1.3 Various types of peptide cyclization

Myelin based protein (MBP) is an example of a peptide cyclized by head to tail cyclization (Figure 1.4a). Cyclization of the linear peptide leads to the formation of an enhanced pharmacological agent. Cyclic MBP shows better *in vivo* stability and efficacy compared to its linear epitope. This epitope is a self-antigen and is known to stimulate CD4<sup>+</sup> T cells.<sup>21</sup> CD4<sup>+</sup> T cells are T-helper cells which help in triggering the body's response to infections and thus are significant in achieving regulated effectual immune response towards pathogens. A study by Gurrath *et.al*, states the importance of cyclization for increased activity of the RGD<sub>F</sub>DV peptide sequence<sup>22</sup> (Figure 1.4 b). Integrin  $\alpha_v\beta_3$  recognizes the tripeptide sequence RGD. Integrins are heterodimeric transmembrane proteins responsible for linking the cells to extracellular matrix. It is composed of two noncovalently associated glycoprotein subunits called  $\alpha$  and  $\beta$ . There are 18  $\alpha$  and 8  $\beta$  units that can bond non covalently to form 24 different pair of integrins. The integrin  $\alpha_v\beta_3$ ,  $\alpha_5\beta_1$ ,  $\alpha_v\beta_6$  are

present in lower concentration in normal tissues but are overexpressed in tumor cells, making them critical for tumor angiogenesis.<sup>23</sup>

The study observed that cyclic peptide RGDF<sub>D</sub>V sequence had more potency than the linear peptide due to the constrained geometry induced by head to tail cyclization. This makes it more suitable to mimic the conformation required to bind to the receptor.

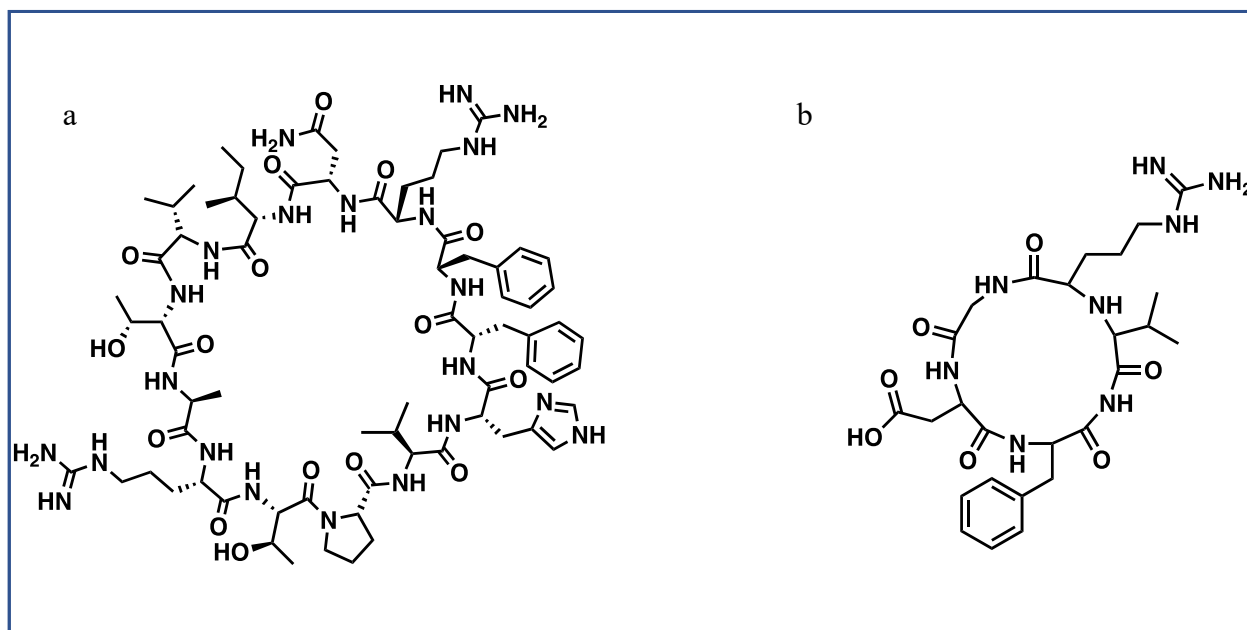


Figure 1.4 Structural constraints introduced through head to tail cyclization, a) MBP, b) Cyclo (Arg-Gly-Asp-DPhe-Val)

Linear peptides constrained through cyclization can alter the specificity of the cyclic peptides to different isoforms or subtypes of targeted receptors. This was demonstrated by a structure- activity study conducted by Pfaff *et al.*, in which the binding affinity of 16 cyclic RGD peptides were compared to the linear GRGDS and RGDFv peptides with respect to several different integrin receptors. Out of all the peptides compared, the cyclic RGDFv had a 3.3-fold greater binding affinity ( $IC_{50} = 11.3 \mu\text{M}$ ) to soluble  $\alpha_v\beta_3$  and a 5.8-fold greater binding affinity ( $IC_{50} = 0.4 \mu\text{M}$ ) to immobilized  $\alpha_v\beta_3$  compared with the linear RGDFv peptide. Interestingly, the linear RGDFv showed a 1.3-fold and 1.5-fold better binding affinity to the soluble and immobilized  $\alpha_{IIb}\beta_3$  integrin, respectively, compared with the cyclic RGDFv. Thus, this study showed that the fixed

geometry created by cyclization of RGDfv sequence made it more specific to  $\alpha_v\beta_3$  compared with its linear counterpart.<sup>24</sup>

Cyclic peptides show enhanced inhibitory properties when compared to their linear derivatives. This was demonstrated in a study conducted by Pakkala *et al.*, which focused on the activity and stability of linear and cyclic human glandular kallikrein (KLK2)-targeting peptides with the sequences ARRPAAPG (KLK2a) and GAARFKVWWAAG (KLK2b). The KLK2 protein is a highly prostate-specific serine protease that can be inhibited to reduce the metastasis of prostate cancer. Enhanced KLK2 inhibition was observed for disulfide-cyclized derivatives of the KLK2b sequence compared with the linear sequence while the cyclic KLK2a peptides were all inactive.<sup>25</sup>

### 1.5 Metal co-ordination

Cyclization can also be induced by metal coordination. Various metals like copper, palladium and iridium have been employed for cyclization of peptides.<sup>26,27,28</sup> Nearly one-third of proteins have metal coordination sites to execute regulatory or enzymatic processes since metal chelation is commonly used for the control of protein quaternary structure.<sup>29</sup>

Metals are known for stabilizing peptide turns. This approach involves use of metal ions that ‘clip’ two or more ligating side chain functional groups of the peptide. In a study by Ghadiri *et al.*,  $Cd^{2+}$  showed similar stabilizing effects for peptide sequence Ac-AEAAAKEAAAEX<sub>1</sub>AAAX<sub>2</sub>A-NH<sub>2</sub> which had (*i, i + 4*) spaced X<sub>1</sub>= Cys, X<sub>2</sub>= His ligating residues whereas  $Cu^{2+}$  stabilized the same peptide sequence when X<sub>1</sub>= His, X<sub>2</sub>= His. This coordination led to the formation of a macrocyclic bidentate complex which concurrently fixed the peptide backbone in an  $\alpha$ -helical conformation.<sup>30</sup> In a study by Giblin *et al.*, radiometals <sup>99m</sup>Tc and <sup>188</sup>Re were shown to cyclize  $\alpha$ -melanocyte stimulating hormone ( $\alpha$ -MSH) which simultaneously provided potential use as an imaging agent and a radiopharmaceutic.<sup>31</sup>  $\alpha$ -MSH is a tridecapeptide [Ac-Ser-Tyr-Ser-Met-Glu-His-Phe-Arg-Trp-Gly-Lys-Pro-Val-NH<sub>2</sub>] that regulates skin pigmentation in most vertebrates, where the core  $\alpha$ -MSH sequence His-Phe-Arg-Trp is sufficient for receptor recognition. Improved chemical stability and bioactivity were observed for the cyclic peptide along with superior receptor-binding properties in comparison to their linear counterparts. Biodistribution and tumor-targeting studies of the corresponding <sup>99m</sup>Tc complex in melanoma-bearing C57 mice showed rapid tumor uptake and significant tumor retention.<sup>31</sup>

A similar study conducted by Cheng *et.al* involved the development of an iodinated  $\alpha$ -MSH peptide Ac-[D-Lys<sup>2</sup> (<sup>125</sup>I-IBA), Arg<sup>11</sup>]-ReCCMSH (Figure 1.5). This peptide sequence consisted of three important components namely ReCCMSH(Arg<sup>11</sup>), which is the receptor targeting component resisting proteolytic degradation, D-Lys which is the residue for label conjugation and IBA (iodobenzoate) label for reducing the dehalogenation *in vivo*. On comparison with the radio-iodinated linear version, the rhenium cyclized radio-iodinated  $\alpha$ -MSH analogue showed higher retention, tumor uptake and biodistribution.<sup>32</sup> This emphasized that metal cyclization enabled high tumor uptake and retention which invariably translates to improved tumor imaging contrast as well as effective therapy at lower doses, sparing the non-target tissues.

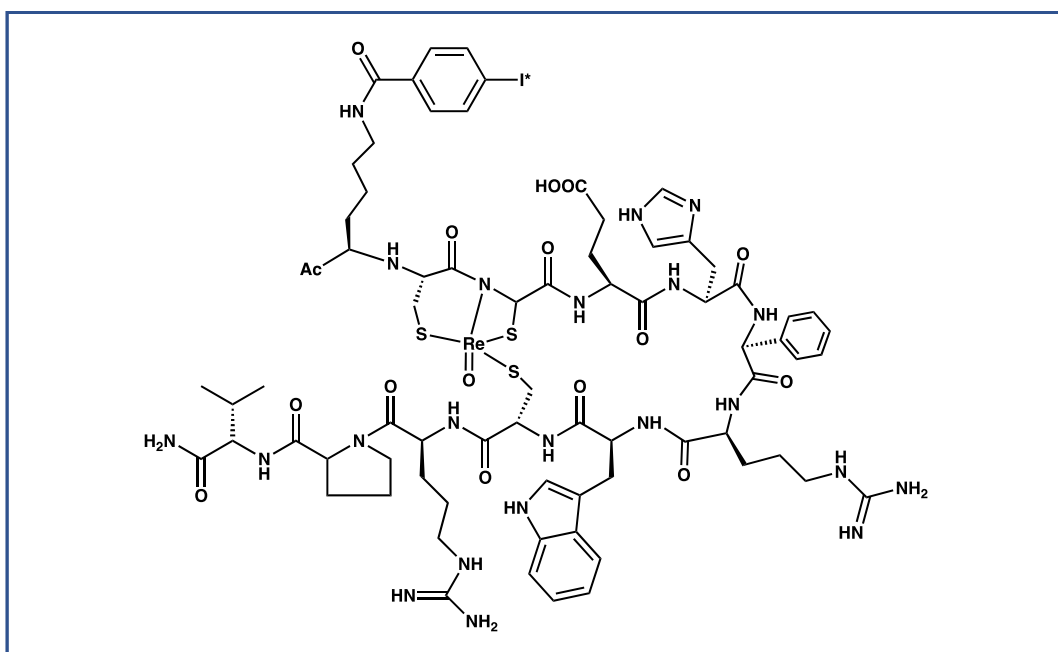


Figure 1.5 Structure of Ac-[D-Lys<sup>2</sup> (<sup>125</sup>I-IBA), Arg<sup>11</sup>]-ReCCMSH

## 1.6 Imaging entity

The imaging entity is the part of an imaging probe that allows for external detection of the probe localization. There exist several imaging modalities, depending on the type of biological process one needs to visualize and the type of imaging data one wants. More commonly used imaging modalities include computed tomography (CT), magnetic resonance imaging (MRI), positron

emission tomography (PET), single photon emission computed tomography (SPECT), and ultrasound (US).

SPECT and PET are radionuclide imaging modalities that enable the evaluation of biochemical changes and the level of molecular targets in the living subject. Although both these techniques have diagnostic advantage over other classical imaging modalities, they have limitations as well. Both of these modalities use ionizing radiation and there are limitations on how many scans a subject can undergo in a year. A very small amount of imaging agent is required for both PET/SPECT, which is advantageous as it is unlikely to cause any pharmacological effects.<sup>2</sup>  $^{18}\text{F}$  ( $t_{1/2} = 109.8$  min),  $^{64}\text{Cu}$  ( $t_{1/2} = 12.7$  h), and  $^{76}\text{Br}$  ( $t_{1/2} = 16.2$  h), or ultra-short lived radionuclides such as  $^{11}\text{C}$  ( $t_{1/2} = 20.3$  min),  $^{13}\text{N}$  ( $t_{1/2} = 10$  min), and  $^{15}\text{O}$  ( $t_{1/2} = 2.04$  min), are the radionuclides most commonly used for PET imaging. These nuclides decay by positron emission.

### 1.7 Single photon emission computed tomography

Single photon computed emission tomography (SPECT) is one of the widely used imaging modalities. SPECT employs radionuclides such as  $^{99\text{m}}\text{Tc}$  ( $t_{1/2} = 6$  h),  $^{123}\text{I}$  ( $t_{1/2} = 13.3$  h), and  $^{111}\text{In}$  ( $t_{1/2} = 2.8$  days). The emission energy emitted by these radionuclides ranges between 100 and 300 keV which is sufficient to pass through the body and be detected externally but does not cause harm to the patient. Unlike PET imaging, radionuclides employed by SPECT emit  $\gamma$  rays, which can be detected directly. The gamma camera in a SPECT scanner rotates  $180^\circ$  or  $360^\circ$  around the patient compared to the detector in a PET scanner, which is stationary. Since the radionuclides used by SPECT imaging is different than PET, the set up required by it to construct and collect the data is completely different than PET<sup>33</sup> (Figure 1.6).





Figure 1.6 SPECT imaging machine

Despite of poor resolution and sensitivity, SPECT is cost effective in comparison with PET due to the fact that majority of the radionuclides can be produced using a generator and have a longer half-life. However, the poor resolution and sensitivity can be overcome by combining SPECT with CT. This makes SPECT a more attractive and accessible imaging modality compared to PET.

### 1.8 Technetium-99m as signaling source for SPECT

$^{99m}\text{Tc}$  is a decay product of molybdenum-99 ( $\text{Mo-99}$ ) and is synthesized using a generator. It is used in 80 % of all nuclear medicine procedures worldwide. It has many favorable qualities, including: 1) easy availability, ii) low cost, iii) easy handling, iv) good imaging characteristics, and v) absence of strong radiation such as  $\alpha$  and  $\beta$  decay. This makes it an isotope of choice for SPECT imaging.  $^{99m}\text{Tc}$  has a half-life of 6 hours, which makes it suitable for radiolabeling biomolecules, as well as acquiring images. Several  $^{99m}\text{Tc}$  radiopharmaceuticals like  $^{99m}\text{Tc}$ -MIBI (sestamibi, **Cardiolite**<sup>®</sup>),  $^{99m}\text{Tc}$ -tetrofosmin (**Myoview**<sup>®</sup>),  $^{99m}\text{Tc}$ -HMPAO (exametazime, **Ceretec**<sup>®</sup>) and  $^{99m}\text{Tc}$ -ECD (bicisate, **Neurolite**<sup>®</sup>) have found clinical application as widely used cardiac and brain imaging agents.<sup>34</sup>

$^{99m}\text{Tc}$  is an artificial element obtained from  $^{99}\text{Mo}/^{99m}\text{Tc}$  generator where  $^{99}\text{Mo}$  decays to  $^{99m}\text{Tc}$  through  $\beta$  decay.  $^{99m}\text{Tc}$  is the metastable form of  $^{99}\text{Tc}$  and decays back to  $^{99}\text{Tc}$  by emitting a  $\gamma$  ray with an energy equal to 140 keV (Figure 1.7). The  $\gamma$  emission can be detected by Single Photon Emission Computer Tomography (SPECT).

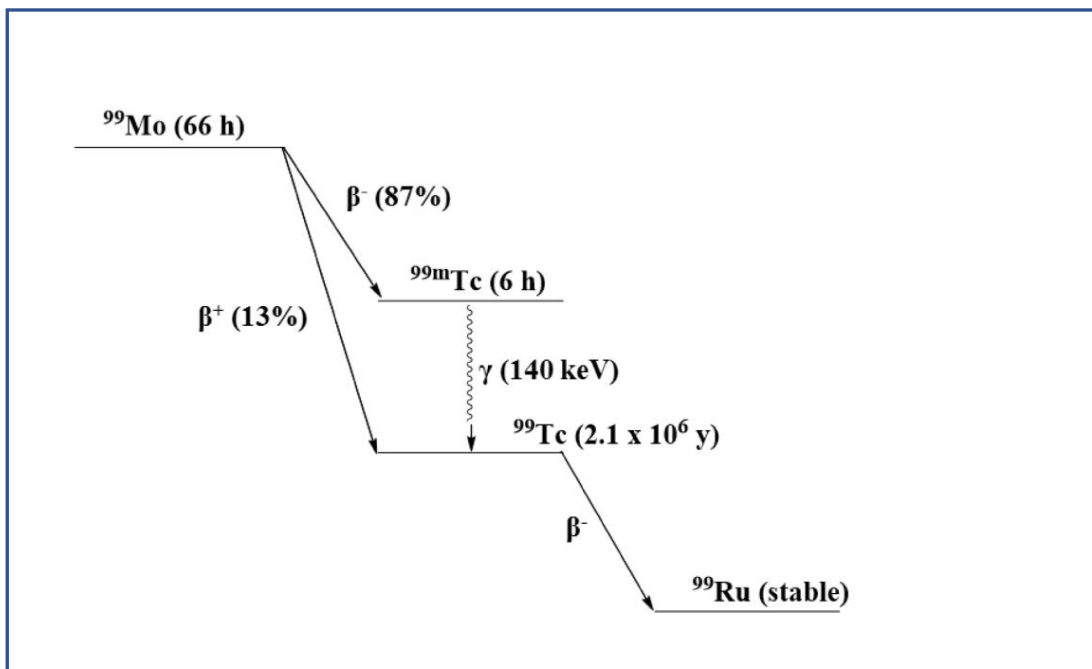


Figure 1.7 Decay scheme of  $^{99}\text{Mo}$  to  $^{99}\text{Ru}$

The  $^{99}\text{Mo}/^{99\text{m}}\text{Tc}$  generator is a simple apparatus composed of an alumina column.  $^{99}\text{Mo}$  is absorbed on this column in the chemical form of molybdate  $[\text{}^{99}\text{Mo}]\text{MoO}_4^{2-}$ .  $^{99}\text{Mo}$  decays into  $^{99\text{m}}\text{Tc}$  which leads to formation of pertechnetate  $[\text{}^{99\text{m}}\text{Tc}]\text{TcO}^-$ . The single negative charge on the pertechnetate makes it less tightly bound to the alumina in comparison to the double negatively charged molybdate. The  $[\text{}^{99\text{m}}\text{Tc}]\text{NaTcO}_4$  can be easily eluted from the column with a saline solution. This becomes possible due to the depression caused by an under-vacuum vial, which is inserted in the pertechnetate collecting area <sup>35</sup> (Figure 1.8).

$^{99\text{m}}\text{Tc}$  is produced in the form of pertechnetate ( $^{99\text{m}}\text{TcO}_4^-$ ) from the generator where its oxidation state is +7. In order to be linked to a bioactive molecule,  $^{99\text{m}}\text{Tc(VII)}$  has been reduced to a suitable oxidation state in presence of suitable ligands.  $^{99\text{m}}\text{Tc}$  exists in oxidation states ranging from -1 to +7. Clinically relevant compounds containing  $^{99\text{m}}\text{Tc}$  with oxidation states of 0, +2, +6 have not been studied in greater detail.  $^{99\text{m}}\text{Tc}$  is most stable in its +4 and +7 oxidation states and exist in the form of oxides, sulfides, halides and pertechnetates.

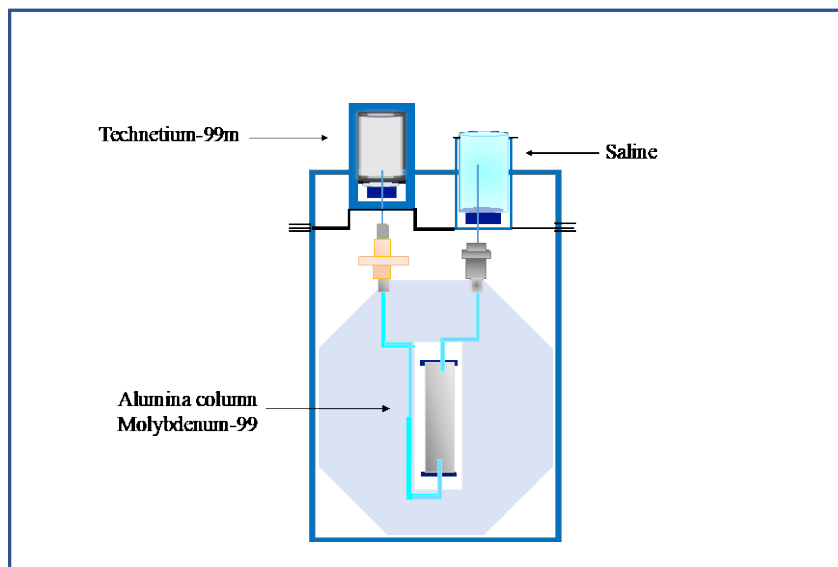


Figure 1.8 Schematic of a  $^{99}\text{Mo}/^{99\text{m}}\text{Tc}$  generator

One of the most extensively studied metal fragment for technetium is the Tc(V) oxo core. Various examples have been studied where Tc(V) is stabilized by oxo groups and contain oxo technetium (Tc=O) core like  $\text{TcO}^{3+}$ ,  $\text{trans-TcO}_2^+$ ,  $\text{trans-}[\text{Tc}_2\text{O}_3]^{4+}$ . This moiety is penta-coordinate and contains an axial oxo group.<sup>36</sup>

$[\text{}^{99\text{m}}\text{Tc}(\text{CO})_3]^+$  is a versatile building block for variety of biomolecules. This moiety consists of technetium coordinated to three carbonyl groups, in +1 oxidation state.  $[\text{}^{99\text{m}}\text{Tc}(\text{CO})_3]^+$  core is typically inert and is air and water stable. Compared to  $^{99\text{m}}\text{Tc}(\text{V})$ -oxo form where the choice of ligand is limited,  $^{99\text{m}}\text{Tc}(\text{I})$  core can be coordinated to almost any bidentate, monodentate and tridentate donor ligands. The carbonyl groups are known to stabilize the metals by increasing the sigma donation of the metal center as a result of  $\pi$  back bonding.<sup>37</sup>  $[\text{}^{99\text{m}}\text{Tc}(\text{CO})_3]^+$  can be easily synthesized in the triaqua form  $[\text{}^{99\text{m}}\text{Tc}(\text{CO})_3(\text{H}_2\text{O})_3]^+$  from  $^{99\text{m}}\text{TcO}_4^-$  by using an Isolink kit. The Isolink kit contains sodium tartrate, sodium tetraborate, sodium bicarbonate, sodium boranocarbonate, which acts as a carbonyl source and reduces pertechnetate from +7 oxidation state to +1 state. This reaction was first reported by Alberto *et.al* and was carried out at  $90^\circ\text{C}$  for 10 minutes.<sup>38</sup> Pitchumony *et al.* optimized this reaction by carrying out a microwave assisted synthesis which reduced the reaction time to 3.5 mins at  $110^\circ\text{C}$ .<sup>39</sup> This leads to the formation of an octahedral complex with the carbonyls trans to the aqua ligand creating a facial orientation.  $[\text{}^{99\text{m}}\text{Tc}(\text{CO})_3(\text{H}_2\text{O})_3]^+$  complex has very good solubility and stability over a broad range of pH. The aqua molecules achieve more lability due to the trans effect of the facial carbonyl groups and are thus an easy target to be replaced by a variety of donors including carboxylic acids, phosphines,

thiols, thioethers, amines or amides as monodentate, bidentate or tridentate ligands. The resulting complexes achieve kinetic stability due to the  $d^6$  low spin configuration.<sup>40</sup>

## 1.9 Rhenium Analogues

$^{99m}\text{Tc}$  is a short-lived radioisotope and is thus used in sub-microgram scale. This makes standard spectroscopic characterization quite difficult. Hence, in order to study the coordination chemistry of technetium, there is a need for a non-radioactive analogue. Rhenium and technetium belong to the same group of the periodic table and therefore have similar physical and chemical properties. Belonging to the same group, rhenium is quite comparable to technetium in its size, shape, formal charge and lipophilicity.<sup>6,41</sup> Rhenium ( $^{185/187}\text{Re}$ ) is therefore a good analogue to study  $^{99m}\text{Tc}$  coordination chemistry where  $^{187}\text{Re}$  (62.6 %) and  $^{185}\text{Re}$  (37.4 %) refers to the two stable isotopes of rhenium. It is quite easy to synthesize and characterize larger quantities of rhenium complexes prior to radio-labelling with  $^{99m}\text{Tc}$ .  $[\text{}^{99m}\text{Tc}(\text{CO})_3(\text{H}_2\text{O})_3]^+$  is quite easy to prepare using the Isolink kit in a microwave synthesizer, but the same method cannot be used for the synthesis of the rhenium analogue  $[\text{Re}(\text{CO})_3(\text{H}_2\text{O})_3]^+$ . This is due to the fact that rhenium is more inert, slower to react and harder to reduce than technetium.<sup>38</sup>

Furthermore, the application of  $\text{Re}(\text{CO})_3^+$  is also extended to fluorescence imaging for complexes having appropriate aromatic donor ligands, since luminescent probes containing  $\text{Re}(\text{I})$  have been described as being useful for the *in vivo* study of biological processes. This was demonstrated by Bartholoma *et.al*, where complimentary pairs of fluorescent and radioactive probes were synthesized to exploit the properties of  $^{99m}\text{Tc}(\text{CO})_3^+$  and  $\text{Re}(\text{CO})_3^+$  cores. The study demonstrated the use of single amino acid chelate (SAAC)-type ligand bis(quinoline-2-methyl)-*N*- $\alpha$ -Fmoc-l-lysine (Figure 1.9). This complex was incorporated in the tetrapeptide fMLF, a targeting sequence used for formyl peptide receptor for neutrophils. The  $\text{Re}(\text{CO})_3^+$  complex of this SAAC-type ligand displayed desired fluorescence and the  $^{99m}\text{Tc}(\text{CO})_3^+$  complex displayed stability in aqueous solution. This approach provided direct correlation between *in vitro* and *in vivo* imaging agents and proved to be instrumental in the development of complimentary *in vitro* fluorescent and *in vivo* radiopharmaceutical probes.<sup>42</sup>

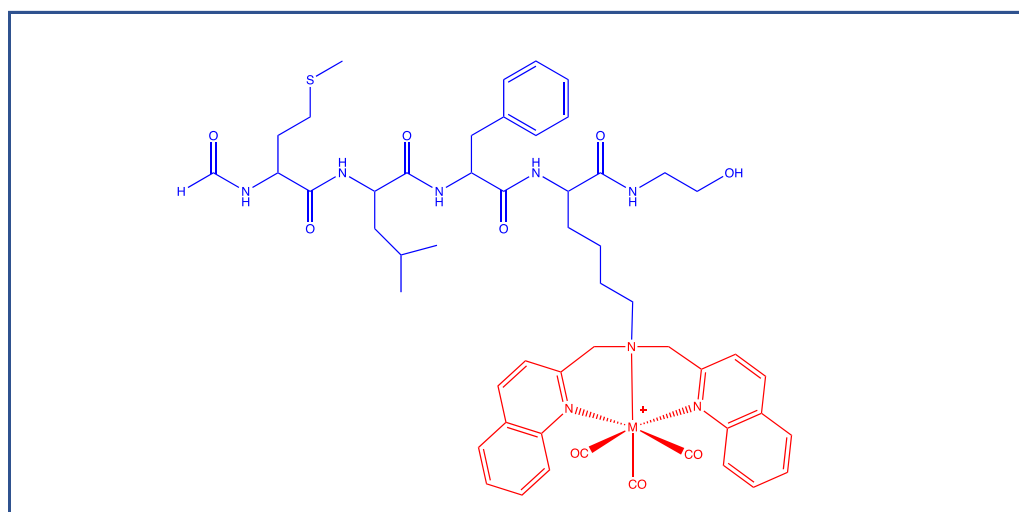


Figure 1.9 SAACQ; the metallated derivative fMLF[Re(CO)<sub>3</sub>-SAACQ]G<sup>42</sup>

Metal complex incorporated in an integrated fashion, forms a crucial part for ligand-receptor interaction. Though, this is usually rare for peptide-based technetium radiopharmaceuticals as metal complexes are typically incorporated in a pendant fashion far away from the active binding site to avoid interference with the area of ligand-receptor interaction. A study by Bigott-Hennkens *et.al* reported the cyclization of the octreotide peptide by successfully replacing the disulfide bridge function through the coordination of Re(V) oxo inorganic core directly to the octreotide peptide backbone.<sup>43</sup> The metal complex, although not located in the receptor binding pocket, was instrumental in binding due to formation of a cyclic constraint. This concept was also demonstrated in a study conducted by Rosita *et.al*, where rhenium tricarbonyl complex was coordinated to cyclopentadienyl moiety and then incorporated into the peptide ghrelin<sup>44</sup> (Figure 1.10). Ghrelin is a 28 amino acid peptide hormone with a unique lipophilic n-octanyl post translational modification in its serine-3-residue. It is known to be the endogenous ligand for the GHSR (growth hormone secretagogue receptor). Cp<sup>99m</sup>Tc(CO)<sub>3</sub> complex was chosen as a good candidate because in addition to being small in size, chemically and metabolically stable and neutral, it was most importantly lipophilic in nature which is a key requirement for the ghrelin side chain.<sup>185/187</sup>Re was used in place of <sup>99m</sup>Tc for chemical and biological analysis. It was observed that the binding affinity of the CpRe(CO)<sub>3</sub> complex suitably improved due to the incorporation of the metal complex. The key component of this success was due to the mimicking of ghrelin side chain by CpRe(CO)<sub>3</sub>. This study formed the first example of incorporating rhenium into a peptide structure where the metal complex formed a crucial part for binding.<sup>44</sup>

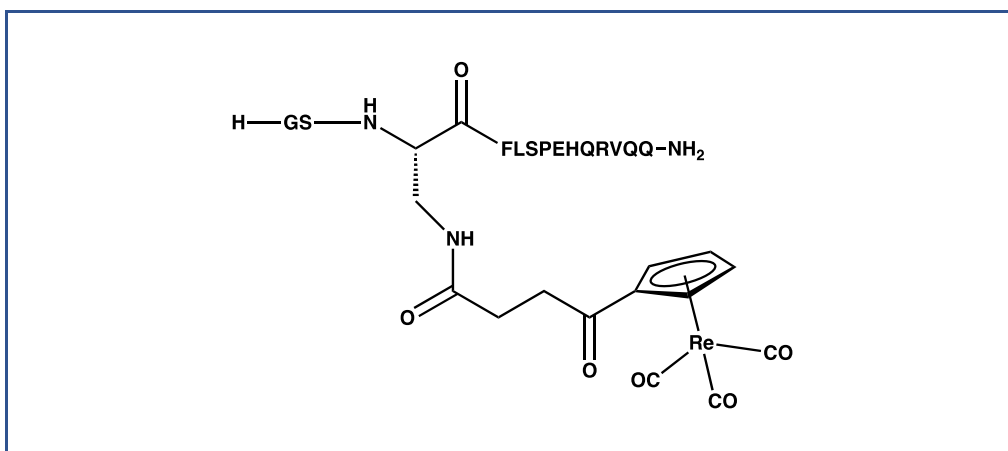


Figure 1.10 Rhenium tricarbonyl bearing Ghrelin (1-14)<sup>44</sup>

## 1.10 Technetium-99m radiopharmaceuticals

Peptide based technetium-99m radiopharmaceuticals are generally composed of a peptide for targeting, the radiometal for external detection, and a chelator to attach the metal to the peptide. Several biologically relevant peptides have been studied in the literature ranging from somatostatin analogues, bombesin, octreotide, neurotensin and Arg-Gly-Asp peptide moiety. A significant fact about <sup>99m</sup>Tc radiopharmaceuticals is that the [<sup>99m</sup>Tc (CO)<sub>3</sub>]<sup>+</sup> complexes can be stabilized either by a tridentate chelator, a '2+1' chelation system, or three mono-dentate ligands. A '2+1' chelation system is the combination of bi-dentate and mono-dentate ligands attached to a metal. Apart from the pendant fashion, the metal complex can also be added to the peptide in an integrated design where the metal is incorporated into the backbone of the peptide. This design hides the metal in the molecule, minimizing interference with binding of the biomolecule to the receptor, and in some cases is an integral component in locking the peptide in its active form, making the metal imperative for biological activity.<sup>45</sup>

## 1.11 Goal of the study

Previously in our lab, a turn conformation was reported by E. Simpson, which was created by coordinating the linear pentapeptide Ac-HAAAH through <sup>99m</sup>Tc/Re(CO)<sub>3</sub>.<sup>45</sup> A 2 + 1 chelation system was formed through the bidentate chelation of the imidazole nitrogen and carboxyl oxygen at one end and monodentate chelation of the imidazole nitrogen at the other end (Figure 1.11).

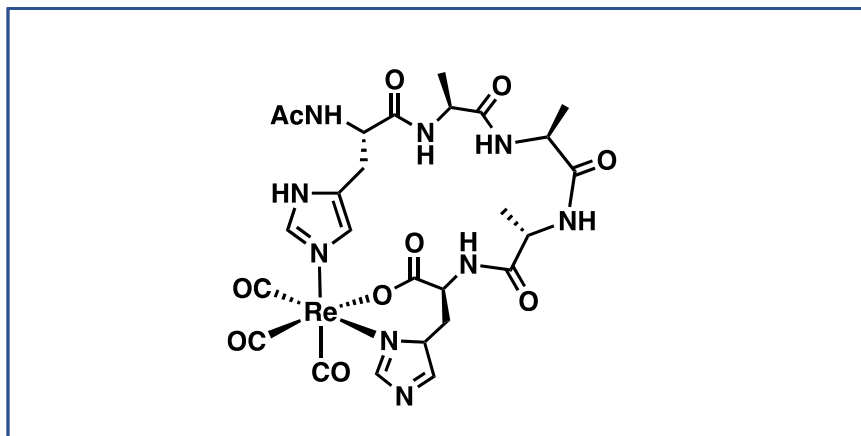


Figure 1.11 Pentapeptide Ac-HAAAH synthesized by Simpson et.al <sup>45</sup>

Although the effort to cyclize the pentapeptide was successful, histidine having multiple coordination sites led to the formation of coordination isomers.<sup>45</sup> To mitigate this problem, a better chelator was proposed, which has fewer coordinating sites and can form a favorable ring size with the metal. This led to the use of unnatural amino acids and synthetic ligands as metal chelators. A. Patel demonstrated the cyclization of the biologically relevant peptide RGD having the unnatural amino acid 3-pyridyl alanine at the C terminus and the ligand pyridyl triazole at the N terminus.<sup>46</sup> This formed a 2+1 chelation system, suggesting that an improved metal complex was discovered. Our current goal is to use the same principle and synthesize a linear peptide sequence AAA with unnatural amino acids and ligand at its terminal ends. In addition, we will also be synthesizing the biologically relevant peptide RGD with a different ligand at its N terminus. Thus, we aim to cyclize these peptides through <sup>99m</sup>Tc/Re(CO)<sub>3</sub> where the metal acts as the central core around which the turn occurs (Figure 1.12).

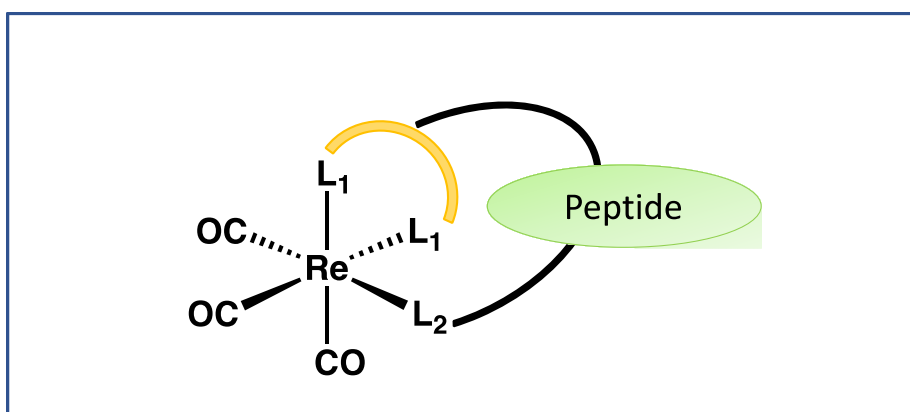


Figure 1.12 2+1 coordination using an integrated design.

## 1.12 References

- (1) Weissleder, R.; Mahmood, U. Molecular Imaging. *Radiology*. **2001**, *219* (2) pp 316–333. <https://doi.org/10.1148/radiology.219.2.r01ma19316>.
- (2) M.L., J.; S.S., G. A Molecular Imaging Primer: Modalities, Imaging Agents, and Applications. *Physiol. Rev.* **2012**, *92* (2), 897–965 doi:10.1152/physrev.00049.2010.
- (3) Sun, X.; Li, Y.; Liu, T.; Li, Z.; Zhang, X.; Chen, X. Peptide-Based Imaging Agents for Cancer Detection. *Adv. Drug Deliv.Rev.* **2017**, *110-111*, pp 38–51. <https://doi.org/10.1016/j.addr.2016.06.007>.
- (4) Chandra, R. *Nuclear Medicine Physics: The Basics.*; **2004**.
- (5) Reubi, J. C. Peptide Receptors as Molecular Targets for Cancer Diagnosis and Therapy. *Endocr.Rev.* **2003**, *24* (4), pp 389–427. <https://doi.org/10.1210/er.2002-0007>.
- (6) Banerjee, S.; Ambikalmajan Pillai, M. R.; Ramamoorthy, N. Evolution of Tc-99m in Diagnostic Radiopharmaceuticals. *Semin. Nucl. Med.* **2001**, *31* (4), 260–277. <https://doi.org/10.1053/snuc.2001.26205>.
- (7) Lee, S.; Xie, J.; Chen, X. Peptides and Peptide Hormones for Molecular Imaging and Disease Diagnosis. *Chem. Rev.* **2010**, *110* (5), 3087–3111. <https://doi.org/10.1021/cr900361p>.
- (8) Igarashi, H.; Fujimori, N.; Ito, T.; Nakamura, T.; Oono, T.; Nakamura, K.; Suzuki, K.; Jensen, R. T.; Takayanagi, R. Vasoactive Intestinal Peptide (VIP) and VIP Receptors-Elucidation of Structure and Function for Therapeutic Applications. *Int. J. Clin. Med.* **2011**, *2* (4), 500–508. <https://doi.org/10.4236/ijcm.2011.24084>.
- (9) De Jong, M.; Breeman, W. A. P.; Kwekkeboom, D. J.; Valkema, R.; Krenning, E. P. Tumor Imaging and Therapy Using Radiolabeled Somatostatin Analogues. *Acc. Chem. Res.* **2009**, *42* (7), 873–880. <https://doi.org/10.1021/ar800188e>.
- (10) Tweedle, M. F. Peptide-Targeted Diagnostics and Radiotherapeutics. *Acc. Chem. Res.* **2009**, *42* (7), 958–968. <https://doi.org/10.1021/ar800215p>.
- (11) Laverman, P.; Sosabowski, J. K.; Boerman, O. C.; Oyen, W. J. G. Radiolabelled Peptides for Oncological Diagnosis. *Eur. J. Nucl. Med. Mol. I.* **2012**, *39*, pp 78–92. <https://doi.org/10.1007/s00259-011-2014-7>.
- (12) Schottelius, M.; Wester, H. J. Molecular Imaging Targeting Peptide Receptors. *Methods.* **2009**, *48* (2), pp 161–177. <https://doi.org/10.1016/j.ymeth.2009.03.012>.
- (13) Charron, C. L.; Hickey, J. L.; Nsiam, T. K.; Cruickshank, D. R.; Turnbull, W. L.; Luyt, L. G. Molecular Imaging Probes Derived from Natural Peptides. *Nat. Prod. Rep.* **2016**, *33* (6), pp 761–800. <https://doi.org/10.1039/c5np00083a>.



- (14) Marshall, G. R. Peptide Interactions with G-Protein Coupled Receptors. *Biopolymers - Peptide Science Section*. **2001**, *60* (3), pp 246–277. [https://doi.org/10.1002/1097-0282\(2001\)60:3<246::AID-BIP10044>3.0.CO;2-V](https://doi.org/10.1002/1097-0282(2001)60:3<246::AID-BIP10044>3.0.CO;2-V).
- (15) Hruby, V.; Balse, P. Conformational and Topographical Considerations in Designing Agonist Peptidomimetics from Peptide Leads. *Curr. Med. Chem.* **2012**, *7* (9), 945–970. <https://doi.org/10.2174/0929867003374499>.
- (16) Hruby, V. J. Prospects for Peptidomimetic Drug Design. *Drug Discov. Today*. **1997**, *2* (5) pp 165–167. [https://doi.org/10.1016/S1359-6446\(96\)20009-1](https://doi.org/10.1016/S1359-6446(96)20009-1).
- (17) Roxin, Á.; Zheng, G. Flexible or Fixed: A Comparative Review of Linear and Cyclic Cancer-Targeting Peptides. *Future Med. Chem.* **2012**, *4* (No. 12), 1601-1618 <https://doi.org/10.4155/fmc.12.75>.
- (18) Bayer, E. Towards the Chemical Synthesis of Proteins. *Angew. Chem. Int. Ed.* **1991**, *30* (2), pp 113–129. <https://doi.org/10.1002/anie.199101133>.
- (19) Srinivasan, M. Interface Peptide Mimetics-Rationale and Application as Therapeutic Agents. *Med. Chem. (Los. Angeles)*. **2016**, *6* (3), 189–194. <https://doi.org/10.4172/2161-0444.1000344>.
- (20) Zorzi, A.; Deyle, K.; Heinis, C. Cyclic Peptide Therapeutics: Past, Present and Future. *Curr. Opin. Chem. Biol.* **2017**, *38*, 24–29. <https://doi.org/10.1016/j.cbpa.2017.02.006>.
- (21) Tapeinou, A.; Matsoukas, M.; Simal, C.; Tselios, T. Review Cyclic Peptides on a Merry-go-round. *Pept. Sci.* 2015, *104* (5), pp 453–461.
- (22) Gurrath, M.; Muller, G.; Kessler, H.; Aumailley, M.; Timpl, R. Conformation/Activity Studies of Rationally Designed Potent Anti-adhesive RGD Peptides. *Eur. J. Biochem.* **1992**, *210* (3), 911–921. <https://doi.org/10.1111/j.1432-1033.1992.tb17495.x>.
- (23) Desgrosellier, J. S.; Cheresh, D. A. Integrins in Cancer: Biological Implications and Therapeutic Opportunities. *Nat. Rev. Cancer.* **2010**, *10*, pp 9–22. <https://doi.org/10.1038/nrc2748>.
- (24) Pfaff, M.; Tangemann, K.; Müller, B.; Gurrath, M.; Müller, G.; Kessler, H.; Timpl, R.; Engel, J. Selective Recognition of Cyclic RGD Peptides of NMR Defined Conformation by Alpha IIb Beta 3, Alpha V Beta 3, and Alpha 5 Beta 1 Integrins. *J. Biol. Chem.* **1994**, *269* (32), 20233–20238.
- (25) Pakkala, M.; Hekim, C.; Soininen, P.; Leinonen, J.; Koistinen, H.; Weisell, J.; Stenman, U. H.; Vepsäläinen, J.; Närvänen, A. Activity and Stability of Human Kallikrein-2-Specific Linear and Cyclic Peptide Inhibitors. *J. Pept. Sci.* **2007**, *13* (5), 348–353. <https://doi.org/10.1002/psc.849>.
- (26) Ma, X.; Jia, J.; Cao, R.; Wang, X.; Fei, H. Histidine-Iridium(III) Coordination-Based Peptide Luminogenic Cyclization and Cyclo-RGD Peptides for Cancer-Cell Targeting. *J.*

- Am. Chem. Soc.* **2014**, *136* (51), 17734–17737. <https://doi.org/10.1021/ja511656q>.
- (27) Ruan, F.; Chen, Y.; Hopkins, P. B. Metal Ion Enhanced Helicity in Synthetic Peptides Containing Unnatural, Metal-Ligating Residues. *J. Am. Chem. Soc.* **1990**, *112* (25), 9403–9404. <https://doi.org/10.1021/ja00181a058>.
- (28) Todd, R. J.; Van Dam, M. E.; Casimiro, D.; Haymore, B. L.; Arnold, F. H. Cu(II)-Binding Properties of a Cytochrome c with a Synthetic Metal-binding Site: His-X3-His in an  $\alpha$ -helix. *Proteins Struct. Funct. Bioinforma.* **1991**, *10* (2), 156–161. <https://doi.org/10.1002/prot.340100209>.
- (29) Hernandez, E. T.; Escamilla, P. R.; Kwon, S. Y.; Partridge, J.; McVeigh, M.; Rivera, S.; Reuther, J. F.; Anslyn, E. V. 2,2'-Bipyridine and Hydrazide Containing Peptides for Cyclization and Complex Quaternary Structural Control. *New J. Chem.* **2018**, *42* (11), 8577–8582. <https://doi.org/10.1039/c8nj00184g>.
- (30) Reza Ghadiri, M.; Choi, C. Secondary Structure Nucleation in Peptides. Transition Metal Ion Stabilized  $\alpha$ -Helices. *J. Am. Chem. Soc.* **1990**, *112* (4), 1630–1632. <https://doi.org/10.1021/ja00160a054>.
- (31) Giblin, M. F.; Wang, N.; Hoffman, T. J.; Jurisson, S. S.; Quinn, T. P. Design and Characterization of  $\alpha$ -Melanotropin Peptide Analogs Cyclized through Rhenium and Technetium Metal Coordination. *Proc. Natl. Acad. Sci. U. S. A.* **1998**, *95* (22), 12814–12818. <https://doi.org/10.1073/pnas.95.22.12814>.
- (32) Cheng, Z.; Chen, J.; Quinn, T. P.; Jurisson, S. S. Radioiodination of Rhenium Cyclized  $\alpha$ -Melanocyte-Stimulating Hormone Resulting in Enhanced Radioactivity Localization and Retention in Melanoma. *Cancer Res.* **2004**, *64* (4), 1411–1418. <https://doi.org/10.1158/0008-5472.CAN-03-0193>.
- (33) Halldin, C.; Gulyás, B.; Langer, O.; Farde, L. Brain Radioligands - State of the Art and New Trends. In *Q. J. Nucl. Med.*; **2001**; *45* (2), pp 139–152.
- (34) INTERNATIONAL ATOMIC ENERGY AGENCY, Technetium Radiopharmaceutical: Manufacture of Kits, TTechnical Reports Series No. 466, IAEA, Vienna (2008).
- (35) Boschi, A.; Uccelli, L.; Martini, P. A Picture of Modern Tc-99m Radiopharmaceuticals: Production, Chemistry, and Applications in Molecular Imaging. *Appl. Sci. (Switzerland)*. **2019**, *9* (12), p 2526. <https://doi.org/10.3390/app9122526>.
- (36) Saha, G. B. *Fundamentals of Nuclear Pharmacy*; 2010. <https://doi.org/10.1007/978-1-4419-5860-0>.
- (37) Atkins, P. W.; Overton, T. L.; Rourke, J. P.; Weller, M. T. *Shriver and Atkins' Inorganic Chemistry, Fifth Edition*; 2010.

- (38) Alberto, R. New Organometallic Technetium Complexes for Radiopharmaceutical Imaging. *Top. Curr. Chem.* **2005**, *252*, 1–44. <https://doi.org/10.1007/b101223>.
- (39) Pitchumony, T. S.; Banevicius, L.; Janzen, N.; Zubieta, J.; Valliant, J. F. Isostructural Nuclear and Luminescent Probes Derived from Stabilized [2 + 1] Rhenium(I)/Technetium(I) Organometallic Complexes. *Inorg. Chem.* **2013**, *52* (23), 13521–13528. <https://doi.org/10.1021/ic401972g>.
- (40) Häfliger, P.; Mundwiler, S.; Ortner, K.; Spingler, B.; Alberto, R.; Andócs, G.; Balogh, L.; Bodo, K. Structure, Stability, and Biodistribution of Cationic [M(CO)<sub>3</sub>]<sup>+</sup> (M = Re, <sup>99</sup>Tc, <sup>99m</sup>Tc) Complexes with Tridentate Amine Ligands. *Synth. React. Inorganic, Met. Nano-Metal Chem.* **2005**, *35* (1), 27–34. <https://doi.org/10.1081/SIM-200047534>.
- (41) Bauer, E. B.; Haase, A. A.; Reich, R. M.; Crans, D. C.; Kühn, F. E. Organometallic and Coordination Rhenium Compounds and Their Potential in Cancer Therapy. *Coord. Chem. Rev.* **2019**, *393*, pp 79–117. <https://doi.org/10.1016/j.ccr.2019.04.014>.
- (42) Bartholomä, M.; Valliant, J.; Maresca, K. P.; Babich, J.; Zubieta, J. Single Amino Acid Chelates (SAAC): A Strategy for the Design of Technetium and Rhenium Radiopharmaceuticals. *Chem. Comm.* **2009**, *5*, pp 493–512. <https://doi.org/10.1039/b814903h>.
- (43) Bigott-Hennkens, H. M.; Junnotula, S.; Ma, L.; Gallazzi, F.; Lewis, M. R.; Jurisson, S. S. Synthesis and in Vitro Evaluation of a Rhenium-Cyclized Somatostatin Derivative Series. *J. Med. Chem.* **2008**, *51* (5), 1223–1230. <https://doi.org/10.1021/jm701056x>.
- (44) Rosita, D.; Dewit, M. A.; Luyt, L. G. Fluorine and Rhenium Substituted Ghrelin Analogues as Potential Imaging Probes for the Growth Hormone Secretagogue Receptor. *J. Med. Chem.* **2009**, *52* (8), 2196–2203. <https://doi.org/10.1021/jm8014519>.
- (45) Simpson, E. J. The Development of Metal-Organic Compounds for Use as Molecular Imaging Agents. **2014**.
- (46) Patel, A. The Development of Cyclic RGD Peptides Stabilized Through <sup>99m</sup>Tc / Re (CO)<sub>3</sub><sup>+</sup>. **2015**.

## Chapter 2

# 2 Optimization of cyclization reaction of linear peptides with rhenium tricarbonyl metal core.

## 2.1 Introduction

Cyclic peptides are known to exhibit enhanced *in vivo* stability and specificity over their linear counterparts. As a result of structural modification, cyclic peptides can mimic the geometries of the biologically active parts of large endogenous proteins. This enhances their binding affinity towards the receptor compared to the linear peptides of the same sequence. Depending on the type of cyclization and the position of cyclization, constrained peptides with different biological activities can be generated.<sup>1</sup>

Apart from cyclizing peptides by lactonization, lactamization or formation of a disulfide bridge, metal coordination can be used as an external means for inducing peptide cyclization. The amino acid side chains of the peptides usually have the ability to be used as ligands to coordinate the metal complex. These ligands chelate the metal which creates a turn in the structure and thus cyclizes the linear peptide. Metal used for cyclization of peptides can influence the secondary structure of the proteins. This was seen in a study by Natale *et.al* where the native prion protein (PrP) was selectively bound to Cu (II) through the chelation of the four histidine residues.<sup>2</sup> Prion protein is a small, cell surface glycoprotein which is responsible for pathogenesis of neurodegenerative disorders called prions diseases.<sup>3</sup> It was the geometrical coordination preferences of the metal along with the stability of the chelate ring formed that forced the coordinated amino acids to adopt a fixed rigid conformation.

Previously in our lab, natural amino acids were used as ligands to coordinate with the group 7 transition metals Re and radioactive <sup>99m</sup>Tc, forming 2+1 chelation systems. A 2+1 chelation system is comprised of a metal complex with coordination to both a bidentate and a monodentate ligand. Simpson *et.al* cyclized the pentapeptide Ac-HAAAH-OH using the *fac* [Re(CO)<sub>3</sub>(OH<sub>2</sub>)<sub>3</sub>]<sup>+</sup> core with histidine as the as the metal chelator.<sup>4</sup> Histidine was chosen as the natural amino acid ligand due to its high biological stability along with its ability to coordinate rapidly and quantitatively in low concentration. In addition, several studies have observed the ability of histidine to coordinate

with different metal centers in metalloproteins like copper in hemocyanin,<sup>5</sup> iron in hemoglobin,<sup>6</sup> and zinc in thermolysin.<sup>7</sup> The imidazole of the histidine on the N-terminus of the pentapeptide was used as a monodentate chelator and the imidazole and carboxylic acid of the histidine at the C-terminus were used as a bidentate chelator to form a 2+1 chelation system. This chelation system was used to coordinate  $\text{Re}/^{99\text{m}}\text{Tc}(\text{CO})_3^+$  and form a cyclic peptide. Although the peptide cyclization attempt was successful, there was formation of numerous linkage isomers due to the multiple coordinating sites on histidine. Linkage isomers are two or more coordination compounds which differ by the donor atom of at least one of the ligands. Imidazole on histidine can coordinate to the metal through N1 and N3 atoms which leads to formation of 7 or 8 membered ring at the C-terminus and a 6 membered ring at the N-terminus (Figure 2.1). Therefore, there was a need for a better chelator that had fewer coordinating sites and can form a stable ring size on coordination with the  $\text{M}(\text{CO})_3$  core.

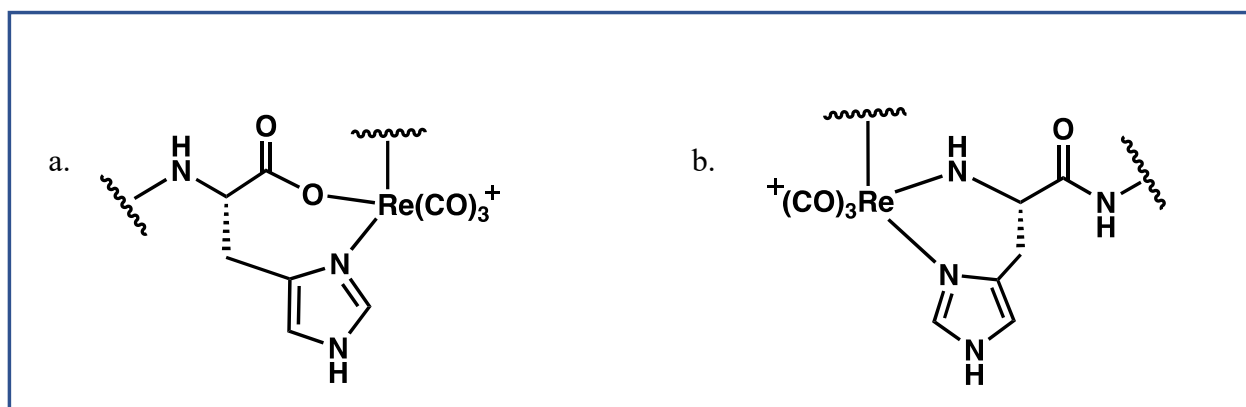


Figure 2.1 a) Rhenium coordination at C-terminal forming 7 or 8 membered ring, b) rhenium coordination at N-terminus forming 6 membered ring.

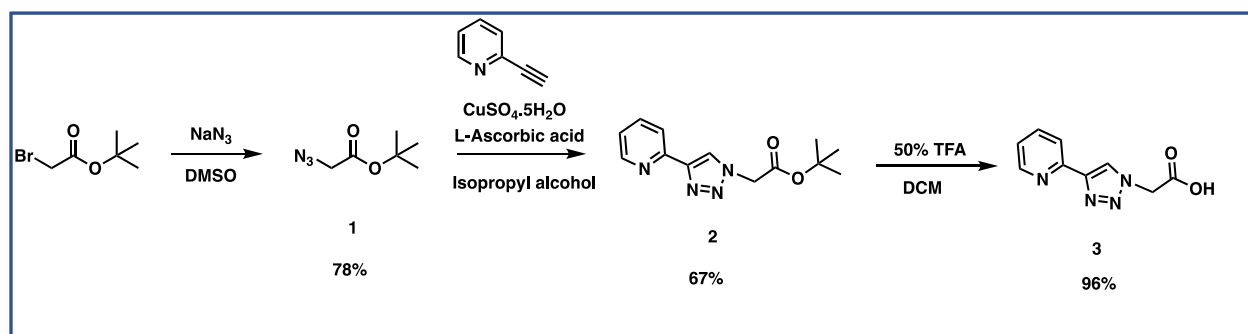
In order to reduce the number of linkage isomers formed and to enable the formation of a stable ring size with the metal, Patel *et.al* proposed the use of unnatural amino acids and synthetic ligands as metal chelators.<sup>8</sup> Pyridyl triazole acetic acid (pyta) and 3-pyridyl alanine (3-Pal) were proposed to be used as bidentate and monodentate ligands respectively whereas the tri-alanine sequence was replaced with the Arg-Gly-Asp to create a biologically relevant peptide. The peptide sequence pyta-RGD-3Pal was then coordinated to the *fac*  $\text{Re}(\text{CO})_3$  core, creating a 2+1 chelation system.<sup>8</sup> However, the isomers of this coordinated peptide were not studied or discussed in detail. Furthermore, the reaction conditions used for the cyclization of the linear peptide by Simpson *et.al*

and Patel *et.al* resulted in low yields of the cyclic product. It was thus essential to optimize the cyclization reaction conditions which would bear high yield of the cyclic product.

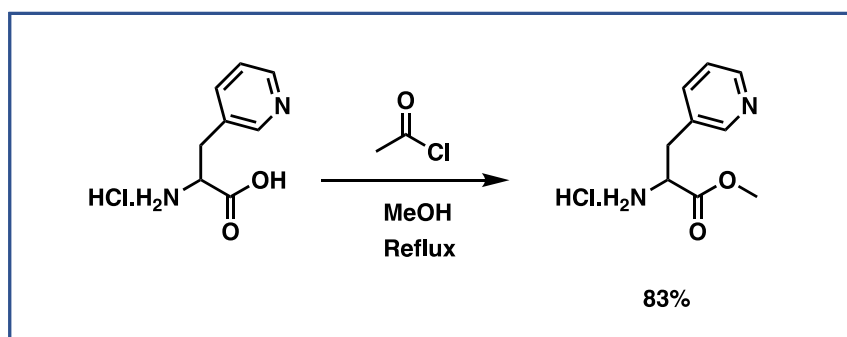
The overall goal of this chapter is to optimize the cyclization reaction conditions and translate the success of the unnatural amino acids and different synthetic ligands as metal chelators on to the model system of Xaa-Ala-Ala-Ala-Xaa (Xaa= unnatural amino acid or synthetic ligand).

## 2.2 Results and Discussion

To optimize the reaction conditions of the coordination reaction, we needed to first synthesize the linear peptides. We chose the model peptide sequence pyta-Ala-Ala-Ala-3Pal for the optimization study. The linear peptide was designed to have two terminal chelators capable of coordinating rhenium, as well as three central alanine residues to aid in forming a turn in the peptide upon coordination. This would allow the peptide to coordinate the rhenium in a [2+1] fashion using the N-terminal and C-terminal chelator, resulting in a neutral peptide-metal complex. Chelation of the peptide to the metal was done using ligand pyridyl triazole acetic acid and unnatural amino acid 3-pyridyl alanine. Pyridyl-triazole would coordinate to  $\text{Re}(\text{CO})_3^+$  in a bi-dentate fashion whereas 3-pyridyl alanine can be used to chelate the metal in a monodentate fashion. Pyridyl triazole acetic acid and the methoxy ester of 3-pyridyl alanine were synthesized as shown in the Scheme 2.1 and Scheme 2.2 respectively.



Scheme 2.1 Synthesis of pyridyl triazole acetic acid <sup>9</sup>, **3**

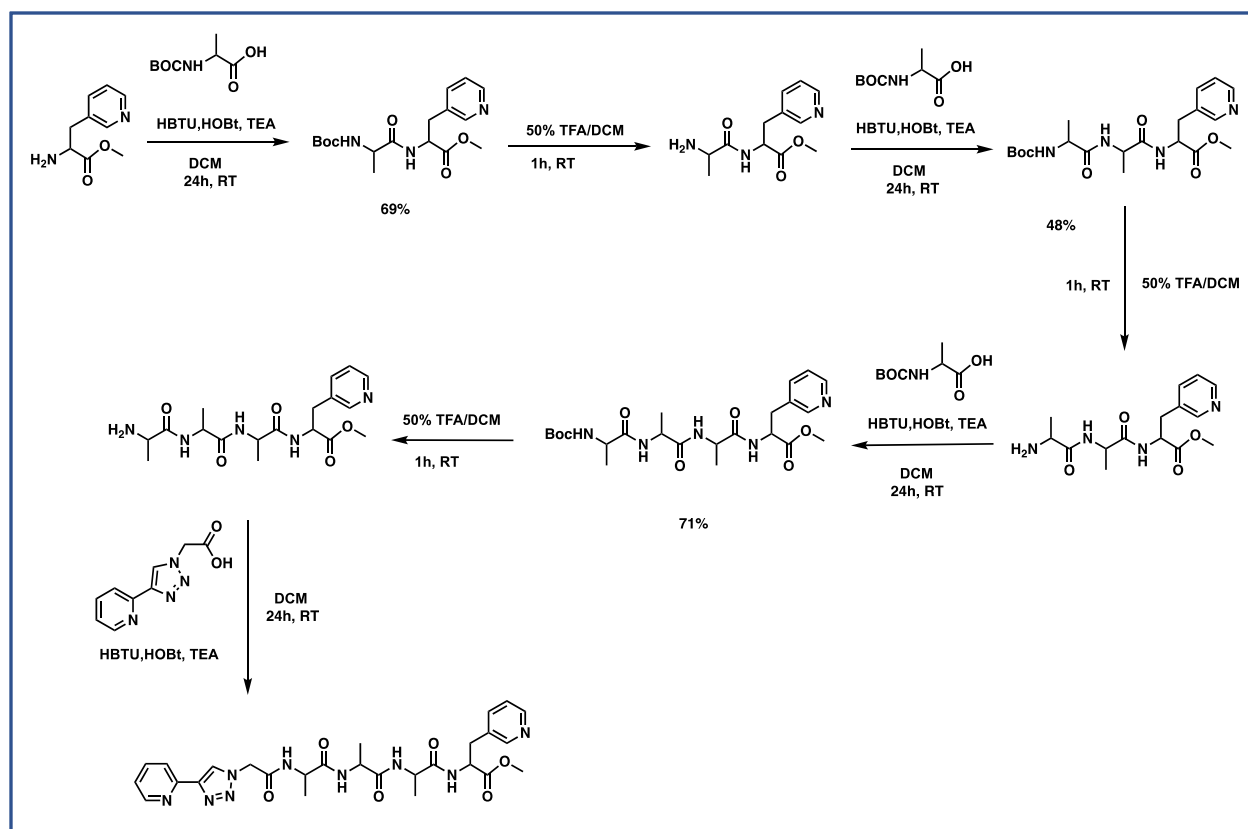


Scheme 2.2 Esterification of 3-pyridyl alanine, 4

Synthesis of linear peptides can be done using the solid phase or solution phase peptide synthesis method. Solid phase peptide synthesis is an efficient method for synthesizing peptides on a small scale but when it comes to scaling up the production, it can become quite expensive. This factor led us to shift our attention to solution phase peptide synthesis. Though a more tedious method, solution phase peptide synthesis can be a comparatively less expensive option for bulk production.

### 2.3 Solution phase peptide synthesis

Peptide sequence pyta-Ala-Ala-Ala-3Pal-OMe was synthesized from the C-terminus unnatural amino acid 3-pyridyl alanine carboxylic acid. 3-Pyridyl alanine was esterified using methanol to protect the C-terminal carboxylic acid<sup>10</sup> (Scheme 2.2). It was then coupled to a *tert*-butoxycarbonyl (Boc)-protected alanine using coupling agents HOBt (1-hydroxybenzotriazole hydrate), HBTU (2-(1H-Benzotriazole-1-yl)-1,1,3,3-tetramethyluronium hexafluorophosphate) in presence of a base TEA (triethyl amine) in dichloromethane. The coupling was followed by removal of the Boc group using trifluoroacetic acid in dichloromethane to yield a free amine. This free amine was then coupled with an incoming Boc-protected alanine. This process was followed by a series of deprotection and coupling steps till the desired peptide sequence Ala-Ala-Ala-3Pal-OMe was achieved. The last stage of peptide deprotection was followed by coupling with the ligand pyridyl triazole acetic acid in a similar manner (Scheme 2.3). Though the coupling of the ligand to the peptide sequence was successful as confirmed by LCMS characterization, purification of the peptide after the last coupling proved to be challenging. Several attempts made to isolate the linear peptide from the mixture of the starting materials and salts proved to be unsuccessful which led us to switch back to solid phase peptide synthesis.



Scheme 2.3 Synthesis of linear peptide sequence pyta-Ala-Ala-Ala-3Pal-OMe, **2.4** using solution phase peptide synthesis

## 2.4 Solid phase peptide synthesis of pyta-AAA-3Pal, **3.1**

The linear sequence of pyta-AAA-3Pal was synthesized by standard Fmoc solid phase peptide synthesis method. Rink amide resin (MBHA) was used as a solid support and the peptide was synthesized from C to N terminus. Each amino acid was vortexed with the coupling agent HCTU (2-(6-chloro-1H-benzotriazole-1-yl)-1,1,3,3-tetramethylammonium hexafluorophosphate), base DIPEA (diisopropyl ethyl amine) in DMF for 10 mins prior to coupling. The N-terminus was coupled with the ligand pyridyl triazole acetic acid (pyta) which was synthesized according to previously published method,<sup>7</sup> (Scheme 2.1). The *tert*-butyl group on the ligand was removed by a method published by Lim and Storr *et al.*<sup>8</sup> Pyta was vortexed for 10 mins with coupling agent TSTU (O-(N-succinimidyl)-1,1,3,3-tetramethyl uronium tetrafluoroborate), DIPEA in DMF to form a pre-activated ester prior to coupling with the tetrapeptide. Removal of all protecting groups and cleaving of the resin was done with 95:2.5:2.5 TFA: TIPS: H<sub>2</sub>O. The peptide was precipitated



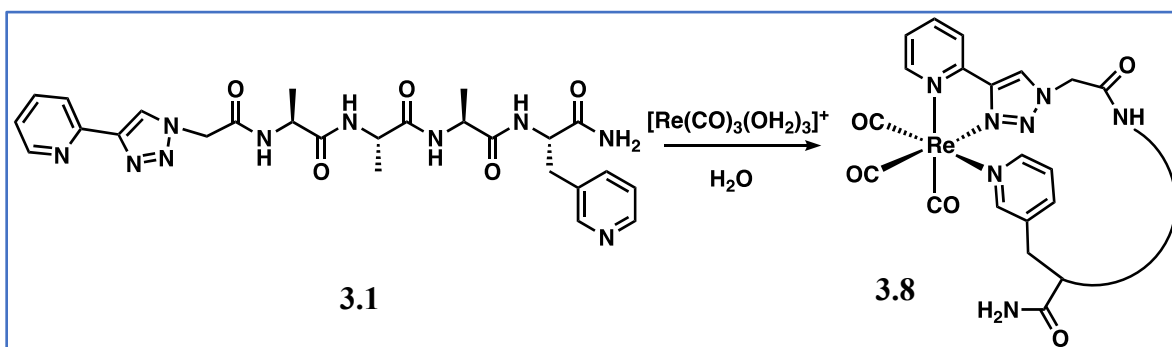
with cold *tert*-butyl methyl ether (TBME), centrifuged, filtered and lyophilized to give crude linear peptide of the desired sequence. The crude linear peptide was then purified by RP-HPLC.

## Optimization of rhenium coordination reaction

Previously in our lab, Simpson *et.al* carried out the coordination reaction at room temperature in the presence of the base NaOH.<sup>2</sup> Replication of these conditions for the coordination of pyta-AAA-3Pal resulted in a poor yield of the coordinated peptide. Patel *et.al* carried out the coordination reaction using microwave conditions at 105° C for 1 hour.<sup>6</sup> This reaction condition resulted in formation of several by-products which could possibly be due to degradation of peptides at higher temperature. The low yield obtained from both the reaction conditions prompted us to carry out an optimization study to get suitable reaction conditions with maximum yield of the cyclic peptide. Optimization was carried out by testing the coordination reaction at different temperatures and time. Impact of solvent change and presence of a base was also examined.

## 2.5 Temperature and time optimization

Linear peptide sequence pyta-AAA-3Pal was used to study the effect of increasing temperature and time during the coordination reaction. Rhenium coordination was carried out at four different temperatures 0° C, RT, 50° C, 100° C respectively for 0-4 hour time points (Scheme 2.4), with aliquots from the reaction being analyzed and quantified using UHPLC. Characterization by UHPLC showed presence of one dominant peak (A) of the cyclic peptide along with two less dominant peaks (B, C) having identical product m/z value as the dominant peak (Figure 2.2).



Scheme 2.4 Rhenium coordination of peptide sequence pyta-Ala-Ala-Ala-3Pal, **3.1**

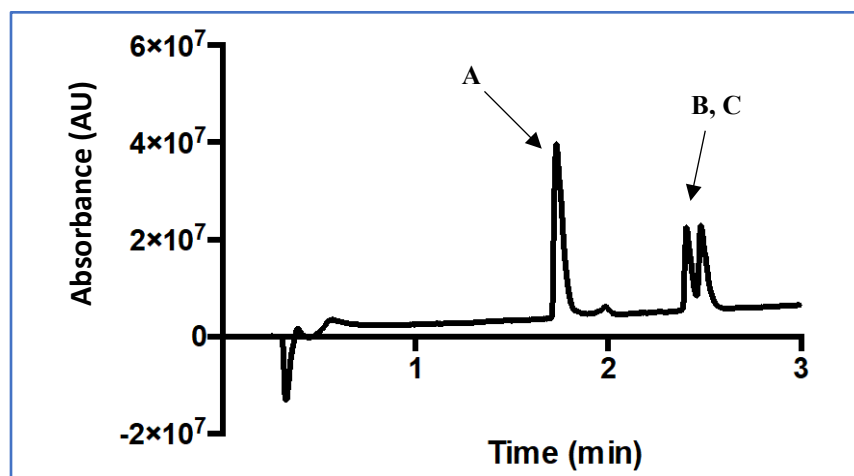


Figure 2.2 UHPLC UV trace of cyclic peptide **3.8**, showing dominant (A) and less dominant conformer (B, C)

The data from the study was plotted in the form of a graph of total coordinated product vs time (Figure 2.3). Total coordinated product constitutes a percentage ratio of the cyclic peptide to the sum of the linear and cyclic peptide. Cyclic peptide consists of a combined sum of the dominant peak of the cyclic peptide (A) along with two other less dominant peaks (B, C). These peaks could be attributed as the conformer/isomer of the dominant peak. The optimization was carried out to isolate the maximum percentage of the dominant peak (A).

It was quite interesting to observe that while the coordination took place at all four temperatures, only the reactions carried out at  $50^\circ\text{C}$  and  $100^\circ\text{C}$  showed significant increase in the percentage of the total coordinated product. Observation from the graph showed that the reaction carried out at  $100^\circ\text{C}$  formed higher percentage of total coordinated product within the first 30 mins of the reaction compared to the reaction carried out at  $50^\circ\text{C}$  (Figure 2.3). However, the total coordinated product seen at  $100^\circ\text{C}$  had maximum percentage of the isomer/conformer than the desired dominant peak. As the reaction progressed at  $100^\circ\text{C}$ , more of the dominant peak was getting converted to its isomer/ conformer state. This can be seen in the graph plotted for the % coordinated peptide v/s time, where % coordinated peptide constitutes to the percentage ratio of dominant (A) and the less dominant peaks (B + C) respectively to the sum of linear and cyclic peptide (Figure 2.4). The reaction at  $50^\circ\text{C}$  in comparison to  $100^\circ\text{C}$ , yielded maximum of dominant cyclic peptide.

Over the course of two hours, least possible amount of the cyclic isomer/conformer was observed at 50° C in addition to a better yield of the cyclic peptide.

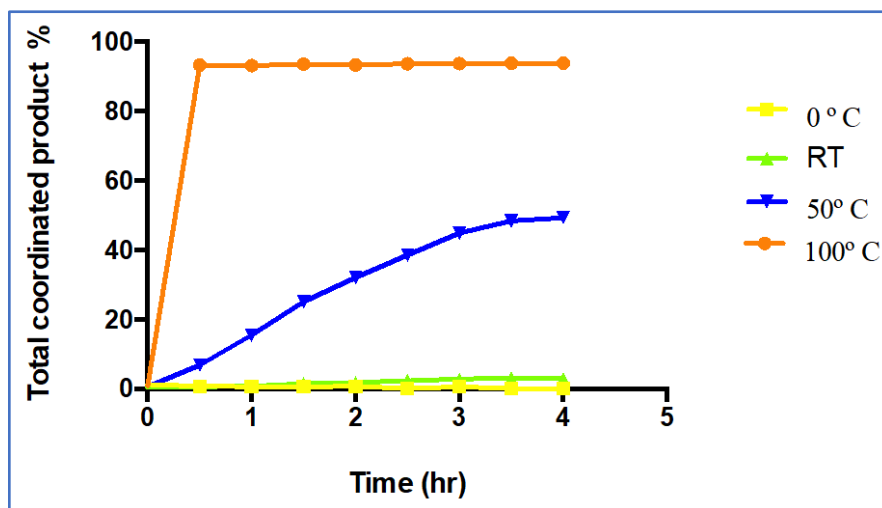


Figure 2.3 Graph of total coordinated product vs time for the four different temperatures used for synthesis of **3.8** (Scheme 2.4), where total coordinated product % = (cyclic peptide / linear peptide + cyclic peptide) %

As a result, in order to maximize the yield of cyclic peptide and limit the formation of cyclic isomer/conformer, the reaction conditions of 50° C for the time period of two hours seems optimal.

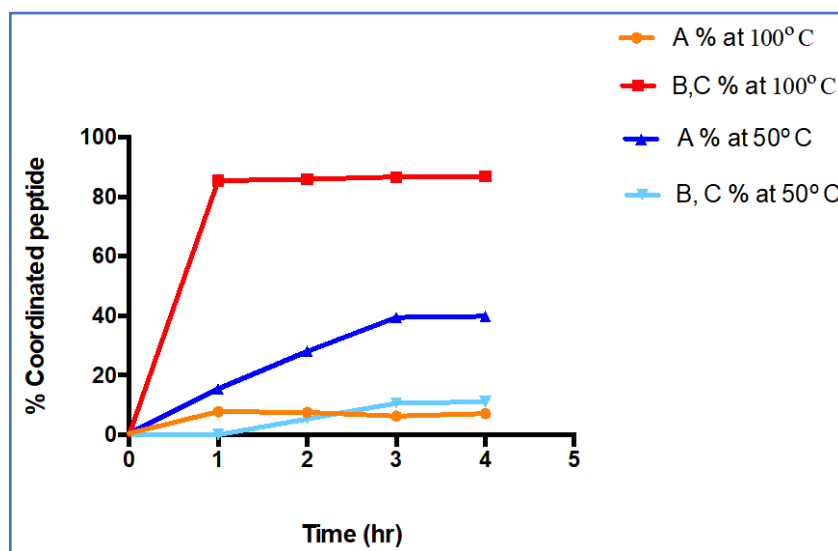


Figure 2.4 Graph of % coordinated peptide vs time for synthesis of **3.8**, where % coordinated peptide = [A or (B + C)/ linear peptide + cyclic peptide] %

## 2.6 Optimization of reaction solvent

The rhenium coordination reaction was carried out in methanol instead of distilled water. It was observed that while there was an increase in the yield of the total coordinated product, the yield of the dominant conformer was lower when compared to the yield obtained with distilled water as the solvent. This means that there was an increase in the yield of the less dominant conformer/isomer over time in methanol.

## 2.7 Optimization using a base

Previously, the coordination reaction carried out by Simpson *et.al* and Patel *et.al* involved the presence of a strong base, NaOH. Impact of the base was examined during the coordination reaction by carrying out the reaction both in presence and absence of the base NaOH. The reaction was performed at 50° C. It was observed that while the coordination took place both in presence and absence of a base, there was a significant difference in the percentage of the cyclic product obtained in the reaction carried out in presence and absence of base. The reaction performed without the base gave better results in comparison to the reaction with base.

## 2.8 Conclusion

Optimization studies were performed to observe the reaction conditions required to improve the efficiency of rhenium coordination reaction. This study was carried out at four different temperatures in order to determine an optimal temperature and reaction time for the coordination reaction. The solvent change from water to methanol and addition of a base both failed to increase the yield of the cyclic peptide. The observations from the optimization experiments led us to conclude that the rhenium coordination reaction carried out at 50° C for 2 hours in distilled water without a base comparatively increased the yield of cyclic peptide.

## 2.9 Experimental data

All the reagents and solvents were purchased from Sigma Aldrich, Fisher Scientific, Alfa-Aesar, Chem- Impex, Novabiochem, Oakwood Chemicals, Peptides International. The Boc-protected amino acids were purchased from Chem-Impex International Ltd. and were used without further purification. For analytical UHPLC-MS, studies were performed on a Waters, Inc. Acquity UHPLC system combined with Xevo QToF mass spectrometer (ESI+, cone voltage = 30V). A

Waters, Inc. Acquity UHPLC BEH C18 2.1 x 50 mm, 1.7  $\mu$ m column was used with a gradient solvent system consisting of 0.1% formic acid in acetonitrile and 0.1% formic acid in water. NMR spectroscopy was performed using Bruker Avance III HD 400 (B400) in deuterated dimethyl sulfoxide (DMSO-  $d_6$ ) or  $CDCl_3$  at 25 °C.

## 2.10 *Small molecule synthesis*

### a) *tert-butyl azido acetate, 1*

A modified procedure was used.<sup>11</sup> To a suspension of sodium azide (2.28 g, 35.07 mmol) in DMSO (15 mL), *tert*-butyl bromo acetate (4.5 g, 23.07 mmol) was added. The resulting opaque white color solution was stirred overnight at RT. This solution was diluted with 300 mL of distilled water and the compound of interest was extracted using diethyl ether and concentrated to afford a colorless oil (2.86 g, 78%) Characterization was identical to published values.<sup>10</sup>  $^1H$  NMR (400 MHz,  $CDCl_3$ ):  $\delta$  1.50 (s, 9H), 3.74 (s, 2H).

### b) *tert-butyl-2-(4-phenyl-1H-1,2,3-triazol-1-yl) acetate, 2*

A modified procedure was used.<sup>9</sup> *tert*-Butyl azido acetate, **1** (1.765 g, 11.23 mmol) and 2- ethynyl pyridine (1.158 g, 11.23 mmol) was dissolved in isopropanol (2 mL) in a 20mL vial. In another 20 mL vial, copper (II) sulphate pentahydrate (0.140 g, 0.56 mmol) and L-ascorbic acid (0.989 g, 5.6 mmol) were dissolved in distilled water. The solids were completely dissolved by sonicating for 20 minutes at room temperature. The aqueous mixture was added dropwise to the stirring organic mixture over 15 minutes. The resulting yellow turbid solution was allowed to stir overnight at RT. The solution was diluted with chloroform (15 mL) and washed thrice with saturated EDTA solution. The organic product was extracted from the aqueous layer using chloroform (2 x 20 mL). The combined organic layers were dried over  $Na_2SO_4$  and then concentrated to remove chloroform. The crude product was purified by crystallization in methanol which afforded white crystals of the mentioned compound. (1.96 g, 67 %) ESI-LCMS:  $m/z$  calculated for  $C_{13}H_{17}N_4O_2$  261.1352; observed  $[M+H]$  261.1306,  $^1H$  NMR (400 MHz,  $CDCl_3$ ):  $\delta$  8.58 (d, 1H, 1H), 8.25 (s, 1H), 8.18 (d,  $^3J_{H-H} = 1.4$  Hz, 1H), 7.78 (m, 1H), 7.23 (m, 1H), 5.12 (s, 2H), 1.49 (s, 9H).

c) 2-(4-phenyl-1H-1,2,3-triazol-1-yl) acetic acid (Pyta), **3**

*tert*-Butyl-2-(4-phenyl-1H-1,2,3-triazol-1-yl) acetate (1.3 g, 5.1 mmol), **2** was dissolved in a 1:1 solution of trifluoroacetic acid and dichloromethane. The resulting solution was allowed to stir overnight at room temperature. After rotary evaporation of dichloromethane, compound of interest was precipitated from the solution by using diethyl ether. This afforded a white color powder of **3**. (1.0 g, 96%) ESI- HRMS: *m/z* calculated for C<sub>9</sub>H<sub>9</sub>N<sub>4</sub>O<sub>2</sub>, 205.0726; observed [M+H]<sup>+</sup> 205.0757, <sup>1</sup>H NMR (400 MHz, D<sub>2</sub>O): δ 8.58 (s, 1H), 8.05 (s, 1H), 7.91 (m, 1H), 7.36 (m, 1H), 5.36 (s, 2H).

d) 3-Pyridyl alanine methoxy ester, **4**

A round bottom flask containing 15 mL of methanol was cooled in ice for 10 mins. Acetyl chloride (1.40 mmol, 1 mL) was added dropwise to the round bottom flask. This was followed by the addition of 3-pyridyl alanine dihydrochloride (6.01 mmol, 1 g). The cloudy reaction mixture was refluxed overnight, following which the solvent was removed by rotary evaporation. This afforded an off-white solid (1.08 g, 83%). This was further used for the coupling reaction and no further purification was required. ESI-HRMS: *m/z* calculated for C<sub>9</sub>H<sub>13</sub>N<sub>2</sub>O<sub>2</sub> 181.0977; observed [M+H]<sup>+</sup> 181.1003, <sup>1</sup>H NMR (400 MHz, DMSO): δ 8.90 (d, <sup>3</sup>J<sub>H-H</sub> = 4.0 Hz, 1H), 8.86 (bs, 2H), 8.82 (dd, <sup>3</sup>J<sub>H-H</sub> = 8.0 Hz, 4.0 Hz, 1H), 8.44 (dt, <sup>3</sup>J<sub>H-H</sub> = 8.0 Hz, 1.6 Hz, 1H), 7.96 (dd, <sup>2</sup>J<sub>H-H</sub> = 8.0 Hz, <sup>3</sup>J<sub>H-H</sub> = 5.2 Hz, 1H), 3.74 (s, 3H), 3.47-3.36 (m, 2H).

e) Tris-aqua tris-carbonyl rhenium (I) triflate, **5**

Commercially available Bromo pentacarbonyl rhenium (1 g, 2.76 mmol) was added to dry dichloromethane (20 mL) and kept for stirring. Silver triflate (0.894 g, 3.47 mmol) was weighed under subdued light and was added to the flask under increased nitrogen flow. The flask was covered with aluminum foil and the solution was allowed to stir at RT for 3h. The resulting white turbid solution was gravity filtered to remove the precipitate of by-product salts, silver bromide. The solution was concentrated to half its volume. Hexanes were degassed in a 50 mL round bottom flask by bubbling nitrogen through for 30 minutes, following which the dry hexane was added slowly to the rhenium pentacarbonyl triflate solution and allowed to crystallize to a white powder. The white powder (0.835 g) was dissolved in distilled water (17.56 mL) to form 0.1 M solution

and was refluxed overnight which afforded  $[\text{Re}(\text{CO})_3(\text{OH}_2)_3]^+$  solution.<sup>12</sup> The resulting solution was characterized by LC-MS. (ESI-MS)<sup>+</sup>:  $m/z$  calculated for  $\text{C}_5\text{H}_7\text{N}_1\text{O}_5\text{Re}$ ,  $[(\text{M} - \text{H}_2\text{O}) + \text{CH}_3\text{CN}]$  347.9882; found 348.0110, calculated for  $\text{C}_7\text{H}_8\text{N}_2\text{O}_4\text{Re}$ ,  $[(\text{M} - 2\text{H}_2\text{O}) + 2\text{CH}_3\text{CN}]$  371.0042; found 371.0145; calculated for  $\text{C}_9\text{H}_9\text{N}_3\text{O}_3\text{Re}$ ,  $[(\text{M} - 3\text{H}_2\text{O}) + 3\text{CH}_3\text{CN}]$  394.0202; found 394.0366.

## 2.11 General procedure for Peptide synthesis (Solution phase)

Peptide was synthesized from C to N terminus with the 3-pyridyl alanine being esterified to protect the carboxylic acid. The amine of the 3-pyridyl alanine was coupled with a *tert*-butoxycarbonyl (Boc) protected amino acid where the Boc group is acid labile. The first coupling was carried out using the coupling agent HOBt (1-hydroxybenzotriazole hydrate), HBTU (2-(1H-Benzotriazole-1-yl)-1,1,3,3-tetramethyluronium hexafluorophosphate) along with the base triethyl amine at room temperature for 24 hours. The resulting solution was given washings with saturated sodium bicarbonate, 10 % citric acid solution and brine to remove any excess base and acid. Purification was done using column chromatography. This was followed by Boc group removal using 50% trifluoroacetic acid in dichloromethane for one hour. This was followed by a series of coupling using Boc protected amino acids and deprotection until the desired peptide sequence is obtained.

### 2.11.1 Boc-Ala-3-Pal-OMe, 2.1

3-Pyridyl alanine methoxy ester, **4** (1.07 g, 4.58 mmol, 1 eq) was added to a round bottom flask containing 20 mL of dichloromethane. This was followed by addition of the base triethyl amine (10.07 mmol, 2.2 eq), HBTU (1.91 g, 5.04 mmol, 1.1 eq) and HOBt (0.68 g, 5.04 mmol, 1.1 eq). The reaction mixture was allowed to stir for 10 minutes at room temperature, followed by addition of Boc-Ala-OH to the reaction mixture. The clear light orangish brown solution was kept for stirring for 24 hours at room temperature. The organic solution was washed with saturated  $\text{NaHCO}_3$  (3 x 50 mL), 10% citric acid solution (3 x 40 mL) and brine (3 x 20 mL). The organic solution was dried using anhydrous  $\text{Na}_2\text{SO}_4$  and dichloromethane was removed using rotary evaporation. The product was purified using column chromatography using ethyl acetate to yield yellow oil (1.11 g, 69 %) ESI-HRMS:  $m/z$  calculated for  $\text{C}_{17}\text{H}_{26}\text{N}_3\text{O}_5$ , 352.1872; observed  $[\text{M}+\text{H}]^+$  352.1863, <sup>1</sup>H NMR (400 MHz,  $\text{CDCl}_3$ ):  $\delta$  8.49 (dd, <sup>3</sup>J<sub>H-H</sub> = 8.0 Hz, 4.0 Hz, 1H), 8.35 (d, <sup>3</sup>J<sub>H-H</sub> = 2.4 Hz, 1H), 7.48 (dt, <sup>3</sup>J<sub>H-H</sub> = 8.0 Hz, 2.0 Hz, 1H), 7.22 (dd, <sup>3</sup>J<sub>H-H</sub> = 8.0 Hz, 4.0 Hz, 1H),

6.72 (d, NH of 3-Pal,  $^3J_{H-H} = 4.0$  Hz, 1H), 4.91 (s, NH of Ala, 1H), 4.86 (m,  $\alpha$  CH of 3-Pal, 1H), 4.12 (m,  $\alpha$  CH of Ala1, 1H), 3.74 (s, 3H), 3.14 (m, CH<sub>2</sub> of 3-Pal, 2H), 1.43 (s, 9H), 1.32 (d, CH<sub>3</sub> of Ala,  $^3J_{H-H} = 8.0$  Hz, 3H)

#### 2.11.2 *Boc-Ala-Ala-3-Pal-OMe*, **2.2**

The *tert*-butoxycarbonyl group (Boc) was removed from Boc-Ala-3-Pal-OMe (**2.1**) using 50 % trifluoroacetic acid in dichloromethane. The reaction mixture was stirred for one hour at room temperature, following which the solvent was removed using rotary evaporation. The deprotected peptide was coupled to another amino acid Boc-Ala-OH using the procedure mentioned for **2.1**. The product was purified using column chromatography using methanol-dichloromethane (06:94) to afford a light yellow oil (0.66 g, 48%) ESI- HRMS: m/z calculated for C<sub>20</sub>H<sub>31</sub>N<sub>4</sub>O<sub>6</sub>, 423.2244; observed [M+H]<sup>+</sup> 423.2243, <sup>1</sup>H NMR (400 MHz, CDCl<sub>3</sub>):  $\delta$  8.48 (dd,  $^3J_{H-H} = 8.0$  Hz, 4.8 Hz, 1H), 8.34 (d,  $^3J_{H-H} = 4.0$  Hz, 1H), 7.48 (dt,  $^3J_{H-H} = 8.0$  Hz, 4.0 Hz, 1H), 7.23 (m, 1H), 6.80 (s,  $^3J_{H-H} = 4.0$  Hz, NH of 3-Pal, 1H), 6.68 (d,  $^3J_{H-H} = 6.0$  Hz, NH of Ala 2, 1H), 5.01 (bs, NH of Ala 1, 1H), 4.85-4.79 (m,  $\alpha$  CH of 3-Pal, 1H), 4.40 (quint,  $^3J_{H-H} = 16.0$  Hz, 8.0 Hz,  $\alpha$  CH of Ala 2, 1H), 4.12 (m,  $\alpha$  CH of Ala 1, 1H), 3.74 (s, 3H), 3.20 (m, CH<sub>2</sub> of 3-Pal, 2H), 1.44 (s, 9H), 1.34 (d, CH<sub>3</sub> of Ala 1 and 2,  $^3J_{H-H} = 8.0$  Hz, 6H)

#### 2.11.3 *Boc-Ala-Ala-Ala-3-Pal-OMe*, **2.3**

Deprotected peptide (**2.2**) was coupled to another amino acid Boc-Ala-OH using the same procedure as **2.1**. The crude product was purified by column chromatography using methanol and ethyl acetate (1:9). This afforded an off white solid (0.53 g, 71%) ESI-HRMS: m/z calculated for C<sub>23</sub>H<sub>36</sub>N<sub>5</sub>O<sub>7</sub> 494.2615; observed [M+H]<sup>+</sup> 494.2654, <sup>1</sup>H NMR (400 MHz, CDCl<sub>3</sub>):  $\delta$  8.45 (dd,  $^2J_{H-H} = 8.0$  Hz,  $^3J_{H-H} = 4.0$  Hz, 1H), 8.42 (s, 1H), 7.55 (dt,  $^3J_{H-H} = 8.0$  Hz, 4.0 Hz, 1H), 7.20 (dd,  $^3J_{H-H} = 8.0$  Hz, 4.0 Hz, 1H), 7.14 (d, NH of 3-Pal,  $^3J_{H-H} = 8.0$  Hz, 1H), 6.73 (d,  $^3J_{H-H} = 8.0$  Hz, 1H), 5.12 (s, NH of Ala, 1H), 4.83 (m,  $\alpha$  CH of 3-Pal, 1H), 4.45 (quint,  $^3J_{H-H} = 12.0$  Hz, 8.0 Hz,  $\alpha$  CH of Ala 3, 1H), 4.40 (m,  $\alpha$  CH of Ala 2, 1H), 4.12 (m,  $\alpha$  CH of Ala 1, 1H), 3.73 (s, 3H), 3.14 (dd,  $^2J_{H-H} = 16.0$  Hz,  $^3J_{H-H} = 2.4$  Hz,  $\beta$ H of CH<sub>2</sub> of 3-Pal, 2H), 3.13 (dd,  $^2J_{H-H} = 16.0$  Hz,  $^3J_{H-H} = 2.4$  Hz,  $\beta'$ H of CH<sub>2</sub> of 3-Pal 1H), 1.45 (s, 9H), 1.40 (d,  $^3J_{H-H} = 8.0$  Hz, 3H), 1.37 (d, CH<sub>3</sub> of Ala,  $^3J_{H-H} = 8.0$  Hz, 3H), 1.33 (d, CH<sub>3</sub> of Ala,  $^3J_{H-H} = 8.0$  Hz, 3H).



#### 2.11.4 *Pyta-Ala-Ala-Ala-3-Pal-OMe*, **2.4**

Deprotected peptide (**2.3**) was coupled to the ligand pyridyl triazole acetic acid (pyta) using the same procedure as **2.1**. Purification was attempted using column chromatography using methanol in dichloromethane (1:9) which afforded a minute amount of white solid (2 mg) ESI-HRMS: m/z calculated for C<sub>27</sub>H<sub>34</sub>N<sub>9</sub>O<sub>6</sub>, 580.2632; observed [M+H]<sup>+</sup> 580.2599

#### 2.12 *Peptide synthesis (Solid phase)*

Peptide was synthesized from C to N terminus on a solid phase support with C terminus being attached to the insoluble resin. Peptides were synthesized using standard solid phase peptide synthesis technique and the linear peptide was synthesized using fluorenyl methyloxycarbonyl (Fmoc) chemistry. The N terminal of each amino acid is Fmoc protected and the side chains are acid labile. Rink amide MBHA resin (0.39 meq/g) was used as a solid support. The rink amide resin was swollen in dimethyl formamide for 15 minutes. Each amino acid was Fmoc deprotected using 20% piperidine in dimethyl formamide for two cycles (5 minutes and 15 minutes). Coupling reactions were carried out with 3 eq. Fmoc protected amino acid, 3 eq. HCTU (2-(6-chloro-1H-benzotriazole-1-yl)-1,1,3,3-tetramethyl ammonium hexafluorophosphate) and 6 eq. of DIPEA (N,N-diisopropylethylamine). The coupling reaction was carried out for 60-90 minutes. The resin beads were washed with excess dimethyl formamide and dichloromethane after each coupling and deprotection cycles. The bidentate ligand (pyta and 2,2'-bipyridyl-4-carboxylic acid) were coupled to the peptide with the (N,N,N',N'-tetramethyl-O-(N-succinimidyl) uronium tetrafluoroborate) TSTU and DIPEA in DMF, to prepare the pre-activated ester. The peptide was cleaved from the resin using a cocktail mixture of 95% (v/v) trifluoroacetic acid (TFA), 2.5% (v/v) tri-isopropyl silane (TIPS) and 2.5% (v/v) water for 5h. The cleaved peptide was precipitated with *tert*-butyl methyl ether (TBME) and centrifuged at 3000 rpm for 10 minutes. After decanting, the peptide was frozen and lyophilized to remove any remaining solvents. The peptide was purified with reverse phase preparative HPLC, and the purity was checked by analytical UHPLC. Each of the following peptides synthesized resulted in purity > 95%.

### 2.12.1 *Pyta-Ala-Ala-Ala-3Pal*, **3.1**

The linear peptide was synthesized using the general procedure for solid phase peptide synthesis mentioned above (2.12). This afforded pure peptide in the form of white fluffy solid (0.017 g, 30%)  $^1\text{H}$  NMR (400 MHz,  $\text{CDCl}_3$ ):  $\delta$  8.67-8.62 (m, Ar-H + NH of Ala 3, 1H), 8.61-8.59 (m, 1H), 8.52 (s, 1H), 8.17 (d,  $^3\text{J}_{\text{H-H}} = 8.0$  Hz, 1H), 8.13 (d,  $^3\text{J}_{\text{H-H}} = 8.0$  Hz, 1H), 8.03 (dt,  $^3\text{J}_{\text{H-H}} = 8.0$  Hz, 1.2 Hz, 1H), 7.93-7.90 (m, NH of 3Pal + Ar-H, 2H), 7.84 (d,  $^3\text{J}_{\text{H-H}} = 4.0$  Hz, NH of Ala1, 1H), 7.72 (dd,  $^3\text{J}_{\text{H-H}} = 8.0$  Hz, 5.2 Hz, 1H), 7.39 (s, 1H), 7.37-7.33 (m, 1H), 7.22 (s, 1H), 5.23 (s, 2H), 4.49 (m,  $\alpha$  CH of 3Pal, 1H), 4.34 (quint,  $^3\text{J}_{\text{H-H}} = 12.0$  Hz, 8.0 Hz,  $\alpha$  CH of Ala 3, 1H), 4.22 (quint,  $^3\text{J}_{\text{H-H}} = 12.0$  Hz, 8.0 Hz,  $\alpha$  CH of Ala 2, 1H), 4.10 (quint,  $^3\text{J}_{\text{H-H}} = 12.0$  Hz, 8.0 Hz,  $\alpha$  CH of Ala 1, 1H), 3.17 (dd,  $^2\text{J}_{\text{H-H}} = 16.0$  Hz,  $^3\text{J}_{\text{H-H}} = 8.0$  Hz,  $\beta$  H of 3pal, 1H), 2.92 (dd,  $^2\text{J}_{\text{H-H}} = 12.0$  Hz,  $^3\text{J}_{\text{H-H}} = 8.0$  Hz,  $\beta'$  H of 3pal, 1H), 1.23 (d,  $^3\text{J}_{\text{H-H}} = 4.0$  Hz,  $\text{CH}_3$  of Ala 3, 3H), 1.16 (d,  $^3\text{J}_{\text{H-H}} = 4.0$  Hz,  $\text{CH}_3$  of Ala 2, 3H), 1.07 (d,  $^3\text{J}_{\text{H-H}} = 4.0$  Hz,  $\text{CH}_3$  of Ala 1, 3H).

### 2.13 *Optimization using temperature and time (general procedure)*

Linear peptide pyta-Ala-Ala-Ala-3Pal (3.5  $\mu\text{mol}$ , 1 eq) was dissolved in 2 mL of distilled water.  $[\text{Re}(\text{CO})_3(\text{OH}_2)_3]\text{OTf}$  (3.2  $\mu\text{mol}$ , 0.9 eq) was added to the reaction mixture. The clear reaction mixture was stirred for 0 - 4 hours at four different temperatures 0 $^\circ$  C, RT, 50 $^\circ$  C, 100 $^\circ$  C. Aliquots (50  $\mu\text{L}$ ) from the reaction mixture were taken after every 30 minutes and diluted with (100  $\mu\text{L}$ ) of Milli Q water. The percentages are obtained by quantification done on the Waters, Inc. Acquity UHPLC.

### 2.14 *Optimization using change of solvent*

Linear peptide pyta-Ala-Ala-Ala-3Pal (3.5  $\mu\text{mol}$ , 1eq) was dissolved in 2 mL of methanol.  $\text{Re}(\text{CO})_3(\text{OH}_2)_3\text{OTf}$  (3.2  $\mu\text{mol}$ , 0.9 eq) was added to the reaction mixture. The clear reaction mixture was stirred for 2 hours at 50 $^\circ$  C. Aliquot (50  $\mu\text{L}$ ) from the reaction mixture were taken at 2-hour time point and diluted with (100  $\mu\text{L}$ ) of Milli Q water and compared with the quantification obtained from reaction using distilled water as a solvent. The percentages are obtained by quantification done on the Waters, Inc. Acquity UHPLC

## 2.15 Optimization by presence of base

Linear peptide pyta-Ala-Ala-Ala-3Pal (3.5  $\mu\text{mol}$ , 1eq) was dissolved in 2 mL of distilled water.  $\text{Re}(\text{CO})_3(\text{OH}_2)_3\text{OTf}$  (3.2  $\mu\text{mol}$ , 0.9 eq) was added to the reaction mixture along with 5M NaOH (17.5  $\mu\text{mol}$ , 5eq) as a base. Reaction was performed at 50° C for 2 hours in presence of a base. Aliquot (50  $\mu\text{L}$ ) from the reaction mixture were taken at 1-hour interval for the 2 hours reaction and diluted with (100  $\mu\text{L}$ ) of Milli Q water and compared with the quantification obtained from reaction carried out in absence of base. The percentages are obtained by quantification done on the Waters, Inc. Acquity UHPLC.

## 2.16 References

- (1) Kumar, A.; Ye, G.; Wang, Y.; Lin, X.; Sun, G.; Parang, K. Synthesis and Structure-Activity Relationships of Linear and Conformationally Constrained Peptide Analogues of CIYKYY as Src Tyrosine Kinase Inhibitors. *J. Med. Chem.* **2006**, *49* (11), 3395–3401. <https://doi.org/10.1021/jm060334k>.
- (2) Di Natale, G.; Grasso, G.; Impellizzeri, G.; La Mendola, D.; Micera, G.; Mihala, N.; Nagy, Z.; Ősz, K.; Pappalardo, G.; Rigó, V.; Rizzarelli, E.; Sanna, D.; Sívágó, I. Copper(II) Interaction with Unstructured Prion Domain Outside the Octarepeat Region: Speciation, Stability, and Binding Details of Copper(II) Complexes with PrP106-126 Peptides. *Inorg. Chem.* **2005**, *44* (20), 7214–7225. <https://doi.org/10.1021/ic050754k>.
- (3) Castle, A. R.; Gill, A. C. Physiological Functions of the Cellular Prion Protein. *Front. Mol. Biosci.* **2017**, *4*, p 19. <https://doi.org/10.3389/fmolb.2017.00019>.
- (4) Simpson, E. J. The Development of Metal-Organic Compounds for Use as Molecular Imaging Agents. **2014**.
- (5) Magnus, K. A.; Hazes, B.; Ton-That, H.; Bonaventura, C.; Bonaventura, J.; Hol, W. G. J. Crystallographic Analysis of Oxygenated and Deoxygenated States of Arthropod Hemocyanin Shows Unusual Differences. *Proteins Struct. Funct. Bioinforma.* **1994**, *19* (4), 302–309. <https://doi.org/10.1002/prot.340190405>.
- (6) El Hage, K.; Hédin, F.; Gupta, P. K.; Meuwly, M.; Karplus, M. Valid Molecular Dynamics Simulations of Human Hemoglobin Require a Surprisingly Large Box Size. *Elife* **2018**, *7*, 35560. <https://doi.org/10.7554/eLife.35560>.
- (7) Holland, D. R.; Hausrath, A. C.; Juers, D.; Matthews, B. W. Structural Analysis of Zinc Substitutions in the Active Site of Thermolysin. *Protein Sci.* **1995**, *4* (10), 1955–1965. <https://doi.org/10.1002/pro.5560041001>.
- (8) Patel, A. The Development of Cyclic RGD Peptides Stabilized Through  $^{99\text{m}}\text{Tc}$  / Re

(CO)<sub>3</sub><sup>+</sup>. **2015**.

- (9) Jones, M. R.; Service, E. L.; Thompson, J. R.; Wang, M. C. P.; Kimsey, I. J.; Detoma, A. S.; Ramamoorthy, A.; Lim, M. H.; Storr, T. Dual-Function Triazole-Pyridine Derivatives as Inhibitors of Metal-Induced Amyloid- $\beta$  Aggregation. *Metallomics* **2012**, *4* (9), 910–920. <https://doi.org/10.1039/c2mt20113e>.
- (10) Pandeewar, M.; Khare, H.; Ramakumar, S.; Govindaraju, T. Crystallographic Insight-Guided Nanoarchitectonics and Conductivity Modulation of an n-Type Organic Semiconductor through Peptide Conjugation. *Chem. Commun.* **2015**, *51* (39), 8315–8318. <https://doi.org/10.1039/c5cc01996f>.
- (11) Boulay, A.; Seridi, A.; Zedde, C.; Ladeira, S.; Picard, C.; Maron, L.; Benoist, E. Tricarbonyl ReI Complexes from Functionalised Pyridine-Triazole Derivatives: From Mononuclear to Unexpected Dimeric Complexes. *Eur. J. Inorg. Chem.* **2010**, No. 32, 5058–5062. <https://doi.org/10.1002/ejic.201000891>.
- (12) Schmidt, S. P.; Nitschke, J.; Trogler, W. C.; Hockett, S. I.; Angelici, R. J. Manganese(I) and Rhenium(I) Pentacarbonyl(Trifluoromethanesulfonato) Complexes; *Inorg Syn* **1989**, *26*, 113-117. <https://doi.org/10.1002/9780470132579.ch20>.

## 3 Chapter Three

### 3 Cyclization of small linear peptides by creating metal foldamers using $^{99m}\text{Tc}/\text{Re}(\text{CO})_3$ core

Short linear peptides having 2-10 amino acids are quite flexible in solution and exist in a fast equilibrium of interconverting conformations.<sup>1</sup> For a biologically active peptide, out of these conformations only a few have a suitable orientation for receptor binding. These short linear peptides tend to lose their bioactive conformation due to their conformational flexibility causing reduced specificity for the target. In addition, short linear peptides have reduced *in vivo* stability due to degradation by proteolytic enzymes. These issues can be combated by various peptidomimetic strategies, one of which is cyclization. Cyclization of these short linear peptides can be envisioned to circumvent the problems by bringing rigidity to the linear structure, thereby forming a limited number of conformations. This results in increased binding affinity and improved stability by producing conformers that are unsusceptible to proteolytic degradation. Cyclization can be brought upon by various techniques like head to tail cyclization, side chain to tail, side chain to side chain cyclization or by metal coordination. In this chapter, the focus is on cyclization induced by metal coordination.

Metals are known to contribute towards the stabilization of protein macromolecular structure.<sup>2</sup> The scope of this chapter is focused on cyclization enabled by the group 7 transition metals rhenium and technetium-99m. Cyclization of linear peptides using the radiometal  $^{99m}\text{Tc}$  would lead to development of a possible SPECT imaging probe, as  $^{99m}\text{Tc}$  is known for its medical imaging properties whereas rhenium, being an analogous group 7 metal, becomes the non-radioactive counterpart. The design of rhenium/technetium-containing diagnostic and therapeutic probes allows the metals to be incorporated into the peptides by two methodologies: the traditional pendant design or the integrated design. The pendant design is one of the most widely used methods of attaching a metal to a peptide, by functionalization of a side chain lysine or a carboxy/amine terminus through a bifunctional chelator. The bifunctional chelator coordinates the metal from one end and is covalently attached to the peptide or targeting entity of interest from the other end (figure 3.1-a). This design places the metal in a position far away from the biological target, which may lead to decreased affinity of the original molecule for the target receptor.<sup>3</sup> On the other hand, the second methodology called the integrated design allows the metal complex to

be incorporated directly into the structure of the biomolecule. This makes the labelling element a critical component of the biologically active region. Integrated design allows cyclization where the metal chelator is present either in the turn region of the peptide (figure 3.1-b) or a chelator is formed at the terminal ends of the peptide through metal coordination (figure 3.1- c). This approach hides the metal core within the ligand framework producing a more stable, compact, low molecular weight chelation system.

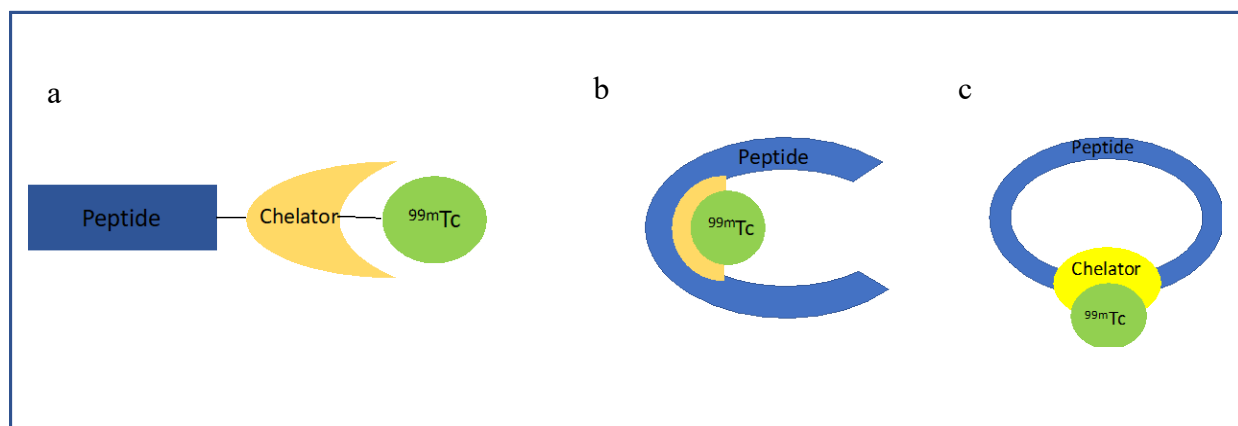


Figure 3.1 a) Pendant design; b-c) Integrated designs

Metal complexes in the form of  $M(\text{CO})_3(\text{H}_2\text{O})_3$  ( $M = \text{Re}, {}^{99\text{m}}\text{Tc}$ ) are attractive organometallic frameworks to be used for chelation with a peptide. This is due to the combined effect of high substitution stability of the CO ligands and lability of water molecules. This allows the substitution of water molecules with different types of monodentate, bidentate and tridentate ligands of different shape, size and different donor atoms.<sup>4</sup> Tridentate chelates have faster clearance and are more stable to substitution in comparison to bidentate  $[{}^{99\text{m}}\text{Tc}(\text{CO})_3]^+$  complexes. However, a bidentate ligand when accompanied by a monodentate ligand shows improved stability and gives rise to a mixed ligand system. This type of mixed ligand system is called a 2+1 chelation system. The 2+1 mixed ligand chelation approach has an advantage of flexibility in structural modifications, high *in vivo* stability and an increased yield of metal complex even at low ligand concentrations ( $10^{-5}$  M). The monodentate ligands can be phosphines (P), isocyanides (CNR) or aromatic amines. The bidentate ligand can be of various donor types which includes (N,O) donors such as 2-picolinic acid,<sup>5</sup> (S,S) donors, such as dithiocarbamate,<sup>6</sup> (P,P) donors, such as biphosphine ligands<sup>7</sup> and (N,N) donors, such as bipyridine<sup>8</sup> (Figure 3.2).

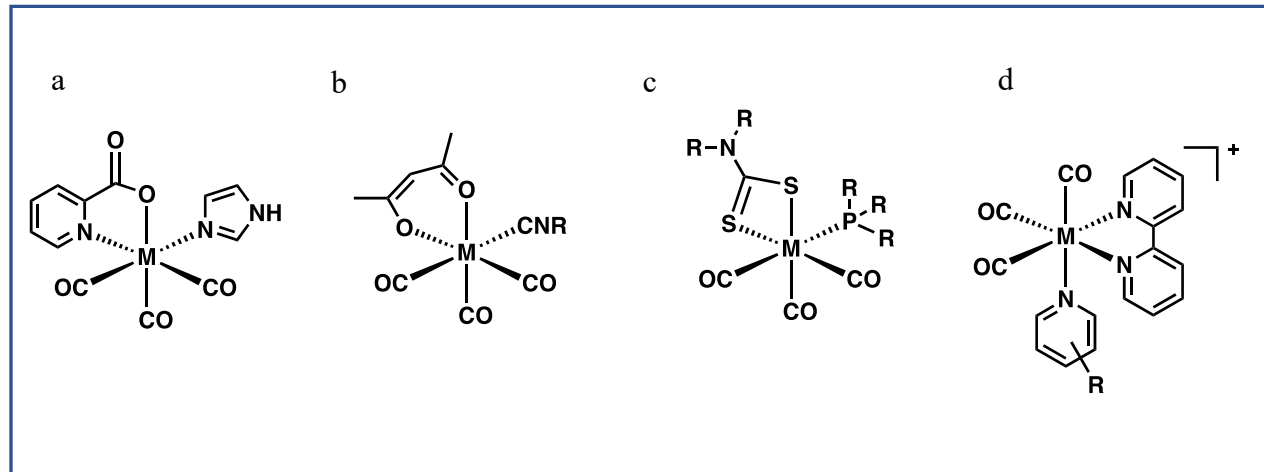


Figure 3.2 Mixed ligand systems having a) N, O bidentate donors; b) O, O donors; c) S, S donors; d) N, N donors.

In recent years, there has been a significant increase in the use of pyridine base ligands as chelators for the  $M(\text{CO})_3^+$  core. Several common examples include 2,2'-bipyridine,<sup>9</sup> picolinic acid,<sup>10</sup> DPA<sup>11</sup> and asymmetrical pyridine base ligands.<sup>7,12,13</sup> Bipyridine has been a widely studied bidentate ligand for metal coordination. It forms a very stable five membered chelate ring with transition metals. Several studies have reported use of bipyridine as a chelator for coordination with rhenium tricarbonyl core.<sup>14,15</sup> Yazdani *et.al* demonstrated the use of 2,2'-bipyridine and imidazole base donors for rhenium tricarbonyl coordination, which led to the development of redox probes and luminescent labels for biomolecules (Figure 3.2-d). The advantage of this 2 + 1 chelation system was the exhibition of broad excitation (350-410 nm) and emission bands (500-700 nm) along with large stokes shift and long lifetimes where an appropriate vector, when attached to either bidentate or monodentate ligand, could lead to the targeting of specific cellular compartments.<sup>8</sup>

In addition to 2,2'- bipyridine, 4-(2-pyridyl)-1,2,3-triazole (pyta) derivatives have garnered increasing attention. This is mainly due to the potent ability of the triazoles to coordinate with various transition metals.<sup>16</sup> A study by Connell *et.al* focused on use of a pyta derivative to coordinate the facial rhenium tricarbonyl core (figure 3.3-a). The ligand was elaborated with a terminal isothiocyanate functional group through both an aromatic and polyethylene glycol spacer. A targeting peptide, arginine–glycine–aspartate (RGD), was conjugated to pyridyl-1,2,3-triazole

bidentate ligands via the isothiocyanate functional group (Figure 3.3-b). The rhenium metal complex of the following compound demonstrated phosphorescence properties which were used in tracking the cellular metabolism and binding affinity of new complexes towards  $\alpha_v\beta_3$  receptor using confocal microscopy.<sup>17</sup>

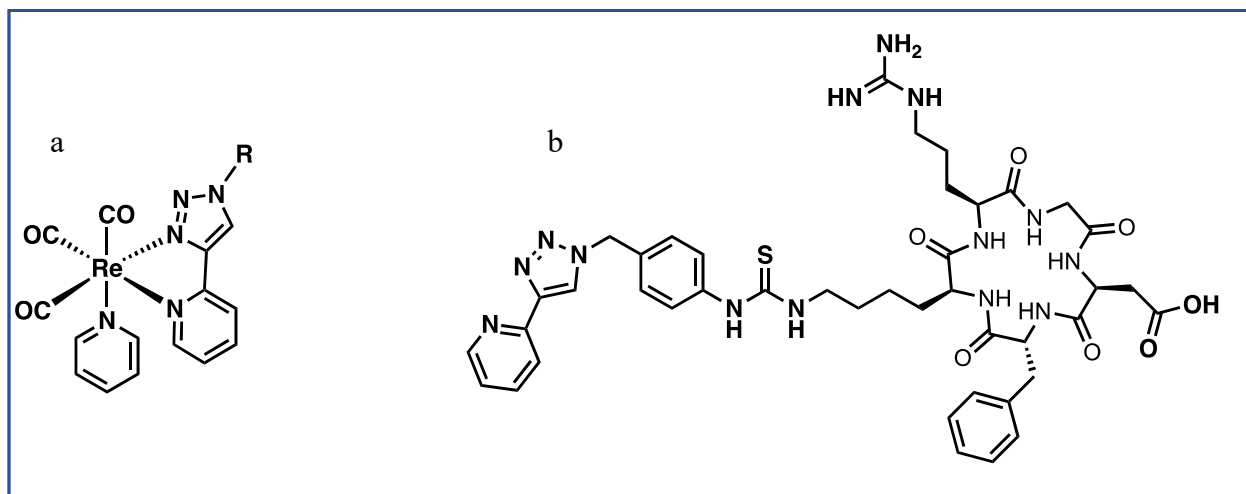


Figure 3.3 a) Rhenium metal complex of isothiocyanate functionalized 4-(2-pyridyl)-1,2,3 triazole and pyridine ligand; b) cyclic cRGDfK conjugate of isothiocyanate functionalized 4-(2-pyridyl)-1,2,3 triazole ligand.

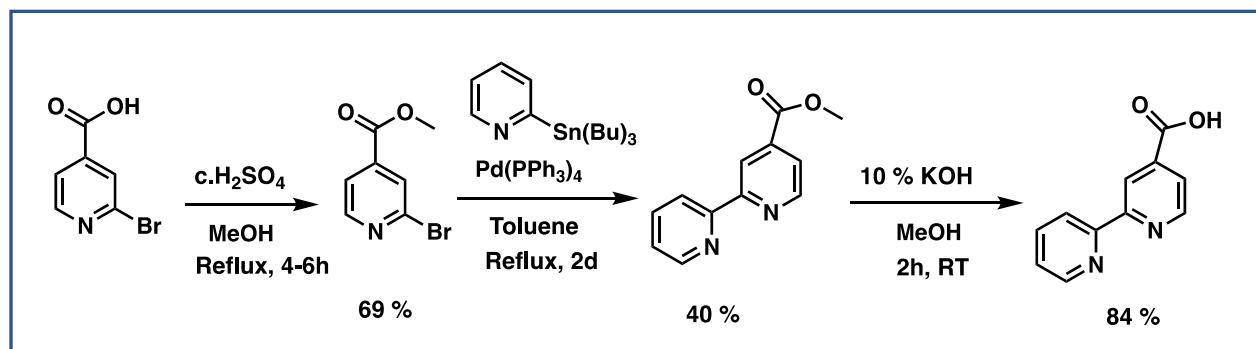
Using this ideology, our project aims to use the bidentate ligands 2,2'-bipyridine and pyridyl triazole along with monodentate pyridine base ligand to cyclize linear peptides in 2+1 chelation fashion. The linear peptides used for the study are the tri-alanine sequence Ala-Ala-Ala and the biologically relevant peptide Arg-Gly-Asp (RGD). The peptide sequence RGD was chosen as it is known to have affinity for  $\alpha_v\beta_3$  which is often overexpressed at tumor sites, including prostate, breast, ovarian, cervical, pancreatic, melanoma, and glioblastoma tumors, whereas the Ala-Ala-Ala peptide sequence is chosen due to its higher propensity to form a helical structure.<sup>18</sup> The model peptide would be studied to demonstrate a turn induced with the aid of the  $M(\text{CO})_3$  core (where  $M = \text{Re}, {}^{99\text{m}}\text{Tc}$ ). Following the study of model tri-alanine peptide sequence, we aim to use  $M(\text{CO})_3$  core to cyclize the biologically relevant peptide sequence RGD and study the effect of cyclization through NMR spectroscopy and mass spectrometry.

### 3.1 Results and Discussion

To investigate the ability of  ${}^{99\text{m}}\text{Tc}/\text{Re}$  tricarbonyl to induce a turn in the linear peptide, we



synthesized linear peptides of sequence Ala-Ala-Ala and the biologically relevant peptide sequence RGD using solid phase peptide synthesis. In addition to pyridyl triazole acetic acid (pyta), a different bidentate ligand, 2,2'-bipyridine-4-carboxylic acid, was synthesized in order to study its ability to coordinate the metal tricarbonyl core. 2,2'-Bipyridine-4-carboxylic acid (Bipyd) was synthesized as shown in the Scheme 3.1.<sup>19</sup>

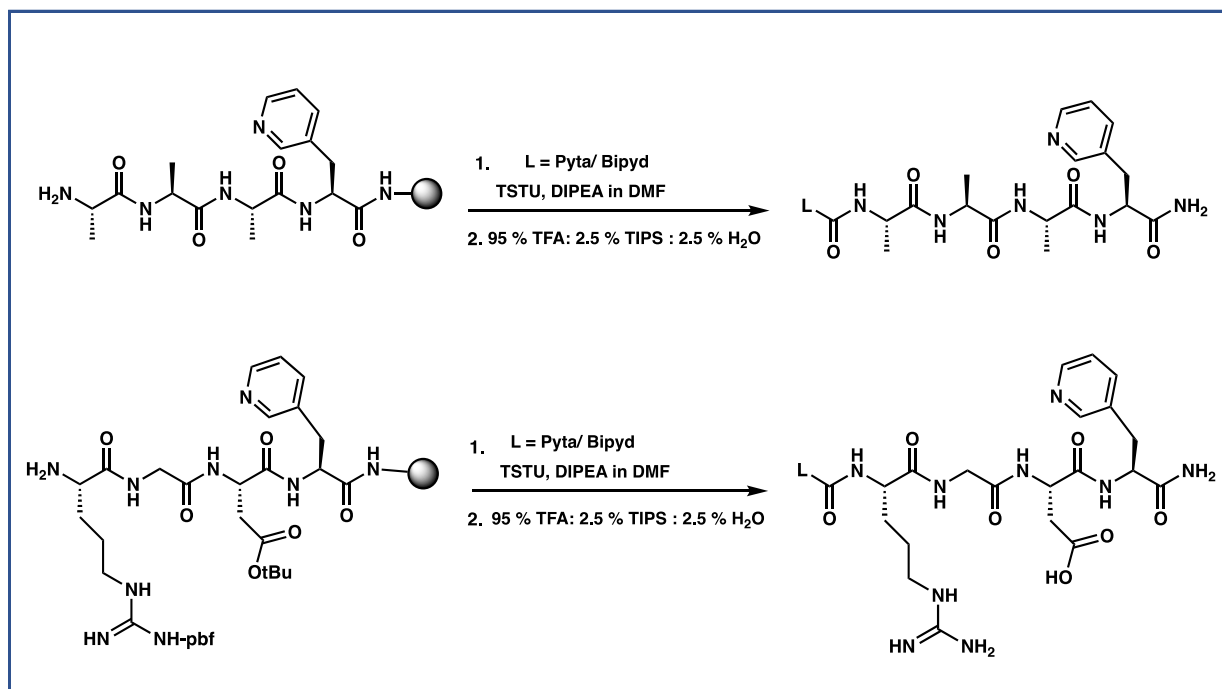


Scheme 3.1 Synthesis of 2,2'-bipyridine-4-carboxylic acid<sup>19</sup>, **8**

Linear peptide sequences pyta-Ala-Ala-Ala-3Pal, pyta-RGD-3Pal, Bipyd-Ala-Ala-Ala-3Pal and Bipyd-RGD-3Pal were synthesized and characterized by NMR spectroscopy and mass spectrometry. The NMR spectroscopy results of the linear peptides would then be used to compare the changes in chemical shifts for amino acids observed on cyclization using the metal tricarbonyl core.

### 3.1.1 Synthesis of linear peptide

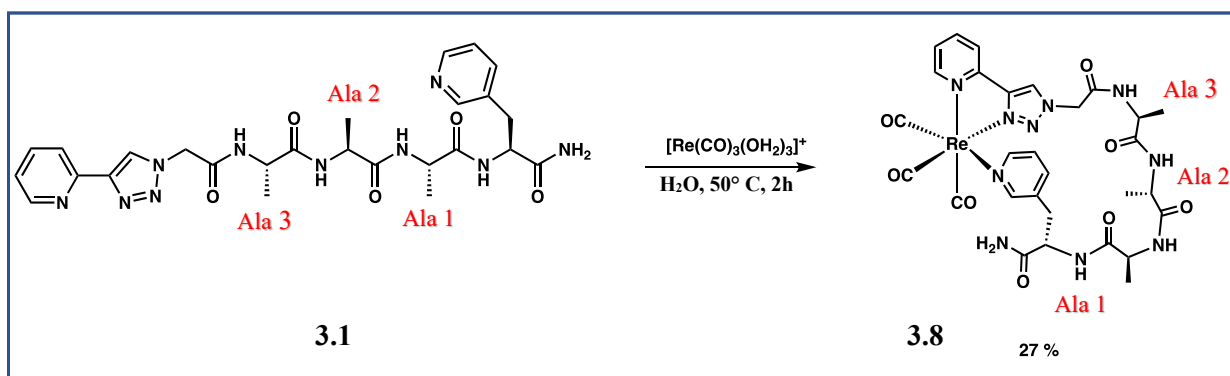
The linear sequences were synthesized by standard Fmoc solid phase peptide synthesis method. Rink amide resin (MBHA) was used as a solid support and the peptide was synthesized from C to N terminus. Each amino acid already had a Fmoc protecting group along with side chains having acid labile protecting groups. After the removal of the Fmoc, amino acid was vortexed with the coupling agent, base in DMF prior to coupling with another amino acid. The N-terminus was coupled with the ligand pyridyl triazole (pyta) and 2,2'-bipyridine-4-carboxylic acid (Bipyd) respectively. Removal of all protecting groups and cleaving of the resin was performed using cleavage cocktail (Scheme 3.2). The peptide was precipitated with cold *tert*-butyl methyl ether (TBME), centrifuged, filtered and lyophilized to give crude linear peptide of the desired sequence. The crude linear peptide was then purified by RP-HPLC to give a purity of > 95%



Scheme 3.2 Synthesis of linear peptide sequences **3.1**, **3.2**, **3.6**, **3.7** using Fmoc strategy

### 3.1.1.1 Cyclization of peptide sequence pyta-Ala-Ala-Ala-3Pal using $[\text{Re}(\text{CO})_3(\text{OH}_2)_3]^+$ , **3.8**

The linear peptide pyta-Ala-Ala-Ala-3Pal, (**3.1**) was coordinated to the rhenium tricarbonyl triaqua  $[\text{Re}(\text{CO})_3(\text{H}_2\text{O})_3]\text{OTf}$  complex where the  $[\text{Re}(\text{CO})_3(\text{H}_2\text{O})_3]\text{OTf}$  complex was synthesized following the method reported by Schmidt *et.al*, by using commercially available bromopentacarbonyl rhenium (I),  $\text{Re}(\text{CO})_5\text{Br}$ .<sup>20</sup> The coordination was done in distilled water at 50°C for 2 hours (Scheme 3.3).



Scheme 3.3 Rhenium coordination of linear peptide pyta-Ala-Ala-Ala-3Pal, **3.1**

Upon coordination, three conformers for rhenium coordinated product were observed. The reaction conditions allowed the formation of one conformer in higher yield in comparison to the other two conformers (Figure 3.4). RP-preparative HPLC did not allow complete separation of the two later eluting conformers due to their proximity to each other, however, the dominant conformer was separated. While, all three conformers show identical product  $m/z$  values, it remains possible that the later eluting products are dimers. However, this requires additional investigation.

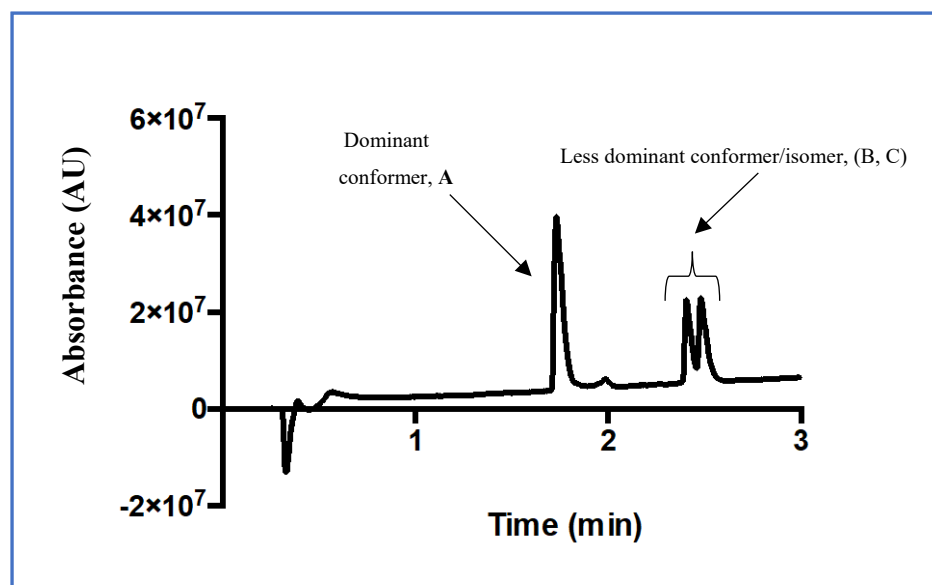


Figure 3.4 UHPLC chromatogram of the cyclic peptide  $\text{Re}(\text{CO})_3[\text{Pyta-Ala-Ala-Ala-3Pal}]$ , **3.8**

Acetonitrile is a remarkable coordinating solvent and in acidic conditions it appears that some of monodentate chelator was replaced by the solvent while passing through the HPLC column. It was observed during the purification of the cyclic peptide using HPLC, acetonitrile adducts of the

cyclic peptide were formed. In contrast, no such issues were encountered when acetonitrile was replaced with methanol as an eluent. Thus, to avoid the formation of the acetonitrile adducts, an eluent system of methanol-water was used for the HPLC purification of the cyclic peptide leading to the isolation of the predominant cyclic peptide with a purity of 96.5%.

### NMR spectroscopic studies of the linear peptide, **3.1** and cyclic peptide, **3.8**

The linear and cyclic peptides were characterized using  $^1\text{H}$  NMR spectroscopy. An overlapping of peaks is seen in the aromatic region of the linear peptide. However, it is observed that cyclization of the linear peptide led to the separation of the peaks. Figure 3.5 shows the aromatic region from the NMR spectra for both the linear and cyclic peptide.

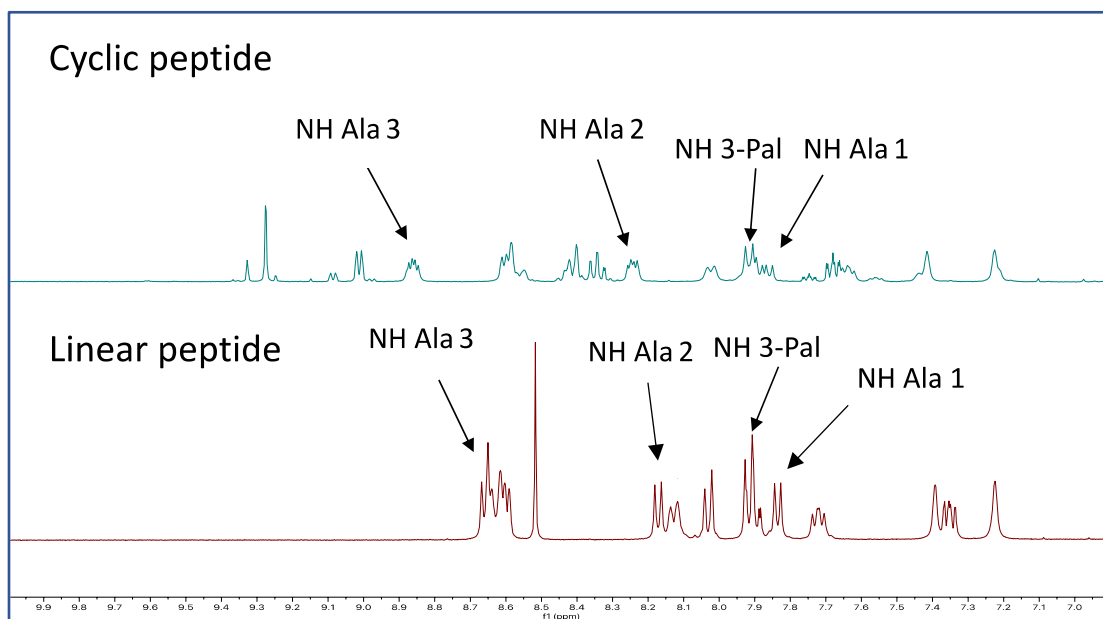


Figure 3.5 Aromatic region from  $^1\text{H}$  NMR spectra of cyclic (**3.8**) and linear peptide (**3.1**)

### 2D- NMR spectroscopic characterization of cyclic peptide, **3.8**

For identification of the individual amino acids, we characterized the linear and cyclic peptides using COSY and NOESY NMR spectroscopy. Shown below is the COSY NMR spectra for the cyclic peptide **3.8** (Figure 3.6). COSY NMR spectra was used by us to observe the correlation of the  $\text{CH}_3$  protons peaks to the neighboring  $\alpha$  CH proton and then to the respective NH proton. This

led to the identification of the individual CH<sub>3</sub>, NH and  $\alpha$  CH protons of each amino acid in the peptide sequence.

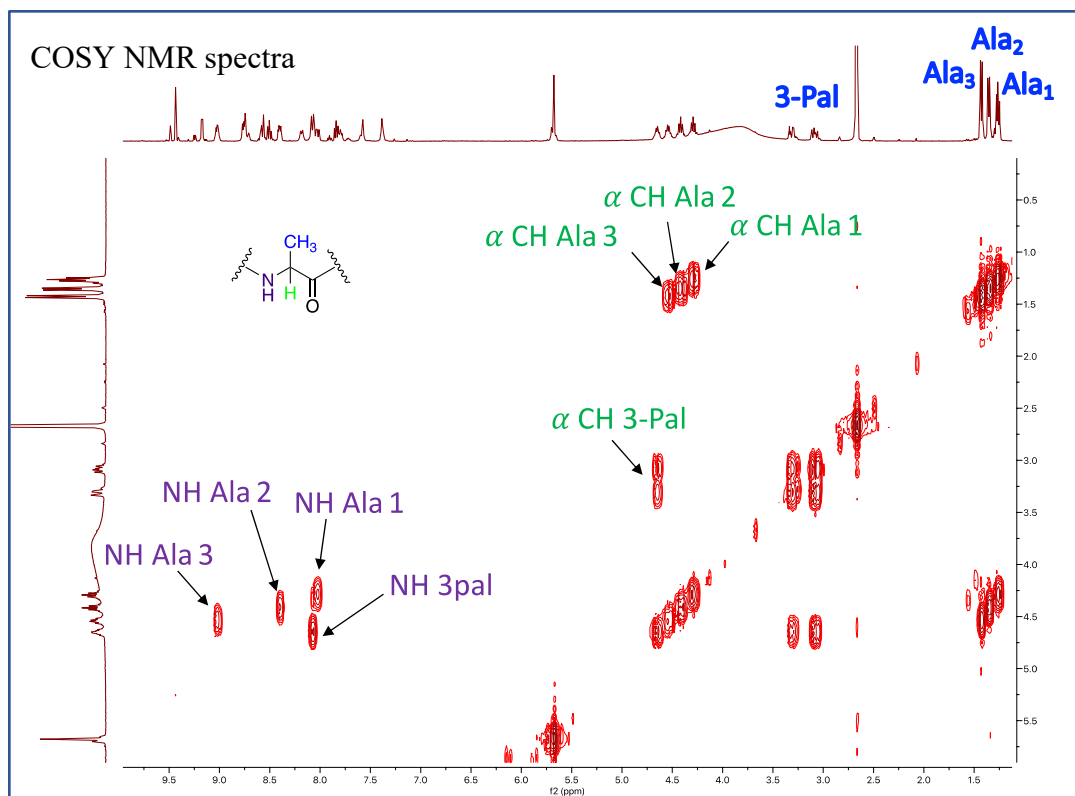


Figure 3.6 COSY NMR spectra of cyclic peptide **3.8**, in DMSO-d<sub>6</sub> at 400 MHz

In order to identify the position of each amino acid in the peptide sequence, we characterized the cyclic peptide, **3.8** using NOESY NMR spectroscopy. Correlation between amide NH protons and  $\alpha$  CH protons of the spatially adjacent amino acids was observed. Using this information, we identified the position of individual amino acids in the peptide sequence and were able to illustrate the structure of the cyclic peptide, **3.8** (Figure 3.7). All the synthesized linear and cyclic peptides were characterized by <sup>1</sup>H, 2D COSY and NOESY NMR spectroscopy in a similar manner.

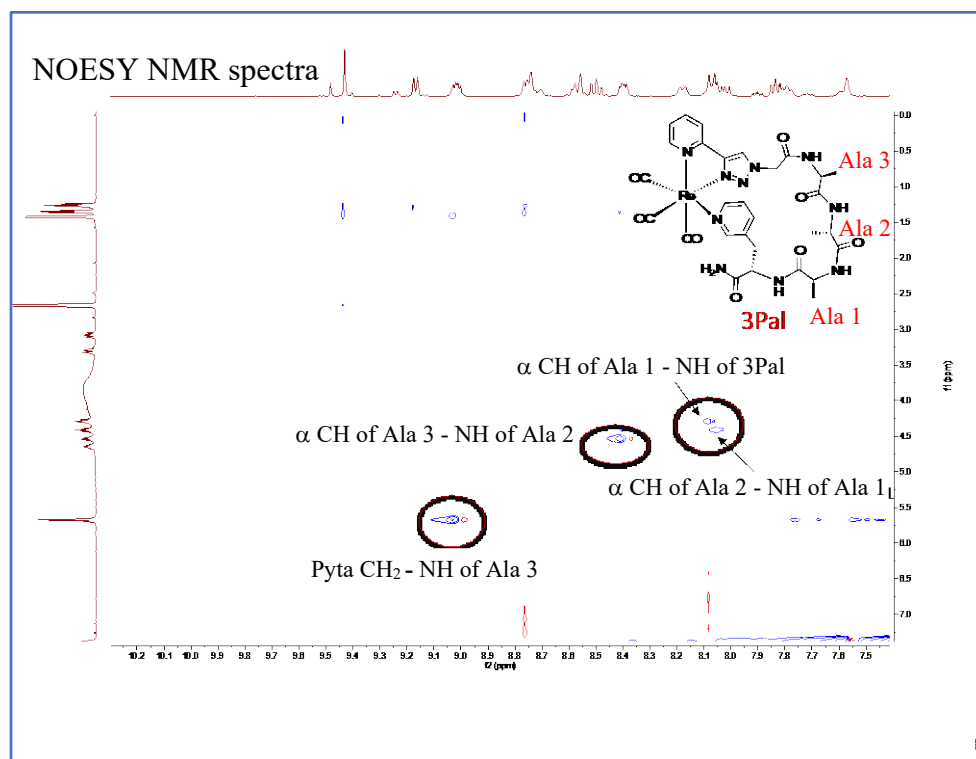


Figure 3.7 NOESY NMR spectra of cyclic peptide **3.8**, in DMSO- $d_6$  at 400 MHz

The slight change in chemical shift before and after cyclization of the peptide is shown in the table 3.1

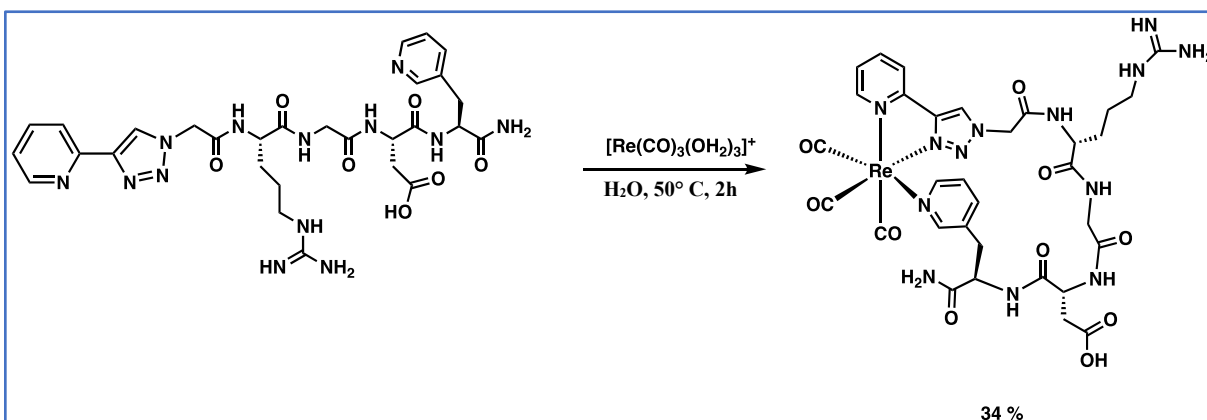
Table 3.1 Amino acids proton shifts (ppm) of the linear peptide Pyta-AAA-3-Pal-NH<sub>2</sub>, **3.1** and rhenium coordinated peptide, **3.8**

Amino acid	Pyta-Ala-Ala-Ala-3Pal			Re(CO) <sub>3</sub> Pyta-Ala-Ala-Ala-3Pal		
	CH <sub>3</sub>	$\alpha$ CH	NH	CH <sub>3</sub>	$\alpha$ CH	NH
Alanine 1	1.07	4.10	7.84	1.10	4.12	7.86
Alanine 2	1.16	4.22	8.17	1.19	4.25	8.24
Alanine 3	1.23	4.34	8.67	1.26	4.36	8.86
3-Pal	3.05, 3.03	4.49	7.93	3.06, 3.04	4.46	7.92

A downfield shift was seen for the amide protons of the three alanine, on comparing the chemical shifts between linear and cyclic peptide. However, a slight upfield shift for amide proton of 3-Pal was observed. Cyclization of the linear peptide deshielded the methyl protons of all three alanine, which can be observed from the difference in their chemical shift. Methylene protons of 3-Pal showed a slight upfield shift on cyclization. All  $\alpha$  CH protons show a downfield shift except the  $\alpha$  CH proton of 3-pyridyl alanine, where an upfield shift is observed. The  $\alpha$  CH protons of 3-pyridyl alanine shows up field shift which may be due to its close proximity to the metal. This proves that 3-Pal is coordinated to metal in monodentate fashion. The distereotopic protons of pyta were equivalent in the linear form of the peptide and had a singlet pattern. However, these protons no longer showcase a singlet pattern on cyclization. This might be due to the restriction in flexibility induced by the metal upon cyclization which makes the two protons non-equivalent. This shows that the ligand has coordinated the metal in a bidentate fashion

### 3.1.1.2 Cyclization of peptide sequence pyta-RGD-3Pal using $[\text{Re}(\text{CO})_3(\text{OH}_2)_3]^+$ , **3.9**

The linear peptide pyta-Arg-Gly-Asp-3Pal was coordinated to the rhenium tricarbonyl triaqua  $[\text{Re}(\text{CO})_3(\text{H}_2\text{O})_3]\text{OTf}$  complex in a similar method as mentioned for **3.8** (Scheme 3.4). Upon analysis by LCMS, three conformers of the cyclic peptide were seen. Purification was done using reverse phase HPLC and the cyclic products were isolated with a collective purity of >99% for the coordinated peptides.



Scheme 3.4 Rhenium coordination of linear peptide pyta-RGD-3Pal, **3.2**

Table 3.2 Chemical shifts for the amino acids in the linear **3.2**, and cyclic peptide Pyta-RGD-3Pal, **3.9**

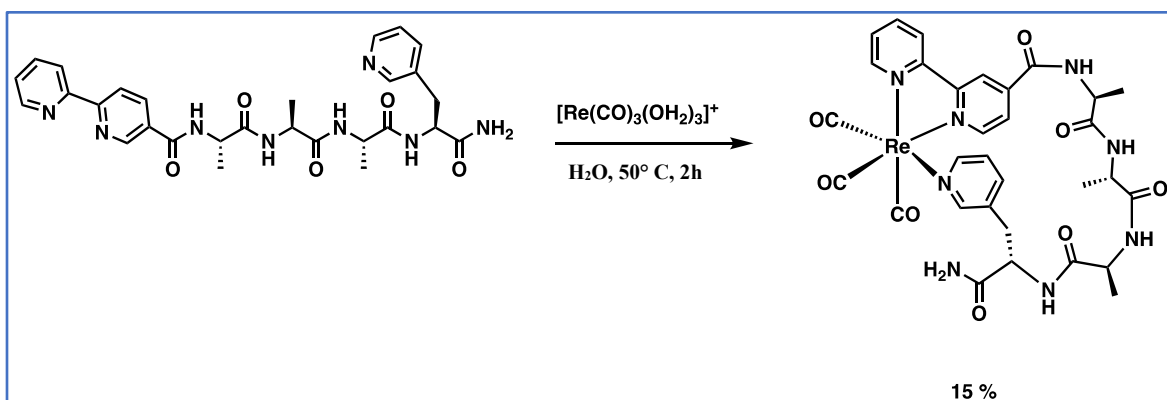
Amino acid	Pyta-RGD-3Pal			Re(CO) <sub>3</sub> Pyta-RGD-3Pal		
	βCH <sub>2</sub>	α CH	NH	βCH <sub>2</sub>	α CH	NH
Arginine	1.75, 1.62	4.40	8.72	1.75, 1.63	4.40	8.88
Glycine	-	3.74	8.42	-	3.74	8.45
Aspartic acid	2.62, 2.42	4.49	8.22	2.62, 2.42	4.52	8.22
3-Pal	3.20, 2.94	4.47	8.07	3.20, 2.95	4.47	8.07

It is interesting to see that the on cyclization, only the amide protons of for arginine and glycine show downfield shifts whereas there is no change seen for aspartic acid and 3-Pal. Similar to **3.8**, separation of the peaks can be seen once the linear peptide is coordinated.

### 3.1.1.3 Cyclization of peptide sequence Bipyd-Ala-Ala-Ala-3Pal using [Re(CO)<sub>3</sub>(OH<sub>2</sub>)<sub>3</sub>]<sup>+</sup>, **3.13**

The conditions for coordinating the linear peptide Bipyd-Ala-Ala-Ala-3Pal with rhenium tricarbonyl triaqua [Re(CO)<sub>3</sub>(H<sub>2</sub>O)<sub>3</sub>]OTf complex were kept similar except for the slight change in time and temperature (Scheme 3.5). The reaction was extended, with stirring for 4 hours at 60° C. Upon analysis by LCMS, two conformers of the cyclic peptide were seen. Purification was done using reverse phase HPLC and the cyclic products were isolated with a collective purity of > 99% for the coordinated peptides





Scheme 3.5 Rhenium coordination of linear peptide Bipyd-Ala-Ala-Ala-3Pal, **3.6**

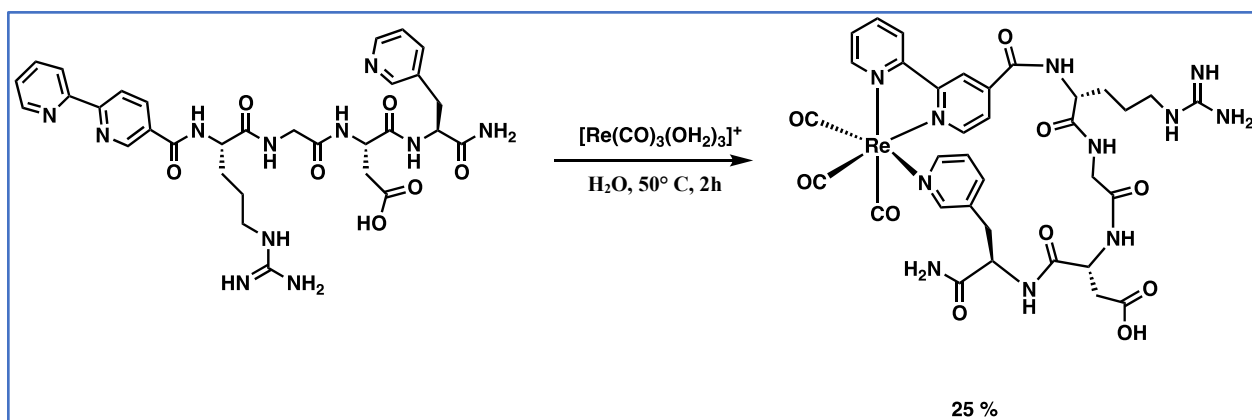
Table 3.3 Chemical shifts for the amino acids in the linear **3.6**, and cyclic peptide Bipyd-Ala-Ala-Ala-3Pal, **3.13**

Amino acid	Bipyd-Ala-Ala-Ala-3Pal			Re(CO) <sub>3</sub> Bipyd-Ala-Ala-Ala-3Pal		
	CH <sub>3</sub>	α CH	NH	CH <sub>3</sub>	α CH	NH
Alanine 1	1.14	4.13	7.88	1.14	4.15	7.89
Alanine 2	1.20	4.26	8.16	1.21	4.27	8.27
Alanine 3	1.37	4.49	9.06	1.39	4.56	9.24
3-Pal	3.10, 3.09	4.53	7.96	3.04, 3.05	4.49	7.94

Similar to **3.8**, there was a downfield shift observed for the α CH protons for all the amino acids except for the 3-pyridyl alanine. 3-Pal being close to the rhenium metal core shows an upfield shift which proves the hypothesis that it is coordinating the metal in monodentate fashion. It is quite interesting to observe that the amide protons for all the amino acids except 3-Pal show downfield shift upon cyclization.

### 3.1.1.4 Cyclization of peptide sequence Bipyd-Arg-Gly-Asp-3Pal using $[\text{Re}(\text{CO})_3(\text{OH}_2)_3]^+$ , **3.14**

The linear peptide Bipyd-Arg-Gly-Asp-3Pal was coordinated to the rhenium tricarbonyl triaqua  $[\text{Re}(\text{CO})_3(\text{H}_2\text{O})_3]\text{OTf}$  complex in a similar method as mentioned for **3.13** (Scheme 3.6). Upon analysis by LCMS, two conformers of the cyclic peptide were seen. Purification was done using reverse phase HPLC and the cyclic products were isolated with a collective purity of >99% for the coordinated peptides. Characterization using  $^1\text{H}$  NMR, 2D g-COSY and NOESY NMR spectroscopy gave results mentioned in the table 3.4.



Scheme 3.6 Rhenium coordination of linear peptide Bipyd-RGD-3Pal, **3.7**

Table 3.4 Chemical shifts for the amino acids in the linear **3.7**, and cyclic peptide Bipyd-RGD-3Pal, **3.14**

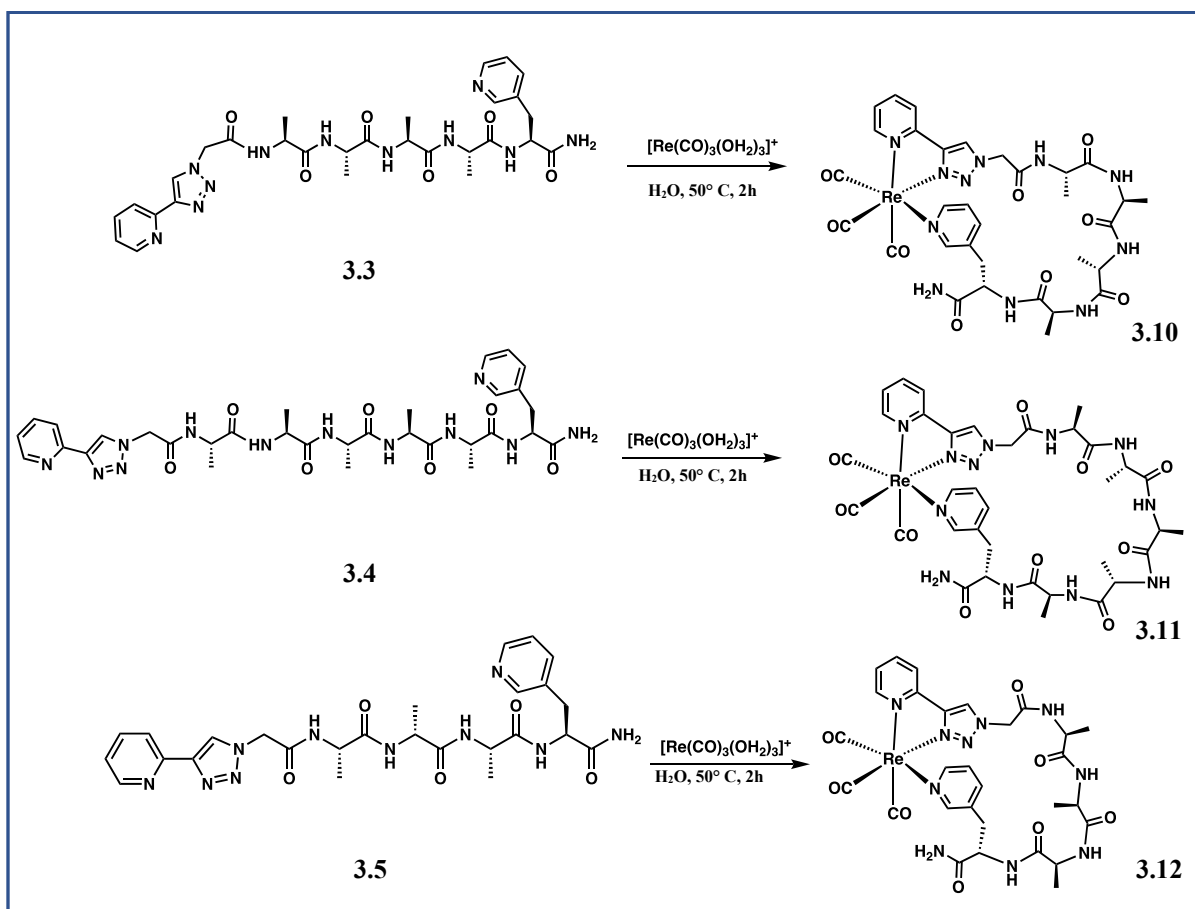
Amino acid	Bipyd-RGD-3Pal			$\text{Re}(\text{CO})_3\text{Bipyd-RGD-3Pal}$		
	$\beta\text{CH}_2$	$\alpha$ CH	NH	$\beta\text{CH}_2$	$\alpha$ CH	NH
Arginine	1.83, 1.77	4.56	9.11	1.81-1.71	4.59	9.32
Glycine	-	3.74	8.40	-	3.76	8.51
Aspartic acid	2.65, 2.44	4.51	8.10	2.65, 2.45	4.52	8.18
3-Pal	3.21, 2.95	4.48	8.10	3.15, 2.91	4.44	8.05

Interesting observations were made on comparing the NMR spectra of the linear and cyclic peptide. A downfield shift is observed in the chemical shift of amide protons for all the amino acids except for 3-Pal. A similar trend is also seen in the chemical shifts of the  $\alpha$  CH proton where, except for 3-Pal, the other amino acids show a slight downfield shift.

## 3.2 Optimization of peptide sequence length

It was observed that despite of carrying out the coordination reaction at conditions to give an optimal yield, not all of the linear peptide was converted into cyclic peptide. The length of the linear peptide might be affecting its flexibility in creating a turn around the metal core. In order to study the effect of the peptide length on the coordination reaction, we synthesized a series of model peptides with increasing peptide length. The peptide sequences synthesized were pyta-Ala-Ala-Ala-Ala-3Pal, pyta-Ala-Ala-Ala-Ala-Ala-3Pal with an increased length to 6 and 7 amino acids respectively. Another chosen peptide sequence was pyta-Ala-D-Ala-Ala-3Pal where the amino acid in the center is a D-amino acid instead of the natural L-amino acid. D- amino acids are known to aid in cyclization by conformational preorganization. All of the three peptides were coordinated to the rhenium tricarbonyl core (Scheme 3.7) and were quantified by analytical UHPLC.

It was assumed that as the length of the peptide would increase, the ease of cyclization would give an increased yield of cyclic product. However, as the number of alanine amino acid increased in the linear sequence, the solubility of the peptide in water was affected. This is due to hydrophobic nature of the methyl group present as a side chain on alanine. Out of the three peptides synthesized, only pyta-Ala-Ala-Ala-Ala-3Pal gave a considerable yield on cyclization. Thus, pyta-Ala-Ala-Ala-Ala-3Pal was used for further studies along with the pentapeptide sequences.



Scheme 3.7 Cyclization reaction of linear peptide sequences with varying length, (3.3 - 3.5)

### 3.3 Variable temperature NMR studies

VT NMR spectroscopy is one of the most common methods used for studying intramolecular hydrogen bonds.<sup>21</sup> There is a strong dependence of the amide protons chemical shift on temperature. Increasing temperature causes an upfield shift in amide protons; however, if the proton is hydrogen bonded, the shift is considerably less. The chemical shifts of amide protons involved in intramolecular hydrogen bonding will not be as sensitive to changes in temperature in contrast to those that are not hydrogen bonded or are intermolecularly hydrogen bonded to the surrounding solvent. This can be tracked quantitatively by dividing the change in shift over the change in temperature ( $\Delta\delta/\Delta T$ ).  $\Delta\delta/\Delta T$  values that are more positive than  $-4.6 \text{ ppbK}^{-1}$  correspond to protons that are involved in intramolecular hydrogen bonding<sup>22</sup>. Thus, the amide peaks were assigned to individual amino acids using g-COSY and NOESY NMR spectroscopy. These peaks were then observed at increasing temperature to determine which of them displays intramolecular hydrogen bonding.

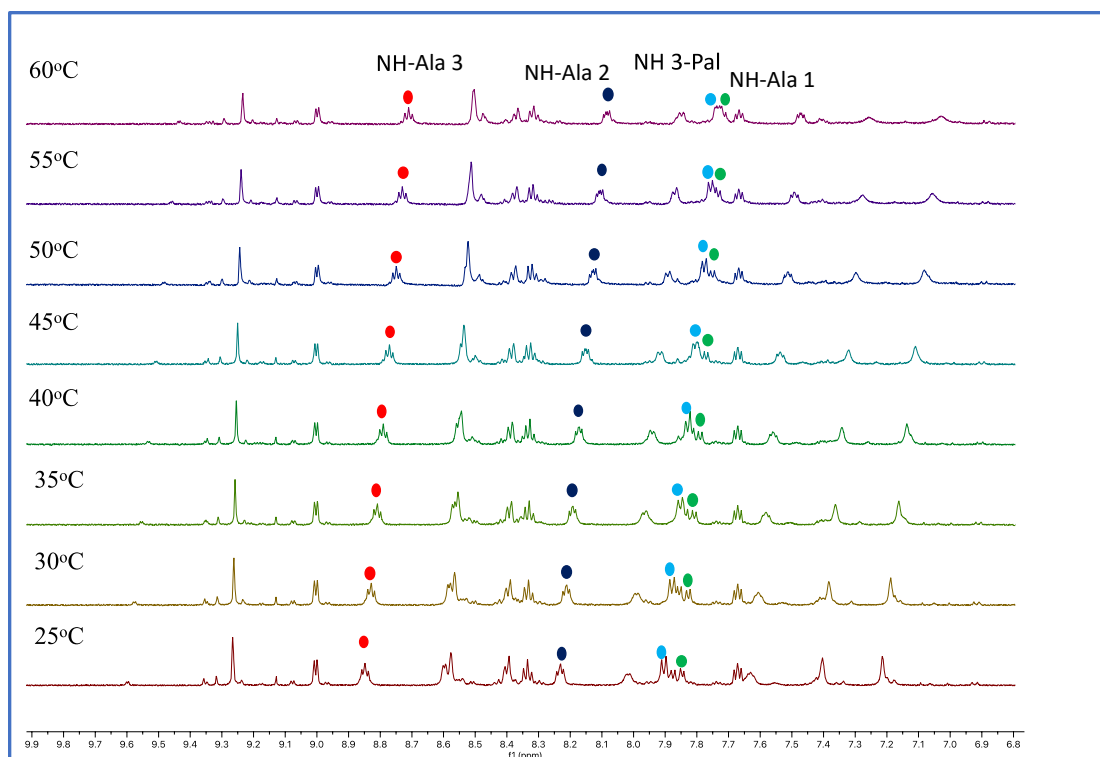


Figure 3.8 VT  $^1\text{H}$  NMR spectra of coordinated peptide **3.8** in  $\text{DMSO-d}_6$  at  $5^\circ\text{C}$  intervals from  $25-60^\circ\text{C}$  at 600 MHz

VT NMR spectroscopy studies were performed on the coordinated peptides in dimethylsulfoxide- $\text{d}_6$  ( $\text{DMSO-d}_6$ ) from  $25-60^\circ\text{C}$  at  $5^\circ\text{C}$  intervals. As the temperature increases, a difference in the magnitude of the change in shift can be seen for each individual proton. When the chemical shifts were converted to numerical values, all the amide bonds except 3-Pal were present in the range of  $0 \geq \Delta\delta/\Delta T \geq -4.6 \text{ ppbK}^{-1}$ , indicating that hydrogen bonding exists within the peptide backbone. 3-Pal showing the value of  $-4.85 \text{ ppbK}^{-1}$  might not be involved in hydrogen bonding. Figure 3.8 shows the superimposed series of  $^1\text{H}$  NMR spectra for **3.8**, obtained at increasing temperature.

Table 3.5 The  $\Delta\delta/\Delta T$  values obtained from the VT  $^1\text{H}$  NMR spectra analysis for each amide proton in peptide **3.8**

$\Delta\delta/\Delta T$ (ppb/K)			
Ala 1 NH	Ala 2 NH	Ala 3 NH	3-Pal NH
- 3.71	- 4.28	- 3.71	- 4.85

### Re(CO)<sub>3</sub>[Pyta-RGD-3Pal], (3.9)

Variable temperature interpretations were done for peptide Re(CO)<sub>3</sub>[Pyta-RGD-3Pal] in a similar manner to **3.8**. The values from VT <sup>1</sup>H NMR spectra suggest that except 3-Pal, all the other three amino acids are involved in intramolecular hydrogen bonding.

Table 3.6 The  $\Delta\delta/\Delta T$  values obtained from the VT <sup>1</sup>H NMR spectra analysis for each amide proton in peptide **3.9**

$\Delta\delta/\Delta T$ (ppb/K)			
Arg NH	Gly NH	Asp NH	3-pal NH
-3.71	- 4.28	-3.14	-6.0

### Re(CO)<sub>3</sub>[Pyta-AAAA-3Pal], 3.10

Variable temperature interpretations were done for peptide Re(CO)<sub>3</sub>[Pyta-AAAA-3Pal] in a similar manner to **3.8** and are presented in the table 3.7. The values from VT NMR spectra suggest that all the amino acids are involved in intramolecular hydrogen bonding. Due to the presence of the amide bonds of Ala 1, Ala 2 and 3-Pal as one multiplet, it was difficult to interpret the chemical shifts individually.

Table 3.7 The  $\Delta\delta/\Delta T$  values obtained from the VT <sup>1</sup>H NMR spectra analysis for each amide proton in peptide **3.10**

$\Delta\delta/\Delta T$ (ppb/K)		
Ala 1/ Ala 2 / 3-pal NH	Ala 3 NH	Ala 4 NH
-3.71	- 4.28	-3.4

Re(CO)<sub>3</sub>[Bipyd-AAA-3Pal], **3.13**

The values from VT NMR suggest that all the amino acids except 3-pyridyl alanine, are involved in intramolecular hydrogen bonding. Figure 3.9 shows the superimposed series of <sup>1</sup>H NMR spectra obtained at increasing temperature.

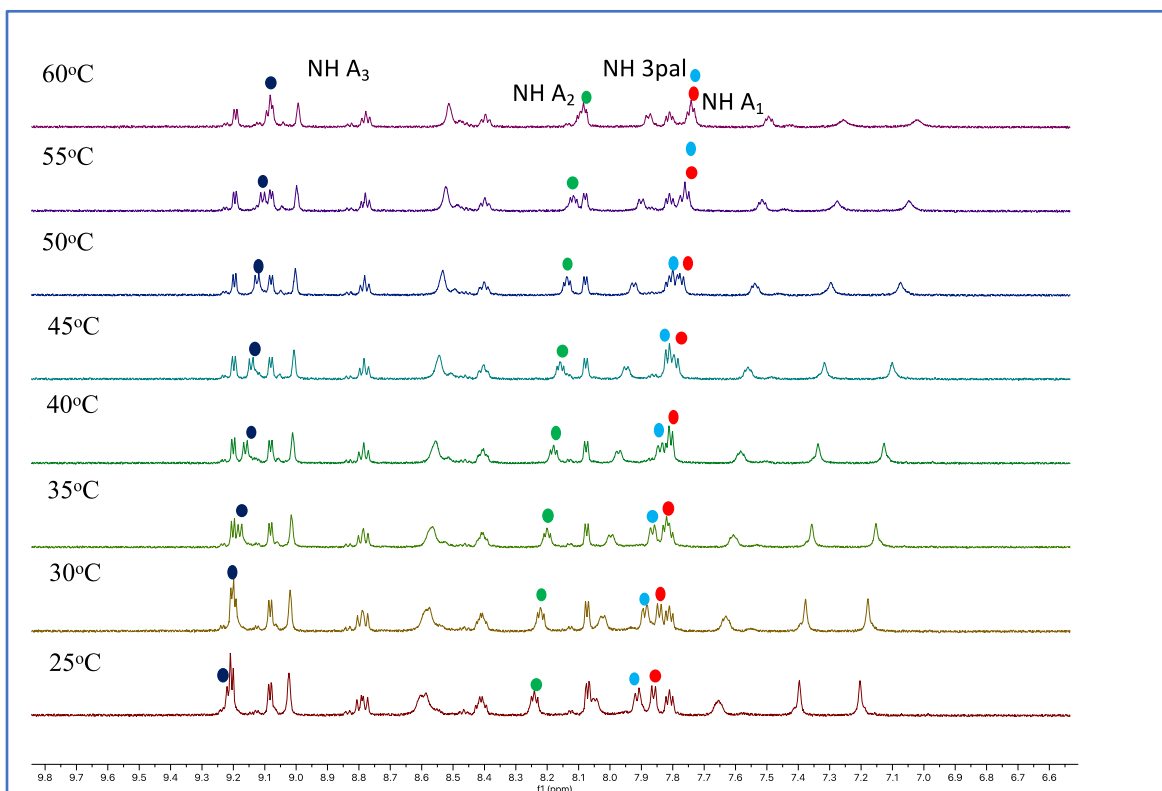


Figure 3.9 VT <sup>1</sup>H NMR spectra of coordinated peptide 3.13 in DMSO-d<sub>6</sub> at 5°C intervals from 25-60°C at 600 MHz

Table 3.8 The  $\Delta\delta/\Delta T$  values obtained from the VT <sup>1</sup>H NMR analysis for each amide proton in peptide **3.13**

$\Delta\delta/\Delta T$ (ppb/K)			
A <sub>1</sub> NH	A <sub>2</sub> NH	A <sub>3</sub> NH	3-Pal NH
-3.14	-4.28	-3.71	-4.85

## Re(CO)<sub>3</sub>[Bipyd-RGD-3Pal], **3.14**

The values from VT NMR suggest that all the amino acids except for 3-pyridyl alanine, are involved in intramolecular hydrogen bonding. The interpretations from the variable temperature NMR are presented in the tabular form (Table 3.9).

Table 3.9 The  $\Delta\delta/\Delta T$  values obtained from the VT <sup>1</sup>H NMR analysis for each amide proton in peptide **3.14**

$\Delta\delta/\Delta T$ (ppb/K)			
Arg NH	Gly NH	Asp NH	3-Pal NH
-3.14	- 2.00	-3.14	-5.71

## 3.4 Circular Dichroism Spectroscopy

Circular dichroism (CD) is a chiroptical method used to analyze chiral molecules like peptides, proteins, nucleic acids, oligo- and polysaccharides. It is a widely used technique to determine the secondary structure and can differentiate between a random coil (linear peptide) and an ordered structure (cyclic peptide).<sup>23,24</sup> All the linear and cyclic peptides were analyzed by CD spectroscopy. The figure 3.8 presents the graphs of mean residue ellipticity vs wavelength for all the linear and cyclic peptides.



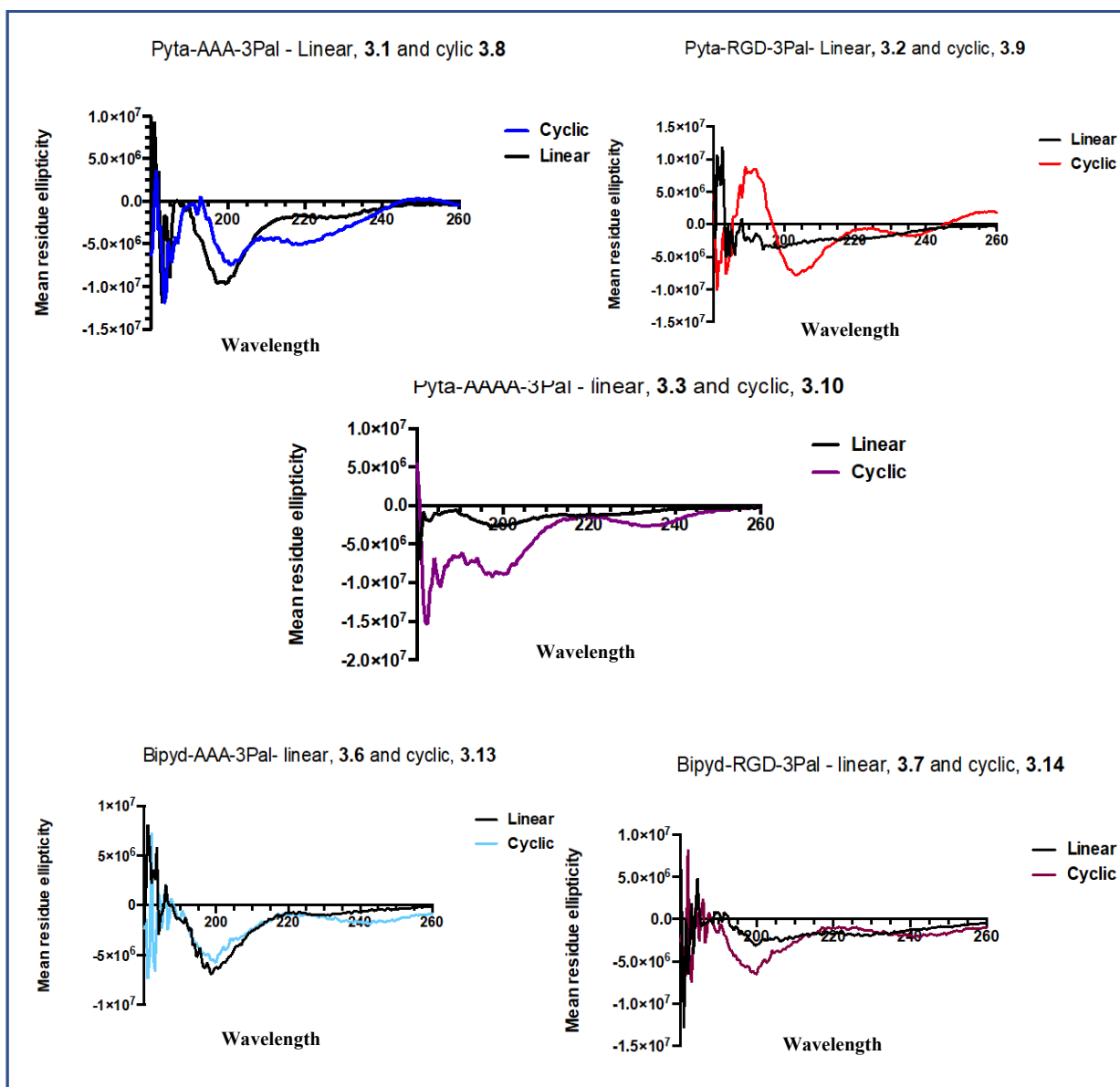


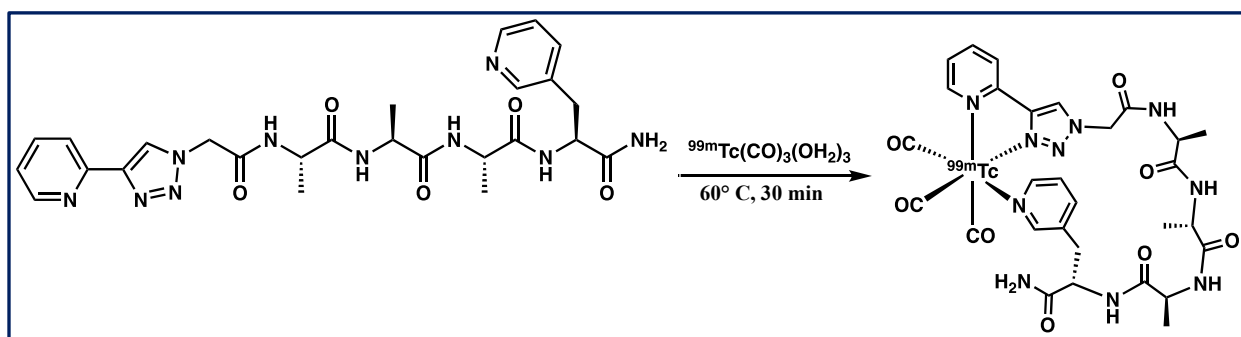
Figure 3.10 CD spectroscopy for the linear (3.1, 3.2, 3.3, 3.6, 3.7) and cyclic peptides, (3.8, 3.9, 3.10, 3.13, 3.14) in MilliQ water at a concentration of 0.25 mg/mL

It is quite interesting to see a change in conformation taking place when the peptide is coordinated to the metal core using the ligand pyridyl triazole acetic acid (pyta). However, the same sequences used with another ligand 2,2'-bipyridine-4-carboxylic acid do not show much change in conformation. The linear peptides (random coil) show a strong minima at 200 nm, a characteristic signal for a random coil, whereas alpha-helical structures usually show two minima at 208 and 222

nm.<sup>25</sup> The cyclic peptide sequence **3.8** shows a two minima at 202 nm and 220 nm along with a maxima at 212 nm and 250 nm. A similar change in conformation is also seen for peptide **3.9**, where the graph shows the presence of two minima at 205 nm and 235 nm along with two maxima at 220 and 260 nm. Peptide **3.10** shows similar minima at 200 and 235 nm along with one maxima at 215 nm. Significant difference seen in the conformation suggests that a turn is induced by the metal upon cyclization of the linear peptide and that peptides **3.8**, **3.9**, **3.10** appear to resemble that of a helical peptide structure.

### 3.5 <sup>99m</sup>Tc labelling of linear peptide pyta-Ala-Ala-Ala-3pal

The linear peptide, pyta-AAA-3Pal-NH<sub>2</sub>, was labelled with technetium-99m to provide <sup>99m</sup>Tc coordinated peptide, [<sup>99m</sup>Tc(CO)<sub>3</sub>(pyta-AAA-3Pal-NH<sub>2</sub>)] (Scheme 3.8). The pertechnetate was added to the isolink kit following the microwave reaction conditions reported by Pitchumony *et al.* which resulted in [<sup>99m</sup>Tc(CO)<sub>3</sub>(OH<sub>2</sub>)<sub>3</sub>]<sup>+</sup>.<sup>9</sup>



Scheme 3.8 <sup>99m</sup>Tc labelling of Pyta-AAA-3Pal, **3.15**

The reduced <sup>99m</sup>Tc was reacted with the linear peptide, producing the radiolabelled peptide. Both technetium and rhenium belong to group 7 and thus it is assumed that they will behave in a similar chemical manner. However, it was quite unique to observe that instead of forming the dominant cyclic product that was observed in the case of rhenium cyclized peptide, <sup>99m</sup>Tc(CO)<sub>3</sub><sup>+</sup> did not form the same cyclic product. A peak was expected at retention time of 7.80 mins, but on technetium labelling two peaks at 9.80 and 10.23 mins were observed. These retention times correlated with the retention times of the less dominant conformer/isomer cyclic product obtained during rhenium coordination. These radiolabelled conformers were then purified with a Waters Sep-Pak C18 Plus Cartridge. To demonstrate that the linear peptide was coordinated through

$^{99m}\text{Tc}(\text{CO})_3^+$ , the crude radiolabelled peptide (A) was compared with the  $\text{Re}(\text{CO})_3^+$  coordinated peptide (B) showing less dominant isomers and the purified dominant peak of  $\text{Re}(\text{CO})_3^+$  coordinated peptide (C) by analytical HPLC. The retention time of the conformer/ isomer of the crude radiolabelled peptide in the gamma trace correlated with the less dominant conformer/isomer peaks in the  $\text{Re}(\text{CO})_3^+$  coordinated peptide in the UV trace, Figure 3.11

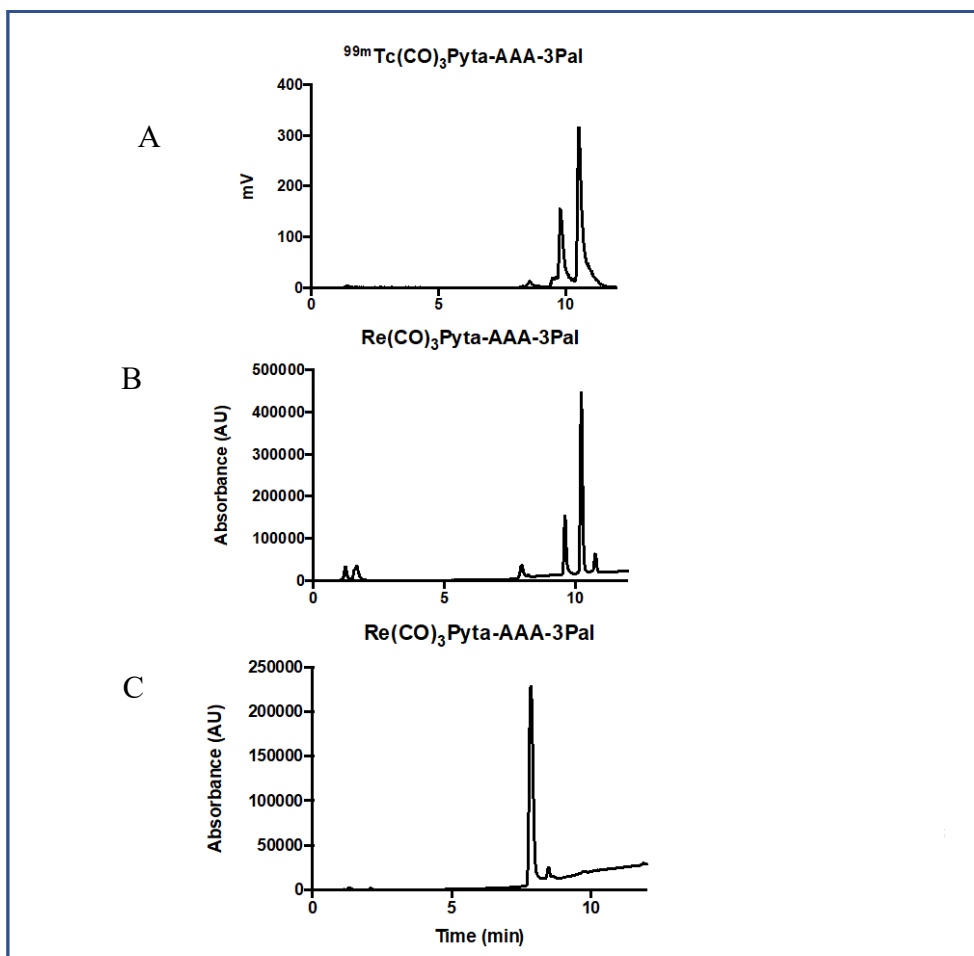


Figure 3.11 Analytical HPLC traces showing correlations between  $\gamma$  trace of crude  $^{99m}\text{Tc}(\text{CO})_3^+$  labelled peptide (A), **3.15** and UV trace of  $\text{Re}(\text{CO})_3^+$  coordinated peptide, **3.8** (B) showing less dominant isomers and no correlation with UV trace of dominant peak of **3.8** (C).

### 3.6 Conclusion

A series of linear peptides were cyclized by bidentate coordination through two nitrogen atoms on the pyridyl-triazole, and mono-dentate coordination from the nitrogen atom on the pyridine, forming a 2+1 chelation system. This was studied by  $^1\text{H}$  NMR spectroscopy of linear and

coordinated peptides, which showed considerable changes in chemical shifts upon cyclization. Circular dichroism (CD) spectroscopy suggested formation of secondary structure upon metal coordination as a change in conformation was seen. The peptides with pyta as the bidentate ligand showed conformation usually seen for helical structures whereas the peptides with 2,2'-bipyridine-4-carboxylic acid showed no significant change. Variable temperature (VT) NMR spectroscopy was used to study the hydrogen bonding where selected amino acids showed intra-molecular hydrogen bonding. Radiolabelling of the linear peptide with  $^{99m}\text{Tc}(\text{CO})_3^+$ , resulted in the formation of conformers which were not dominant during  $\text{Re}(\text{CO})_3^+$  coordination. However, there was a correlation observed between the radiolabelled peak and two of the conformers formed during rhenium coordination. We successfully demonstrated cyclization of linear pentapeptide sequences using  $^{99m}\text{Tc}/\text{Re}(\text{CO})_3^+$  coordination by 2+1 chelation fashion.

### 3.7 Experimental data

All the reagents and solvents were purchased from Sigma Aldrich, Fischer Scientific, Alfa-Aesar, Chem-Impex, Novabiochem, Oakwood Chemicals, Peptides International. For analytical UHPLC-MS, studies were performed on a Waters, Inc. Acquity UHPLC system combined with Xevo QToF mass spectrometer (ESI+, cone voltage = 30V). A Waters, Inc. Acquity UHPLC BEH C18 2.1 x 50 mm, 1.7  $\mu\text{m}$  column was used with a gradient solvent system consisting of 0.1% formic acid in acetonitrile and 0.1% formic acid in water. Analysis of the peptides was carried out using a reversed-phase analytical HPLC column (Agilent Zorbax SB-C18 column 4.6 x 150 mm, 3.5  $\mu\text{m}$ ). The mobile phases employed were 0.1% TFA in water (solvent A) and 0.1% TFA in acetonitrile (solvent B) and 0.1% TFA in methanol (solvent C) with a flow rate of 1.5 ml/min over 15 minutes. The absorbance was monitored using a Waters 2998 Photodiode array detector set at 220 nm, 254 nm, and 400 nm. All peptides were purified using a reversed-phase preparative HPLC column (Agilent Zorbax SB-C18 column 21.2 x 150 mm, 5  $\mu\text{m}$ ) with all system specifics being the same as those used for the analytical system. The flowrate for the preparative HPLC was set at 20 mL/min. The collected fractions were then lyophilized to a solid, and subsequently analysed by ESI-MS on a Acquity UHPLC-MS system (Waters Co.). The NMR spectroscopy experiments were performed using Bruker Avance III HD 400 (B400) in deuterated dimethyl sulfoxide ( $\text{DMSO}-d_6$ ) or  $\text{CDCl}_3$  at 25°C. Varian INOVA 600 NMR spectrometer was used for  $^1\text{H}$ , g-COSY

and NOESY NMR spectroscopy studies. Chemical shifts are reported in parts per million (ppm) relative to TMS (0.00 ppm).

### 3.7.1 *Small molecule synthesis*

#### 3.7.2 *4-methyl-2-bromo pyridine carboxylate, 6*

2-Bromopyridine-4-carboxylic acid (0.01 mol, 2.02 g) was added to a round bottom flask containing 40 mL of methanol. A few drops of concentrated sulfuric acid were added to the solution and the reaction mixture was brought to reflux for 5-6 hours. Methanol was removed from the clear solution using rotary evaporation. The product was diluted with distilled water and transferred to a separatory funnel. Extraction of the organic product was done using chloroform followed by washings with 20 % solution of sodium bicarbonate. The organic layer was dried and concentrated to afford a pale yellowish white solid. ESI-LCMS: m/z calculated for C<sub>7</sub>H<sub>7</sub>BrNO<sub>2</sub>, 217.9917, observed, 217.9817 (1.5 g, 69 %) <sup>1</sup>H NMR (400 MHz, CDCl<sub>3</sub>): δ 8.53 (d, J = 4.0 Hz, 1H), 8.04 (s, 1H), 7.80 (d, J = 4.0 Hz, 1H), 3.97 (s, 3H).

#### 3.7.3 *4-Methyl-2,2'-bipyridine carboxylate, 7*

4-Methyl-2-bromo pyridine carboxylate, (**6**) (0.9 g, 4.16 mmol) was dissolved in a microwave vial containing 10 mL of dry toluene, followed by addition of 2-(tri-n-butylstannyl) pyridine (1.574 g, 4.27 mmol). The resulting clear solution was degassed for 10 minutes followed by the addition of tetrakis(triphenylphosphine)palladium (0.120 mg, 2.5 mol%). The yellow-coloured transparent solution was allowed to stir in refluxing conditions at 110° C for 2 days. Potassium fluoride (0.288 g, 1.189 mmol dissolved in distilled water) was added and the reaction mixture was allowed to stir for 30 minutes at room temperature. A blackish grey precipitate was filtered off from the reaction mixture followed by extraction of the organic product using toluene (3 x 40 mL). The organic layers were combined, dried and concentrated. Column chromatography was used to purify the crude product using ethyl acetate: hexanes (1:4) which afforded a white solid. Characterization was identical to published values<sup>19</sup> (0.892 g, 40 %) ESI-HRMS: m/z calculated for C<sub>12</sub>H<sub>11</sub>N<sub>2</sub>O<sub>2</sub>, 215.0821, observed, 215.0812, <sup>1</sup>H NMR (400 MHz, CDCl<sub>3</sub>): δ 8.94 (m, 1H), 8.83 (d, <sup>3</sup>J<sub>H-H</sub> = 4.0 Hz, 1H), 8.73 (m, 1H), 8.42 (d, <sup>3</sup>J<sub>H-H</sub> = 8.0 Hz, 1H), 7.88-7.82 (m, 2H), 7.35 (dd, <sup>3</sup>J<sub>H-H</sub> = 8.0 Hz, 4.0 Hz, 1H), 3.98 (s, 3H). <sup>13</sup>C{<sup>1</sup>H} NMR (400 MHz, CDCl<sub>3</sub>): δ 165.7, 157.3, 155.1, 149.9, 149.4, 138.5, 137.0, 124.1, 122.7, 121.3, 120.3, 52.6.

### 3.7.4 2,2'-bipyridine carboxylic acid, **8**

4-Methyl-2,2'-bipyridine carboxylate, **7** (0.360 g, 1.68 mmol) was dissolved in 10 mL of methanol in a round bottom flask. To it was added 10 % KOH aqueous solution (2-3 mL). The reaction mixture was kept for stirring at room temperature for 3 hours. The resulting clear solution was concentrated, and the product was precipitated out of the solution using 1M HCl which afforded a white colored solid (0.28 g, 84 %), ESI-HRMS:  $m/z$  calculated for  $C_{11}H_9N_2O_2$ , 201.0664, observed, 201.0647;  $^1H$  NMR (400 MHz, DMSO):  $\delta$  13.78 (bs, 1H), 8.87 (dd,  $^3J_{H-H} = 4.0$  Hz, 1.7 Hz, 1H), 8.83 (m, 1H), 8.73 (m, 1H), 8.41 (m, 1H), 7.98 (td,  $^3J_{H-H} = 8.0$  Hz, 1.8 Hz 1H), 7.87 (dd,  $^3J_{H-H} = 4.0$  Hz, 1.7 Hz, 1H), 7.50 (m, 1H).  $^{13}C\{^1H\}$  NMR (400 MHz, DMSO):  $\delta$  166.6, 156.6, 154.7, 150.8, 150.1, 140.1, 138.2, 125.3, 123.3, 121.1, 120.21.

### 3.7.5 Peptide synthesis

Peptide was synthesized from C to N terminus on a solid phase support with C terminus being attached to the insoluble resin. Peptides were synthesized using standard solid phase peptide synthesis technique and the linear peptide was synthesized using fluorenylmethyloxycarbonyl (Fmoc) chemistry. The N terminal of each amino acid is Fmoc protected and the side chains are acid labile. Rink amide MBHA resin (0.39 meq/g) was used as a solid support. The rink amide resin was swollen in dimethyl formamide for 15 minutes. Each amino acid was Fmoc deprotected using 20% piperidine in dimethyl formamide for two cycles (5 minutes and 15 minutes). Coupling reactions were carried out with 3 eq. Fmoc protected amino acid, 3 eq. HCTU(2-(6-chloro-1H-benzotriazole-1-yl)-1,1,3,3-tetramethyl ammonium hexafluorophosphate) and 6 eq. of DIPEA (N, N- diisopropylethylamine). The coupling reaction was carried out for 60-90 minutes. The resin beads were washed with excess dimethyl formamide and dichloromethane after each coupling and deprotection cycles. The bidentate ligand (pyta and 2,2'-bipyridyl-4-carboxylic acid) were coupled to the peptide with the (N,N,N',N'-tetramethyl-O- (N-succinimidyl) uronium tetrafluoroborate) TSTU and DIPEA in DMF, to prepare the pre-activated ester. The peptide was cleaved from the resin using a cocktail mixture of 95% (v/v) trifluoroacetic acid (TFA), 2.5% (v/v) tri-isopropyl silane (TIPS) and 2.5% (v/v) water for 5h. The cleaved peptide was precipitated with *tert*-butyl methyl ether (TBME) and centrifuged at 3000 rpm for 10 minutes. After decanting, the peptide was frozen and lyophilized to remove any remaining solvents. The peptide was purified with reverse phase preparative HPLC, and the purity was checked by analytical UHPLC. Each of the following peptides synthesized resulted in purity > 95%.

*a) Pyta-AAA-3Pal, 3.1*

The linear peptide was synthesized using the general procedure for solid phase peptide synthesis mentioned above (3.7.5). This afforded pure peptide in the form of white fluffy solid (yield = 0.017 g, 30%) ESI HRMS:  $m/z$  calculated for  $C_{26}H_{33}N_{10}O_5$ , 565.2635 observed  $[M+H]^+$  565.2552  $^1H$  NMR (400 MHz, DMSO- $d_6$ ):  $\delta$  8.67-8.62 (m, Ar-H + NH of Ala 3, 1H), 8.61-8.59 (m, 1H), 8.52 (s, 1H), 8.17 (d,  $^3J_{H-H} = 8.0$  Hz, 1H), 8.13 (d,  $^3J_{H-H} = 8.0$  Hz, 1H), 8.03 (dt,  $^3J_{H-H} = 8.0$  Hz, 1.2 Hz, 1H), 7.93-7.90 (m, NH of 3-Pal + Ar-H, 2H), 7.84 (d,  $^3J_{H-H} = 4.0$  Hz, NH of Ala 1, 1H), 7.72 (dd,  $^3J_{H-H} = 8.0$  Hz, 5.2 Hz, 1H), 7.39 (s, 1H), 7.37-7.33 (m, 1H), 7.22 (s, 1H), 5.23 (s, 2H), 4.49 (m,  $\alpha$  CH of 3Pal, 1H), 4.34 (quint,  $^3J_{H-H} = 12.0$  Hz, 8.0 Hz, CH of Ala 3, 1H), 4.22 (quint,  $^3J_{H-H} = 12.0$  Hz, 8.0 Hz,  $\alpha$  CH of Ala 2, 1H), 4.10 (quint,  $^3J_{H-H} = 12.0$  Hz, 8.0 Hz,  $\alpha$  CH of Ala 1, 1H), 3.05 (dd,  $^2J_{H-H} = 12.0$  Hz,  $^3J_{H-H} = 6.1$  Hz,  $\beta$  H of 3-Pal, 1H), 3.03 (dd,  $^2J_{H-H} = 12.0$  Hz,  $^3J_{H-H} = 6.1$  Hz,  $\beta'$  H of 3-Pal, 1H), 1.23 (d,  $^3J_{H-H} = 4.0$  Hz,  $CH_3$  of Ala 3, 3H), 1.16 (d,  $^3J_{H-H} = 4.0$  Hz,  $CH_3$  of Ala 2, 3H), 1.07 (d,  $^3J_{H-H} = 4.0$  Hz,  $CH_3$  of Ala 1, 3H).

*b) Pyta-RGD-3Pal, 3.2*

The linear peptide was synthesized using the general procedure for solid phase peptide synthesis mentioned above (3.7.5). This afforded pure peptide in the form of white fluffy solid (yield = 0.020 g, 29 %) ESI HRMS:  $m/z$  calculated for  $C_{29}H_{38}N_{13}O_7$ , 680.3017 observed  $[M+H]^+$  680.3047,  $^1H$  NMR (400 MHz, DMSO- $d_6$ ):  $\delta$  8.72 (d, NH of Arg,  $^3J_{H-H} = 8.0$  Hz, 1H), 8.60 (m, 3H), 8.53 (s, 1H), 8.42 (t, NH of Gly,  $^3J_{H-H} = 8.0$  Hz, 1H), 8.22 (d, NH of Asp,  $^3J_{H-H} = 8.0$  Hz, 1H), 8.09-8.02 (m, NH of 3-Pal + Ar-H, 3H), 7.91 (dt,  $^3J_{H-H} = 8.0$  Hz, 4.0 Hz, 1H), 7.65 (m, 1H), 7.55 (t, NH next to  $\delta$   $CH_2$  of Arg,  $^3J_{H-H} = 4.0$  Hz, 1H), 7.38-7.33 (m, 2H), 7.29 (s, 1H), 5.27 (s, 2H), 4.52-4.44 (m,  $\alpha$  CH of 3Pal and Asp, 3H), 4.43-4.38 (m,  $\alpha$  CH of Arg, 2H), 3.80-3.67 (m,  $CH_2$  of Gly, 3H), 3.20 (dd,  $^2J_{H-H} = 16.0$  Hz,  $^3J_{H-H} = 8.0$  Hz,  $\beta$  H of  $CH_2$  of 3-Pal, 1H), 3.12 (quint,  $^3J_{H-H} = 8.0$  Hz,  $\delta$   $CH_2$  of Arg, 3H), 2.93 (dd,  $^2J_{H-H} = 12.0$  Hz,  $^3J_{H-H} = 8.0$  Hz,  $\beta'$  H of 3pal, 1H), 2.62 (dd,  $\beta$  H of  $CH_2$  of Asp,  $^2J_{H-H} = 16.0$  Hz,  $^3J_{H-H} = 8.0$  Hz, 1H), 2.42 (dd,  $\beta'$  H of  $CH_2$  of Asp,  $^2J_{H-H} = 16.0$  Hz,  $^3J_{H-H} = 8.0$  Hz, 1H), 1.79 -1.70 (m,  $\beta$  H of  $CH_2$  of Arg, 1H), 1.63-1.50 (m,  $\beta'$  H of  $CH_2$  of Arg +  $\gamma$   $CH_2$  of Arg, 4H).

*c) Pyta-AAAA-3Pal, 3.3*

The linear peptide was synthesized using the general procedure for solid phase peptide synthesis mentioned above (3.7.5). This afforded pure peptide in the form of white fluffy solid (yield = 0.015 g, 24 %) ESI-HRMS:  $m/z$  calculated for  $C_{29}H_{38}N_{11}O_6$ , 636.3007 observed  $[M+H]^+$  636.2969,  $^1H$  NMR (400 MHz, DMSO- $d_6$ ):  $\delta$  8.65 (d,  $^3J_{H-H} = 4.0$  Hz, NH of Ala 4, 1H), 8.59 (bs, 2H), 8.51 (s, 1H), 8.21 (d,  $^3J_{H-H} = 8.0$  Hz, 1H), 8.03 (t,  $^3J_{H-H} = 8.0$  Hz, 2H), 7.92-7.83 (m, NH of Ala 1, Ala 2 and 3-Pal, 4H), 7.65 (bs, 1H), 7.38 (s, 1H), 7.34 (s, 1H), 7.21 (s, 1H), 5.22 (s, 2H), 4.47 (m,  $\alpha$  CH of 3Pal, 1H), 4.34 (quint,  $^3J_{H-H} = 12.0$  Hz, 4.0 Hz, CH of Ala 4, 1H), 4.24 (m,  $\alpha$  CH of Ala 3, 1H), 4.18 (m,  $\alpha$  CH of Ala 2, 1H), 4.12 (m,  $\alpha$  CH of Ala 1, 1H), 3.15 (m,  $\beta$  H of 3-Pal, 1H), 2.91 (m,  $\beta'$  H of 3-Pal, 1H), 1.24 (d,  $^3J_{H-H} = 4.0$  Hz,  $CH_3$  of Ala 4, 3H), 1.20 (d,  $^3J_{H-H} = 4.0$  Hz,  $CH_3$  of Ala 3, 3H), 1.12 (d,  $^3J_{H-H} = 4.0$  Hz,  $CH_3$  of Ala 1 and Ala 2, 6H).

*d) Pyta-AAAAA-3Pal, 3.4*

The linear peptide was synthesized using the general procedure for solid phase peptide synthesis mentioned above (3.7.5). This afforded pure peptide in the form of white fluffy solid (yield = 0.021 g, 30 %) ESI-HRMS:  $m/z$  calculated for  $C_{32}H_{43}N_{12}O_7$ , 707.3378 observed  $[M+H]^+$  707.3381,  $^1H$  NMR (400 MHz, DMSO- $d_6$ ):  $\delta$  8.65 (d,  $^3J_{H-H} = 8.0$  Hz, NH of Ala 5, 1H), 8.59 (m, 1H), 8.57-8.53 (m, 2H), 8.51 (s, 1H), 8.21 (d, NH of Ala 4,  $^3J_{H-H} = 8.0$  Hz, 1H), 8.02 (d,  $^3J_{H-H} = 4.0$  Hz, H), 7.92-7.86 (m, NH of Ala 1, Ala 2, Ala 3, 3-Pal, 4H), 7.57 (m, 1H), 7.38 (bs, 1H), 7.36-7.32 (m, 1H), 7.23 (s, 1H), 7.20 (s, 1H), 7.10 (s, 1H), 6.97 (s, 1H), 5.22 (s, 2H), 4.48-4.43 (m, 1H), 4.34 (quint,  $^3J_{H-H} = 12.0$  Hz, 4.0 Hz, CH of Ala 5, 1H), 4.27-4.17 (m,  $\alpha$  CH of Ala 2, Ala 3 and Ala 4, 3H), 4.11 (quint,  $^3J_{H-H} = 12.0$  Hz, 4.0 Hz, CH of Ala 1, 1H), 3.16-3.11 (m,  $\beta$  H of 3-Pal, 1H), 2.92-2.87 (m,  $\beta'$  H of 3-Pal, 1H), 1.24 (d,  $^3J_{H-H} = 8.0$  Hz,  $CH_3$  of Ala 5, 3H), 1.22 (d,  $^3J_{H-H} = 8.0$  Hz,  $CH_3$  of Ala 4, 3H), 1.21 (d,  $^3J_{H-H} = 8.0$  Hz,  $CH_3$  of Ala 3), 1.16 (d,  $^3J_{H-H} = 8.0$  Hz,  $CH_3$  of Ala 2, 3H), 1.11 (d,  $^3J_{H-H} = 8.0$  Hz,  $CH_3$  of Ala 1)

*e) Pyta-Aaa-3Pal, 3.5*

The linear peptide was synthesized using the general procedure for solid phase peptide synthesis mentioned above (3.7.5). This afforded pure peptide in the form of white fluffy solid (yield = 0.010



g, 18 %) ESI-HRMS: m/z calculated for C<sub>26</sub>H<sub>33</sub>N<sub>10</sub>O<sub>5</sub>, 565.2635 observed [M+H]<sup>+</sup> 565.2552 <sup>1</sup>H NMR (400 MHz, DMSO-d<sub>6</sub>): δ 8.67-8.62 (m, Ar-H + NH of Ala 3, 1H), 8.60-8.58 (m, 2H), 8.52 (s, 1H), 8.38 (d, NH of Ala 2, <sup>3</sup>J<sub>H-H</sub> = 8.0 Hz, 1H), 8.13 (d, <sup>3</sup>J<sub>H-H</sub> = 8.0 Hz, 1H), 8.05-8.02 (m, NH of Ala 1, 1H), 8.00 (m, 1H), 7.96 (d, <sup>3</sup>J<sub>H-H</sub> = 12.0 Hz, NH of 3-Pal, 1H), 7.90 (dt, <sup>3</sup>J<sub>H-H</sub> = 8.0 Hz, 1.8 Hz, 1H), 7.72-7.68 (m, 1H), 7.28 (s, 1H), 7.21 (s, 1H), 5.23 (s, 2H), 4.49 - 4.44 (m, α CH of 3-Pal, 1H), 4.36 (quint, <sup>3</sup>J<sub>H-H</sub> = 16.0 Hz, 8.0 Hz, CH of Ala 3, 1H), 4.18 (quint, <sup>3</sup>J<sub>H-H</sub> = 16.0 Hz, 8.0 Hz, α CH of Ala 2, 1H), 4.05 (quint, <sup>3</sup>J<sub>H-H</sub> = 16.0 Hz, 8.0 Hz, α CH of Ala 1, 1H), 3.09 (dd, <sup>2</sup>J<sub>H-H</sub> = 16.0 Hz, <sup>3</sup>J<sub>H-H</sub> = 3.8 Hz, β H of 3-Pal, 1H), 3.07 (dd, <sup>2</sup>J<sub>H-H</sub> = 12.0 Hz, <sup>3</sup>J<sub>H-H</sub> = 4.2 Hz, β' H of 3-Pal, 1H), 1.26 (d, <sup>3</sup>J<sub>H-H</sub> = 8.0 Hz, CH<sub>3</sub> of Ala 3, 3H), 1.18 (d, <sup>3</sup>J<sub>H-H</sub> = 8.0 Hz, CH<sub>3</sub> of Ala 2, 3H), 1.00 (d, <sup>3</sup>J<sub>H-H</sub> = 8.0 Hz, CH<sub>3</sub> of Ala 1, 3H).

*f) Bipyd-AAA-3Pal, 3.6*

The linear peptide was synthesized using the general procedure for solid phase peptide synthesis mentioned above (3.7.5). This afforded pure peptide in the form of white fluffy solid (yield = 0.012 g, 24 %) ESI-HRMS: m/z calculated for C<sub>28</sub>H<sub>33</sub>N<sub>8</sub>O<sub>5</sub>, 561.2574 observed [M+H]<sup>+</sup> 561.2532 <sup>1</sup>H NMR (400 MHz, DMSO-d<sub>6</sub>): δ 9.06 (d, <sup>3</sup>J<sub>H-H</sub> = 8.0 Hz, NH of Ala 3, 1H), 8.84 (d, <sup>3</sup>J<sub>H-H</sub> = 8.0 Hz, 1H), 8.82 (m, 1H), 8.74 (m, 1H), 8.71 (m, 1H), 8.68 (d, <sup>3</sup>J<sub>H-H</sub> = 2.0 Hz, 1H), 8.43 (dt, <sup>3</sup>J<sub>H-H</sub> = 8.0 Hz, 1.1 Hz, 1H), 8.24 (dt, <sup>3</sup>J<sub>H-H</sub> = 8.0 Hz, 1H), 8.01 (td, <sup>3</sup>J<sub>H-H</sub> = 8.0 Hz, 5.2 Hz, 1H), 7.96 (d, <sup>3</sup>J<sub>H-H</sub> = 8.0 Hz, 1H), 7.88 (d, <sup>3</sup>J<sub>H-H</sub> = 4.0 Hz, 1H), 7.86 (dd, <sup>3</sup>J<sub>H-H</sub> = 5.0 Hz, 1.0 Hz, 1H), 7.82 (dd, <sup>3</sup>J<sub>H-H</sub> = 8.0 Hz, 4.3 Hz, 1H), 7.52 (m, 1H), 7.41 (bs, 1H), 7.26 (bs, 1H), 4.55 - 4.47 (m, α CH of 3Pal and Ala 3, 2H), 4.26 (quint, <sup>3</sup>J<sub>H-H</sub> = 12.0 Hz, 4.0 Hz, CH of Ala 2, 1H), 4.13 (quint, <sup>3</sup>J<sub>H-H</sub> = 12.0 Hz, 4.0 Hz, α CH of Ala 1, 1H), 3.10 (dd, <sup>2</sup>J<sub>H-H</sub> = 12.0 Hz, <sup>3</sup>J<sub>H-H</sub> = 2.3 Hz, β' H of CH<sub>2</sub> of 3pal, 1H), 3.09 (dd, <sup>2</sup>J<sub>H-H</sub> = 12.0 Hz, <sup>3</sup>J<sub>H-H</sub> = 1.7 Hz, β H of CH<sub>2</sub> of 3pal, 1H), 1.37 (d, <sup>3</sup>J<sub>H-H</sub> = 8.0 Hz, CH<sub>3</sub> of Ala 3, 3H), 1.20 (d, <sup>3</sup>J<sub>H-H</sub> = 8.0 Hz, CH<sub>3</sub> of Ala 2, 3H), 1.14 (d, <sup>3</sup>J<sub>H-H</sub> = 8.0 Hz, CH<sub>3</sub> of Ala 1, 3H).

*g) Bipyd-RGD-3Pal, 3.7*

The linear peptide was synthesized using the general procedure for solid phase peptide synthesis mentioned above (3.7.5). This afforded pure peptide in the form of white fluffy solid (yield = 9 mg, 13 %) ESI-HRMS: m/z calculated for C<sub>31</sub>H<sub>38</sub>N<sub>11</sub>O<sub>7</sub>, 676.2956 observed [M+H]<sup>+</sup> 676.2927, <sup>1</sup>H NMR (400 MHz, DMSO-d<sub>6</sub>): δ 9.11 (d, NH of Arg, <sup>3</sup>J<sub>H-H</sub> = 8.0 Hz, 1H), 8.43-8.38 (m, NH of Gly

+ Ar-H, 2H), 8.17 (d,  $^3J_{\text{H-H}} = 8.0$  Hz, 1H), 8.13-8.08 (m, NH of Asp + Gly, 2H), 8.00 (td,  $^3J_{\text{H-H}} = 8.0$  Hz, 4.0 Hz, 1H), 7.87 (dd,  $^3J_{\text{H-H}} = 8.0$  Hz, 4.0 Hz, 3H), 7.71(m, 1H), 7.57( t, NH next to  $\delta$  CH<sub>2</sub> of Arg,  $^3J_{\text{H-H}} = 4.0$  Hz, 1H), 7.51 (m, 1H), 7.30 (d,  $^3J_{\text{H-H}} = 4.0$  Hz, 1H), 4.58 - 4.44 (m, 4H), 3.74 (m, CH<sub>2</sub> of Gly, 2H), 3.21 (dd,  $^2J_{\text{H-H}} = 8.0$  Hz,  $^3J_{\text{H-H}} = 4.0$  Hz,  $\beta$  H of CH<sub>2</sub> of 3-Pal, 1H), 3.14 (quint,  $^3J_{\text{H-H}} = 8.0$  Hz,  $\delta$  CH<sub>2</sub> of Arg, 2H), 2.95 (dd,  $^2J_{\text{H-H}} = 16.0$  Hz,  $^3J_{\text{H-H}} = 12.0$  Hz,  $\beta'$  H of 3-Pal, 1H), 2.65 (dd,  $\beta$  H of CH<sub>2</sub> of Asp,  $^2J_{\text{H-H}} = 16.0$  Hz,  $^3J_{\text{H-H}} = 8.0$  Hz, 1H), 2.44 (dd,  $\beta'$  H of CH<sub>2</sub> of Asp,  $^2J_{\text{H-H}} = 16.0$  Hz,  $^3J_{\text{H-H}} = 8.0$  Hz, 1H) 1.81-1.72 (m,  $\beta$  CH<sub>2</sub> of Arg, 1H), 1.63-1.53 (m,  $\gamma$  CH<sub>2</sub> of Arg, 2H).

### 3.7.6 Metal coordination

#### 1) $[\text{Re}(\text{CO})_3(\text{Pyta-AAA-3Pal-NH}_2)]\text{OTf}$ , **3.8**

The purified linear peptide, **3.1** (50.0 mg, 0.088 mmol) was coordinated  $[\text{Re}(\text{CO})_3(\text{OH}_2)_3]\text{OTf}$  (797  $\mu\text{L}$  of 0.1 M solution, 0.0797 mmol) in water (6 mL). The solution was stirred for 2 hours at 50 °C. Upon completion of reaction, the crude mixture was lyophilized and purified by preparative HPLC. (Linear gradient of 35-95 % of solvent C in B) (yield = 19.5 mg, 27%), ESI-HRMS: m/z calculated for C<sub>29</sub>H<sub>32</sub>N<sub>10</sub>O<sub>8</sub><sup>185/187</sup>Re, 835.1962; observed [M]<sup>+</sup> 835.2040. <sup>1</sup>H NMR (400 MHz, DMSO-d<sub>6</sub>):  $\delta$  9.27 (d,  $^3J_{\text{H-H}} = 8.0$  Hz, 1H), 9.01 (d,  $^3J_{\text{H-H}} = 4.0$  Hz, 1H), 8.86 (d, NH of Ala 3,  $^3J_{\text{H-H}} = 4.0$  Hz, 1H), 8.60 (m, 1H), 8.58 (s, 1H), 8.43 - 8.41 (m, 1H), 8.40 - 8.38 (m, 1H), 8.33 (td,  $^3J_{\text{H-H}} = 4.0$  Hz, 1.5 Hz, 1H), 8.23 (dd, NH of Ala 2,  $^3J_{\text{H-H}} = 8.0$  Hz, 4.0 Hz, 1H), 8.02 (d,  $^3J_{\text{H-H}} = 8.0$  Hz, 1H), 7.91 ( d, NH of 3-Pal,  $^3J_{\text{H-H}} = 8.0$  Hz, 1H), 7.86 (dd, NH of Ala 1,  $^3J_{\text{H-H}} = 12.0$  Hz, 8.0 Hz, 1H), 7.69 - 7.65(m, 1H), 7.64-7.61 (m, 1H), 7.41 (s, 1H), 7.22 (s, 1H), 5.51 (s, 2H), 4.51- 4.44 (m,  $\alpha$  CH of 3Pal,1H), 4.40 - 4.34 (m,  $\alpha$  CH of Ala 3, 1H), 4.25 (quint,  $^3J_{\text{H-H}} = 12.0$  Hz, 8.0 Hz,  $\alpha$  CH of Ala 2, 1H), 4.12 (quint,  $^3J_{\text{H-H}} = 12.0$  Hz, 8.0 Hz,  $\alpha$  CH of Ala 1, 1H), 3.06 (dd,  $^2J_{\text{H-H}} = 12.0$  Hz,  $^3J_{\text{H-H}} = 6.1$  Hz,  $\beta$  H of 3-Pal, 1H), 3.04 (dd,  $^2J_{\text{H-H}} = 12.0$  Hz,  $^3J_{\text{H-H}} = 6.1$  Hz,  $\beta'$  H of 3pal, 1H), 1.26 (d,  $^3J_{\text{H-H}} = 8.0$  Hz, CH<sub>3</sub> of Ala 3, 3H), 1.19 (d,  $^3J_{\text{H-H}} = 8.0$  Hz, CH<sub>3</sub> of Ala 2, 3H), 1.10 (d,  $^3J_{\text{H-H}} = 8.0$  Hz, CH<sub>3</sub> of Ala 1, 3H)

#### 2) $[\text{Re}(\text{CO})_3(\text{Pyta-RGD-3Pal-NH}_2)]\text{OTf}$ , **3.9**

The purified linear peptide, **3.2** (120.0 mg, 0.177 mmol) was coordinated  $[\text{Re}(\text{CO})_3(\text{OH}_2)_3]\text{OTf}$  (1.59 mL of 0.1 M solution, 0.159 mmol) in water (10 mL). The solution was stirred for 2 hours at 50 °C.

Upon completion of reaction, the crude mixture was lyophilized and purified by preparative HPLC. (Linear gradient of 25-80 % of solvent C in B) (yield = 0.058 g, 34 %), ESI-LCMS: m/z calculated for  $C_{32}H_{37}N_{13}O_{10}^{185/187}Re$ , 950.2344; observed  $[M + H]^+$  950.2310  $^1H$  NMR (400 MHz, DMSO- $d_6$ ):  $\delta$  9.25 (s, 1H), 9.00 (m, 1H), 8.89 (d, NH of Arg,  $^3J_{H-H} = 8.0$  Hz, 1H), 8.57 (m, 2H), 8.45 (d, NH of Gly,  $^3J_{H-H} = 4.0$  Hz, 1H), 8.38 (m, 1H), 8.33 (td,  $^3J_{H-H} = 8.0$  Hz, 4.0 Hz, 1H), 8.22 (dd, NH of Asp,  $^3J_{H-H} = 8.0$  Hz, 4.0 Hz, 1H), 8.06 (dd,  $^3J_{H-H} = 8.0$  Hz, 4.0 Hz, NH of 3-Pal, 1H), 7.98 (d,  $^3J_{H-H} = 8.0$  Hz, 1H), 7.69-7.65 (m, 1H), 7.62-7.56 (m, 1H), 7.51 (t,  $^3J_{H-H} = 8.0$  Hz, NH next to  $\gamma$  CH<sub>2</sub> of Arg, 1H), 7.34 (s, 1H), 7.28 (s, 1H), 5.54 (s, 2H), 4.52-4.37 (m,  $\alpha$ CH of 3Pal, Arg, Asp, 6H), 3.80-3.68 (m, CH<sub>2</sub> of Gly, 2H), 3.18 (m,  $\beta$  H of CH<sub>2</sub> of 3-Pal, 1H), 3.11 (m,  $\delta$  CH<sub>2</sub> of Arg, 2H), 2.93 (dd,  $^2J_{H-H} = 12.0$  Hz,  $^3J_{H-H} = 8.0$  Hz,  $\beta'$  H of 3pal, 1H), 2.67-2.59 (m,  $\beta$  H of CH<sub>2</sub> of Asp, 1H), 2.42 (m,  $\beta'$  H of CH<sub>2</sub> of Asp, 1H), 1.82-1.69 (m,  $\beta$  H of CH<sub>2</sub> of Arg, 1H), 1.67-1.49 (m,  $\beta'$  H of CH<sub>2</sub> of Arg +  $\gamma$  CH<sub>2</sub> of Arg, 4H).

### 3) $[Re(CO)_3$ Pyta-AAAA-3Pal], **3.10**

The purified linear peptide, (**3.3**), (83.0 mg, 0.131 mmol) was coordinated  $[Re(CO)_3(OH_2)_3]OTf$  (1.17 mL of 0.1 M solution, 0.117 mmol) in water (8 mL). The solution was stirred for 2 hours at 50 °C. Upon completion of reaction, the crude mixture was lyophilized and purified by preparative HPLC. (Linear gradient of 35-95 % of solvent C in B) (yield = 0.023 g, 21 %) ESI-LCMS: m/z calculated for  $C_{32}H_{37}N_{11}O_9^{185/187}Re$ , 906.2333 observed  $[M+H]^+$  906.2170,  $^1H$  NMR (400 MHz, DMSO- $d_6$ ):  $\delta$  9.27 (s, 1H), 9.01 (d,  $^3J_{H-H} = 8.0$  Hz, 1H), 8.86 (m, NH of Ala 4, 1H), 8.53 (bs, 1H), 8.42-8.38 (m, 1H), 8.34 (m, 1H), 8.26 (dd, NH of Ala 3,  $^3J_{H-H} = 8.0$  Hz, 4 Hz, 1H), 7.91-7.86 (m, NH of Ala 1, Ala 2 and 3-Pal, 4H), 7.70-7.66 (m, 1H), 7.50 (bs, 1H), 7.40 (s, 1H), 7.20 (s, 1H), 5.51 (s, 2H), 4.49 - 4.44 (m,  $\alpha$  CH of 3Pal, 1H), 4.41-4.36 (m, CH of Ala 4, 1H), 4.27 (quint,  $^3J_{H-H} = 12.0$  Hz, 4.0 Hz,  $\alpha$  CH of Ala 3, 1H), 4.24 - 4.11 (m,  $\alpha$  CH of Ala 2 and Ala 1, 2H), 3.01 (dd,  $^2J_{H-H} = 16.0$  Hz,  $^3J_{H-H} = 5.9$  Hz,  $\beta$  H of 3-Pal, 1H), 2.99 (dd,  $^2J_{H-H} = 16.0$  Hz,  $^3J_{H-H} = 6.0$  Hz,  $\beta'$  H of 3-Pal, 1H), 1.28 (d,  $^3J_{H-H} = 4.0$  Hz, CH<sub>3</sub> of Ala 4, 3H), 1.22 (d,  $^3J_{H-H} = 4.0$  Hz, CH<sub>3</sub> of Ala 3, 3H), 1.16-1.13 (d,  $^3J_{H-H} = 4.0$  Hz, CH<sub>3</sub> of Ala 1 and Ala 2, 6H).

4) [Re(CO)<sub>3</sub> Pyta-AAAAA-3Pal], **3.11**

The purified linear peptide, (**3.4**), (85.0 mg, 0.120 mmol) was coordinated [Re(CO)<sub>3</sub>(OH<sub>2</sub>)<sub>3</sub>]OTf (1.08 mL of 0.1 M solution, 0.1082 mmol) in water (8 mL). The solution was stirred for 2 hours at 50 °C. Upon completion of reaction, the crude mixture was lyophilized and purified by preparative HPLC. (Linear gradient of 35-95 % of solvent C in B) (yield = 0.015g, 13 %) ESI-HRMS: m/z calculated for C<sub>35</sub>H<sub>42</sub>N<sub>12</sub>O<sub>10</sub><sup>185/187</sup>Re, 977.2705 observed [M+H]<sup>+</sup> 977.2711, <sup>1</sup>H NMR (400 MHz, DMSO-d<sub>6</sub>): δ 9.27 (s, 1H), 9.01 (d, <sup>3</sup>J<sub>H-H</sub> = 8.0 Hz, 1H), 8.87-8.84 (m, NH of Ala 5, 1H), 8.56 (m, 2H), 8.41 (m, 1H), 8.33 (m, 1H), 8.26 (dd, NH of Ala 4, <sup>3</sup>J<sub>H-H</sub> = 8.0 Hz, 4.0 Hz, 1H), 7.97 (d, <sup>3</sup>J<sub>H-H</sub> = 8.0 Hz, 1H), 7.92-7.87 (m, NH of Ala 1, Ala 2, Ala 3 and 3-Pal, 4H), 7.69-7.65 (m, 1H), 7.60-7.57 (m, 1H), 7.39 (s, 1H), 7.21 (s, 1H), 5.50 (m, 2H), 4.49 - 4.44 (m, α CH of 3Pal, 1H), 4.40-4.36 (m, CH of Ala 5, 1H), 4.27 (quint, <sup>3</sup>J<sub>H-H</sub> = 12.0 Hz, 8.0 Hz, α CH of Ala 4, 1H), 4.23 - 4.17 (m, α CH of Ala 2 and Ala 3, 2H), 4.13 (m, <sup>3</sup>J<sub>H-H</sub> = 12.0 Hz, 4.0 Hz, α CH of Ala 1, 1H), 3.01 (dd, <sup>2</sup>J<sub>H-H</sub> = 12.0 Hz, <sup>3</sup>J<sub>H-H</sub> = 5.9 Hz, β H of 3pal, 1H), 2.99 (dd, <sup>2</sup>J<sub>H-H</sub> = 12.0 Hz, <sup>3</sup>J<sub>H-H</sub> = 6.0 Hz, β' H of 3pal, 1H), 1.27 (d, <sup>3</sup>J<sub>H-H</sub> = 4.0 Hz, CH<sub>3</sub> of Ala 5, 3H), 1.22 (d, <sup>3</sup>J<sub>H-H</sub> = 4.0 Hz, CH<sub>3</sub> of Ala 4, 3H), 1.17 (d, <sup>3</sup>J<sub>H-H</sub> = 4.0 Hz, CH<sub>3</sub> of Ala 1 and Ala 2, 6H), 1.12 (d, <sup>3</sup>J<sub>H-H</sub> = 8.0 Hz, 3H).

5) [Re(CO)<sub>3</sub>(Pyta-AaA-3Pal-NH<sub>2</sub>)]OTf, **3.12**

The purified linear peptide, (**3.5**), (50.0 mg, 0.088 mmol) was coordinated [Re(CO)<sub>3</sub>(OH<sub>2</sub>)<sub>3</sub>]OTf (797 μL of 0.1 M solution, 0.0797 mmol) in water (8 mL). The solution was stirred for 2 hours at 50 °C. Upon completion of reaction, the crude mixture was lyophilized and purified by preparative HPLC. (Linear gradient of 32-95 % of solvent C in B) (yield = 0.016 g, 21%), ESI-HRMS: m/z calculated for C<sub>29</sub>H<sub>32</sub>N<sub>10</sub>O<sub>8</sub><sup>185/187</sup>Re, 835.1962; observed [M]<sup>+</sup> 835.1857 <sup>1</sup>H NMR (400 MHz, DMSO-d<sub>6</sub>): δ 9.27 (d, <sup>3</sup>J<sub>H-H</sub> = 8.0 Hz, 1H), 9.00 (d, NH of Ala 3, <sup>3</sup>J<sub>H-H</sub> = 4.0 Hz, 1H) 8.83 (dd, <sup>3</sup>J<sub>H-H</sub> = 8.0 Hz, 4.0 Hz, 1H), 8.64 (s, 1H), 8.62 (s, 1H), 8.41 (m, 1H), 8.38-8.31 (m, 2H), 8.13 (d, <sup>3</sup>J<sub>H-H</sub> = 8.0 Hz, 1H), 8.12-8.09 (m, 2H), 7.97 (d, <sup>3</sup>J<sub>H-H</sub> = 8.0 Hz, 1H), 7.69-7.65 (m, 2H), 7.25 (d, <sup>3</sup>J<sub>H-H</sub> = 12.0 Hz, 1H), 5.53-5.49 (m, 2H), 4.50- 4.37 (m, α CH of 3Pal and Ala 3, 2H), 4.19 (quint, <sup>3</sup>J<sub>H-H</sub> = 12.0 Hz, 8.0 Hz, α CH of Ala 2, 1H), 4.05 (quint, <sup>3</sup>J<sub>H-H</sub> = 12.0 Hz, 8.0 Hz, α CH of Ala 1, 1H), 3.26-3.19 (m, β H of 3pal, 1H), 3.03-2.95 (m, β' H of 3pal, 1H), 1.28 (d, <sup>3</sup>J<sub>H-H</sub> = 8.0 Hz, CH<sub>3</sub> of Ala 3, 3H), 1.19 (d, <sup>3</sup>J<sub>H-H</sub> = 8.0 Hz, CH<sub>3</sub> of Ala 2, 3H), 1.03 (d, <sup>3</sup>J<sub>H-H</sub> = 8.0 Hz, CH<sub>3</sub> of Ala 1, 3H)

6) *Re(CO)<sub>3</sub>[Bipyd-AAA-3Pal]*, **3.13**

The purified linear peptide (**3.6**), (60.0 mg, 0.107 mmol) was coordinated [Re(CO)<sub>3</sub>(OH<sub>2</sub>)<sub>3</sub>]OTf (963 μL of 0.1 M solution, 0.096 mmol) in water (6 mL). The solution was stirred for 2 hours at 50 °C. Upon completion of reaction, the crude mixture was lyophilized and purified by preparative HPLC. (Linear gradient of 35-95 % of solvent C in B), (yield = 0.013g, 15%) ESI-HRMS: m/z calculated for C<sub>31</sub>H<sub>32</sub>N<sub>8</sub>O<sub>8</sub><sup>185/187</sup>Re, 831.1901 observed [M+H]<sup>+</sup> 831.1965 <sup>1</sup>H NMR (400 MHz, DMSO-d<sub>6</sub>): δ 9.25- 9.22 (m, NH of Ala 3, 2H), 9.10 (m, 1H), 9.04 (bs, 1H), 8.81 (t, <sup>3</sup>J<sub>H-H</sub> = 8.0 Hz, 1H), 8.62 (bs, 2H), 8.45-8.40 (m, 1H), 8.26 (m, 1H), 8.10-8.08 (m, 1H), 7.94 (d, NH of 3-Pal, <sup>3</sup>J<sub>H-H</sub> = 8.0 Hz, 1H), 7.88 (d, <sup>3</sup>J<sub>H-H</sub> = 4.0 Hz, 1H), 7.83 (t, NH of Ala 1, <sup>3</sup>J<sub>H-H</sub> = 8.0 Hz, 1H), 7.68 (t, <sup>3</sup>J<sub>H-H</sub> = 8.0 Hz, 1H), 7.42 (s, 1H), 7.23 (s, 1H), 4.56 (quint, α CH of Ala 3, <sup>3</sup>J<sub>H-H</sub> = 16.0 Hz, 8.0 Hz, 2H), 4.53-4.47 (m, 1H), 4.27 (quint, <sup>3</sup>J<sub>H-H</sub> = 12.0 Hz, 4.0 Hz, α CH of Ala 2, 1H), 4.15 (quint, <sup>3</sup>J<sub>H-H</sub> = 12.0 Hz, 8.0 Hz, α CH of Ala 1, 1H), 3.05 (dd, <sup>2</sup>J<sub>H-H</sub> = 12.0 Hz, <sup>3</sup>J<sub>H-H</sub> = 6.1 Hz, β' H of CH<sub>2</sub> of 3-Pal, 1H), 3.04 (dd, <sup>2</sup>J<sub>H-H</sub> = 12.0 Hz, <sup>3</sup>J<sub>H-H</sub> = 6.1 Hz, β H of CH<sub>2</sub> of 3-Pal, 1H), 1.39 (d, <sup>3</sup>J<sub>H-H</sub> = 8.0 Hz, CH<sub>3</sub> of Ala 3, 3H), 1.21 (d, <sup>3</sup>J<sub>H-H</sub> = 8.0 Hz, CH<sub>3</sub> of Ala 2, 3H), 1.14 (d, <sup>3</sup>J<sub>H-H</sub> = 8.0 Hz, CH<sub>3</sub> of Ala 1, 3H).

7) *[Re(CO)<sub>3</sub>(Bipyd-RGD-3Pal-NH<sub>2</sub>)]OTf*, **3.14**

The purified linear peptide, (**3.7**), (35.0 mg, 0.051 mmol) was coordinated [Re(CO)<sub>3</sub>(OH<sub>2</sub>)<sub>3</sub>]OTf (465 μL of 0.1 M solution, 0.0465 mmol) in water (10 mL). The solution was stirred for 2 hours at 50 °C. Upon completion of reaction, the crude mixture was lyophilized and purified by preparative HPLC. (Linear gradient of 36-95 % of solvent C in B) (yield = 12 mg, 25 %), ESI-LCMS: m/z calculated for C<sub>34</sub>H<sub>37</sub>N<sub>11</sub>O<sub>10</sub><sup>185/187</sup>Re, 946.2283; observed [M + H]<sup>+</sup> 946.2487 <sup>1</sup>H NMR (400 MHz, DMSO-d<sub>6</sub>): δ 9.32 (d, NH of Arg, <sup>3</sup>J<sub>H-H</sub> = 8.0 Hz, 1H), 9.23 (dd, <sup>3</sup>J<sub>H-H</sub> = 4.0 Hz, 2.0 Hz, 1H), 9.11 (m, 1H), 9.04 (m, 1H), 8.79 (dd, <sup>3</sup>J<sub>H-H</sub> = 8.0 Hz, 4.0 Hz 1H), 8.58 - 8.48 (m, NH of Gly + Ar-H, <sup>3</sup>J<sub>H-H</sub> = 4.0 Hz, 2H), 8.43 (m, 1H), 8.18 (d, NH of Asp, <sup>3</sup>J<sub>H-H</sub> = 8.0 Hz, 1H), 8.11 (m, 1H), 8.05 (d, <sup>3</sup>J<sub>H-H</sub> = 8.0 Hz, NH of 3-Pal, 1H), 7.93 (bs, 1H), 7.84 (m, 1H), 7.56 (m, NH next to γ CH<sub>2</sub> of Arg, 1H), 7.32 (s, 1H), 7.26 (s, 1H), 4.61- 4.50 (m, α CH of Arg and Asp, 2H), 4.44 (m, αCH of 3-Pal, 2H), 3.76 (m, CH<sub>2</sub> of Gly, 2H), 3.17-3.14 (m, β H of CH<sub>2</sub> of 3-Pal + δ CH<sub>2</sub> of Arg, 3H), 2.94-2.88 (m, β' H of CH<sub>2</sub> of 3-Pal, 1H), 2.65 (dd, <sup>2</sup>J<sub>H-H</sub> = 16.0 Hz, <sup>3</sup>J<sub>H-H</sub> = 8.0 Hz, β' H of Asp, 1H), 2.45 (dd, <sup>2</sup>J<sub>H-H</sub> =

16.0 Hz,  $^3J_{H-H} = 8.0$  Hz,  $\beta$  H of Asp, 1H), 1.81-1.71 (m,  $\beta$  CH<sub>2</sub> of Arg, 2H), 1.67-1.56 (m,  $\gamma$  CH<sub>2</sub> of Arg, 2H).

### 8) $^{99m}\text{Tc}(\text{CO})_3\text{-Pyta-AAA-3Pal}$ , **3.15**

Isolink kit containing sodium potassium tartrate, sodium tetraborate, sodium carbonate, and sodium boranocarbonate was dissolved in 1 mL of distilled water. To it was added 1093 MBq (0.300 mL) of [ $^{99m}\text{Tc}$ ]-pertechnetate. This was stirred at 110 °C for 3.5 mins in the microwave reactor. After 3.5 min, 200  $\mu\text{L}$  of 1 M HCl was added and was allowed to stand for 5 min. 180 MBq (200  $\mu\text{L}$ ) was then added to (**3.1**) (0.5 mg, 8.8  $\mu\text{mol}$ ) and was diluted with H<sub>2</sub>O to total volume of 1 mL. This reaction was carried out in the microwave reactor at 60 °C for 30 min. HPLC analysis showed retention time of 9.80 and 10.23 min at a linear gradient of 25-75% solvent C in B for 15 min. The labelled conformers were then purified using a Waters Sep-Pak Plus C18 Cartridge. This resulted in a 24% and 44% decay corrected radiochemical yield for the respective conformers.

## 3.8 Circular Dichroism spectroscopy

CD was carried out on a Jasco J-810 spectropolarimeter and recorded in the range of 180-260 nm. All the linear and cyclic peptides (>90% purity, lyophilized) were dissolved in Milli-Q water to a concentration of 0.25 mg/mL. The measurement was carried out at 20° C, using a quartz cuvette with a path length of 1 mm. The instrument measured at a scanning speed of 100 nm/min with a response rate of 0.5s. A blank solution of Milli-Q water was run before the measurements. Graph pad Prism (version 6.0c) was used to plot the graphs.

## 3.9 References

- (1) Roxin, Á.; Zheng, G. Flexible or Fixed: A Comparative Review of Linear and Cyclic Cancer-Targeting Peptides. *Future Med. Chem.* **2012**, *4* (12), 1601–1618. <https://doi.org/10.4155/fmc.12.75>.
- (2) Barber-Zucker, S.; Shaanan, B.; Zarivach, R. Transition Metal Binding Selectivity in Proteins and Its Correlation with the Phylogenomic Classification of the Cation Diffusion Facilitator Protein Family. *Sci. Rep.* **2017**, *7*, 16381. <https://doi.org/10.1038/s41598-017->

16777-5.

- (3) Hickey, J. L.; Simpson, E. J.; Hou, J.; Luyt, L. G. An Integrated Imaging Probe Design: The Synthesis of  $^{99m}\text{Tc}/\text{Re}$ -Containing Macrocyclic Peptide Scaffolds. *Chem. - A Eur. J.* **2015**, *21* (2), 568–578. <https://doi.org/10.1002/chem.201404774>.
- (4) Alves, S.; Paulo, A.; Correia, J. D. G.; Gano, L.; Smith, C. J.; Hoffman, T. J.; Santos, I. Pyrazolyl Derivatives as Bifunctional Chelators for Labeling Tumor-Seeking Peptides with the  $\text{Fac-}[\text{M}(\text{CO})_3]^+$  Moiety ( $\text{M} = ^{99m}\text{Tc}, \text{Re}$ ): Synthesis, Characterization, and Biological Behavior. *Bioconjug. Chem.* **2005**, *16* (2), 438–449. <https://doi.org/10.1021/bc0497968>.
- (5) Mundwiler, S.; Kündig, M.; Ortner, K.; Alberto, R. A New  $[2 + 1]$  Mixed Ligand Concept Based on  $[\text{99}(\text{m})\text{Tc}(\text{OH}_2)_3(\text{CO})_3]^+$ : A Basic Study. *J. Chem. Soc. Dalton Trans.* **2004**, No. 9, 1320–1328. <https://doi.org/10.1039/b400220b>.
- (6) Gorshkov, N. I.; Schibli, R.; Schubiger, A. P.; Lumpov, A. A.; Miroslavov, A. E.; Suglobov, D. N. “ $2 + 1$ ” Dithiocarbamate-Isocyanide Chelating Systems for Linking  $\text{M}(\text{CO})_3^+$  ( $\text{M} = ^{99m}\text{Tc}, \text{Re}$ ) Fragment to Biomolecules. In *J. Organomet. Chem.*; 2004; *689* (25), pp 4757–4763. <https://doi.org/10.1016/j.jorganchem.2004.09.019>.
- (7) Schibli, R.; Katti, K. V.; Higginbotham, C.; Volkert, W. A.; Alberto, R. In Vitro and in Vivo Evaluation of Bidentate, Water-Soluble Phosphine Ligands as Anchor Groups for the Organometallic  $\text{Fac-}[\text{99mTc}(\text{CO})_3]^+$ -Core. *Nucl. Med. Biol.* **1999**, *26* (6), 711–716. [https://doi.org/10.1016/S0969-8051\(99\)00028-1](https://doi.org/10.1016/S0969-8051(99)00028-1).
- (8) Yazdani, A.; Janzen, N.; Banevicius, L.; Czorny, S.; Valliant, J. F. Imidazole-Based  $[2 + 1]$   $\text{Re}(\text{I})/^{99m}\text{Tc}(\text{I})$  Complexes as Isostructural Nuclear and Optical Probes. *Inorg. Chem.* **2015**, *54* (4), 1728–1736. <https://doi.org/10.1021/ic502663p>.
- (9) Pitchumony, T. S.; Banevicius, L.; Janzen, N.; Zubieta, J.; Valliant, J. F. Isostructural Nuclear and Luminescent Probes Derived from Stabilized  $[2 + 1]$  Rhenium(I)/Technetium(I) Organometallic Complexes. *Inorg. Chem.* **2013**, *52* (23), 13521–13528. <https://doi.org/10.1021/ic401972g>.
- (10) Schibli, R.; La Bella, R.; Alberto, R.; Garcia-Garayoa, E.; Ortner, K.; Abram, U.; Schubiger, P. A. Influence of the Denticity of Ligand Systems on the in Vitro and in Vivo Behavior of  $^{99m}\text{Tc}(\text{I})$ -Tricarbonyl Complexes: A Hint for the Future Functionalization of Biomolecules. *Bioconjug. Chem.* **2000**, *11* (3), 345–351. <https://doi.org/10.1021/bc990127h>.
- (11) Banerjee, S. R.; Levalada, M. K.; Lazarova, N.; Wei, L.; Valliant, J. F.; Stephenson, K. A.; Babich, J. W.; Maresca, K. P.; Zubieta, J. Bifunctional Single Amino Acid Chelates for Labeling of Biomolecules with the  $\{\text{Tc}(\text{CO})_3\}^+$  and  $\{\text{Re}(\text{CO})_3\}^+$  Cores. Crystal and Molecular Structures of  $[\text{ReBr}(\text{CO})_3(\text{H}_2\text{NCH}_2\text{C}_5\text{H}_4\text{N})]$ ,  $[\text{Re}(\text{CO})_3\{(\text{C}_5\text{H}_4\text{NCH}_2)_2\text{NH}\}]\text{Br}$ . *Inorg. Chem.* **2002**, *41* (24), 6417–6425. <https://doi.org/10.1021/ic020476e>.

- (12) Haiyang, H.; Morley, J. E.; Twamley, B.; Groeneman, R. H.; Bucar, D. K.; MacGillivray, L. R.; Benny, P. D. Investigation of the Coordination Interactions of S-(Pyridin-2-Ylmethyl)-L- Cysteine Ligands with  $M(\text{CO})_3^+$  ( $M = \text{Re}, 99\text{mTc}$ ). *Inorg. Chem.* **2009**, *48* (22), 10625–10634. <https://doi.org/10.1021/ic901159r>.
- (13) Karagiorgou, O.; Papagiannopoulou, D.; Kyprianidou, P.; Patsis, G.; Panagiotopoulou, A.; Tsoukalas, C.; Raptopoulou, C. P.; Pelecanou, M.; Pirmettis, I.; Papadopoulos, M. Synthesis and Structural Characterization of Novel Neutral Fac- $M(\text{CO})_3(\text{NSO})$  Complexes ( $M = \text{Re}, 99\text{mTc}$ ) with N-Acetylcysteine Derivatives as Tridentate NSO Ligands. *Polyhedron* **2009**, *28* (15), 3317–3321. <https://doi.org/10.1016/j.poly.2009.05.010>.
- (14) Leonidova, A.; Pierroz, V.; Adams, L. A.; Barlow, N.; Ferrari, S.; Graham, B.; Gasser, G. Enhanced Cytotoxicity through Conjugation of a “Clickable” Luminescent Re(I) Complex to a Cell-Penetrating Lipopeptide. *ACS Med. Chem. Lett.* **2014**, *5* (7), 809–814. <https://doi.org/10.1021/ml500158w>.
- (15) Amoroso, A. J.; Arthur, R. J.; Coogan, M. P.; Court, J. B.; Fernández-Moreira, V.; Hayes, A. J.; Lloyd, D.; Millet, C.; Pope, S. J. A. 3-Chloromethylpyridyl Bipyridine Fac-Tricarbonyl Rhenium: A Thiol-Reactive Luminophore for Fluorescence Microscopy Accumulates in Mitochondria. *New J. Chem.* **2008**, *32* (7), 1097–1102. <https://doi.org/10.1039/b802215a>.
- (16) Huang, D.; Zhao, P.; Astruc, D. Catalysis by 1,2,3-Triazole- and Related Transition-Metal Complexes. *Coord. Chem. Rev.* **2014**, *272*, pp 145–165. <https://doi.org/10.1016/j.ccr.2014.04.006>.
- (17) Connell, T. U.; Hayne, D. J.; Ackermann, U.; Tochon-Danguy, H. J.; White, J. M.; Donnelly, P. S. Rhenium and Technetium Tricarbonyl Complexes of 1,4-Substituted Pyridyl-1,2,3-Triazole Bidentate “click” Ligands Conjugated to a Targeting RGD Peptide. *J. Label. Compd. Radiopharm.* **2014**, *57* (4), 262–269. <https://doi.org/10.1002/jlcr.3169>.
- (18) Pace, C. N.; Scholtz, J. M. A Helix Propensity Scale Based on Experimental Studies of Peptides and Proteins. *Biophys. J.* **1998**, *75* (1), 422–427. [https://doi.org/10.1016/s0006-3495\(98\)77529-0](https://doi.org/10.1016/s0006-3495(98)77529-0).
- (19) Lin, H. C.; Kim, H.; Barlow, S.; Hales, J. M.; Perry, J. W.; Marder, S. R. Synthesis and Linear and Nonlinear Optical Properties of Metal-Terminated Bis(Dioxaborine) Polymethines. *Chem. Commun.* **2011**, *47* (2), 782–784. <https://doi.org/10.1039/c0cc02003f>.
- (20) Schmidt, S. P.; Nitschke, J.; Trogler, W. C.; Hockett, S. I.; Angelici, R. J. Manganese(I) and Rhenium(I) Pentacarbonyl(Trifluoromethanesulfonato) Complexes; *Inorg Syn* **1989**, *26*, 113-117. <https://doi.org/10.1002/9780470132579.ch20>.
- (21) Baxter, N. J.; Williamson, M. P. Temperature Dependence of  $^1\text{H}$  Chemical Shifts in Proteins. *J. Biomol. NMR* **1997**, *9*, 359–369. <https://doi.org/10.1023/A:1018334207887>.



- (22) Cierpicki, T.; Otlewski, J. Amide Proton Temperature Coefficients as Hydrogen Bond Indicators in Proteins. *J. Biomol. NMR* **2001**, *21*, 249–261.  
<https://doi.org/10.1023/A:1012911329730>.
- (23) Johnson, W. C. Secondary Structure of Proteins through Circular Dichroism Spectroscopy. *Annu. Rev. Biophys. Biophys. Chem.* **1988**, *17*, pp 145–166.  
<https://doi.org/10.1146/annurev.bb.17.060188.001045>.
- (24) Johnson, W. C. Analyzing Protein Circular Dichroism Spectra for Accurate Secondary Structures. *Proteins Struct. Funct. Genet.* **1999**, *35* (3), 307–312.  
[https://doi.org/10.1002/\(SICI\)1097-0134\(19990515\)35:3<307::AID-PROT4>3.0.CO;2-3](https://doi.org/10.1002/(SICI)1097-0134(19990515)35:3<307::AID-PROT4>3.0.CO;2-3).
- (25) Gopal, R.; Park, J. S.; Seo, C. H.; Park, Y. Applications of Circular Dichroism for Structural Analysis of Gelatin and Antimicrobial Peptides. *Int. J. Mol. Sci.* **2012**, *13* (3), 3229–3244. <https://doi.org/10.3390/ijms13033229>.

## Chapter Four

### 4 Conclusion

In recent years, cyclic peptides have achieved significant success as diagnostics and therapeutics. Constrained geometry of the cyclic peptides leads to improved properties like enhanced *in vivo* stability, good binding affinity and target selectivity. This gives them an edge over their linear counterparts and thus find application in the development of pharmaceutical products.<sup>1</sup> Peptides can be cyclized by various methods like head to tail, head to side chain, side chain to side chain cyclization or through formation of a disulfide bond. In addition to these classical methods, cyclization can be induced in peptides through metal coordination. The scope of the thesis is limited to the ability of group 7 metals, Re and the radioactive <sup>99m</sup>Tc, to induce cyclization in linear peptides.

Previously, Simpson *et.al* cyclized a pentapeptide sequence Ac-HAAAH using [Re(CO)<sub>3</sub>(OH)<sub>2</sub>]<sub>3</sub>OTf.<sup>2</sup> Terminal histidine amino acids were used as a chelator for coordinating with the metal tricarbonyl core. The tri-alanine sequence was selected due to the ability of alanine to form stable helices in water.<sup>3</sup> Histidine was used as a mono and a bidentate ligand where the monodentate coordination took place using the nitrogen of the imidazole side chain of histidine and bidentate chelation using the nitrogen of the imidazole and oxygen of the carboxylic acid present on the peptide C-terminus. This led to formation of a cyclic peptide where a turn was induced using the chelation of the ligands to the metal core, creating a 2+1 chelation complex. However, this system had numerous linkage isomers due to histidine having multiple coordinating sites. Separation of the isomers proved to be a challenging task. It was thus critical to select a chelator having lesser coordinating sites. Patel *et.al* used an unnatural amino acid 3-pyridyl alanine (3-Pal) along with a synthetic ligand pyridyl triazole (pyta) to cyclize the biologically relevant peptide sequence pyta-RGD-3Pal.<sup>4</sup> The sequence RGD was chosen due its increased affinity for the integrin  $\alpha_v\beta_3$  which is overexpressed in several cancer types<sup>5</sup>. The design involved the use of pyta as a bidentate ligand with its two-nitrogen atoms on the triazole ring chelating the metal and 3-pyridyl alanine as a monodentate ligand. The use of this unnatural amino acid and synthetic ligand combination, along with natural amino acid sequence RGD, led to formation of a peptidomimetic scaffold which would have the potential to improve the binding properties of the RGD motif.

The goal of this thesis was to apply this concept of using unnatural amino acid and synthetic ligand as chelators, for cyclization of the linear peptide sequence X-Ala-Ala-Ala-X (X= unnatural amino acid/synthetic ligand). We used the peptide sequence Ala-Ala-Ala since alanine is known to have higher propensity to form an alpha-helix.<sup>6</sup> Furthermore, alanine being one of the simplest amino acids, would be used as a model sequence to study the effect of metal based cyclization on the pentapeptide. It would then be possible to replace it with the biological relevant peptide sequence RGD.

Apart from pyta, we also aimed to use a different bidentate chelator 2,2'-bipyridine-4-carboxylic acid and study its effect on coordination. Both pyridyl triazole acetic acid and 2,2'-bipyridine-4-carboxylic acid forms a 5-membered ring with the metal complex, which considered to be a more stable ring size in contrast to the 7 membered ring formed by histidine as a chelator (Figure 4.1).

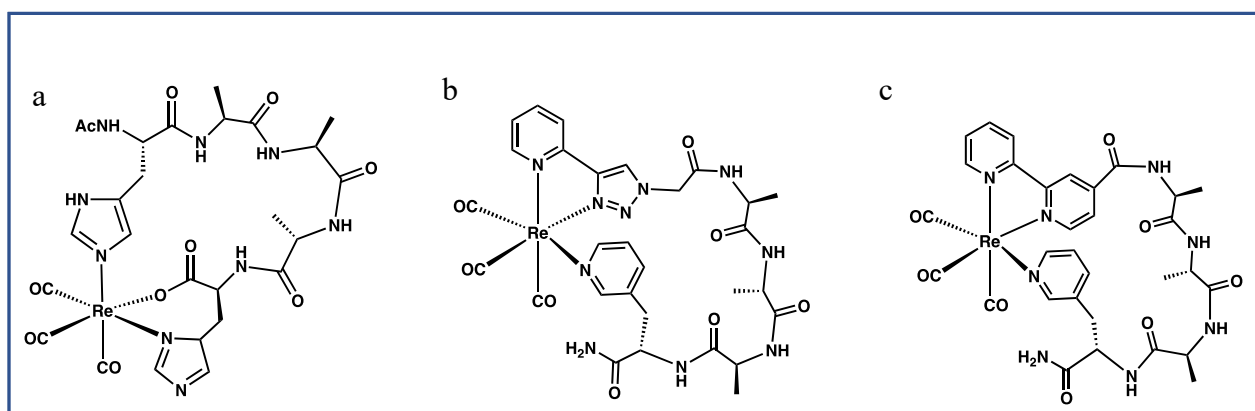


Figure 4.1 a) Formation of a 7 membered ring with histidine as a chelator, b), c) 5 membered ring formed by pyridyl triazole acetic acid and 2,2'-bipyridine-4-carboxylic acid

Prior to moving towards cyclization, it was critical to optimize the reaction conditions used for rhenium coordination. The replication of the coordination reaction conditions used previously by Simpson *et.al* and Patel *et.al* did not lead to effective yield of cyclic product. Thus, chapter two describes the optimization methods carried out to improve the yield of cyclic peptide. Temperature and time proved to be the essential factors which helped in reaction optimization. It was observed that on increasing the temperature, there was an increase in the yield of the cyclic product. However, excessive heat leads to formation of conformers/isomers which were observed on analysis of the crude product on the LCMS. In order to effectively increase the yield as well keep

the formation of the less dominant conformer/isomer to the minimum, a reaction condition was decided based on the quantification done by UHPLC. In addition to time and temperature, factors like change in solvents and presence/absence of base was also taken in consideration.

It was observed that even after applying optimal conditions, some of the linear peptide would still remain uncyclized. It was then imperative to acknowledge the effect of peptide length on the cyclization reaction. Assuming that the short pentapeptide would not be flexible enough to form a turn and chelate the metal in 2+1 fashion, we synthesized the peptide sequences with increasing length. Thus, peptide sequences pyta-Ala-Ala-Ala-Ala-3pal, pyta-Ala-Ala-Ala-Ala-Ala-3pal were synthesized. In addition to above mentioned peptides, another peptide sequence pyta-Ala-ala-Ala-3pal was synthesized with D-alanine in the center. D-amino acids are known to aid in cyclization by conformational preorganization.<sup>7</sup> All of these linear peptides were cyclized using  $[\text{Re}(\text{CO})_3(\text{OH}_2)_3] \text{OTf}$  and the yields were compared to the pentapeptide sequence pyta-Ala-Ala-Ala-3Pal. It was observed that a relatively better yield was obtained when using the hexapeptide sequence having four alanine in the center. In contrast, the other peptide modifications did not provide any improvement in the yield. The hexapeptide sequence was used for further studies along with the pentapeptide sequences synthesized using the two different chelators. Peptides were cyclized using rhenium tricarbonyl core and it was observed that there was formation of a dominant conformer along with some minor conformer/isomer peaks. Complete separation of the later eluting conformers through RP-HPLC was not feasible, however, the dominant product was separated. The dominant conformers from all the cyclization reaction were studied using NMR spectroscopy and suggested specific changes in chemical shift which proved that the peptide was coordinated to the metal in 2+1 chelation fashion. Further studies were done using circular dichroism spectroscopy which revealed a change in conformation in cyclic peptide. This suggests that a turn was induced in the linear peptide. However, the change in conformation was more predominant with peptides having pyta as a ligand in comparison to bipyridine. Further confirmation of the secondary structure was done using variable temperature NMR spectroscopy which helps in the detection of intramolecular hydrogen bonds. VT NMR spectroscopy studies suggested the intramolecular hydrogen bonding does take place based on the values of  $\Delta\delta/\Delta T$ .

We then aimed to cyclize the linear peptide pyta-Ala-Ala-Ala-3Pal using  $[\text{}^{99\text{m}}\text{Tc}(\text{CO})_3(\text{OH}_2)_3]^+$ . It was assumed that rhenium and technetium being in the same group would behave in a similar

manner and would coordinate to the linear peptide to form the same dominant cyclic conformer. However, a unique scientific observation was made when technetium, instead of coordinating and forming the same dominant cyclic product, chelated and formed a cyclic product which correlated to the other conformer/isomers obtained as minor products in the rhenium coordination reaction. Though  $^{99m}\text{Tc}(\text{CO})_3^+$  did not coordinate the way we assumed it would, we were still successful in performing the coordination reaction and cyclizing the linear peptide.

In conclusion, we were able to cyclize the linear peptide sequences using  $\text{Re}/^{99m}\text{Tc}(\text{CO})_3^+$  metal coordination creating a 2+1 chelation complex. Future work can involve the use of different chelators for both C- and N- terminals and observation of the effect of chelation. X-ray crystal structure studies would be impactful in studying the different conformers/isomers produced due to cyclization.

## 4.1 References

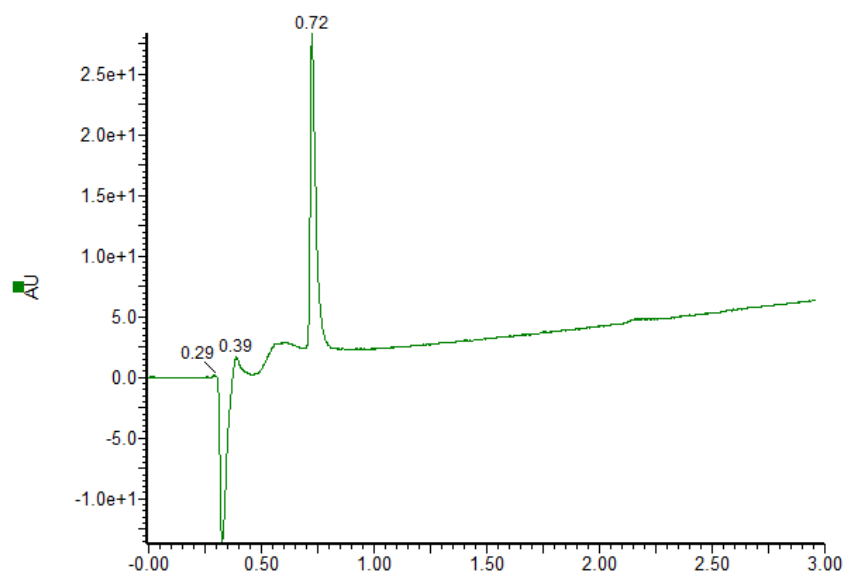
- (1) Marsault, E.; Peterson, M. L. Macrocycles Are Great Cycles: Applications, Opportunities, and Challenges of Synthetic Macrocycles in Drug Discovery. *J. Med. Chem.* **2011**, *54* (7), 1961–2004. <https://doi.org/10.1021/jm1012374>.
- (2) Simpson, E. J. The Development of Metal-Organic Compounds for Use as Molecular Imaging Agents. **2014**.
- (3) Courter, J. R.; Abdo, M.; Brown, S. P.; Tucker, M. J.; Hochstrasser, R. M.; Smith, A. B. The Design and Synthesis of Alanine-Rich  $\alpha$ -Helical Peptides Constrained by an s,s-Tetrazine Photochemical Trigger: A Fragment Union Approach. *J. Org. Chem.* **2014**, *79* (2), 759–768. <https://doi.org/10.1021/jo402680v>.
- (4) Patel, A. The Development of Cyclic RGD Peptides Stabilized Through  $^{99m}\text{Tc} / \text{Re}(\text{CO})_3^+$ . **2015**.
- (5) Xiong, J. P.; Stehle, T.; Zhang, R.; Joachimiak, A.; Frech, M.; Goodman, S. L.; Arnaout, M. A. Crystal Structure of the Extracellular Segment of Integrin  $\text{AV}\beta 3$  in Complex with an Arg-Gly-Asp Ligand. *Science*. **2002**, *296* (5565), 151–155. <https://doi.org/10.1126/science.1069040>.

- (6) Pace, C. N.; Scholtz, J. M. A Helix Propensity Scale Based on Experimental Studies of Peptides and Proteins. *Biophys. J.* **1998**, *75* (1), 422–427. [https://doi.org/10.1016/s0006-3495\(98\)77529-0](https://doi.org/10.1016/s0006-3495(98)77529-0).
- (7) Yongye, A. B.; Li, Y.; Giulianotti, M. A.; Yu, Y.; Houghten, R. A.; Martínez-Mayorga, K. Modeling of Peptides Containing D-Amino Acids: Implications on Cyclization. *J. Comput. Aided. Mol. Des.* **2009**, *23*, 677–689. <https://doi.org/10.1007/s10822-009-9295-y>.

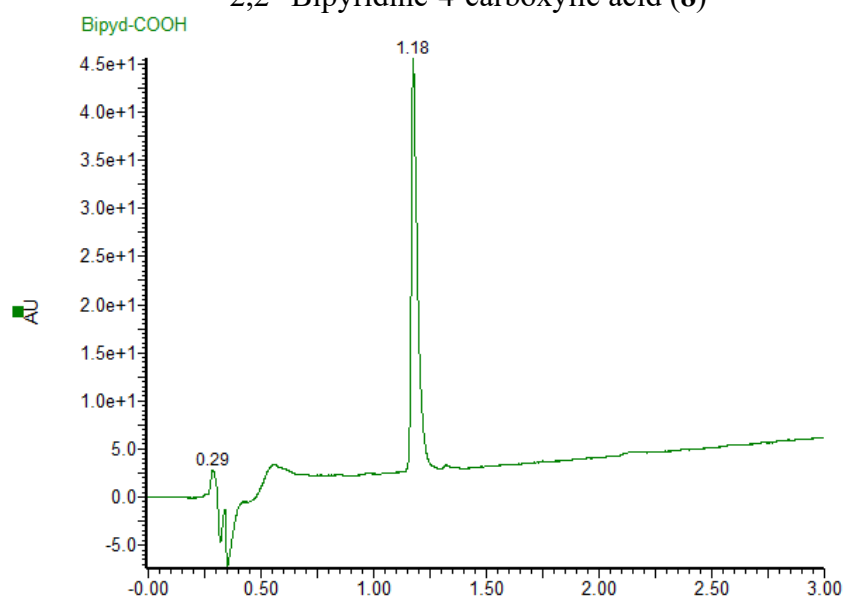
## Appendices

### Appendix A Chromatographs of selected compounds (UHPLC-MS UV traces)

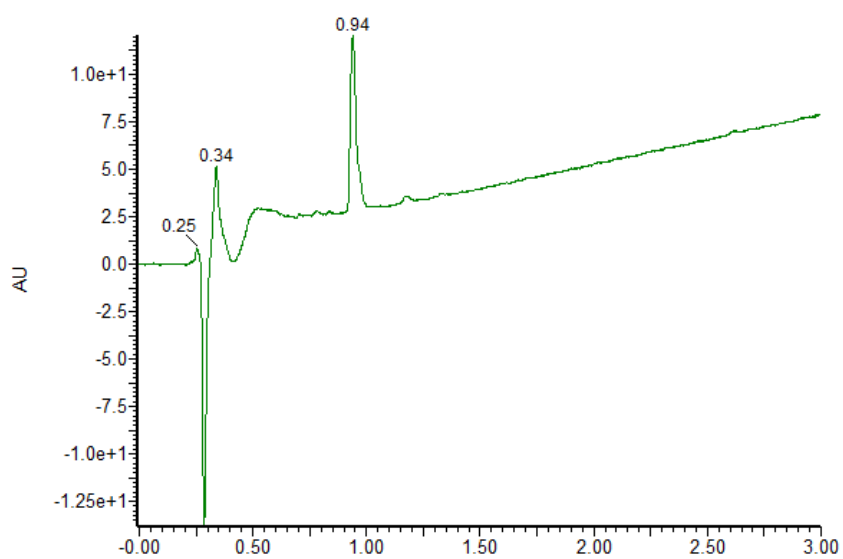
Pyridyl triazole acetic acid (**3**)



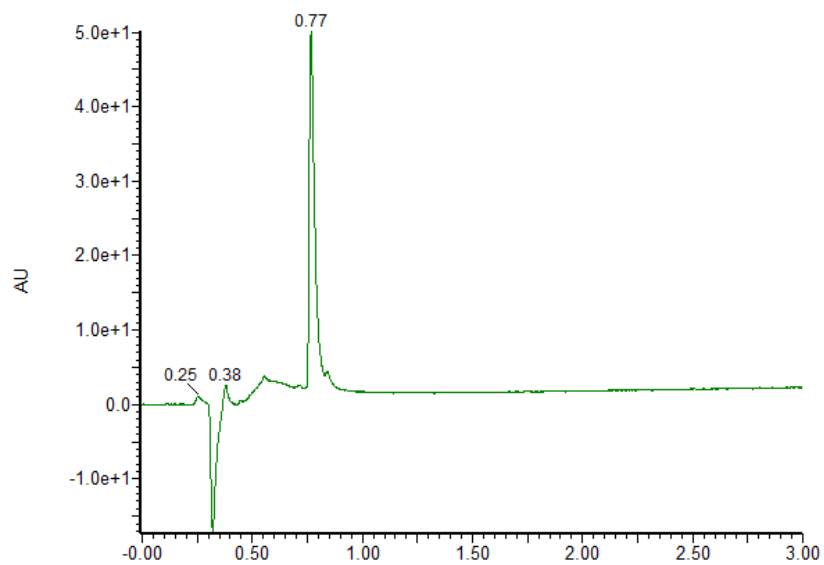
2,2'-Bipyridine-4-carboxylic acid (**8**)



Pyta-Ala-Ala-Ala-3pal, (3.1)

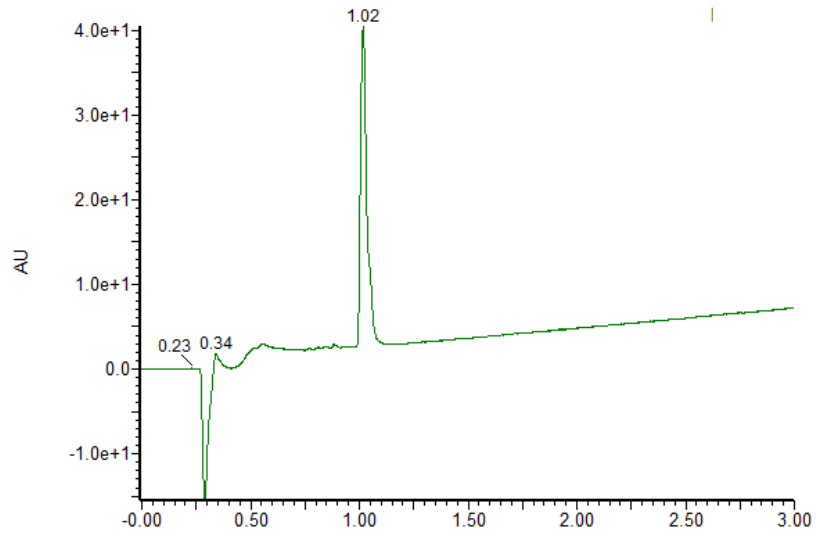


Pyta-Arg-Gly-Asp-3pal (3.2)

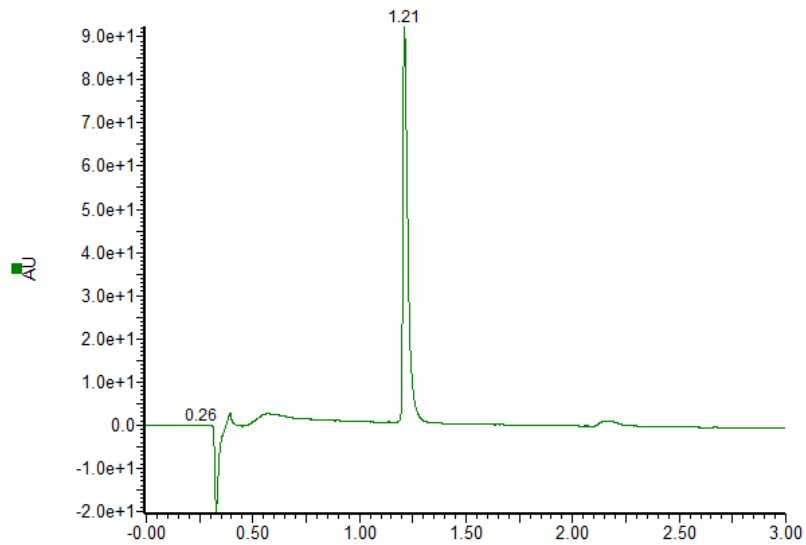




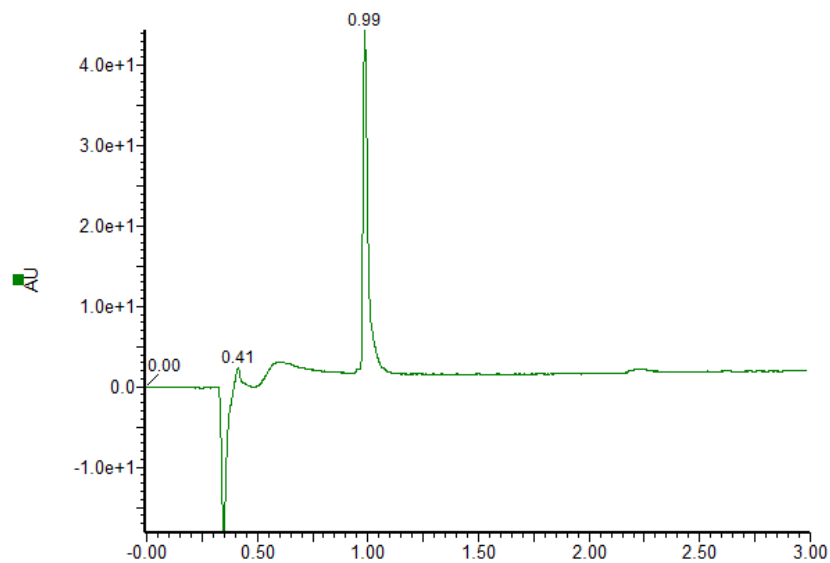
Pyta-Ala-Ala-Ala-Ala-3pal (3.3)



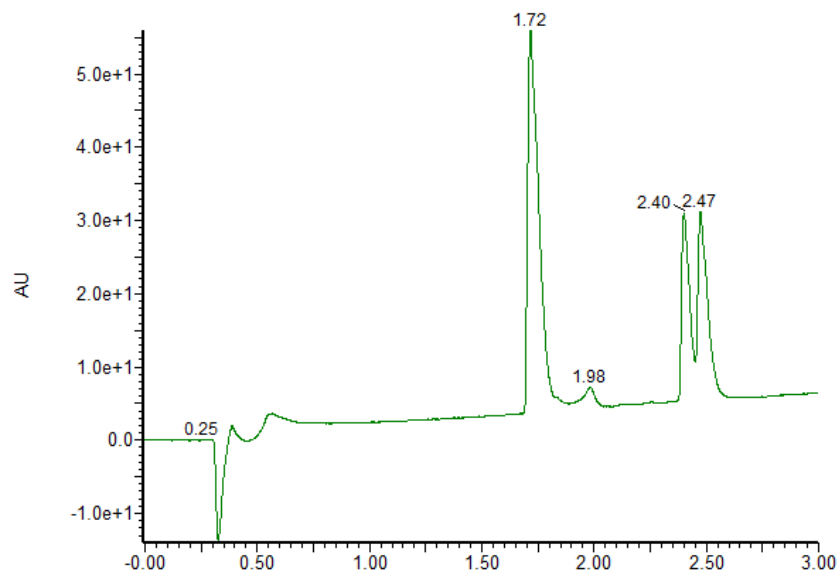
Bipyd-Ala-Ala-Ala -3pal (3.6)



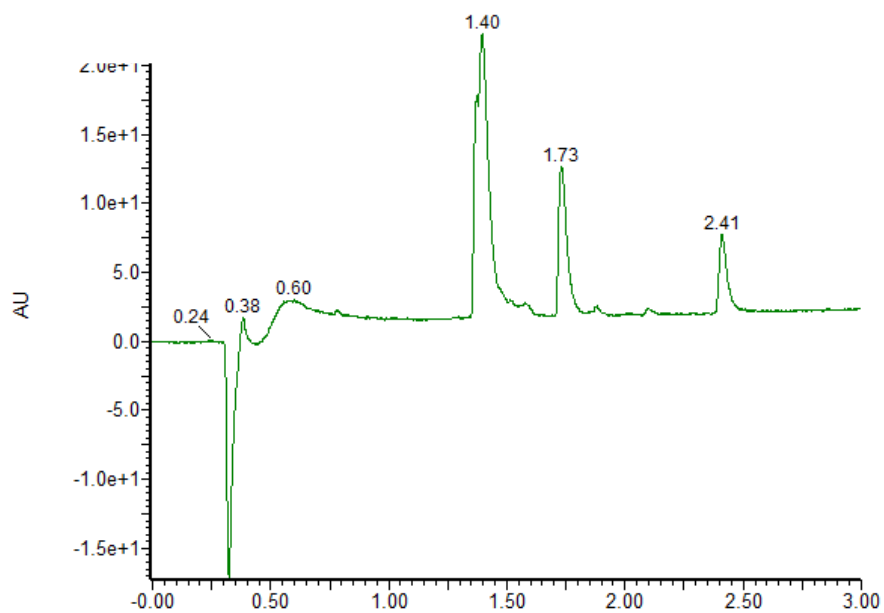
Bipyd-Arg-Gly-Asp -3pal (3.7)



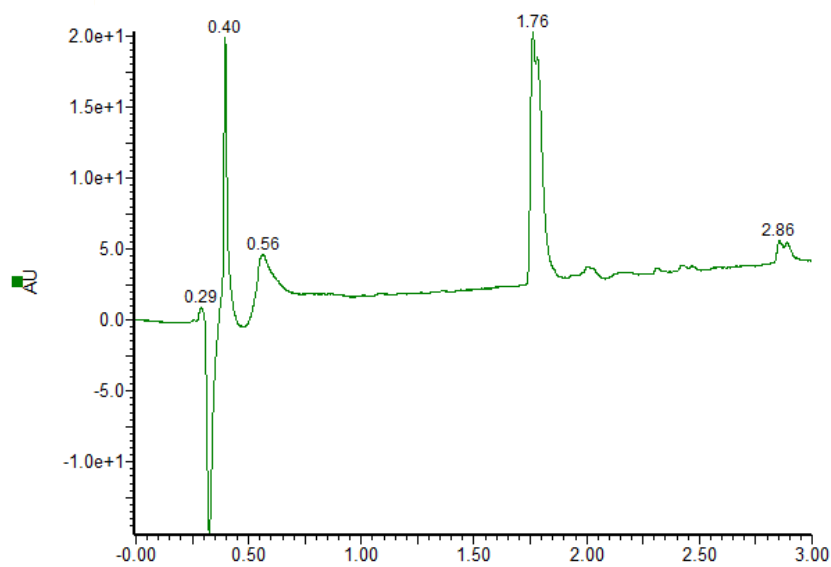
Re(CO)<sub>3</sub>[Pyta-Ala-Ala-Ala-3pal] (3.8)



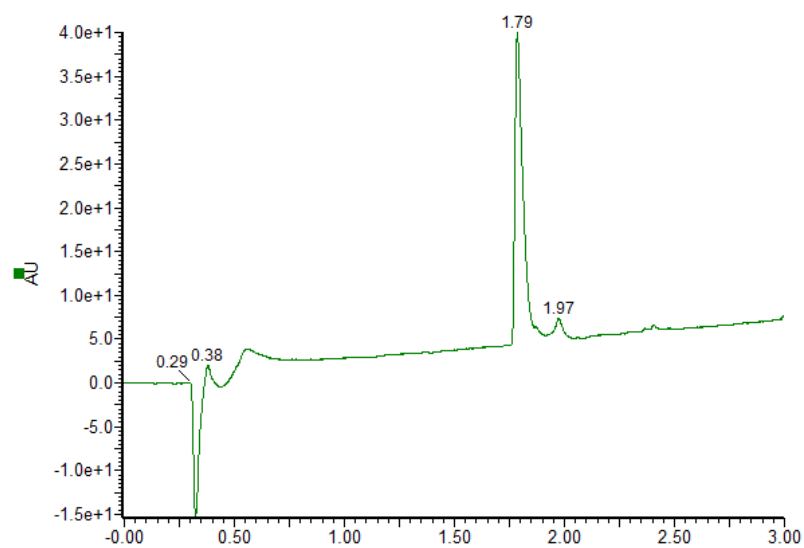
$\text{Re}(\text{CO})_3[\text{Pyta-Arg-Gly-Asp-3pal}]$  (3.9)



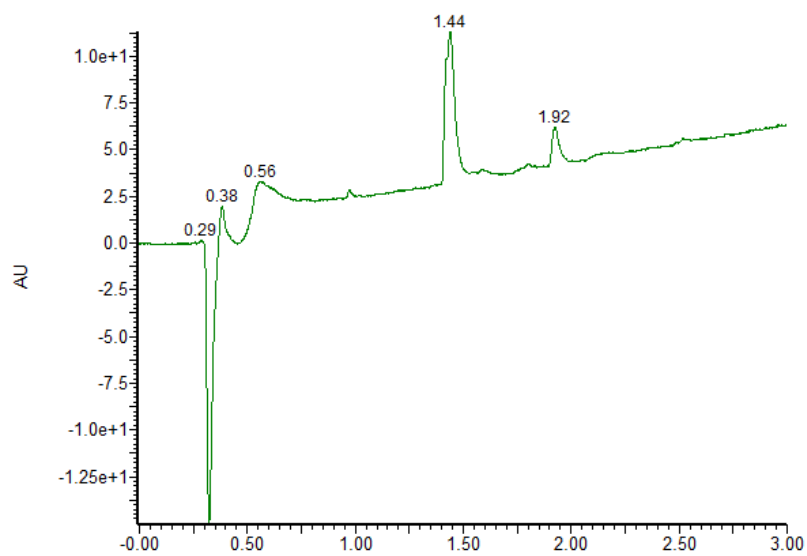
$\text{Re}(\text{CO})_3[\text{Pyta-Ala-Ala-Ala-Ala-3pal}]$  (3.10)



$\text{Re}(\text{CO})_3[\text{Bipyd-Ala-Ala-Ala-3pal}]$  (3.13)

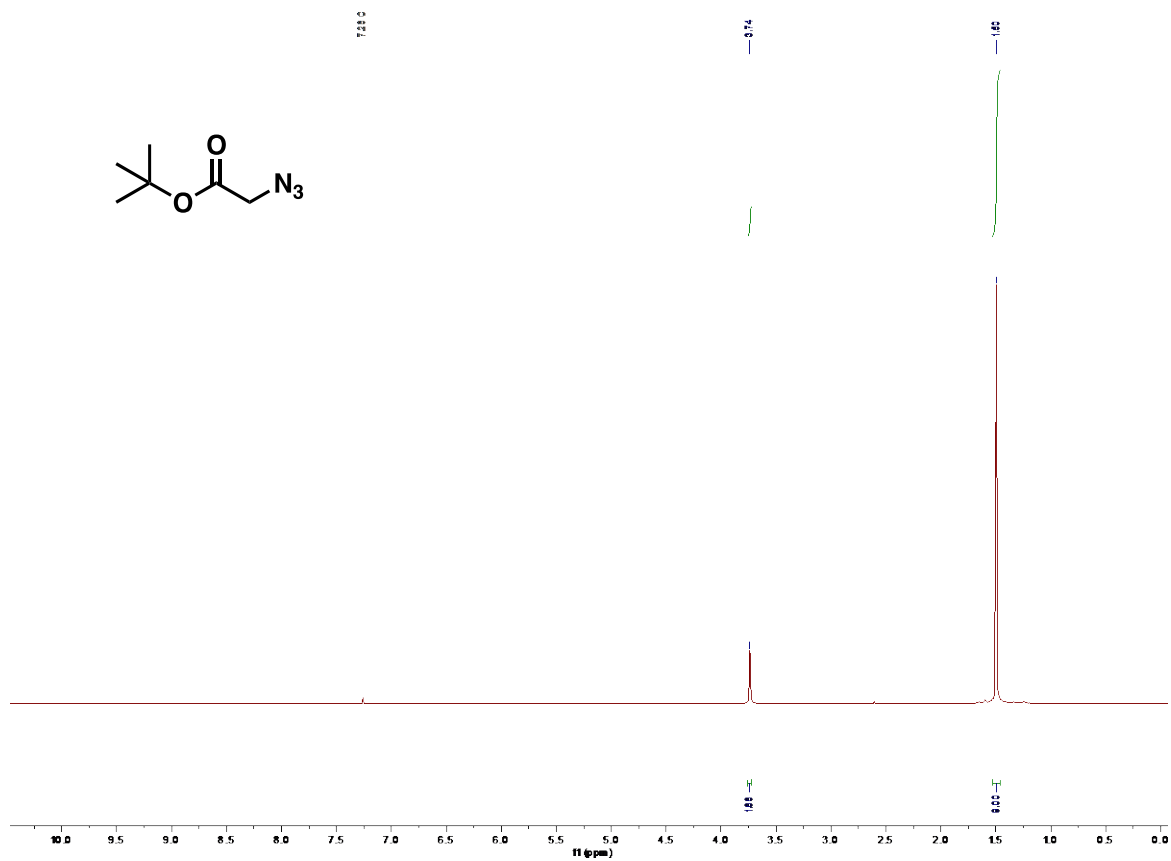


$\text{Re}(\text{CO})_3[\text{Bipyd-Arg-Gly-Asp-3pal}]$  (3.14)



Appendix B.  $^1\text{H}$  and 2D g-COSY, NOESY NMR spectra of linear and cyclic peptides

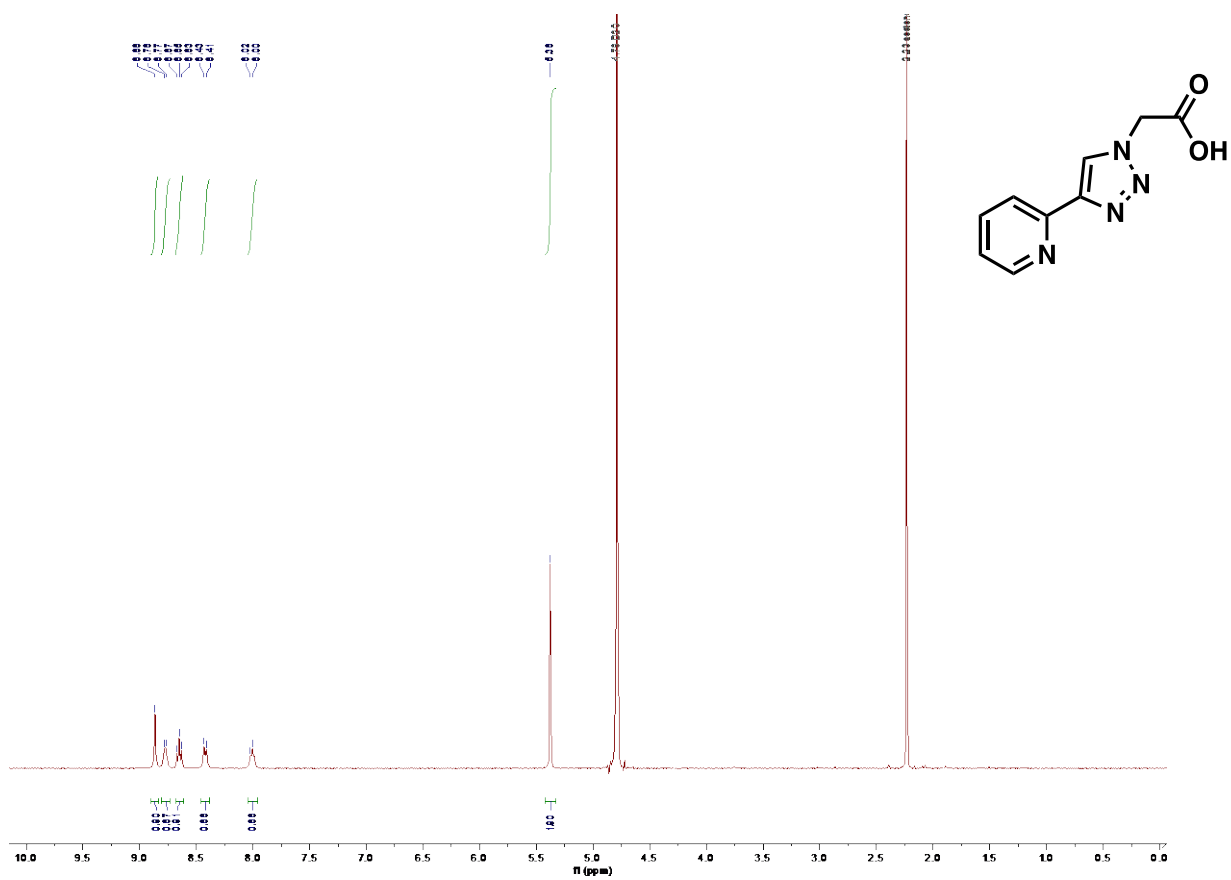
$^1\text{H}$  NMR spectra of *tert*-butyl azido acetate (**1**) in  $\text{CDCl}_3$  at 400 MHz



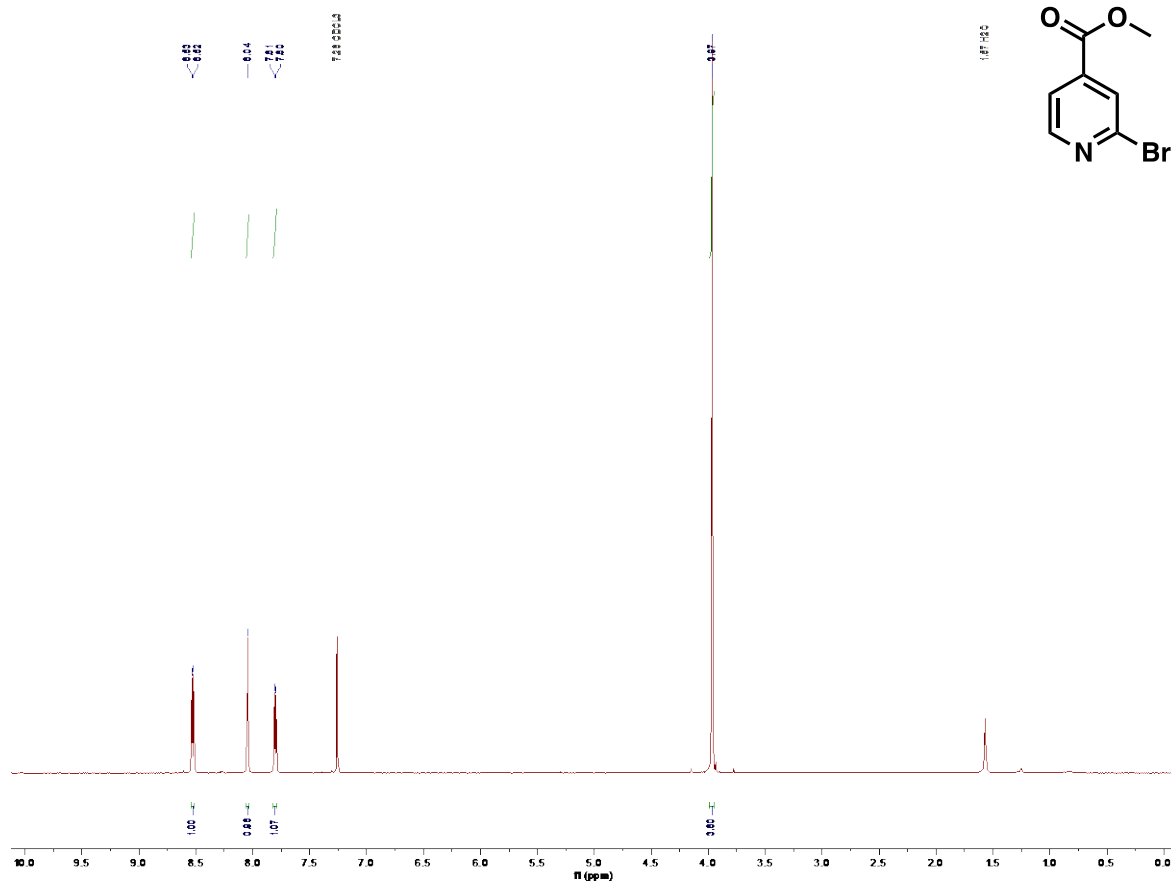
$^1\text{H}$  NMR spectra of pyridyl triazole *tert*-butyl acetate (**2**) in  $\text{CDCl}_3$  at 400 MHz



$^1\text{H}$  NMR spectra of pyridyl triazole acetic acid (pyta) (**3**) in  $\text{DMSO-d}_6$  at 400 MHz

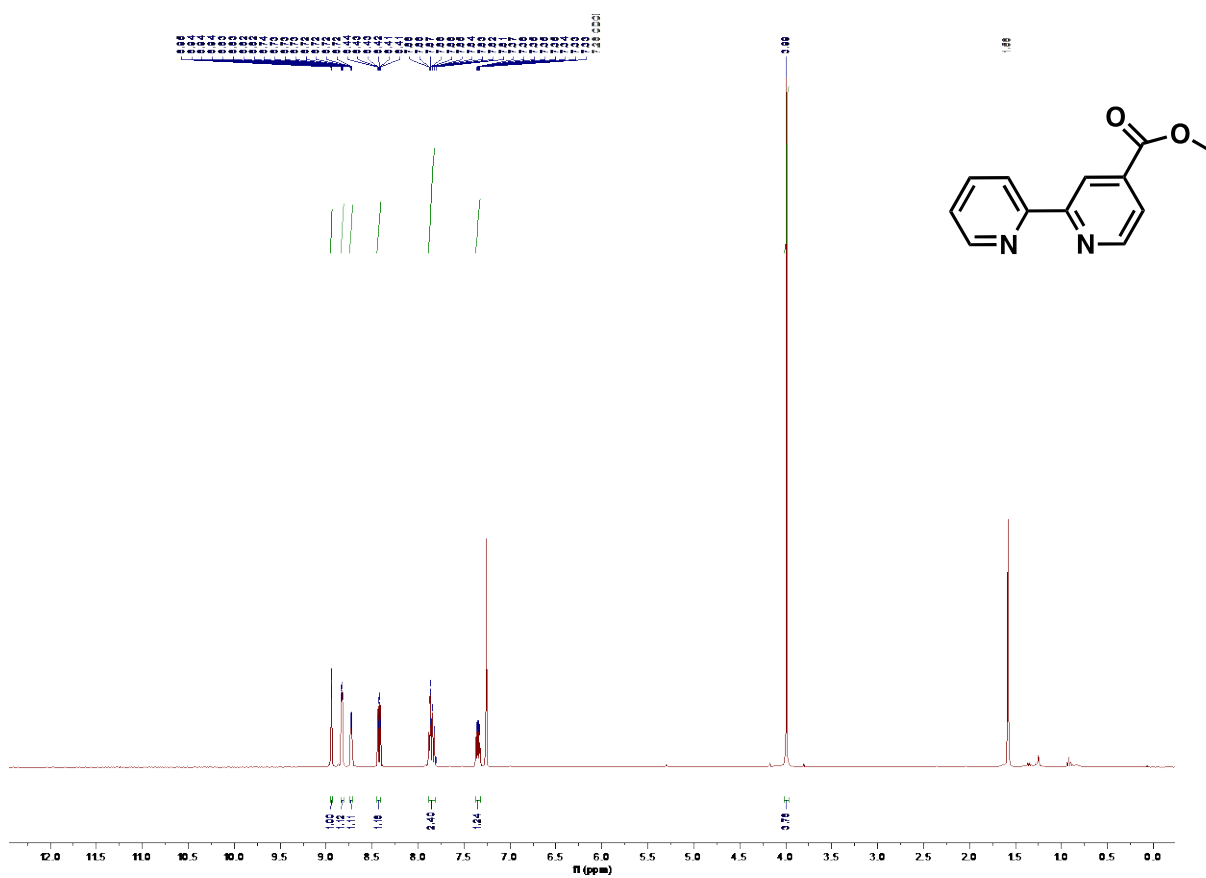


$^1\text{H}$  NMR spectra of 4-Methyl-2-bromopyridine carboxylate (**6**) in  $\text{CDCl}_3$  at 400 MHz

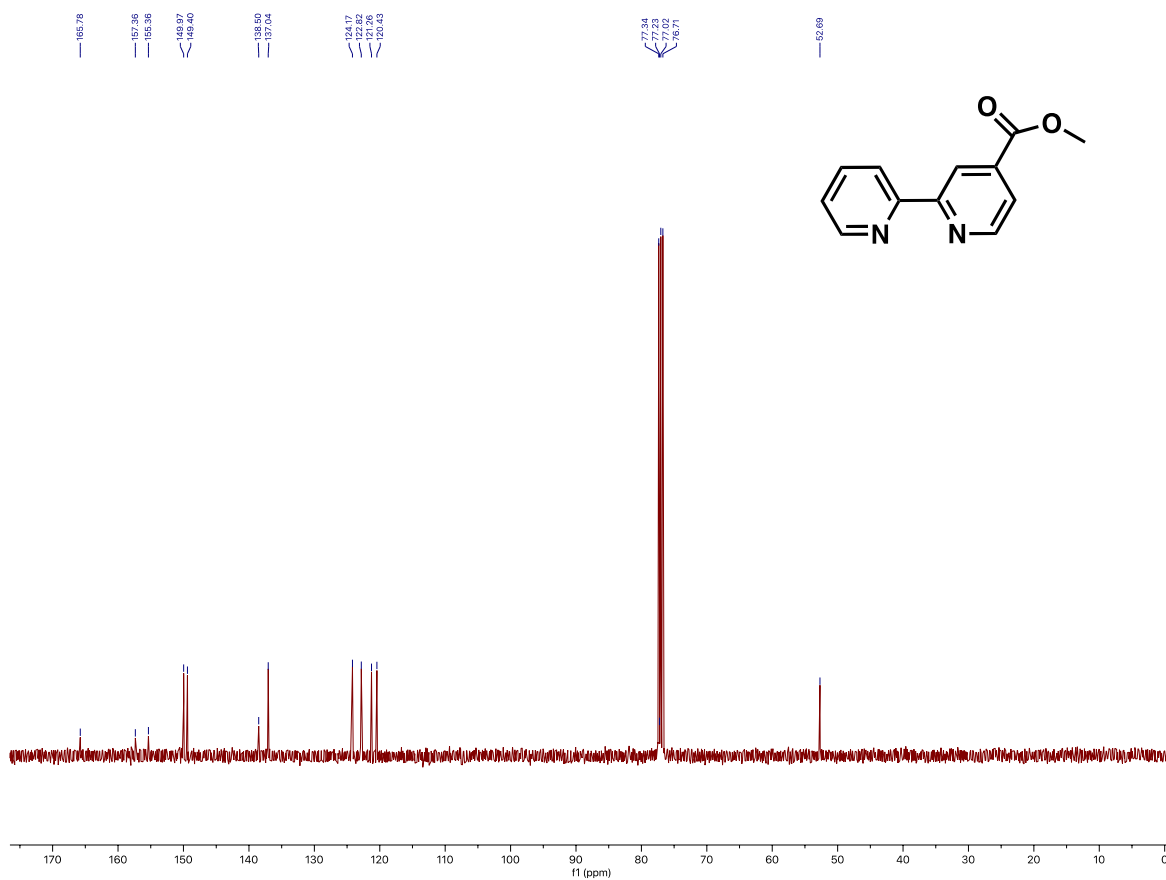




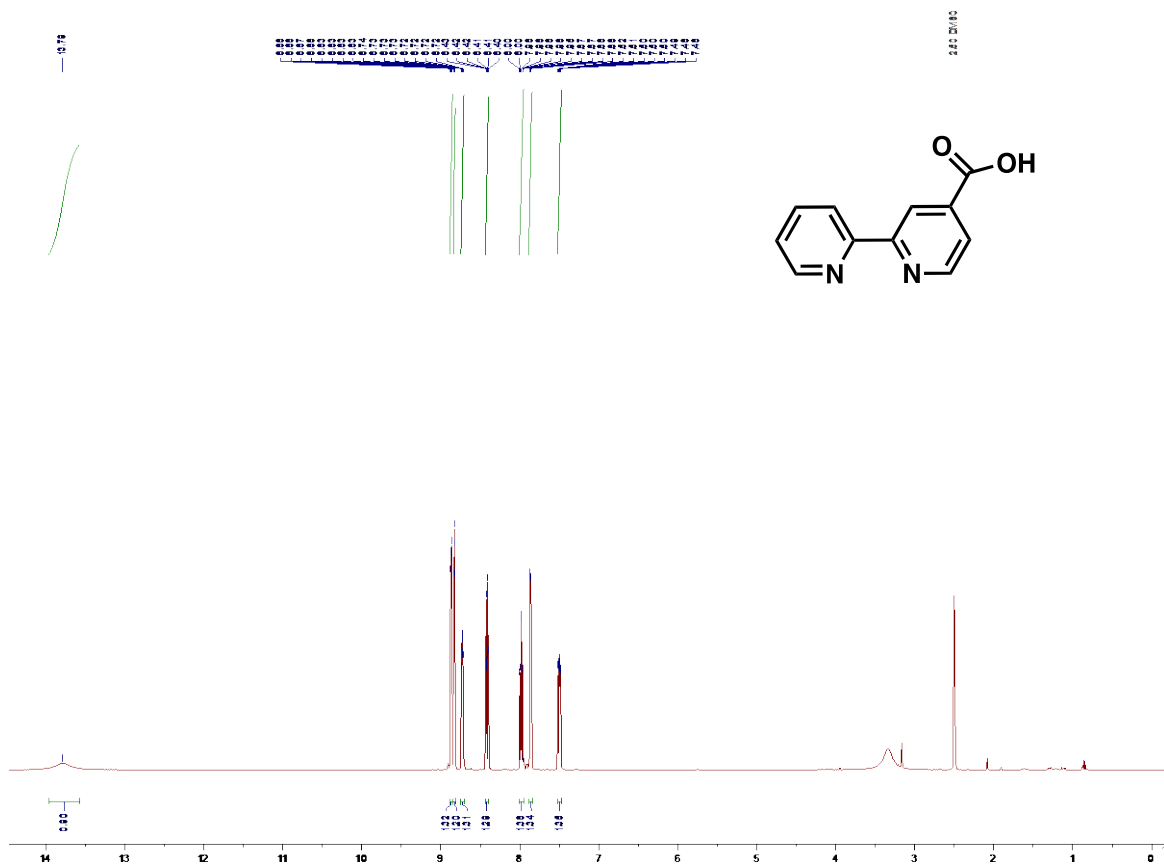
$^1\text{H}$  NMR spectra of 4-Methyl-2,2'-bipyridine carboxylate (7) in  $\text{CDCl}_3$  at 400 MHz



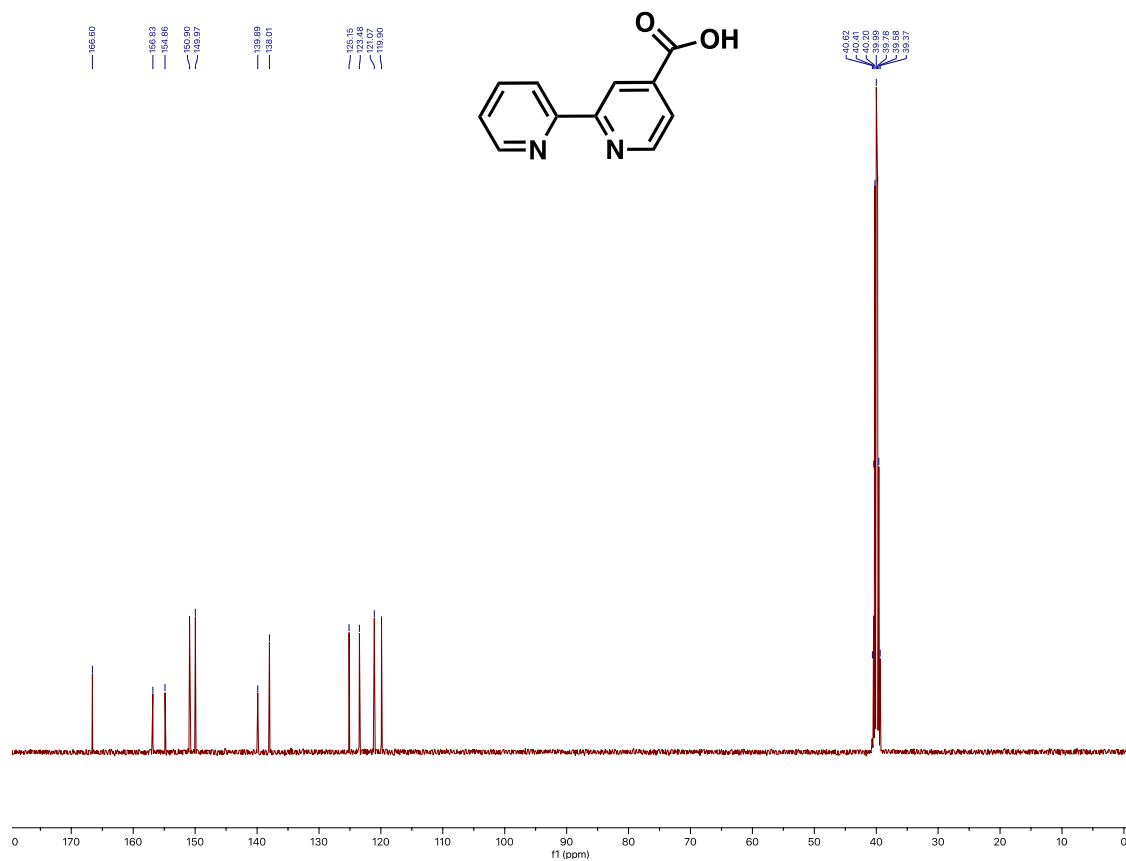
$^{13}\text{C}$  NMR spectra of 4-Methyl-2,2'-bipyridine carboxylate (**7**) in  $\text{CDCl}_3$  at 400 MHz



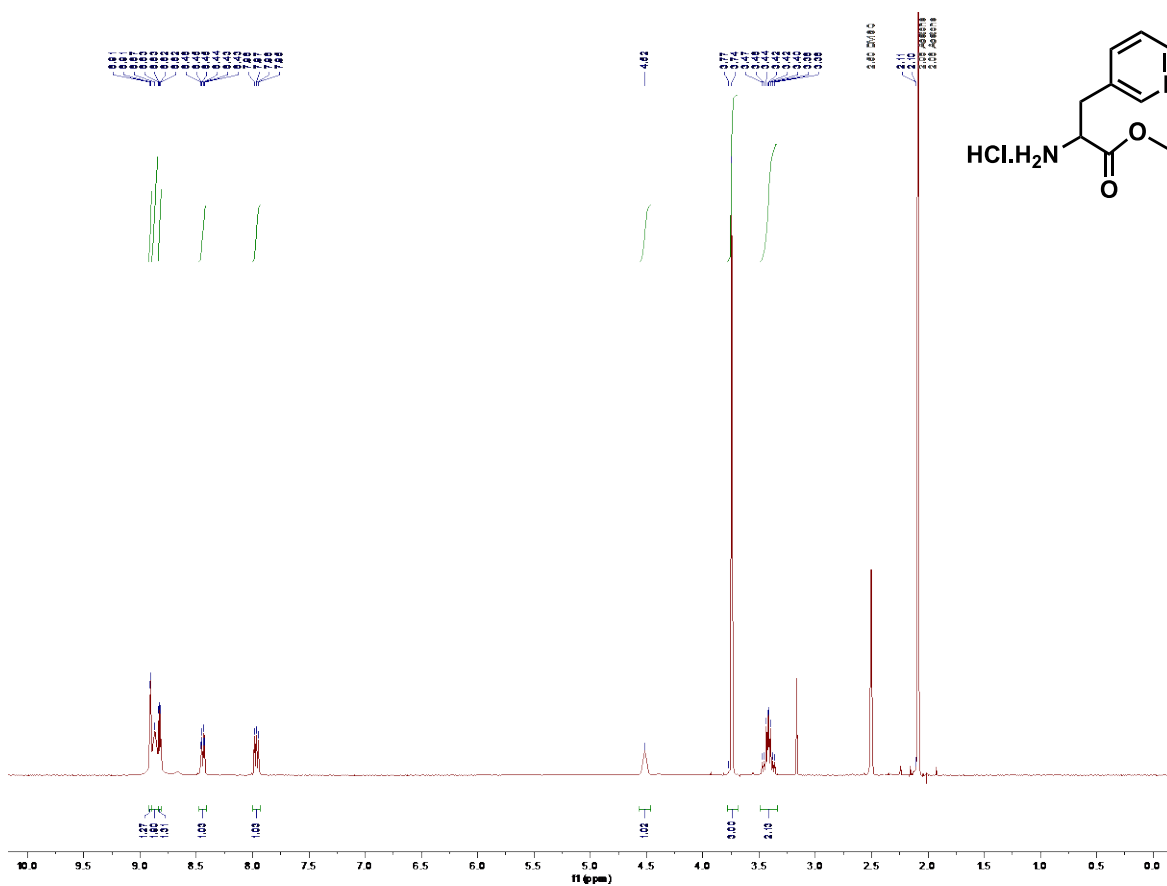
$^1\text{H}$  NMR spectra of 2,2'-Bipyridine-4-carboxylic acid (**8**) in  $\text{DMSO-d}_6$  at 400 MHz



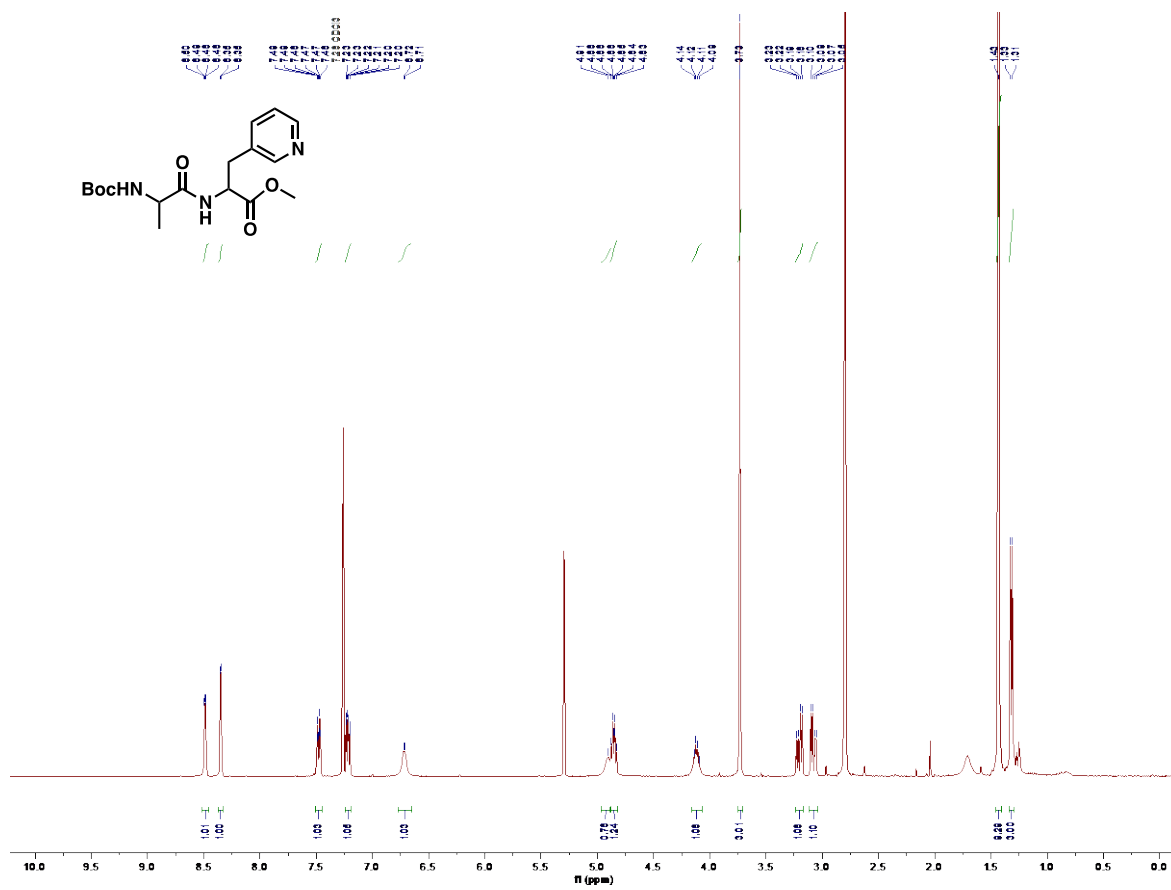
$^{13}\text{C}$  NMR spectra of 2,2'-Bipyridine-4-carboxylic acid (**8**) in DMSO- $d_6$  at 400 MHz



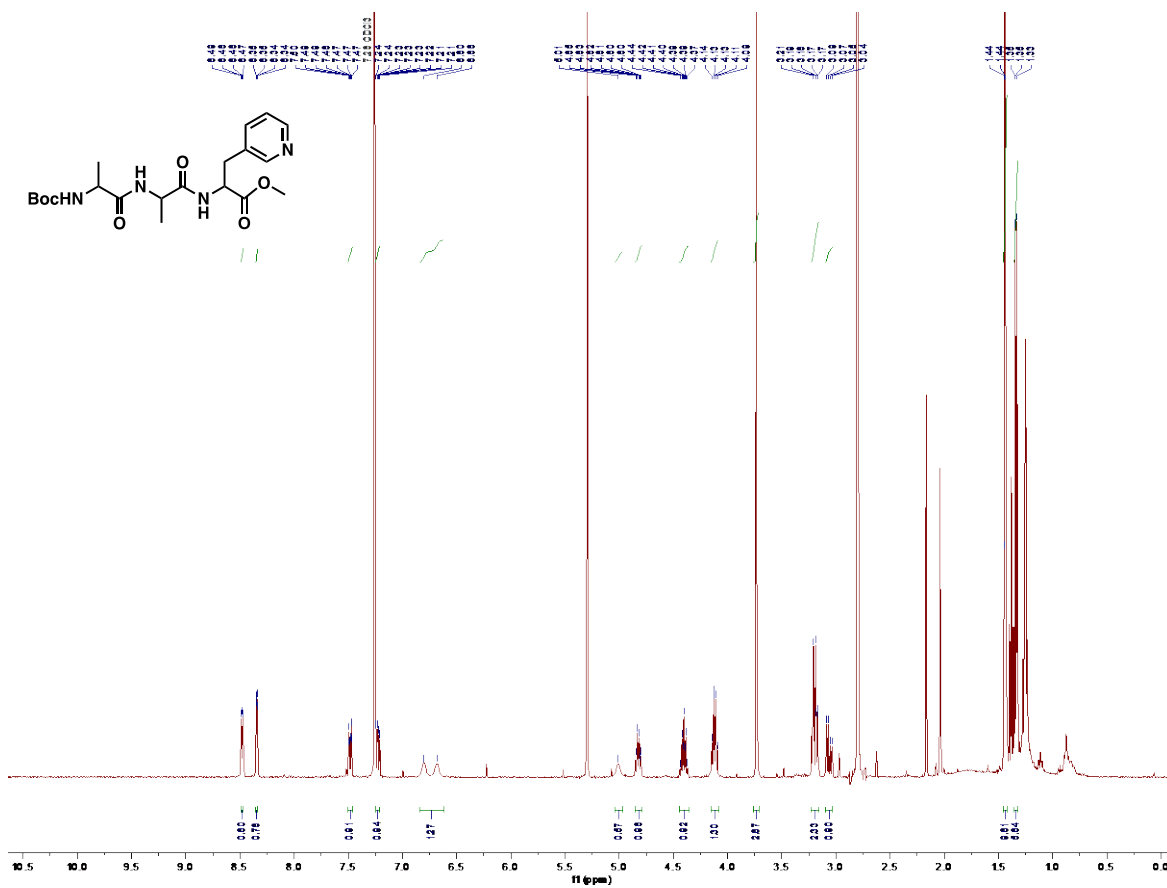
$^1\text{H}$  NMR spectra of 3-pyridyl alanine methyl ester (**4**) in  $\text{DMSO-d}_6$  at 400 MHz



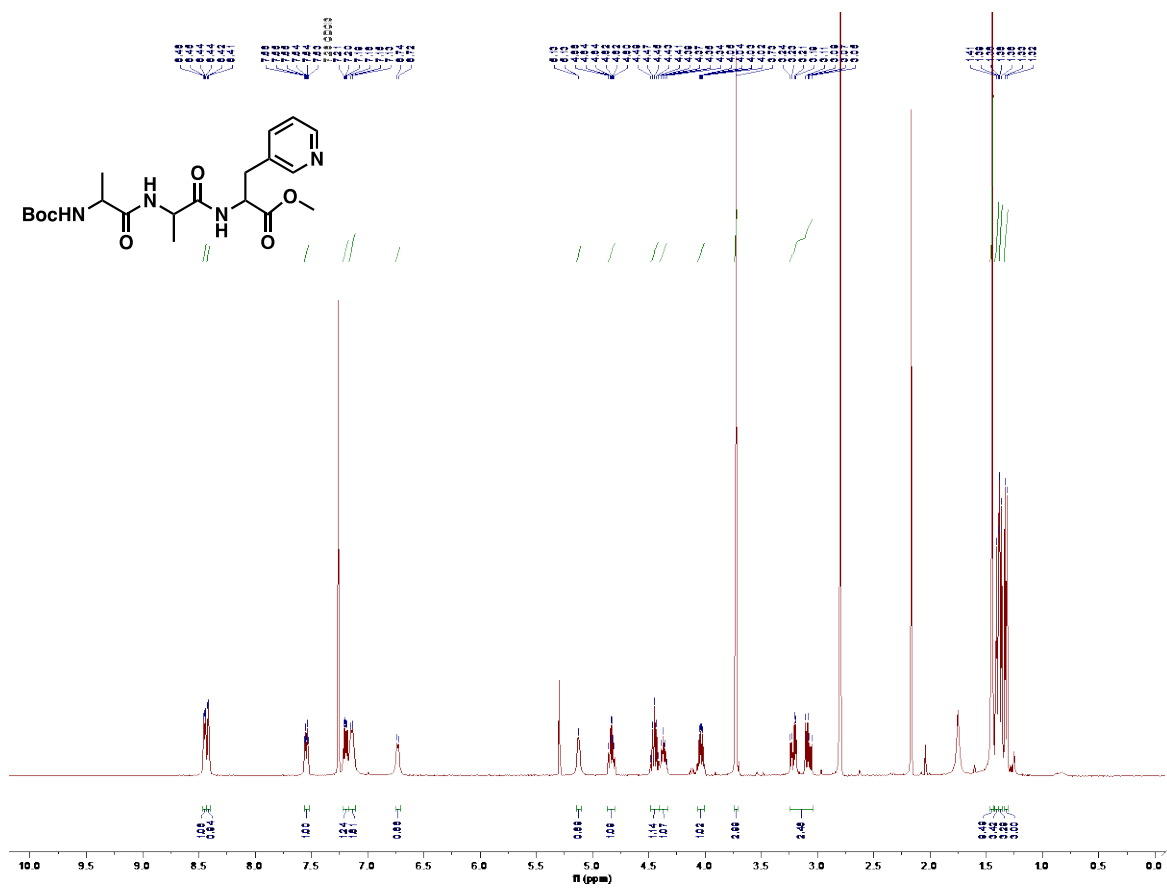
$^1\text{H}$  NMR spectra of Boc-Ala-3Pal-OMe (**2.1**) in  $\text{CDCl}_3$  at 400 MHz



$^1\text{H}$  NMR spectra of Boc-Ala-Ala-3Pal-OMe (**2.2**) in  $\text{CDCl}_3$  at 400 MHz

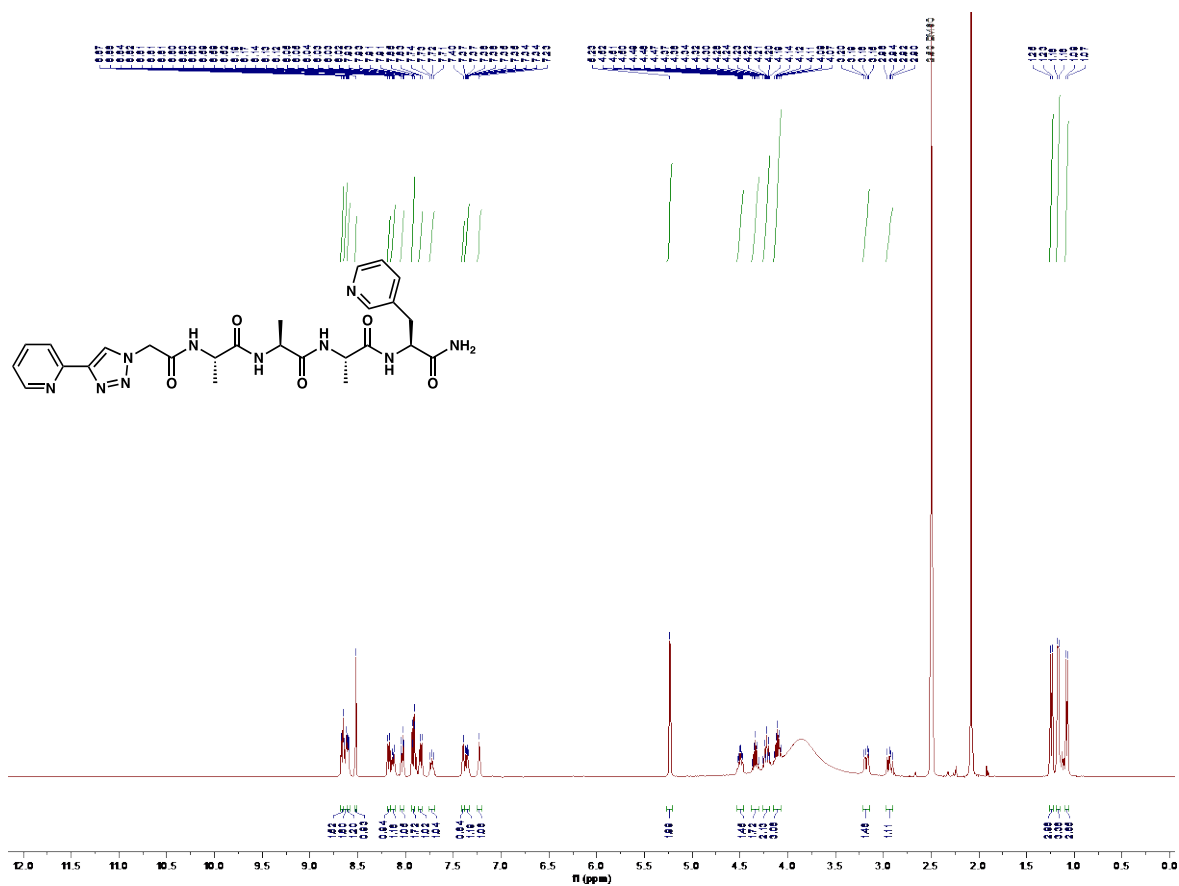


$^1\text{H}$  NMR spectra of Boc-Ala-Ala-Ala-3Pal-OMe (**2.3**) in  $\text{CDCl}_3$  at 400 MHz

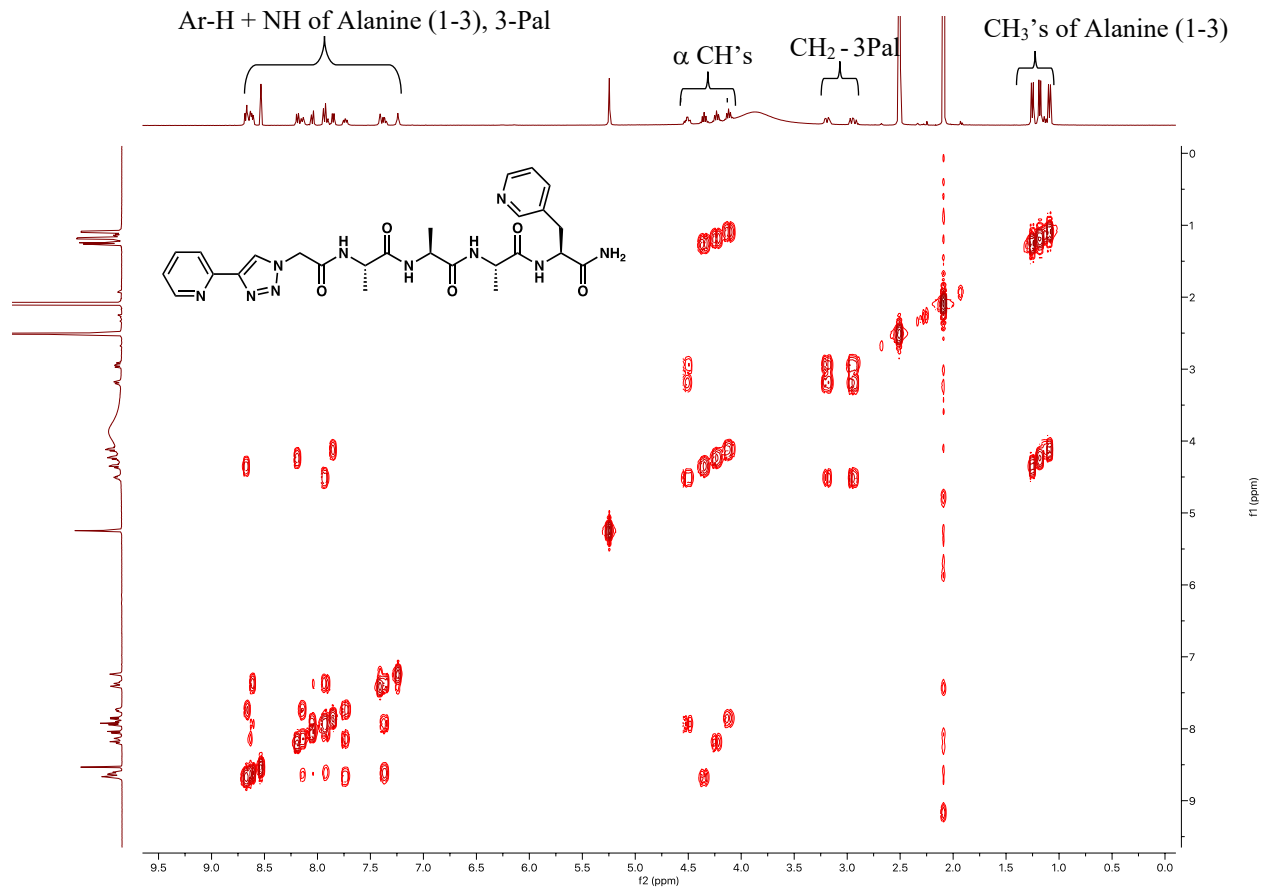




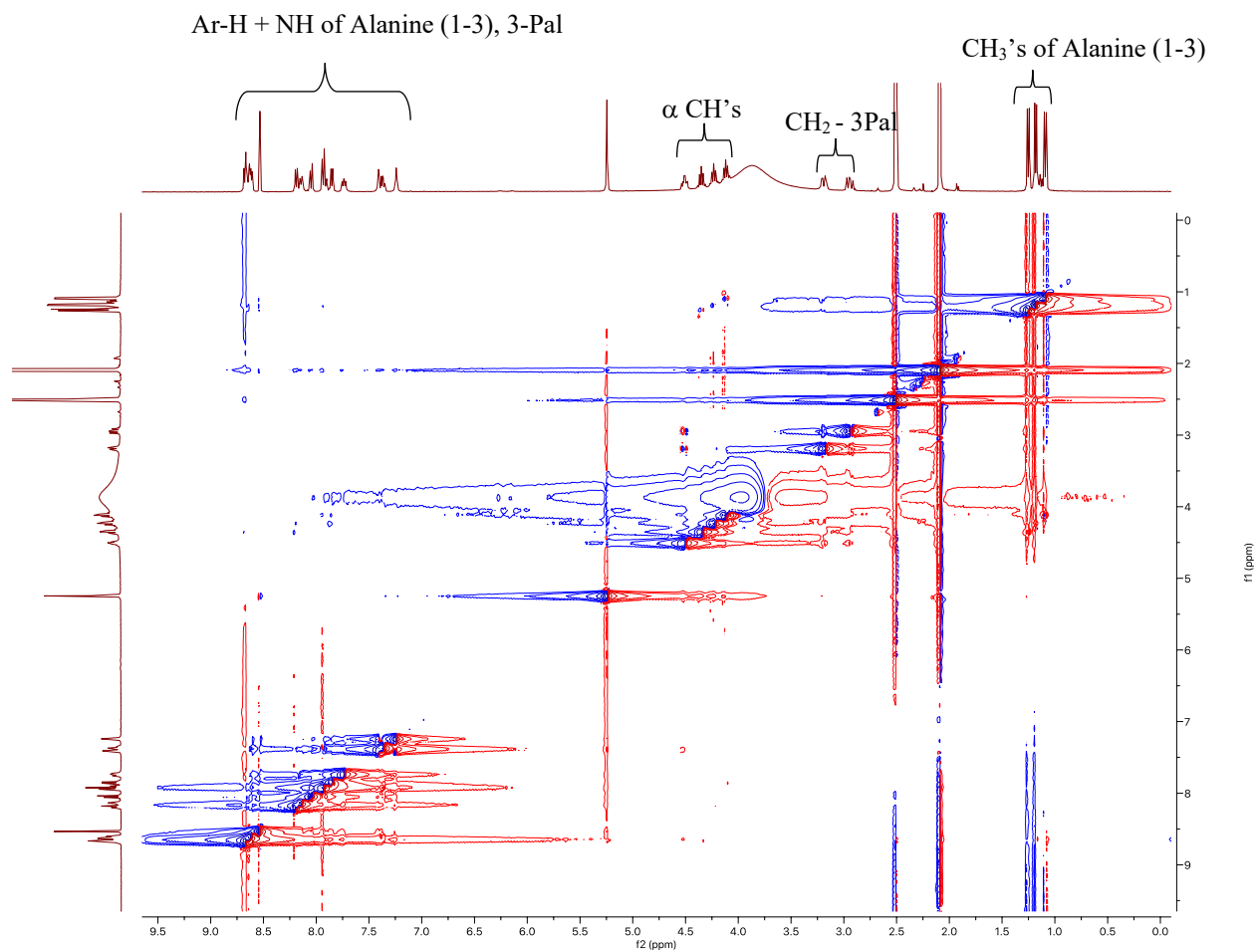
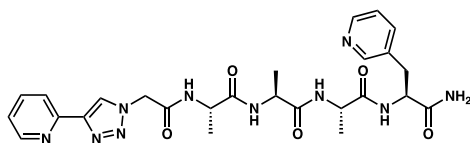
$^1\text{H}$  NMR spectra of pyta-Ala-Ala-Ala-3Pal (**3.1**) in DMSO- $d_6$  at 400 MHz



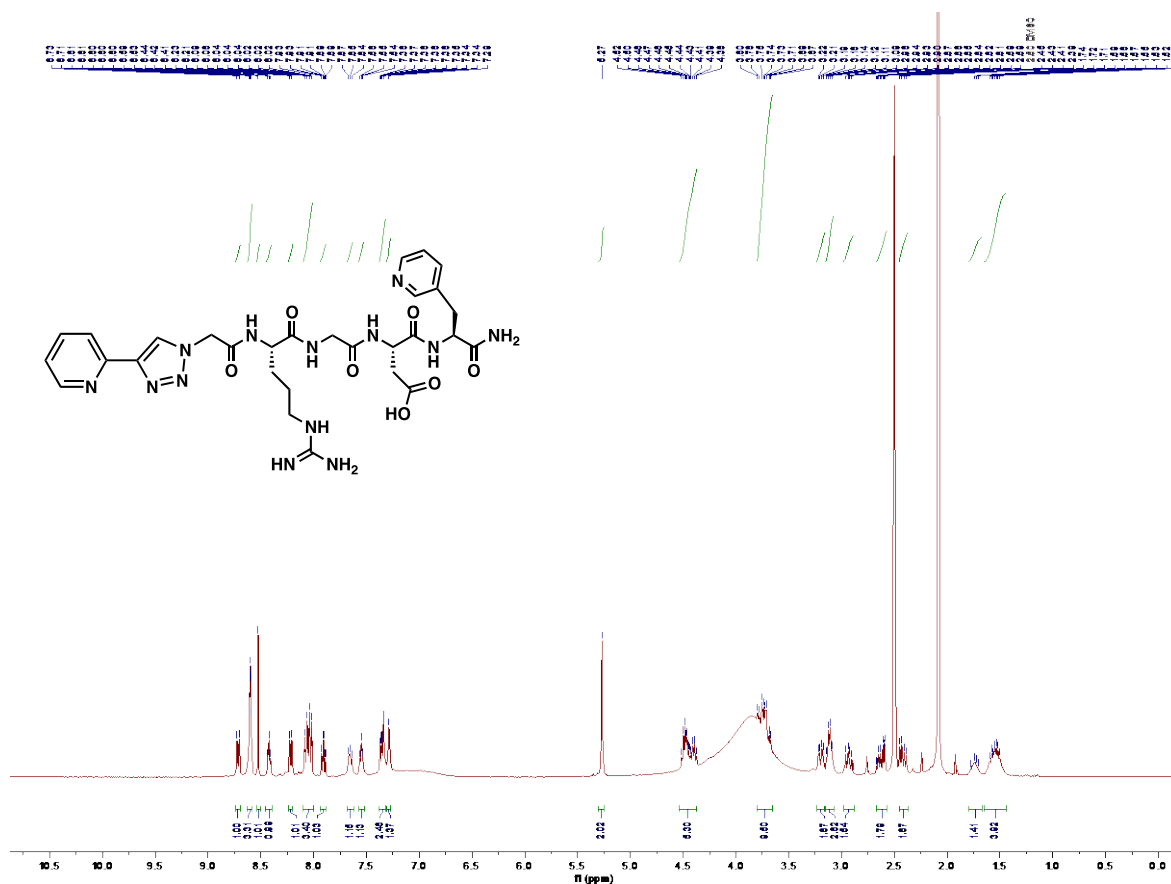
g-COSY NMR spectra of pyta-Ala-Ala-Ala-3Pal (**3.1**) in DMSO-d<sub>6</sub> at 400 MHz



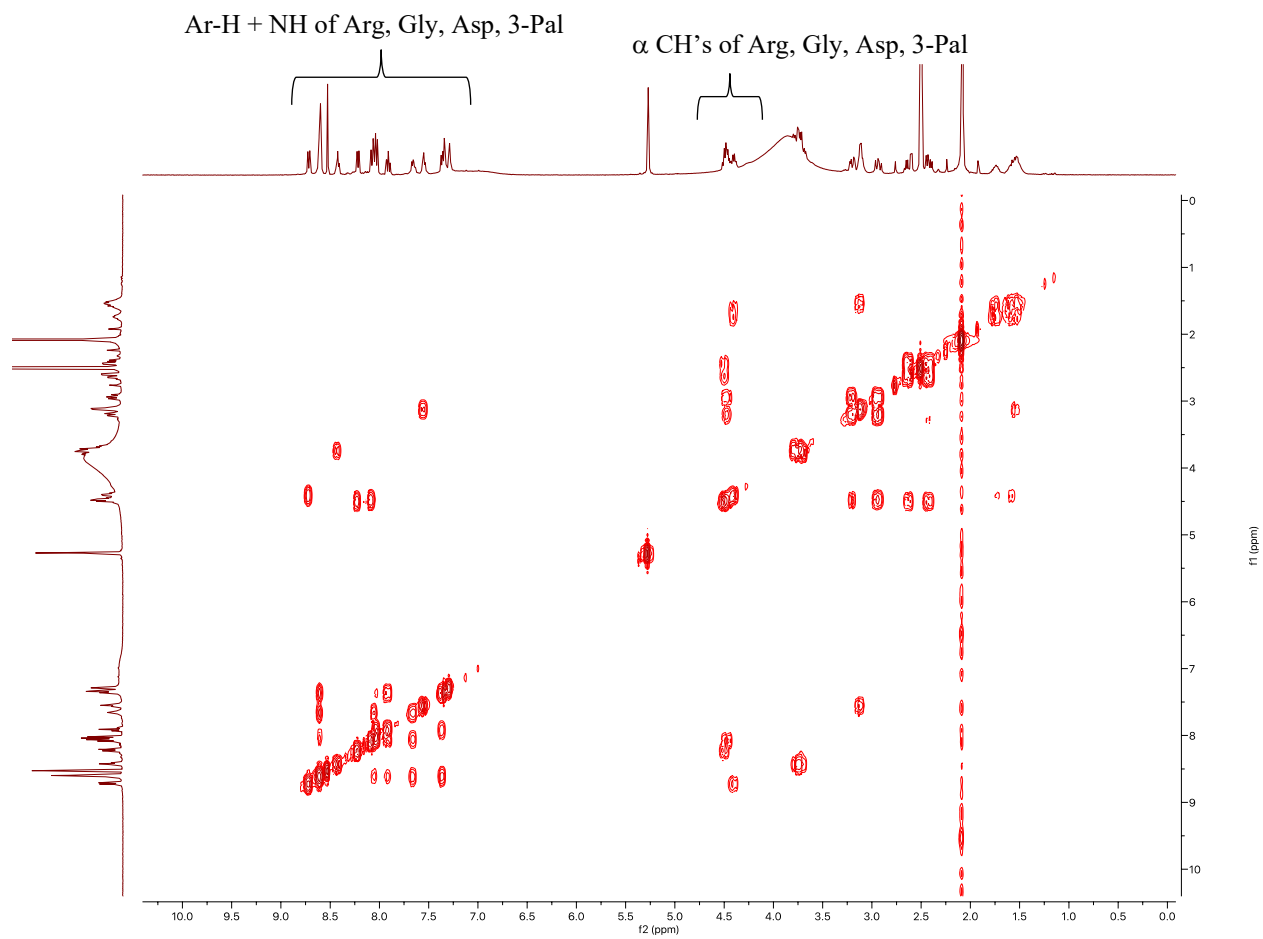
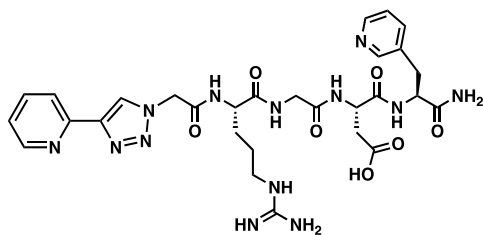
NOESY NMR spectra of pyta-Ala-Ala-Ala-3Pal (**3.1**) in DMSO-d<sub>6</sub> at 400 MHz



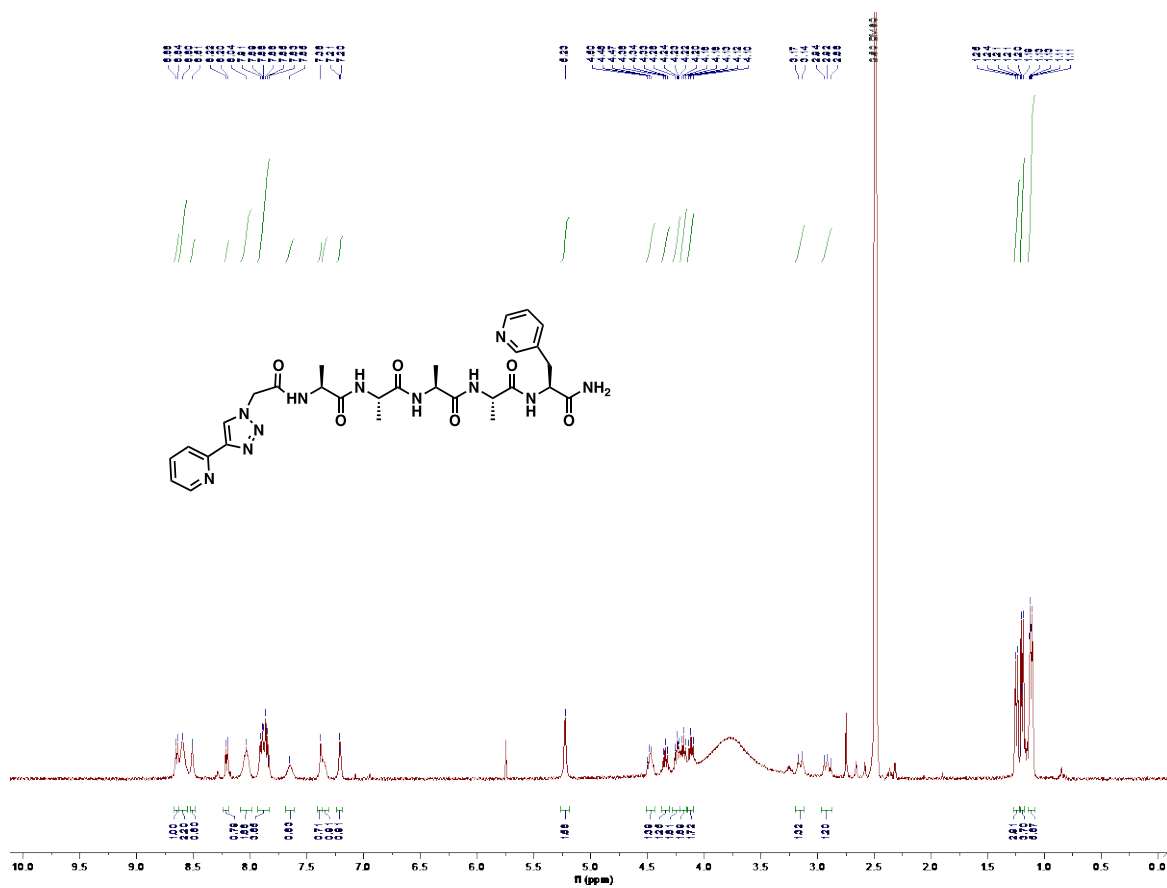
$^1\text{H}$  NMR spectra of pyta-Arg-Gly-Asp-3Pal (**3.2**) in  $\text{DMSO-d}_6$  at 400 MHz



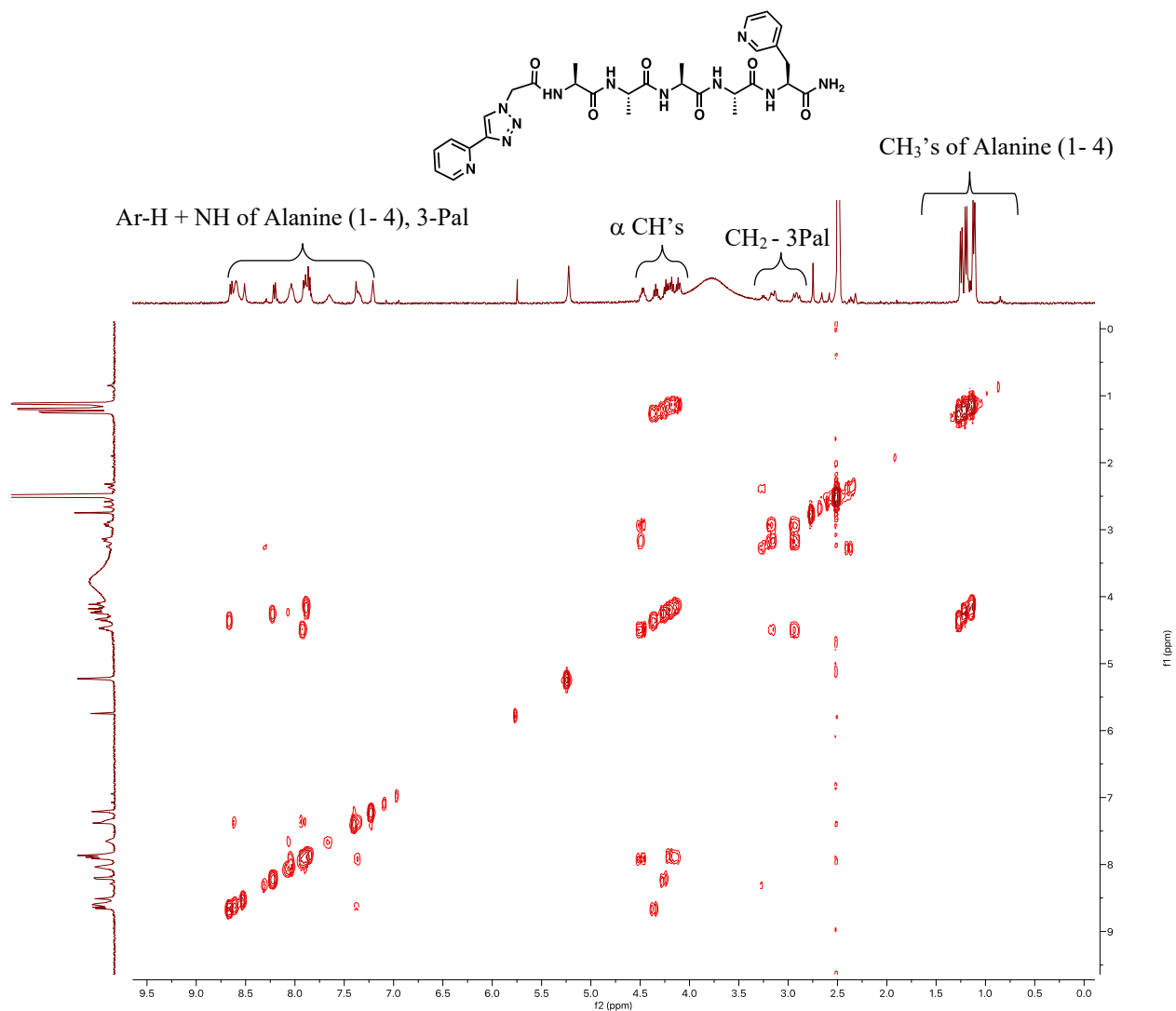
g-COSY NMR spectra of pyta-Arg-Gly-Asp-3Pal (**3.2**) in DMSO-d<sub>6</sub> at 400 MHz



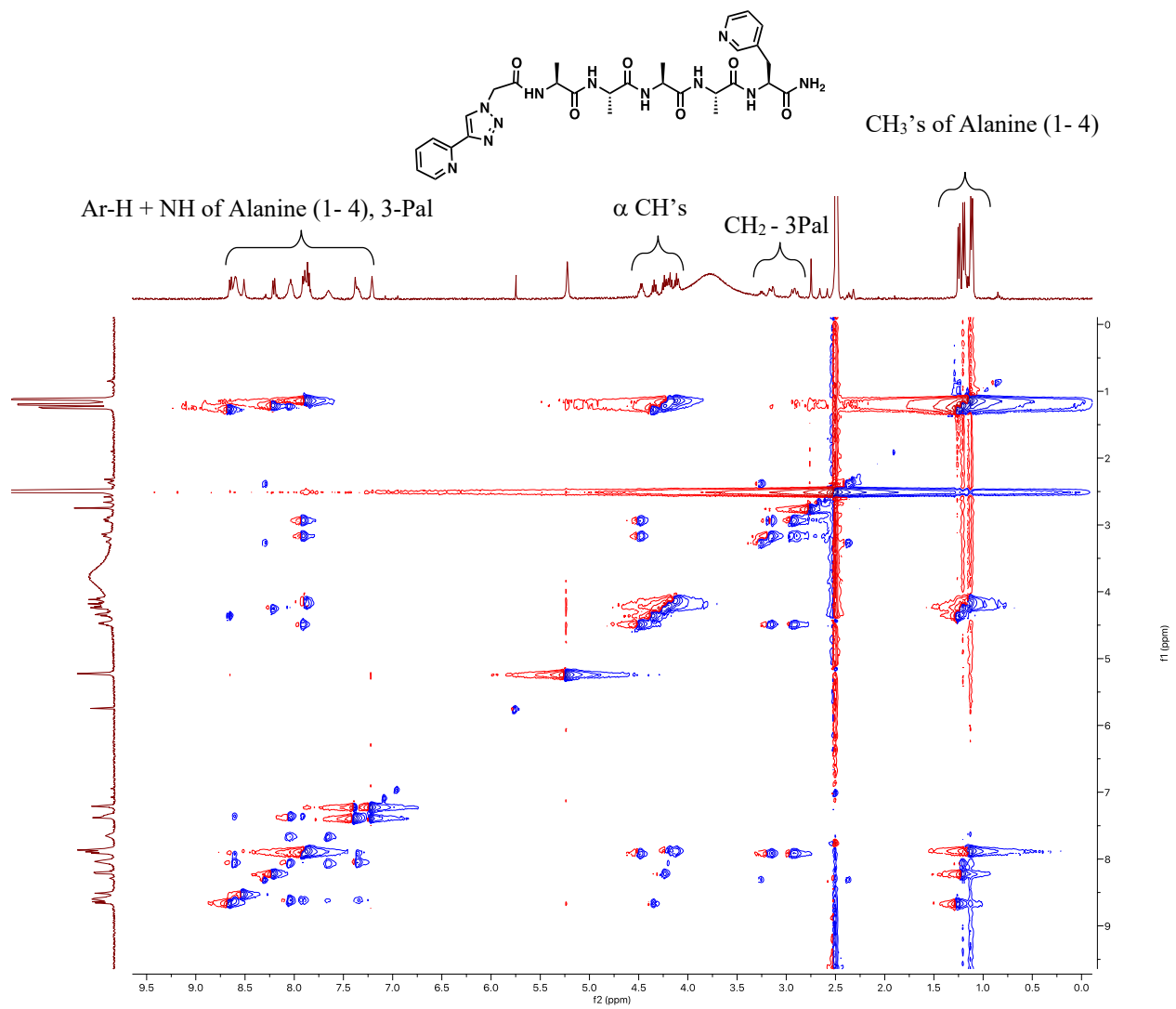
$^1\text{H}$  NMR spectra of pyta-Ala-Ala-Ala-Ala-3Pal (3.3) in DMSO- $d_6$  at 400 MHz



g-COSY NMR spectra of pyta-Ala-Ala-Ala-Ala-3Pal (**3.3**) in DMSO-d<sub>6</sub> at 400 MHz

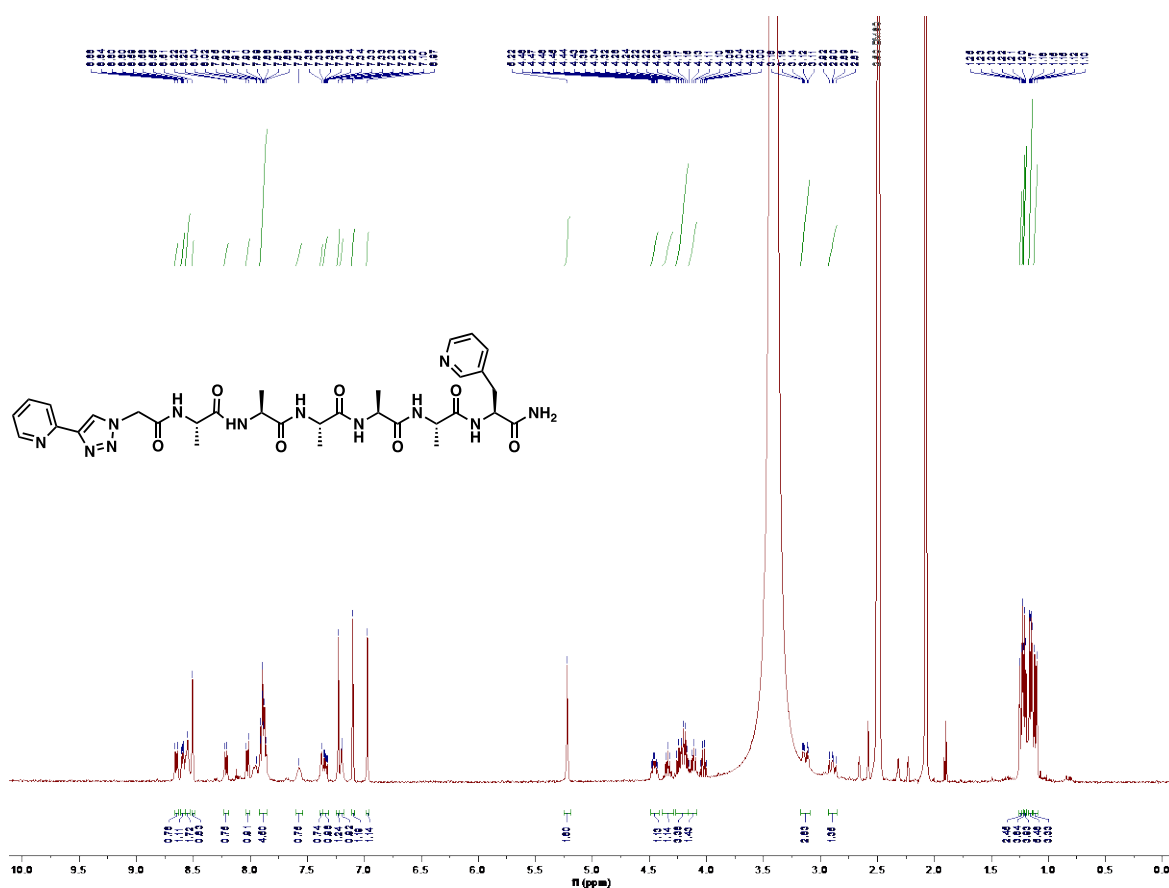


NOESY NMR spectra of pyta-Ala-Ala-Ala-Ala-3Pal (**3.3**) in DMSO-d<sub>6</sub> at 400 MHz

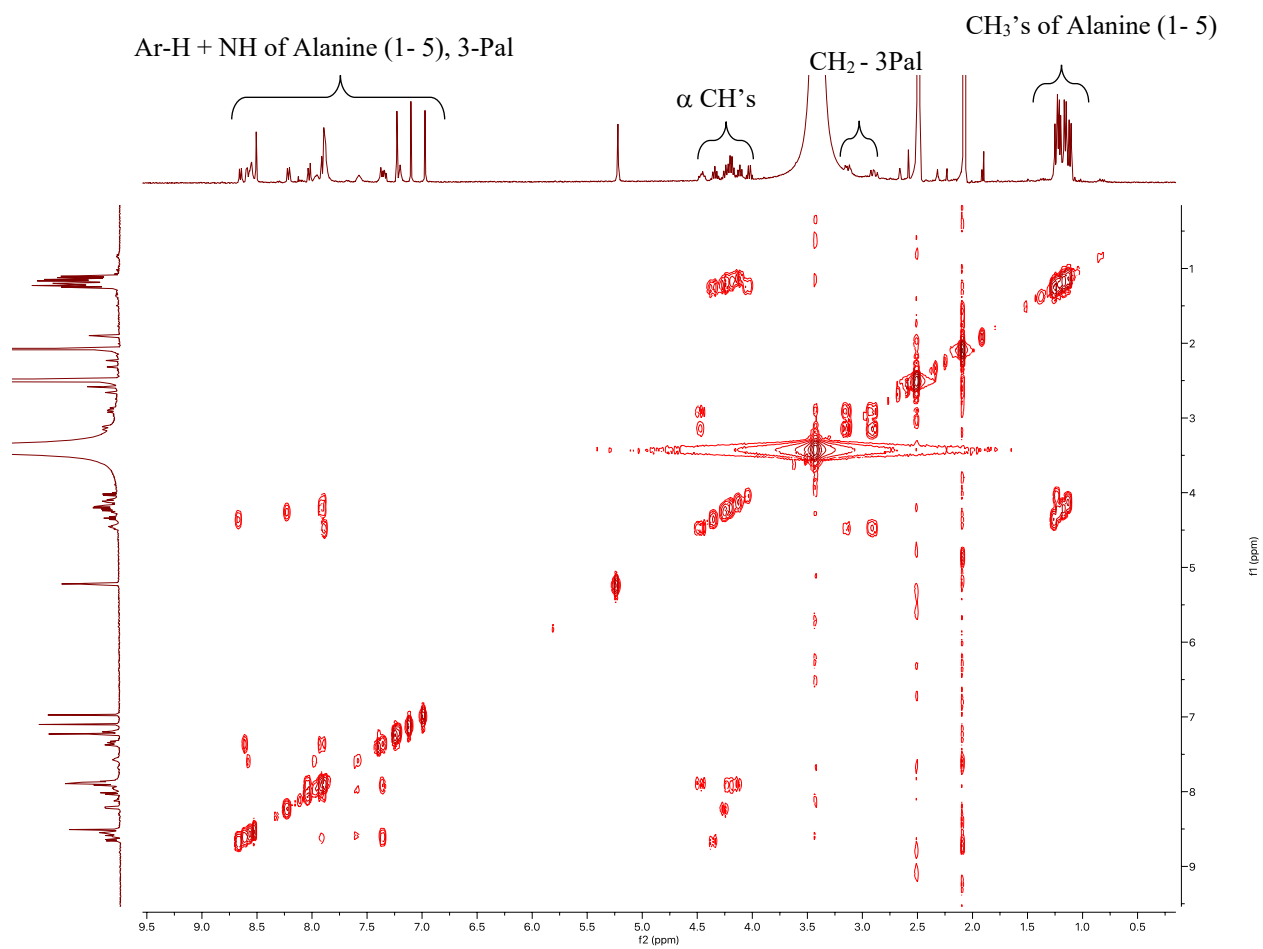
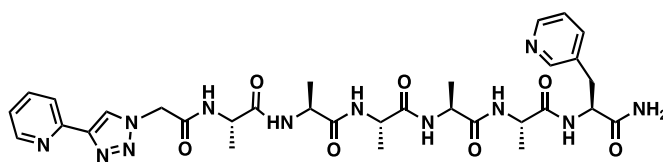




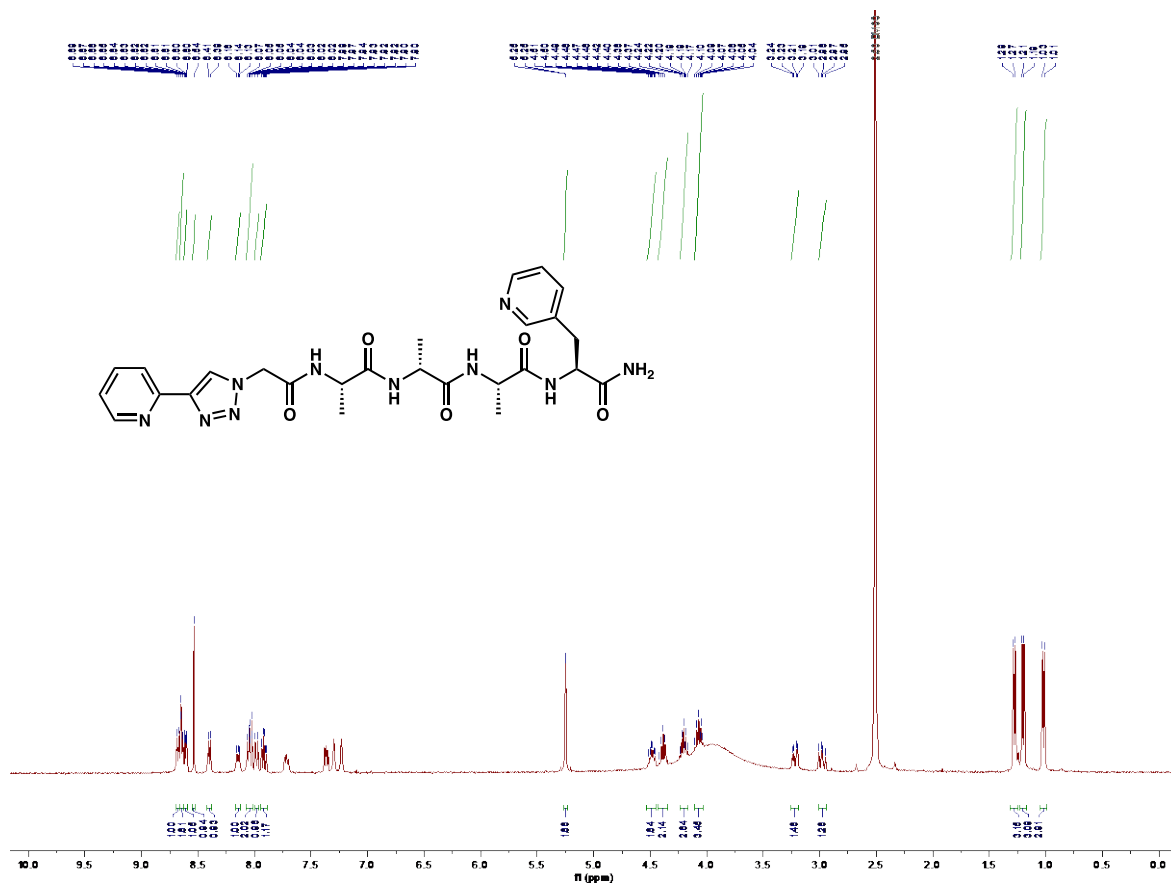
$^1\text{H}$  NMR spectra of pyta-Ala-Ala-Ala-Ala-Ala-3Pal (**3.4**) in  $\text{DMSO-d}_6$  at 400 MHz



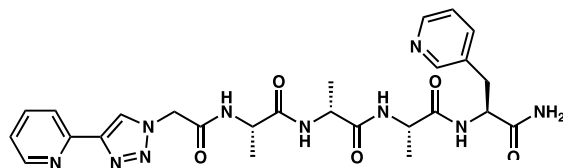
g-COSY NMR spectra of pyta-Ala-Ala-Ala-Ala-Ala-3Pal (**3.4**) in DMSO- $d_6$  at 400 MHz



$^1\text{H}$  NMR spectra of pyta-Ala-ala-Ala-3Pal (**3.5**) in  $\text{DMSO-d}_6$  at 400 MHz

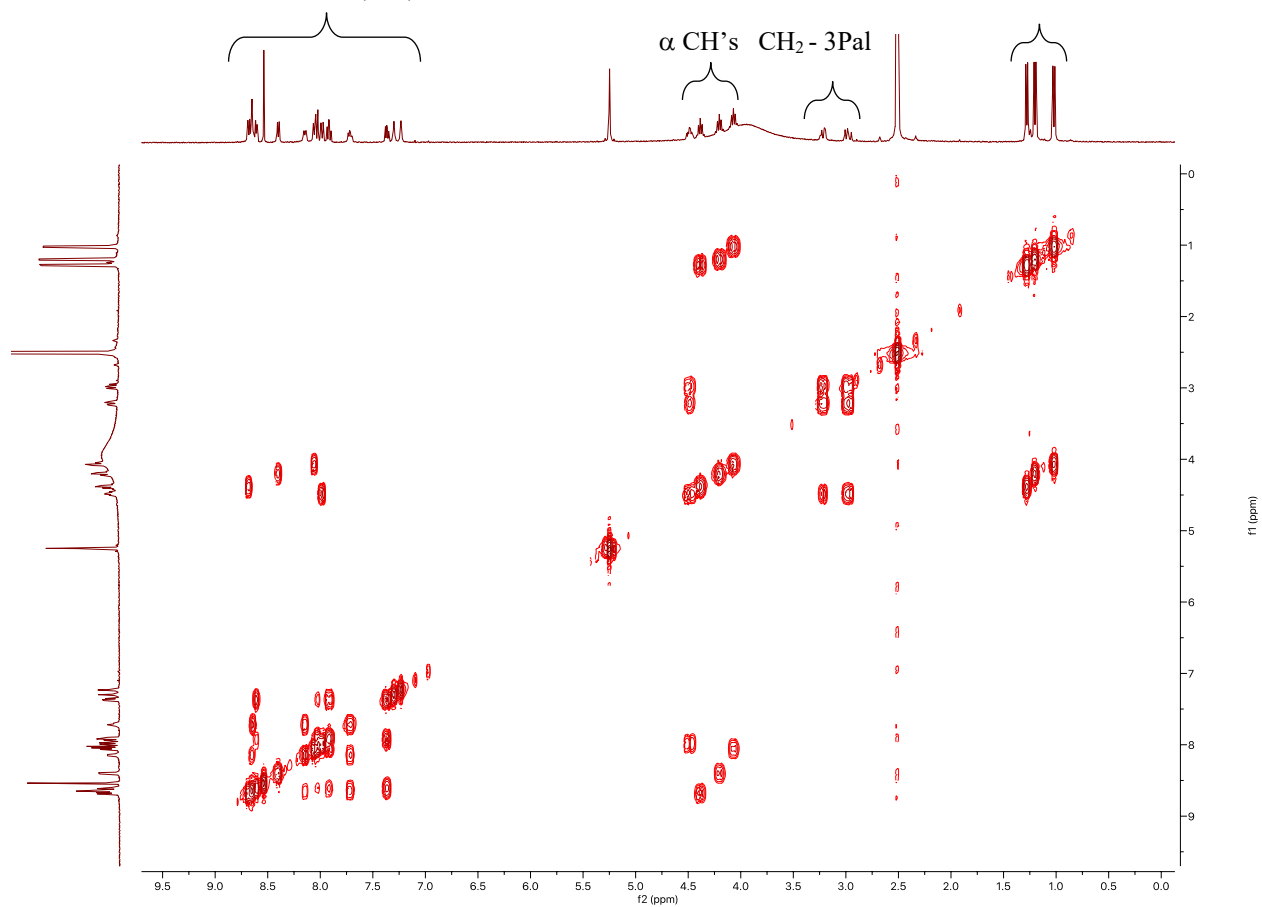


g- COSY NMR spectra of pyta-Ala-ala-Ala-3Pal (**3.5**) in DMSO-d<sub>6</sub> at 400 MHz

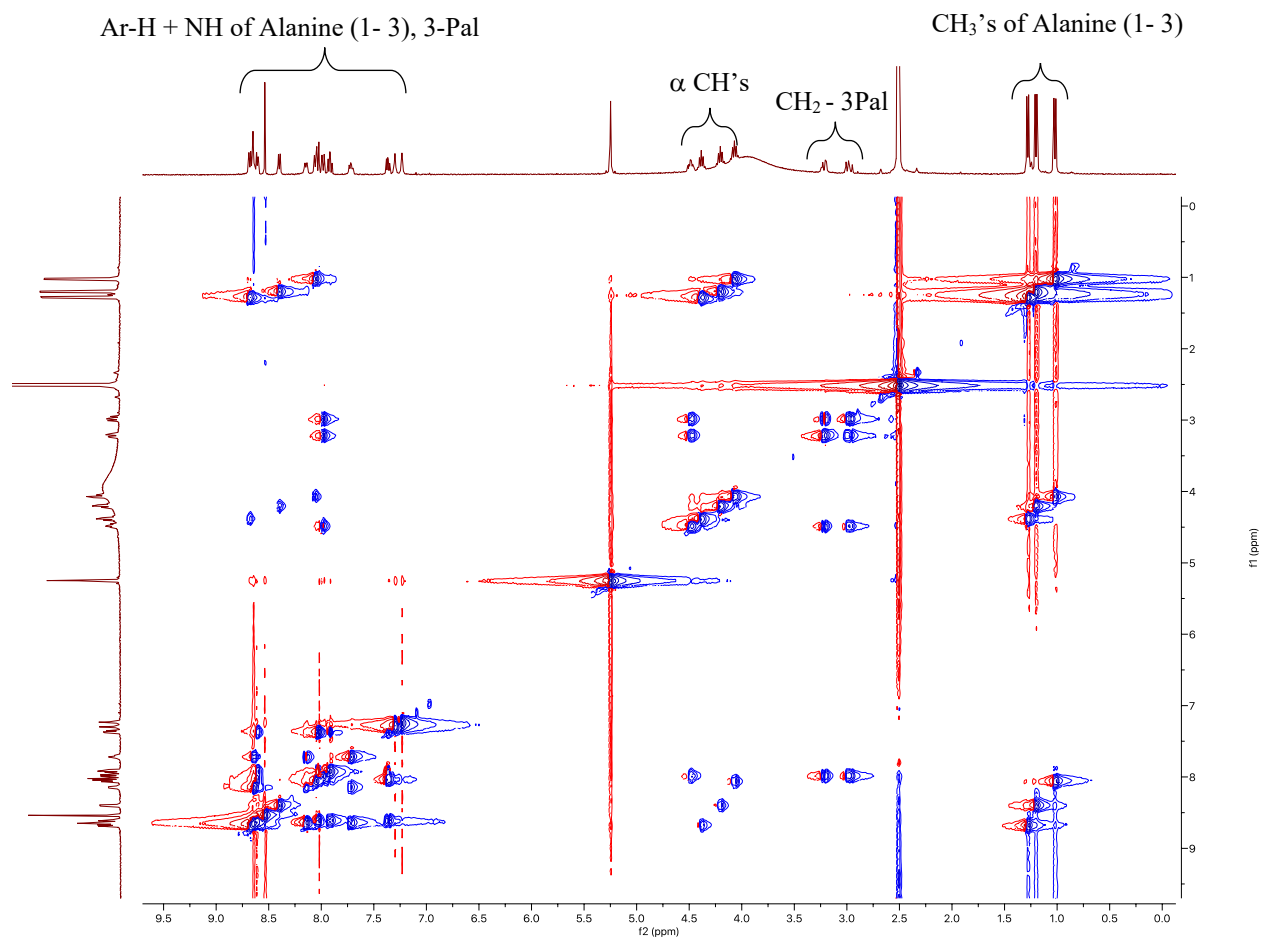
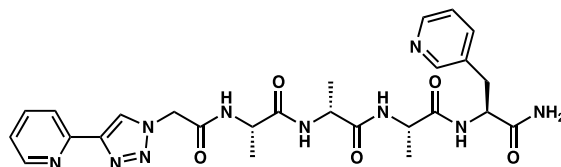


Ar-H + NH of Alanine (1- 3), 3-Pal

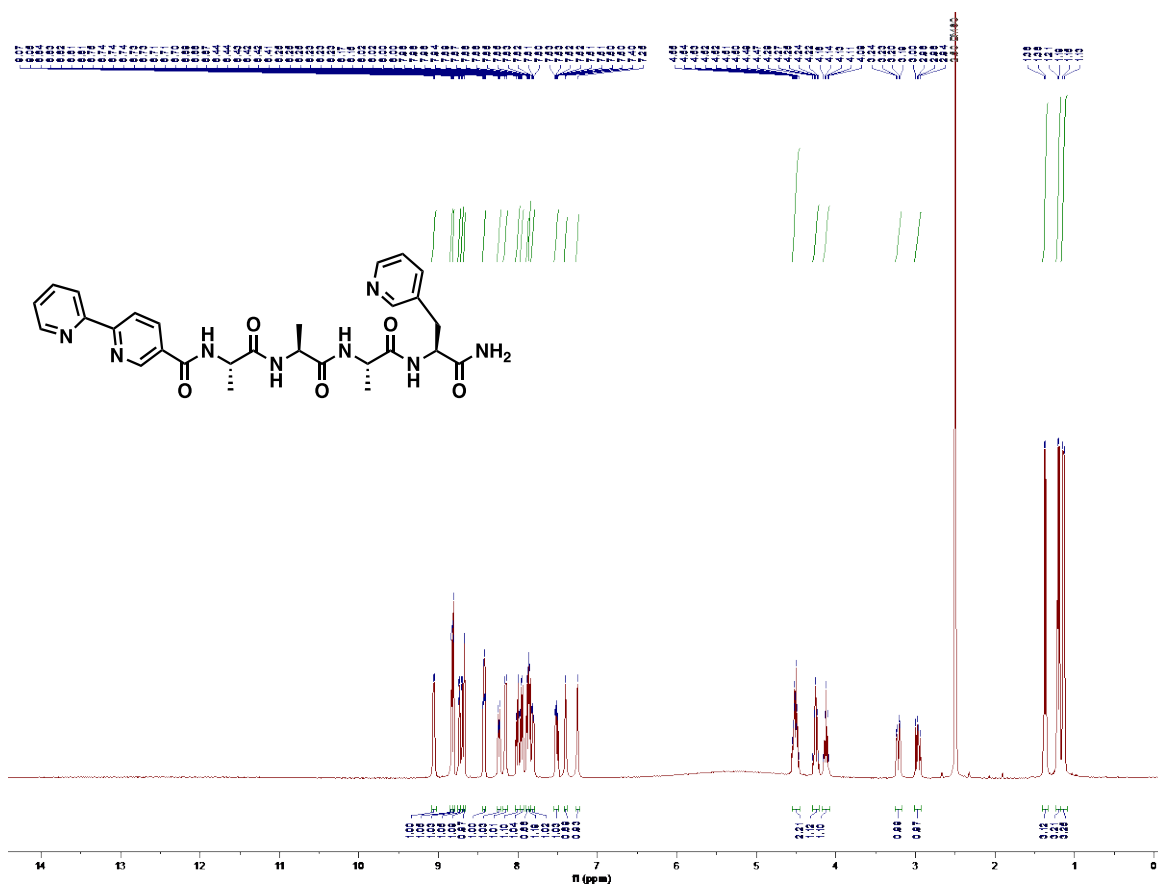
CH<sub>3</sub>'s of Alanine (1- 3)



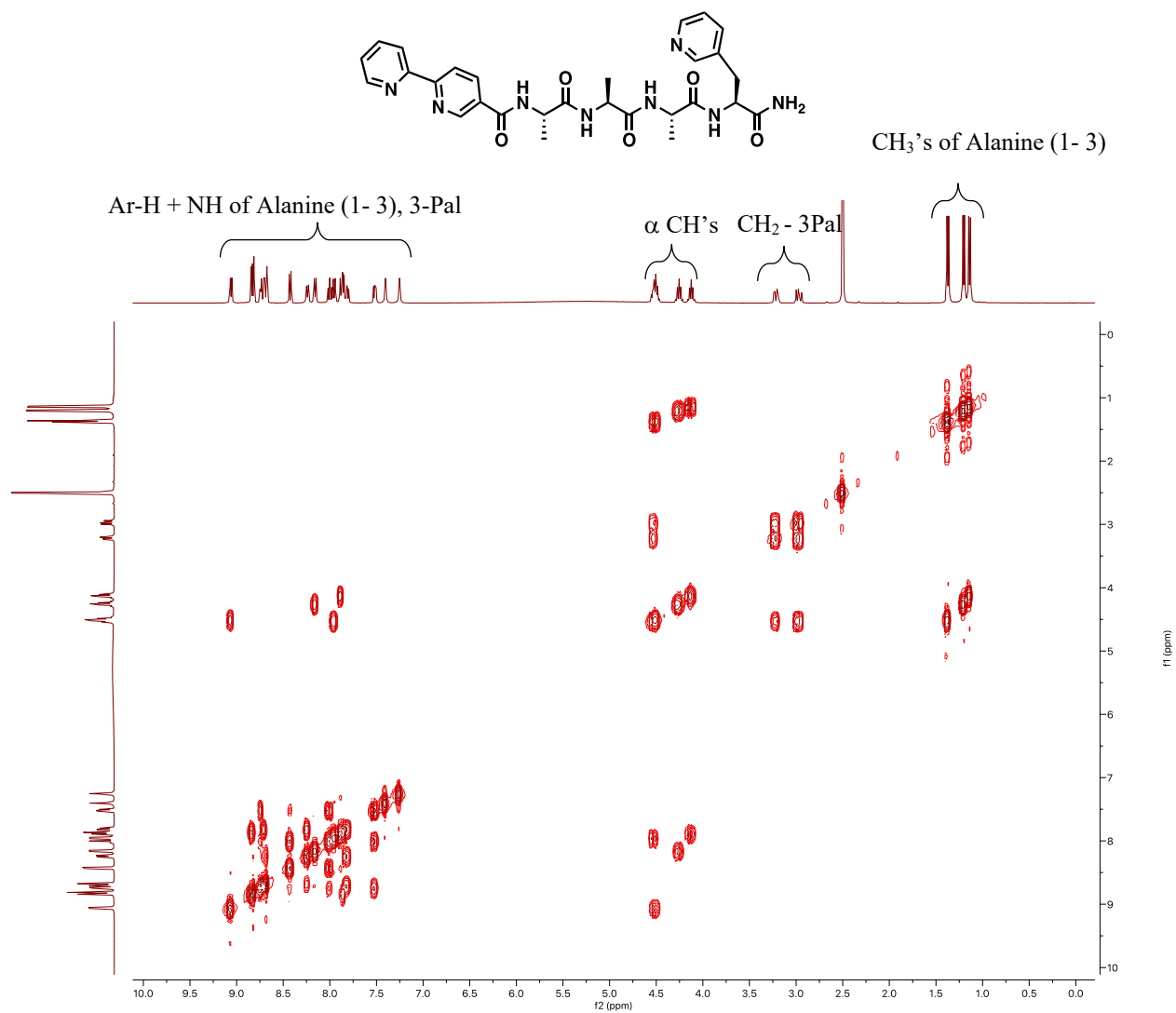
NOESY NMR spectra of pyta-Ala-ala-Ala-3Pal (**3.5**) in DMSO-d<sub>6</sub> at 400 MHz



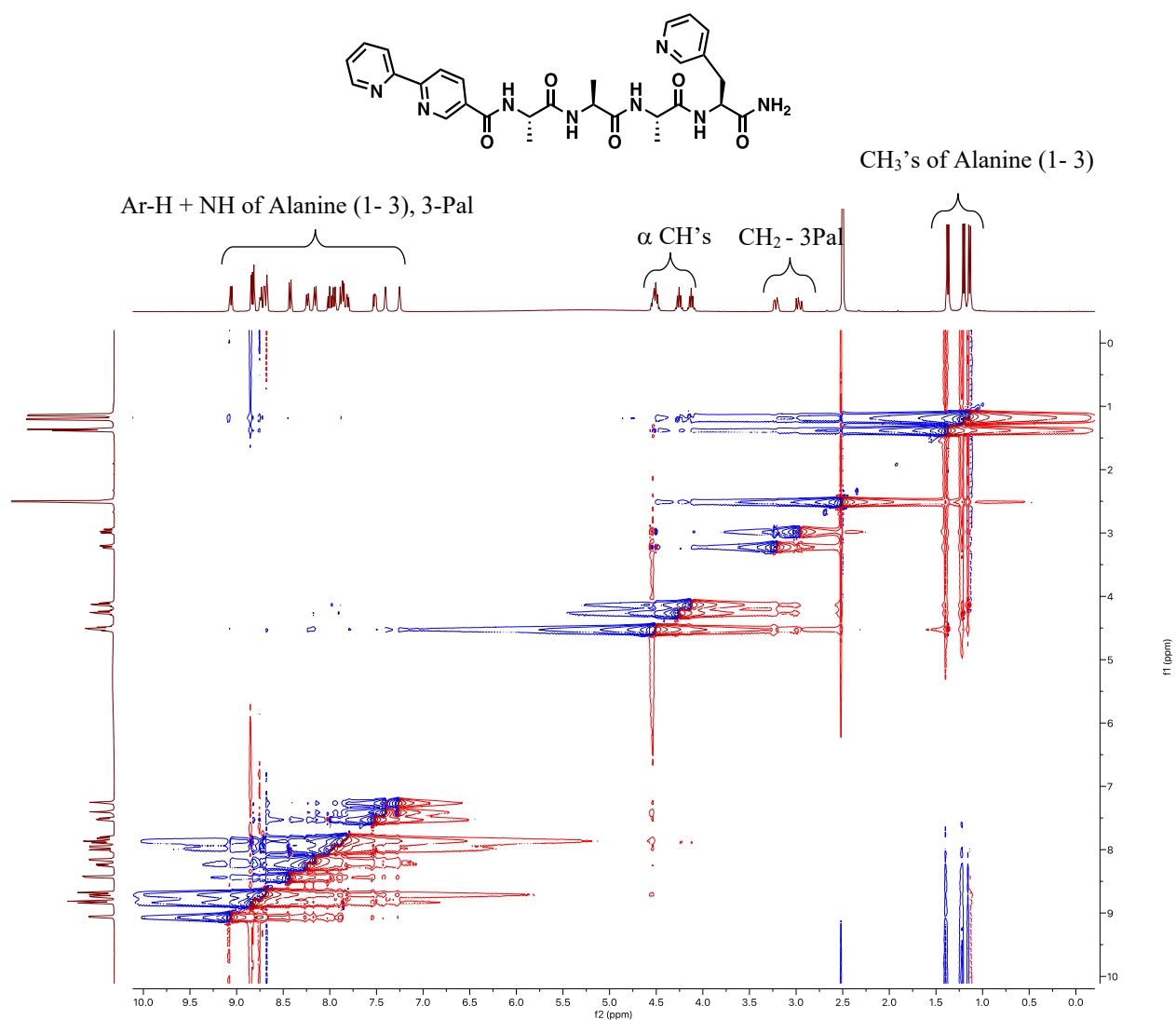
<sup>1</sup>H NMR spectra of Bipyd-Ala-Ala-Ala-3Pal (**3.6**) in DMSO-d<sub>6</sub> at 400 MHz



g-COSY NMR spectra of Bipyd-Ala-Ala-Ala-3Pal (**3.6**) in DMSO-d<sub>6</sub> at 400 MHz

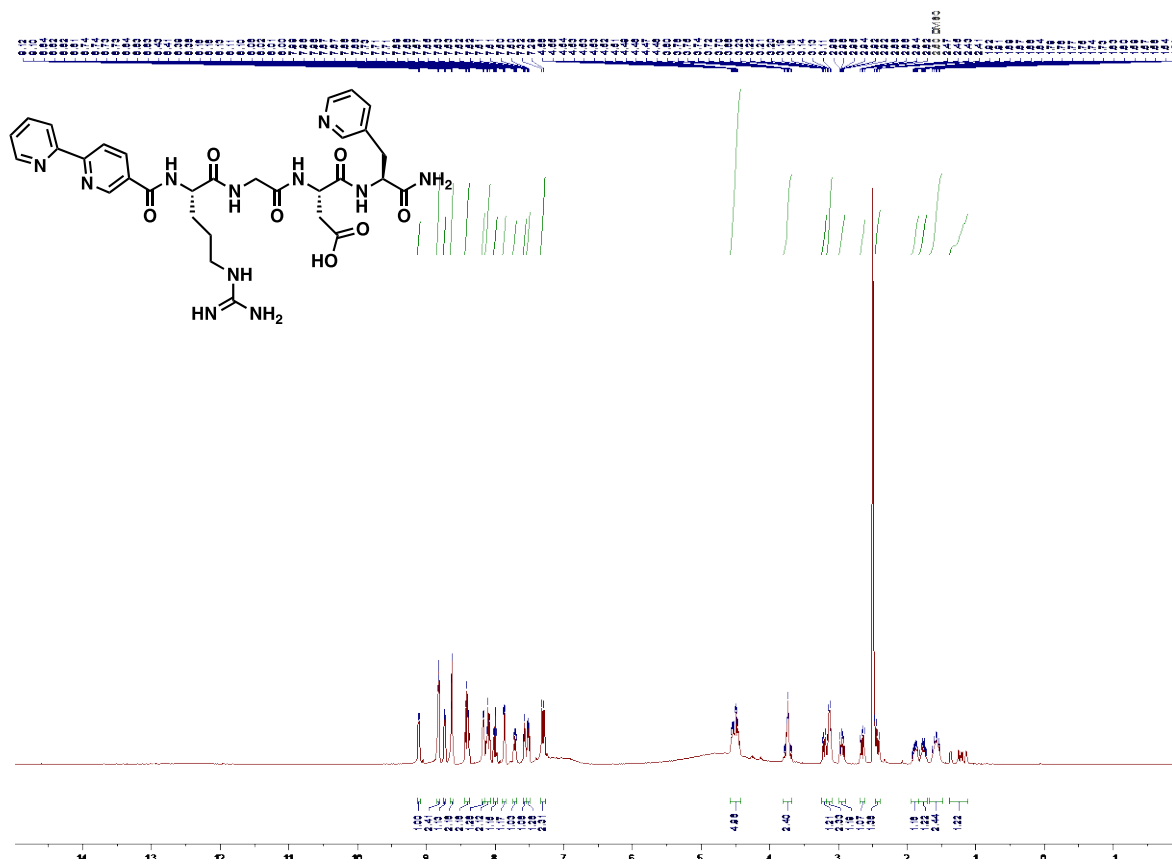


NOESY NMR spectra of Bipyd-Ala-Ala-Ala-3Pal (**3.6**) in DMSO-d<sub>6</sub> at 400 MHz

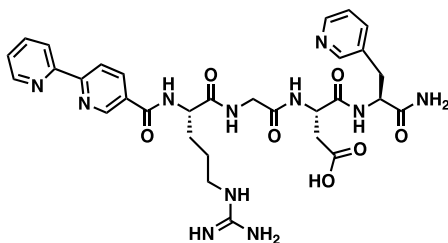




$^1\text{H}$  NMR spectra of Bipyd-Arg-Gly-Asp-3Pal (3.7) in DMSO- $d_6$  at 400 MHz

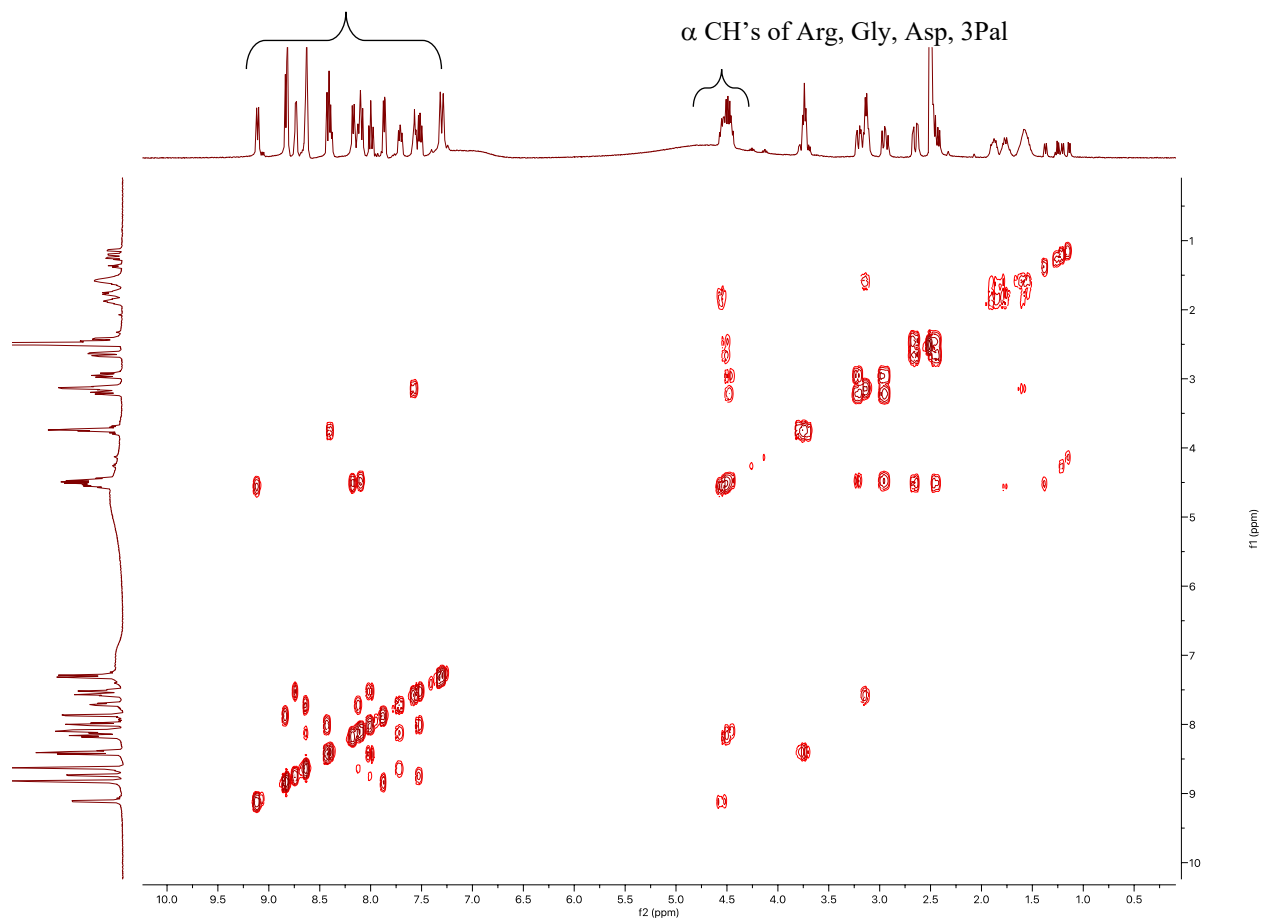


g-COSY NMR spectra of Bipyd-Arg-Gly-Asp-3Pal (3.7) in DMSO-d<sub>6</sub> at 400 MHz

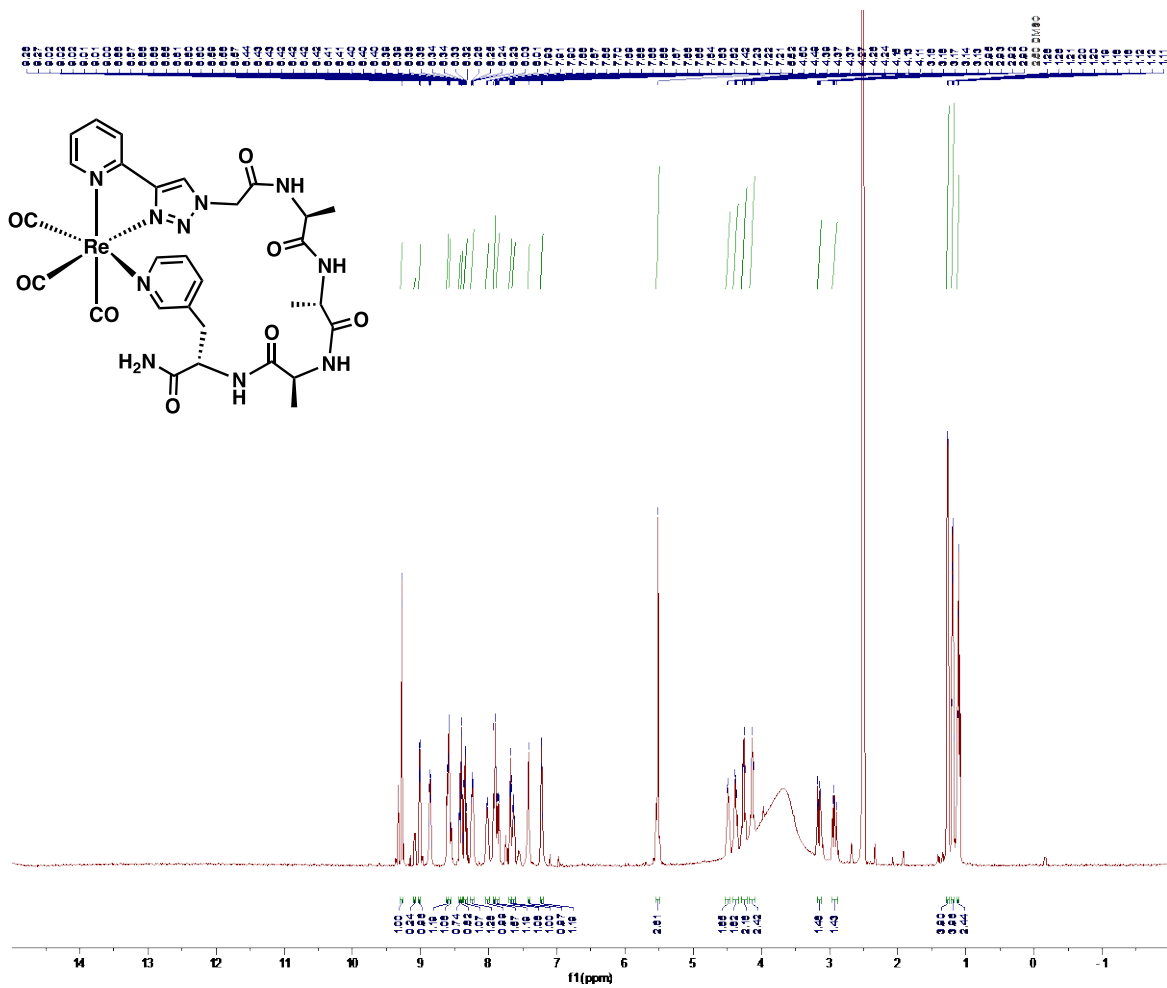


Ar-H + NH of Arg, Gly, Asp, 3-Pal

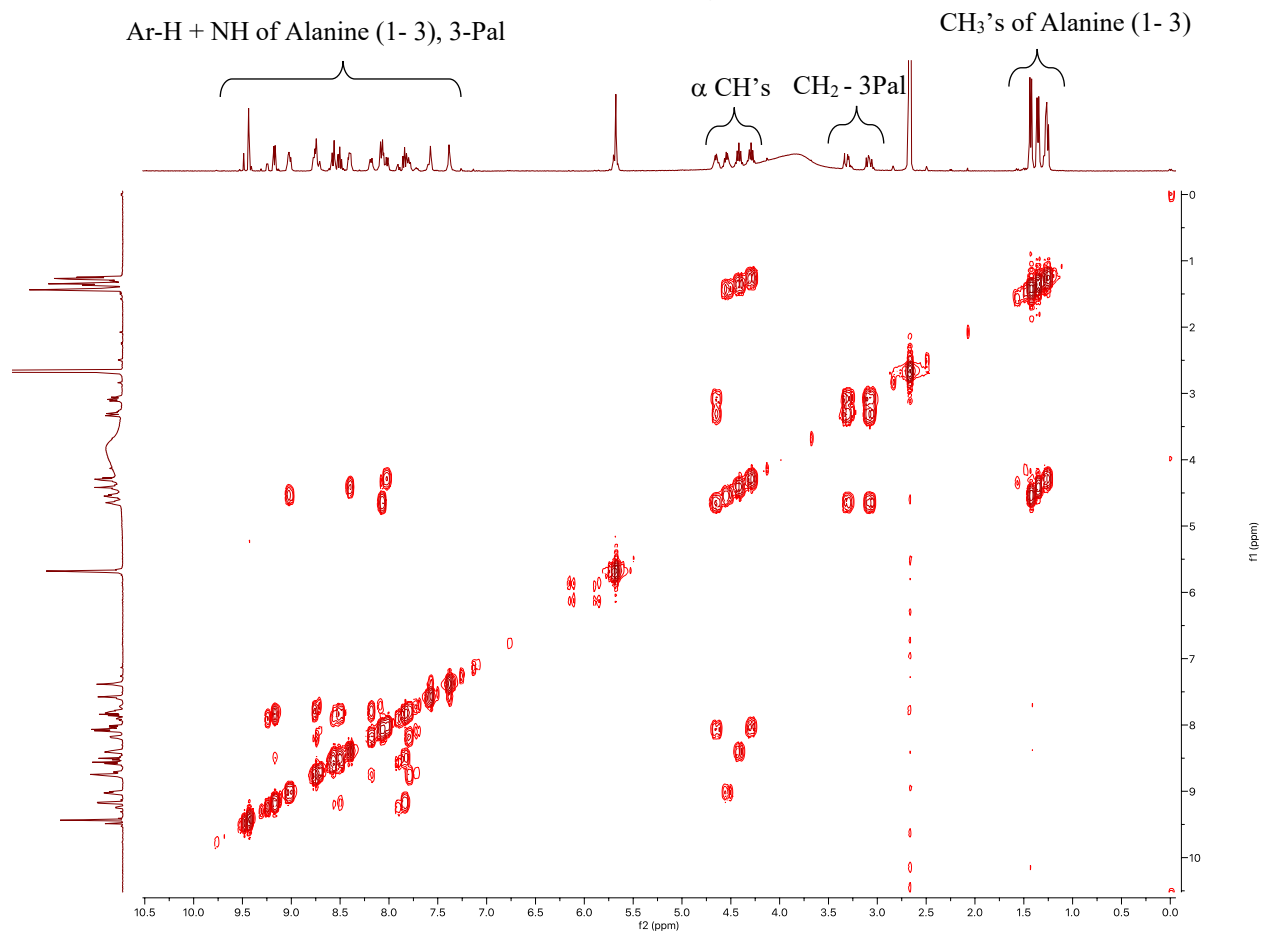
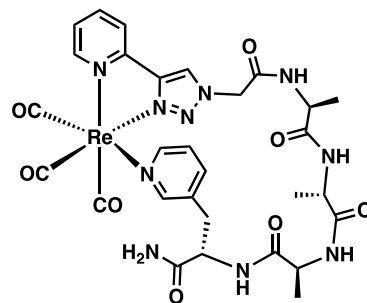
$\alpha$  CH's of Arg, Gly, Asp, 3Pal



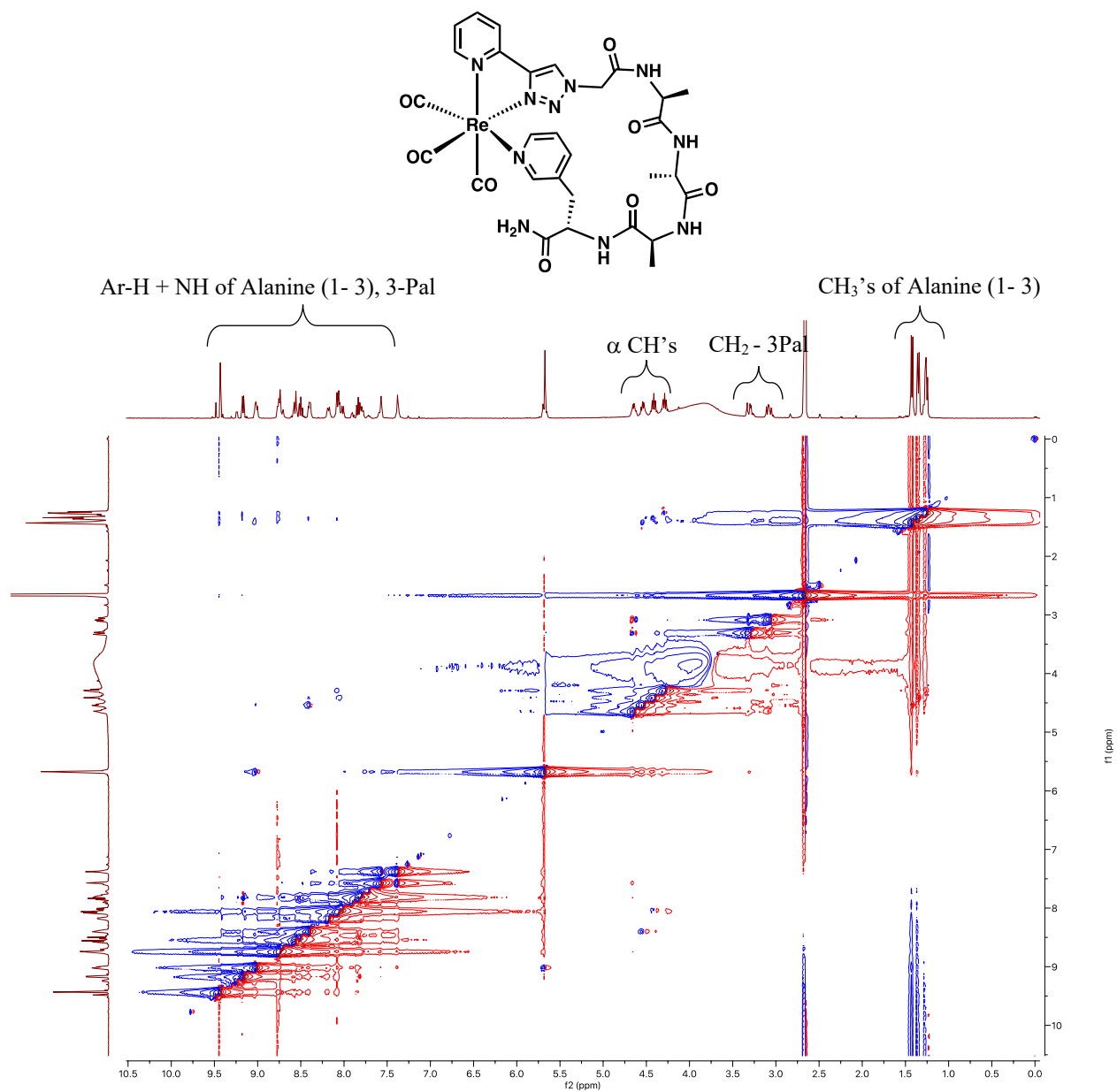
$^1\text{H}$  NMR spectra of  $\text{Re}(\text{CO})_3[\text{pyta-Ala-Ala-Ala-3Pal}]$  (**3.8**) in  $\text{DMSO-d}_6$  at 400 MHz



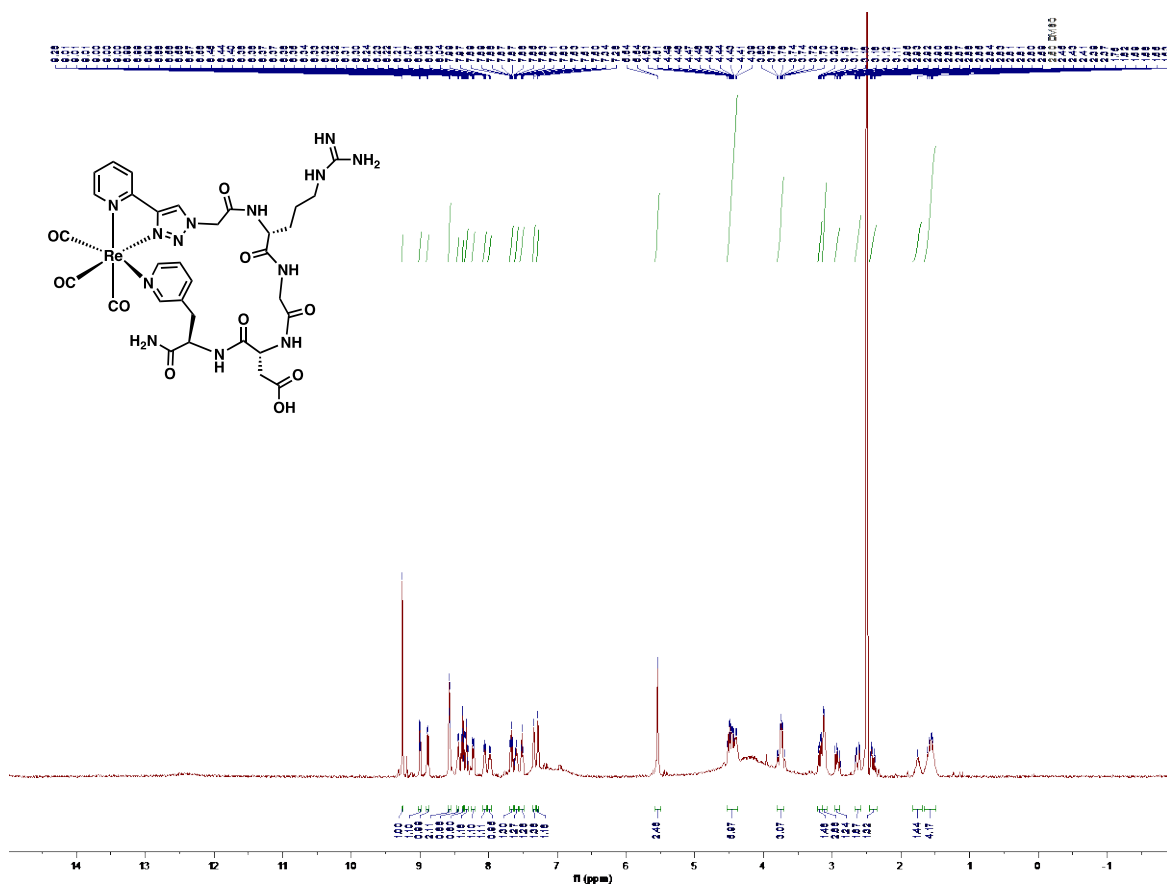
g-COSY NMR spectra of  $\text{Re}(\text{CO})_3[\text{pyta-Ala-Ala-Ala-3Pal}]$  (**3.8**) in  $\text{DMSO-d}_6$  at 400 MHz



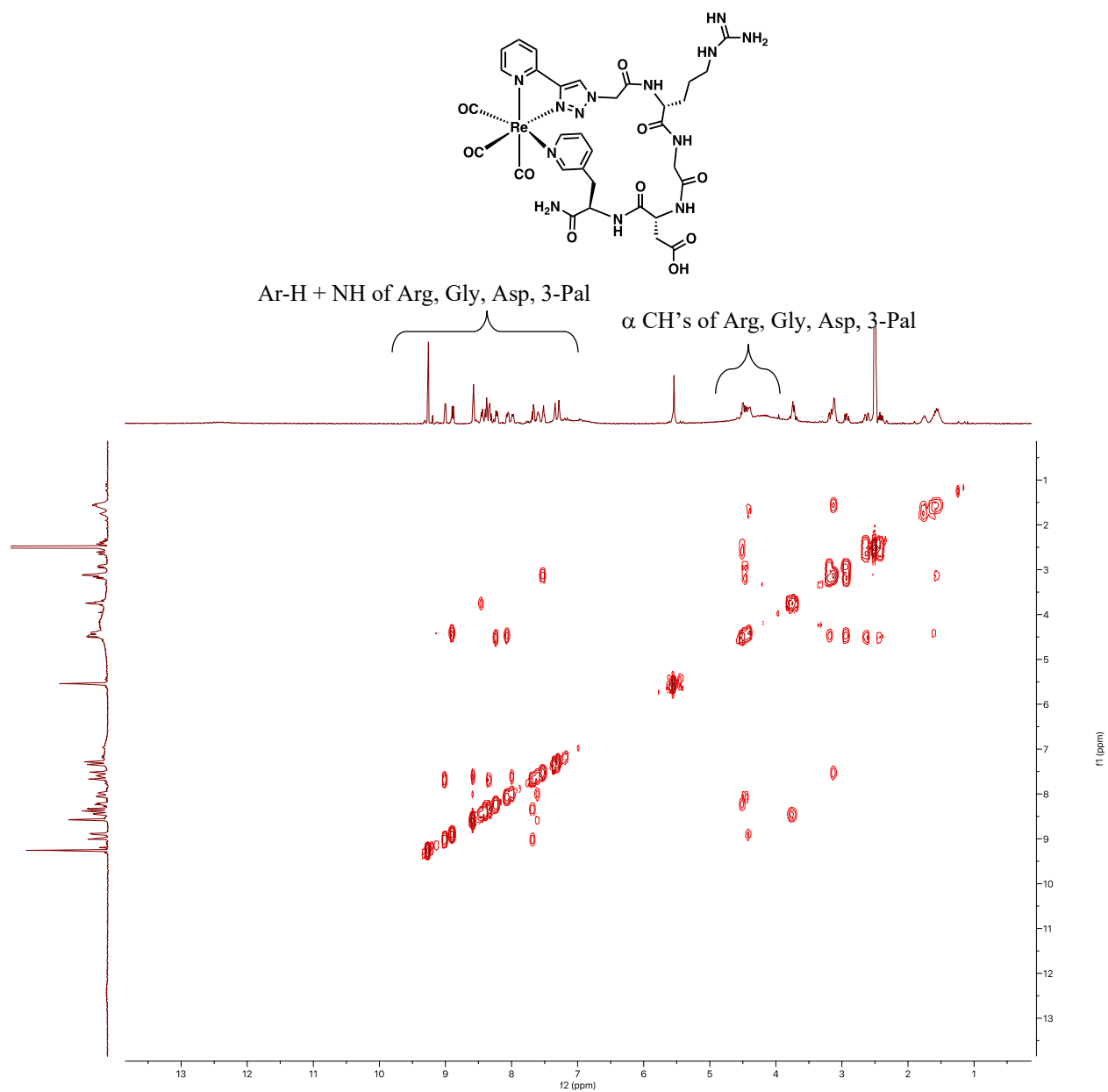
NOESY NMR spectra of  $\text{Re}(\text{CO})_3[\text{pyta-Ala-Ala-Ala-3Pal}]$  (**3.8**) in  $\text{DMSO-d}_6$  at 400 MHz



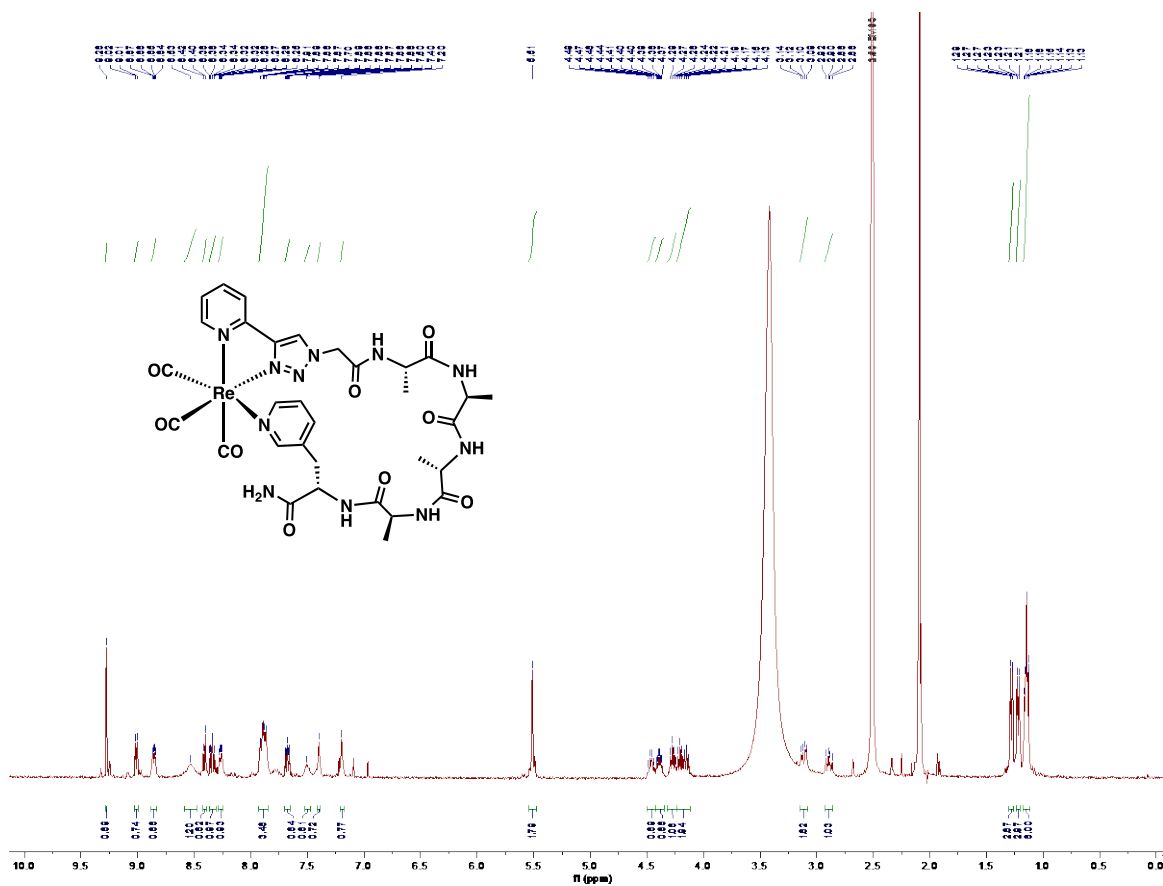
$^1\text{H}$  NMR spectra of  $\text{Re}(\text{CO})_3[\text{pyta-Arg-Gly-Asp-3Pal}]$  (**3.9**) in  $\text{DMSO-d}_6$  at 400 MHz



g-COSY NMR spectra of  $\text{Re}(\text{CO})_3[\text{pyta-Arg-Gly-Asp-3Pal}]$  (**3.9**) in  $\text{DMSO-d}_6$  at 400 MHz

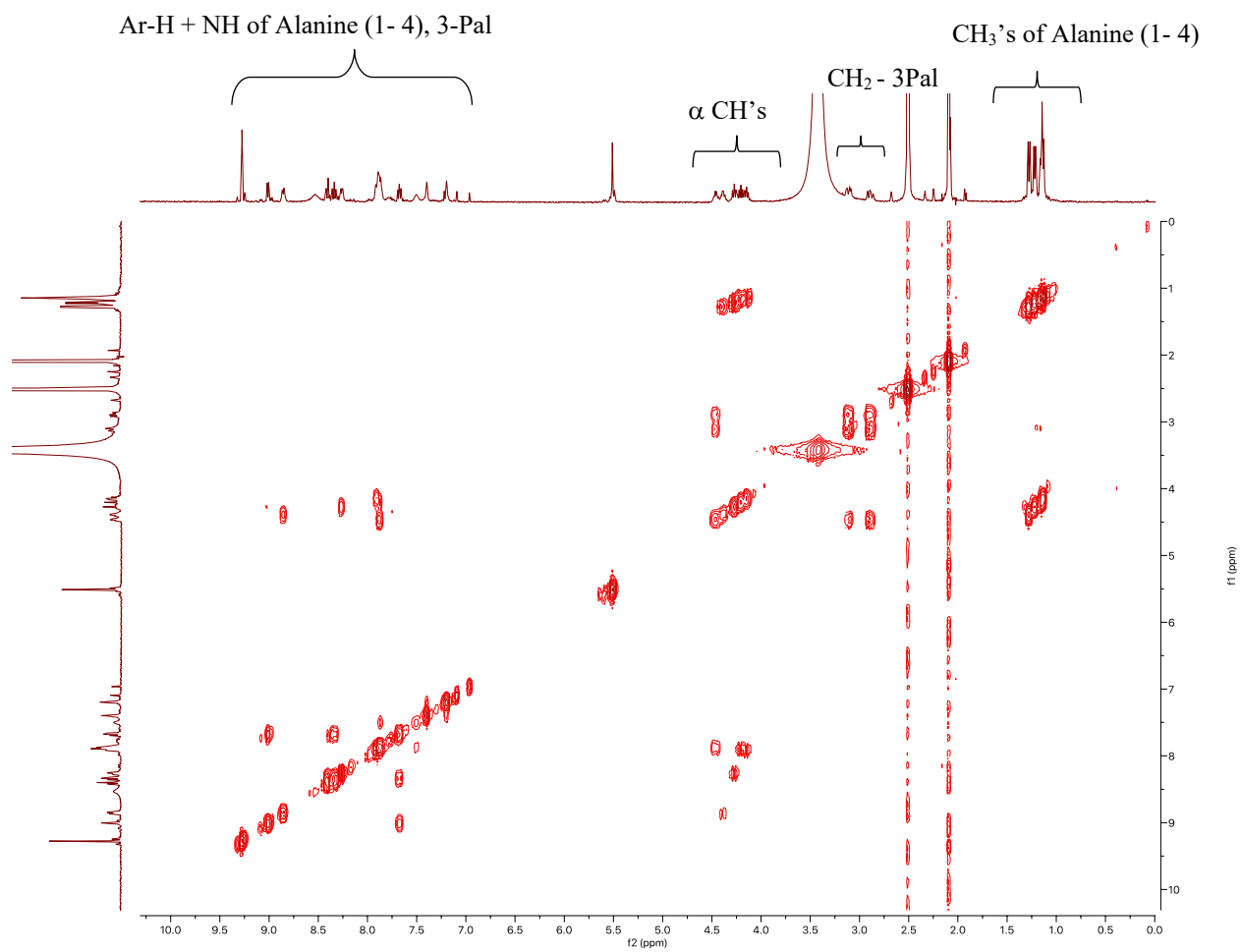
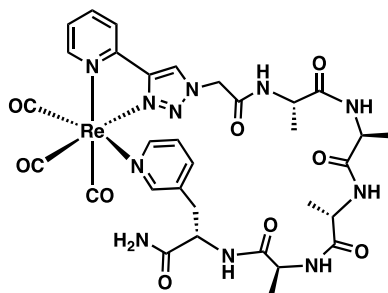


$^1\text{H}$  NMR spectra of  $\text{Re}(\text{CO})_3[\text{pyta-Ala-Ala-Ala-Ala-3Pal}]$  (**3.10**) in  $\text{DMSO-d}_6$  at 400 MHz

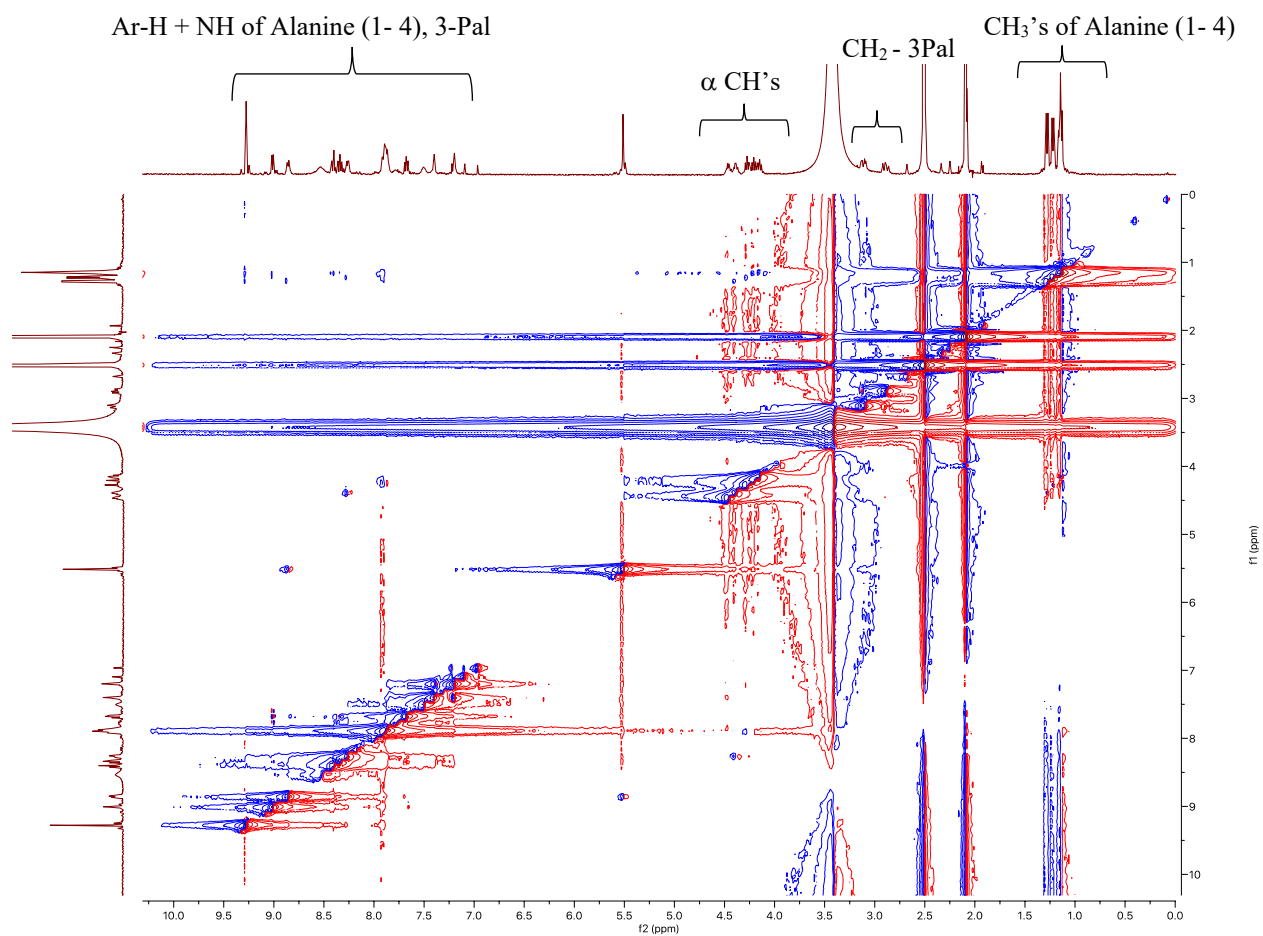
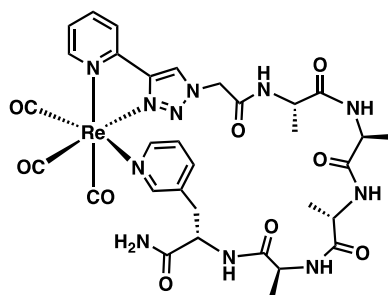




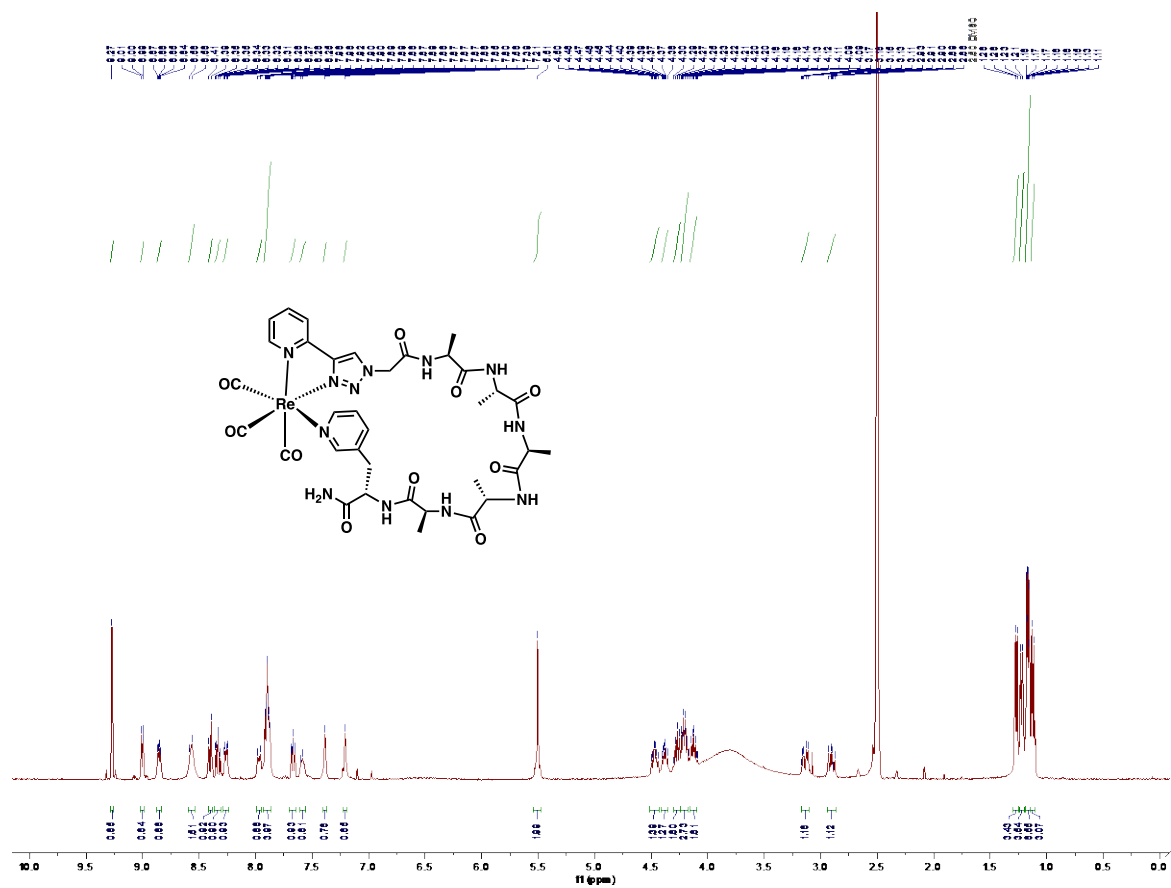
g-COSY NMR spectra of  $\text{Re}(\text{CO})_3[\text{pyta-Ala-Ala-Ala-Ala-3Pal}]$  (**3.10**) in  $\text{DMSO-d}_6$  at 400 MHz



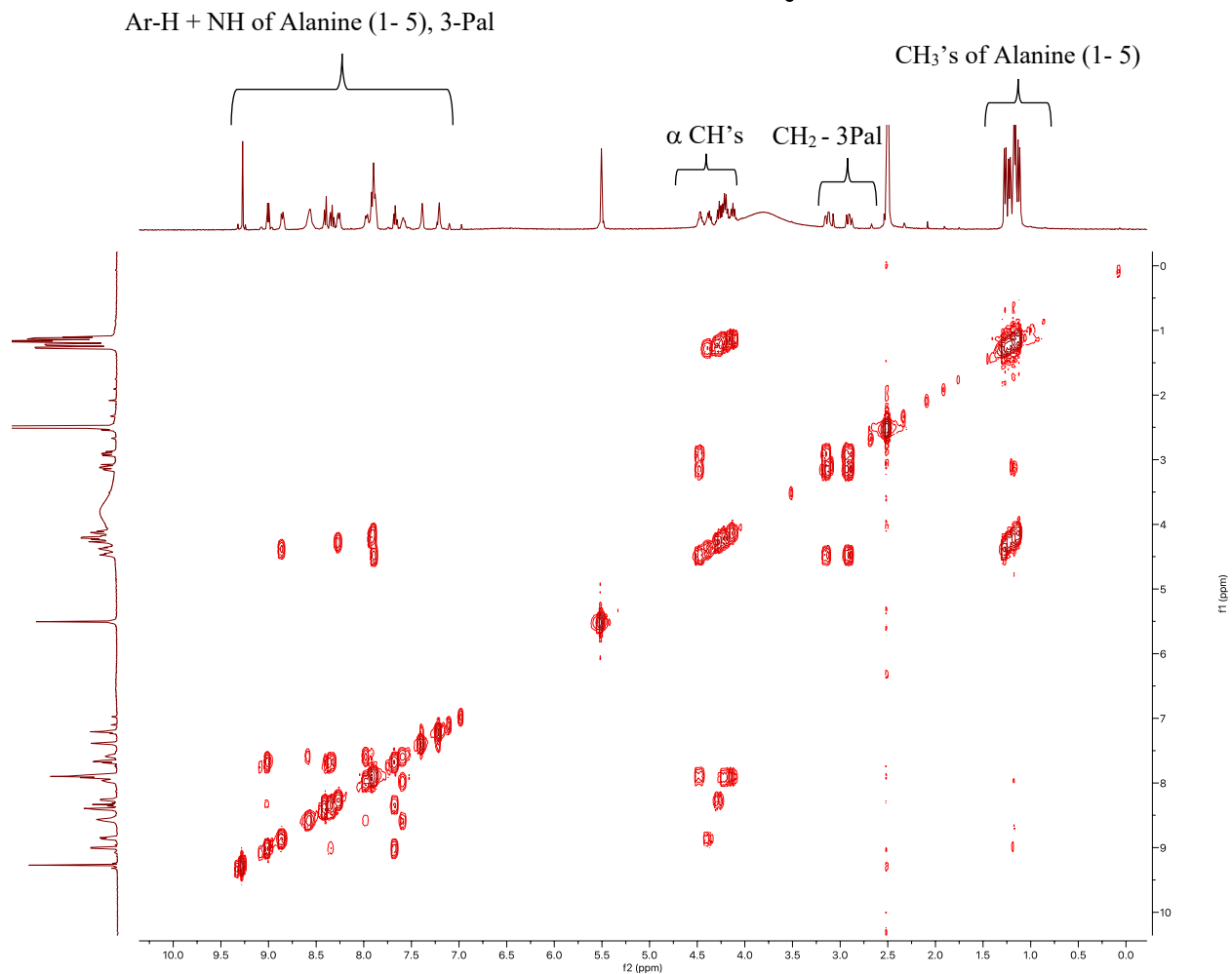
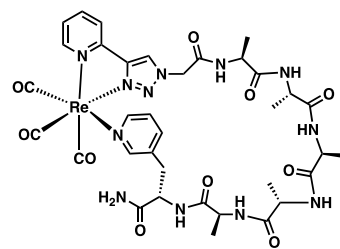
NOESY NMR spectra of  $\text{Re}(\text{CO})_3[\text{pyta-Ala-Ala-Ala-Ala-3Pal}]$  (**3.10**) in  $\text{DMSO-d}_6$  at 400 MHz



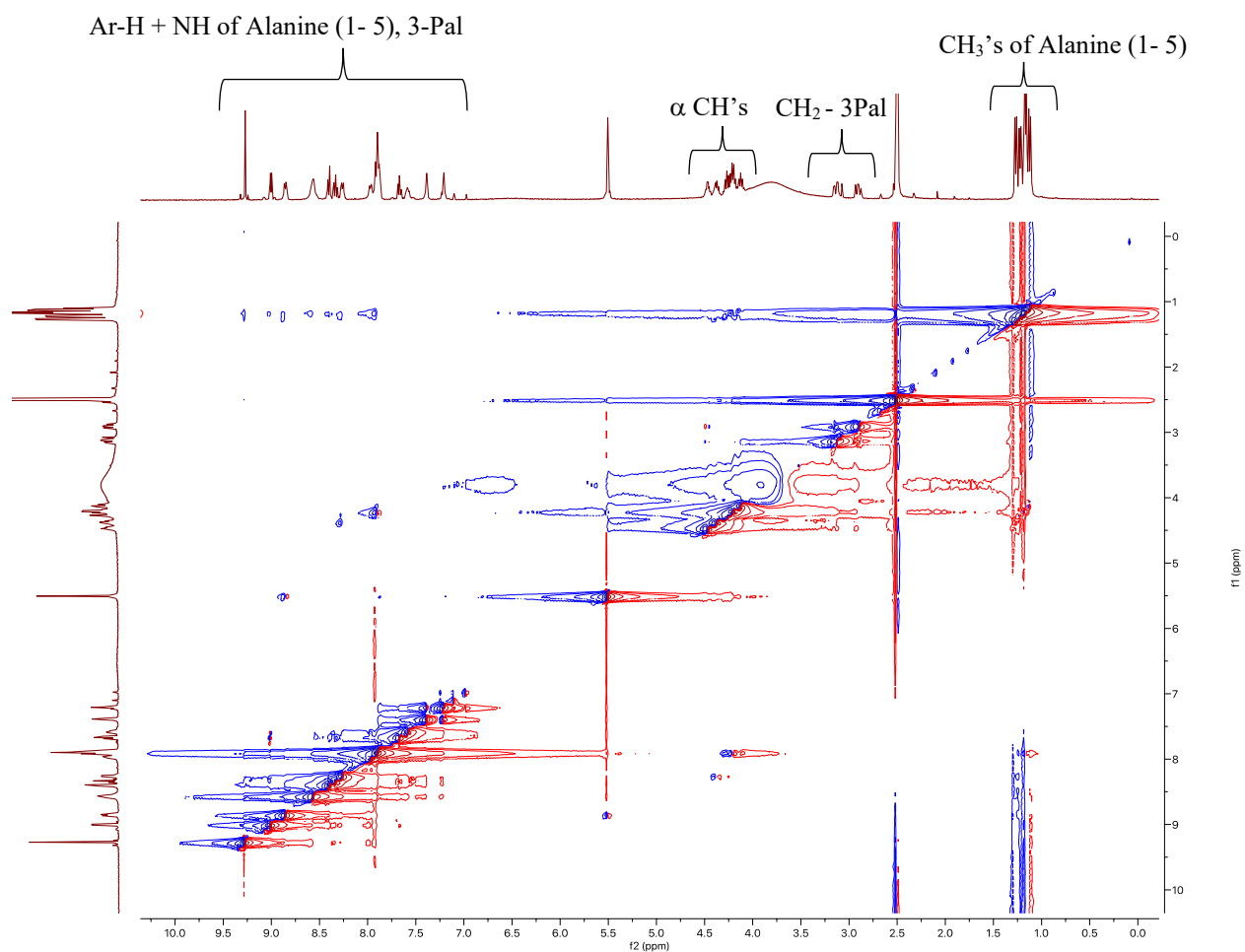
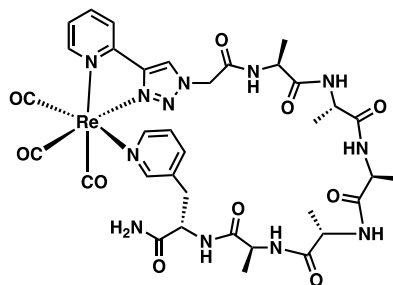
$^1\text{H}$  NMR spectra of  $\text{Re}(\text{CO})_3[\text{pyta-Ala-Ala-Ala-Ala-Ala-3Pal}]$  (**3.11**) in  $\text{DMSO-d}_6$  at 400 MHz



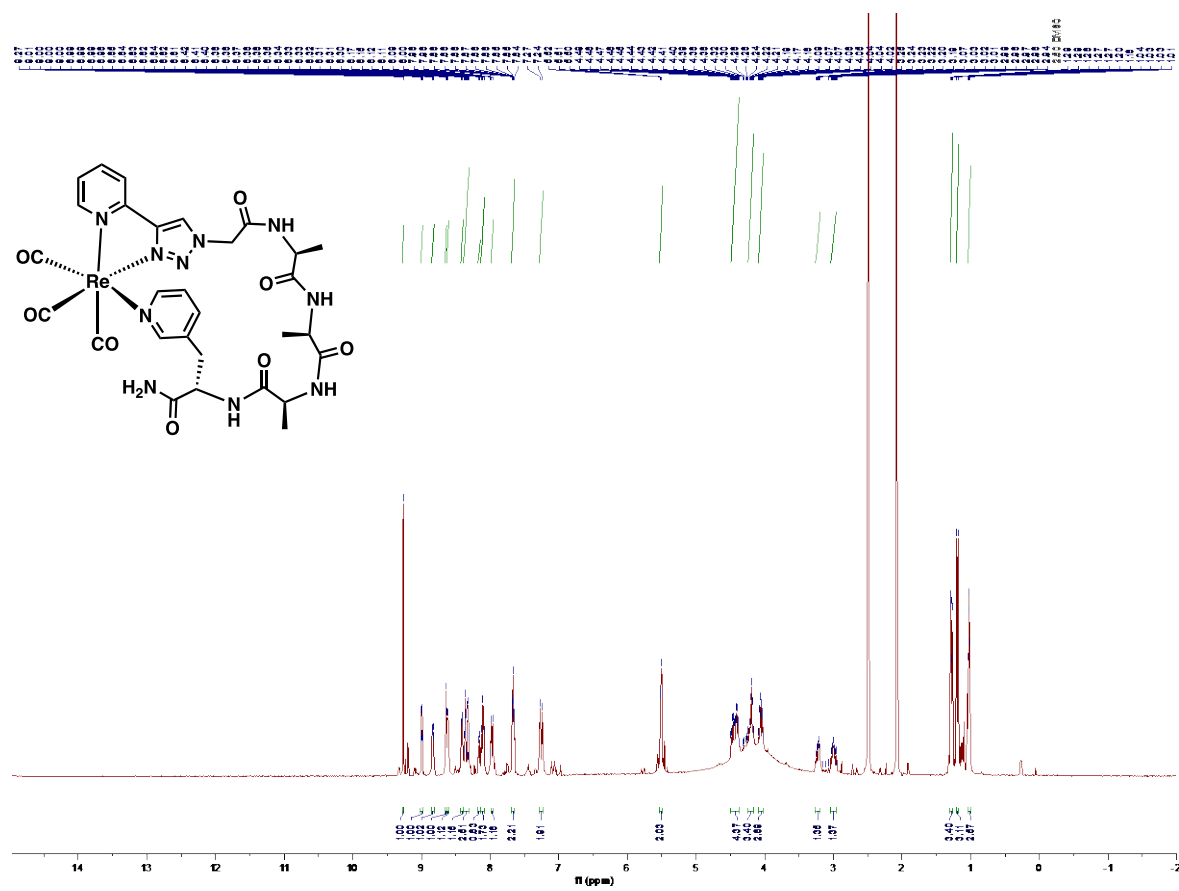
g-COSY NMR spectra of  $\text{Re}(\text{CO})_3[\text{pyta-Ala-Ala-Ala-Ala-Ala-3Pal}]$  (**3.11**) in  $\text{DMSO-d}_6$  at 400 MHz



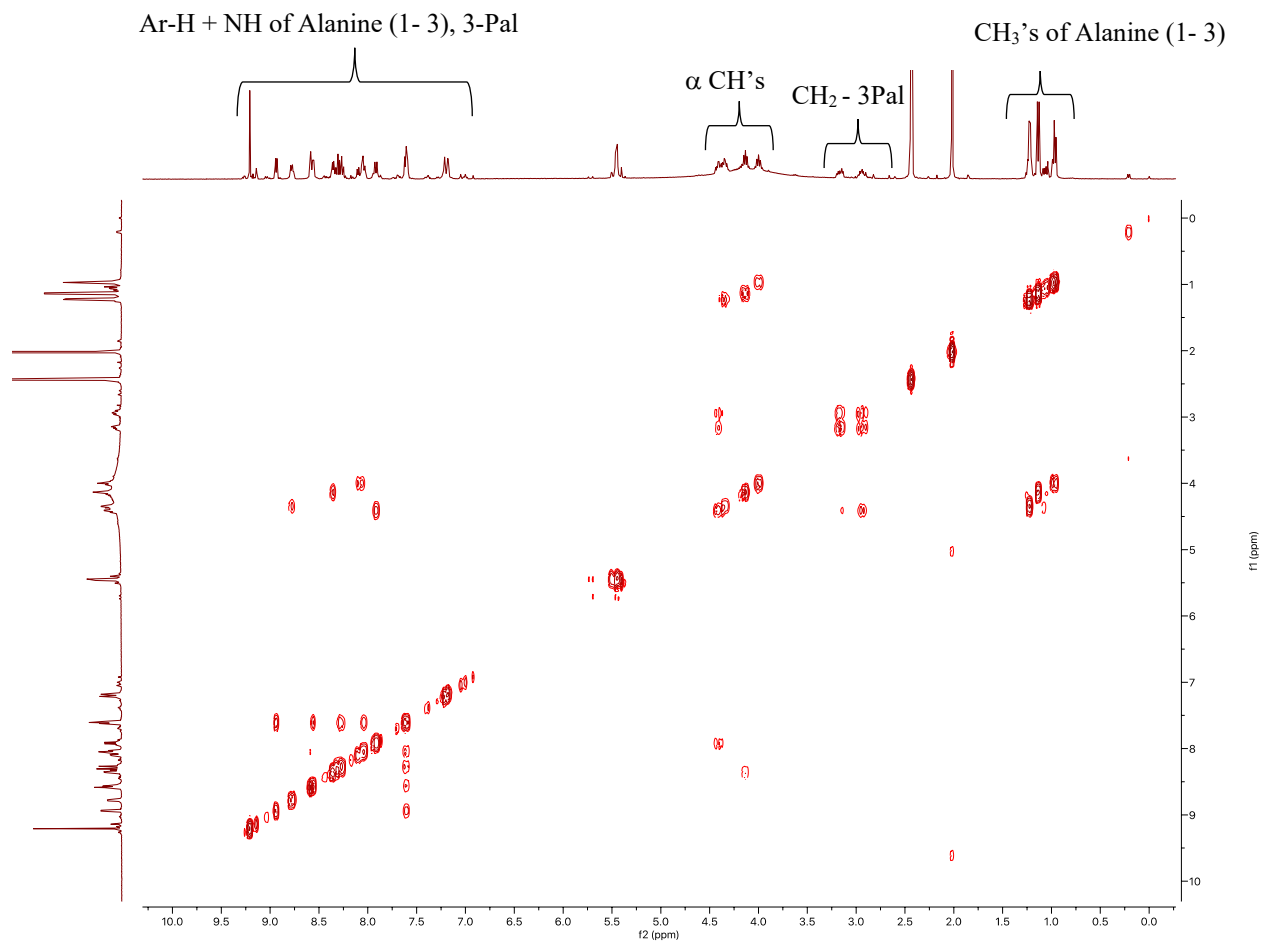
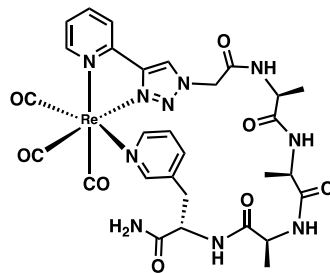
NOESY NMR spectra of  $\text{Re}(\text{CO})_3[\text{pyta-Ala-Ala-Ala-Ala-Ala-3Pal}]$  (**3.11**) in  $\text{DMSO-d}_6$  at 400 MHz



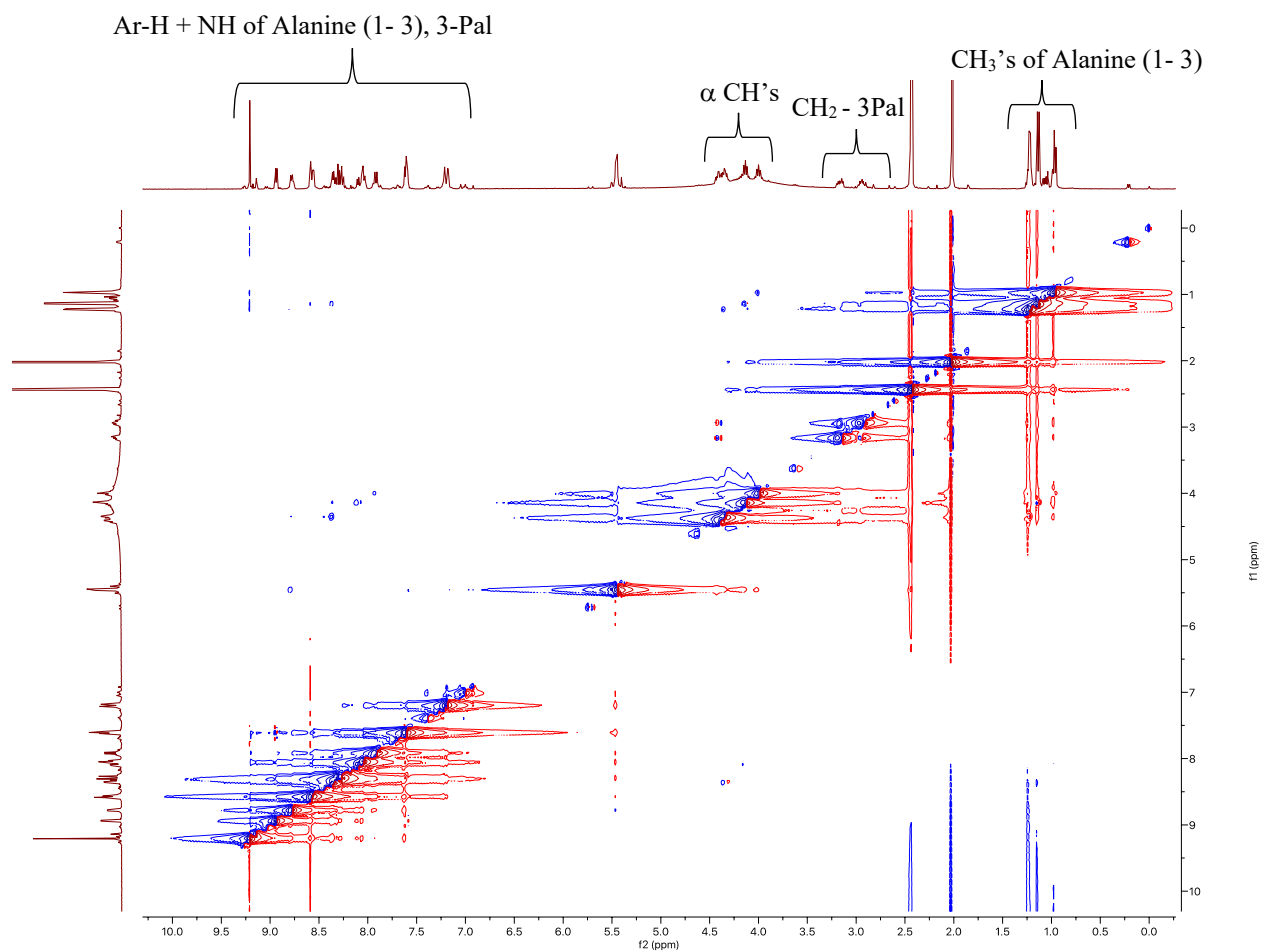
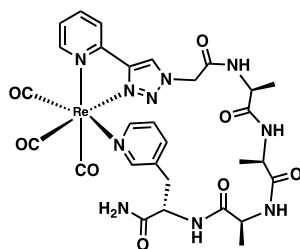
$^1\text{H}$  NMR spectra of  $\text{Re}(\text{CO})_3[\text{pyta-Ala-ala-Ala-3Pal}]$  (**3.12**) in  $\text{DMSO-d}_6$  at 400 MHz



g-COSY NMR spectra of  $\text{Re}(\text{CO})_3[\text{pyta-Ala-ala-Ala-3Pal}]$  (**3.12**) in  $\text{DMSO-d}_6$  at 400 MHz

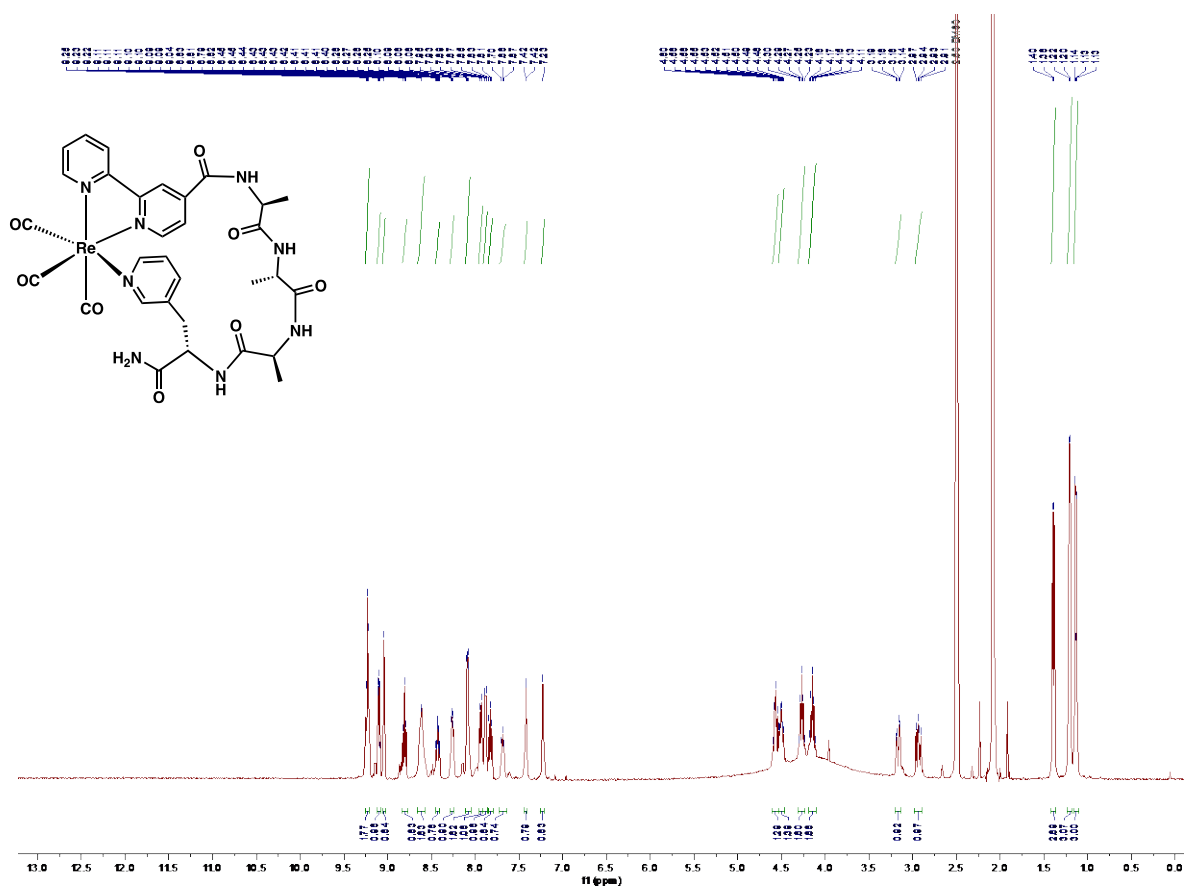


NOESY NMR spectra of  $\text{Re}(\text{CO})_3[\text{pyta-Ala-ala-Ala-3Pal}]$  (**3.12**) in  $\text{DMSO-d}_6$  at 400 MHz

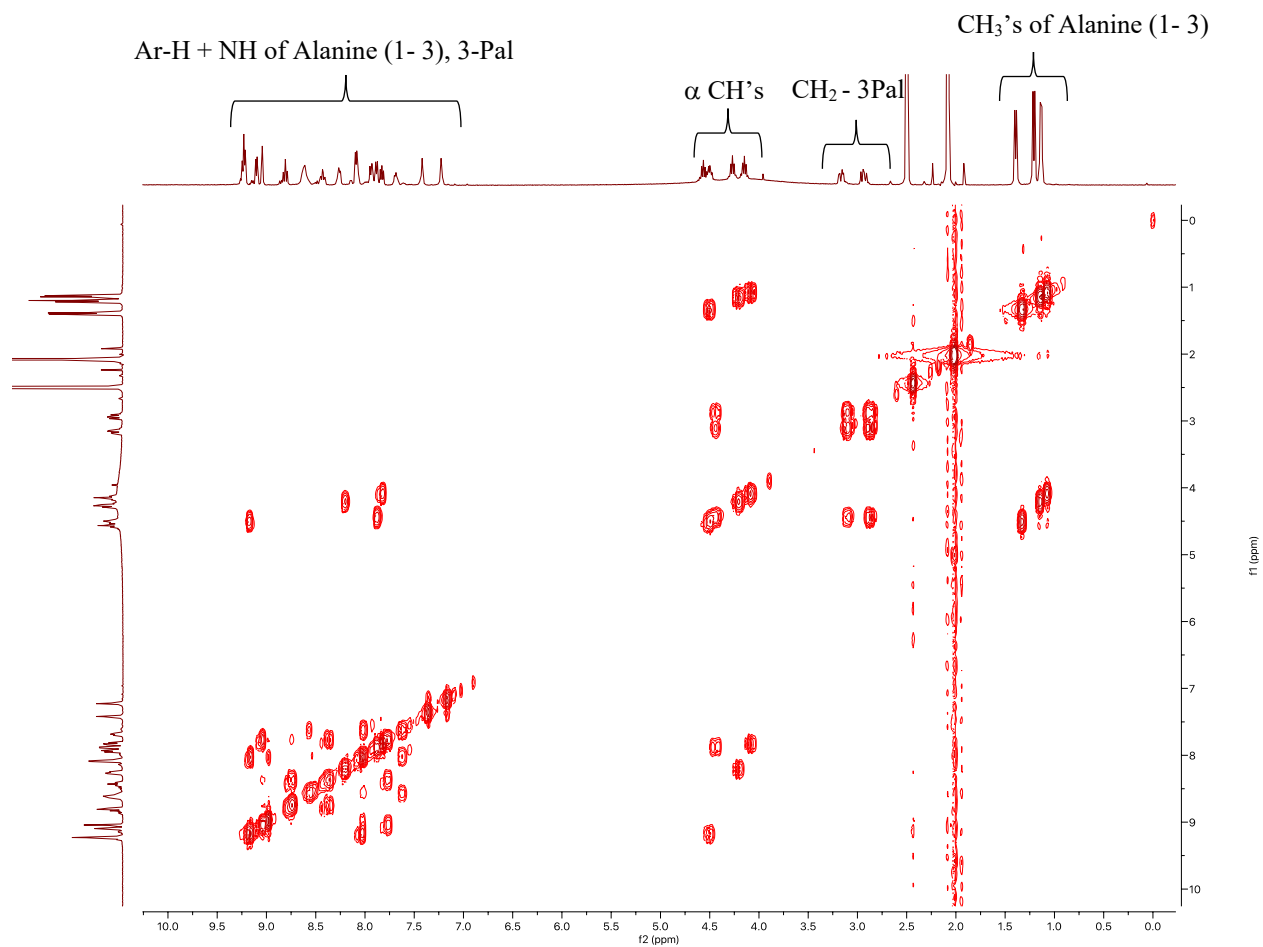
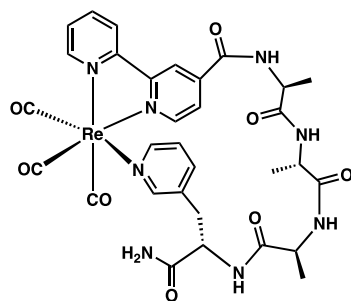




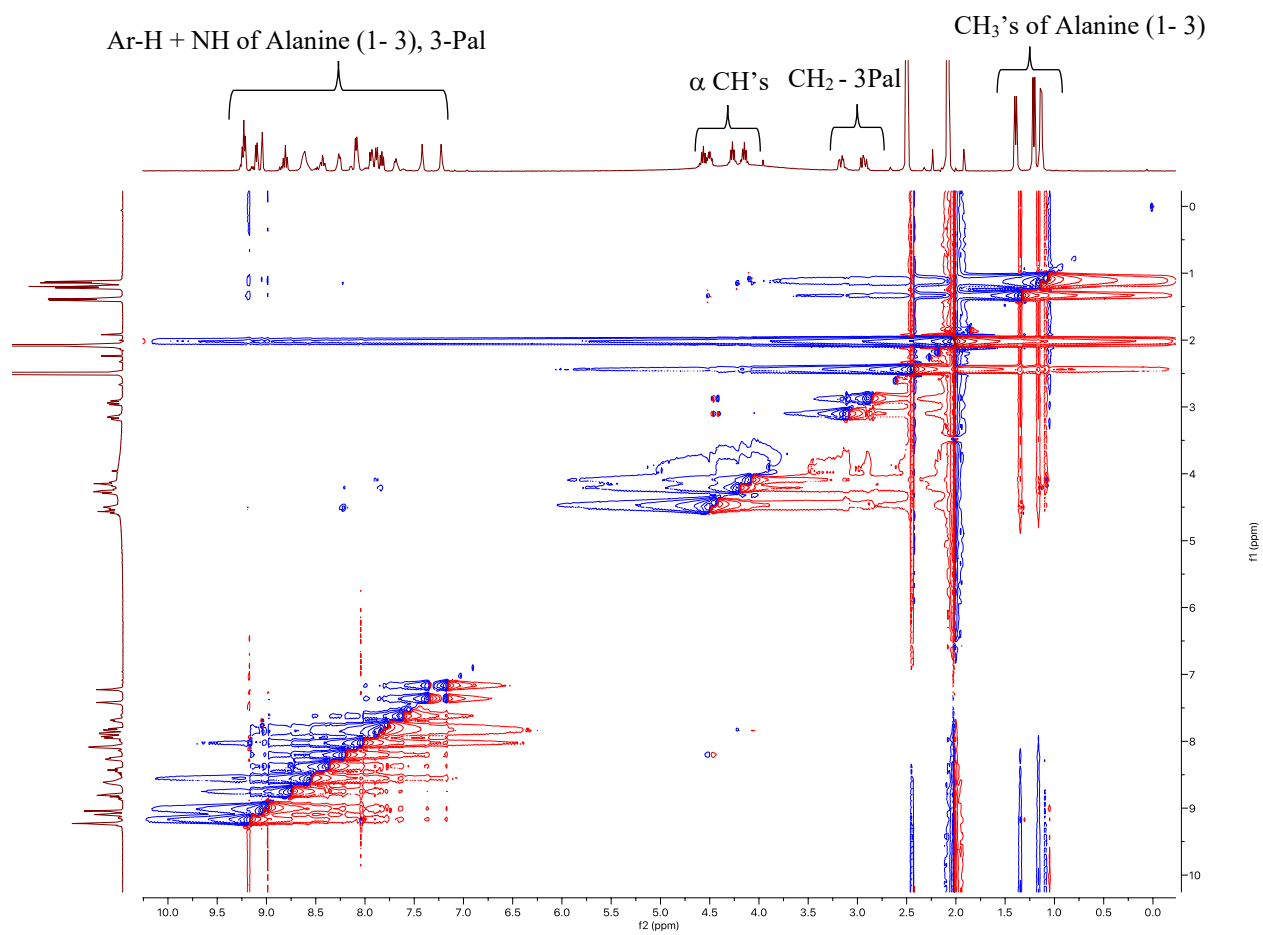
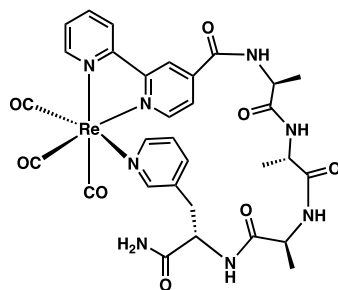
$^1\text{H}$  NMR spectra of  $\text{Re}(\text{CO})_3[\text{Bipyd-Ala-Ala-Ala-3Pal}]$  (**3.13**) in  $\text{DMSO-d}_6$  at 400 MHz



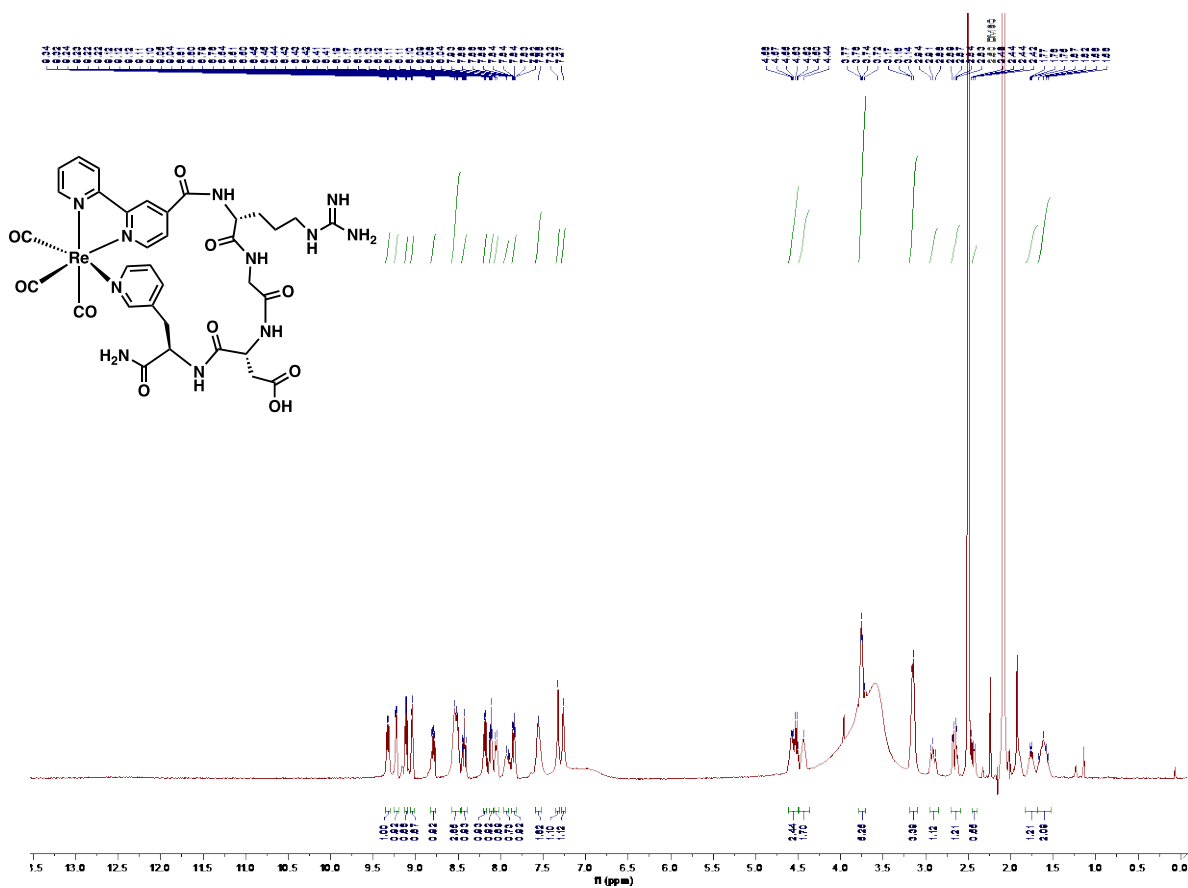
g-COSY NMR spectra of  $\text{Re}(\text{CO})_3[\text{Bipyd-Ala-Ala-Ala-3Pal}]$  (**3.13**) in  $\text{DMSO-d}_6$  at 400 MHz



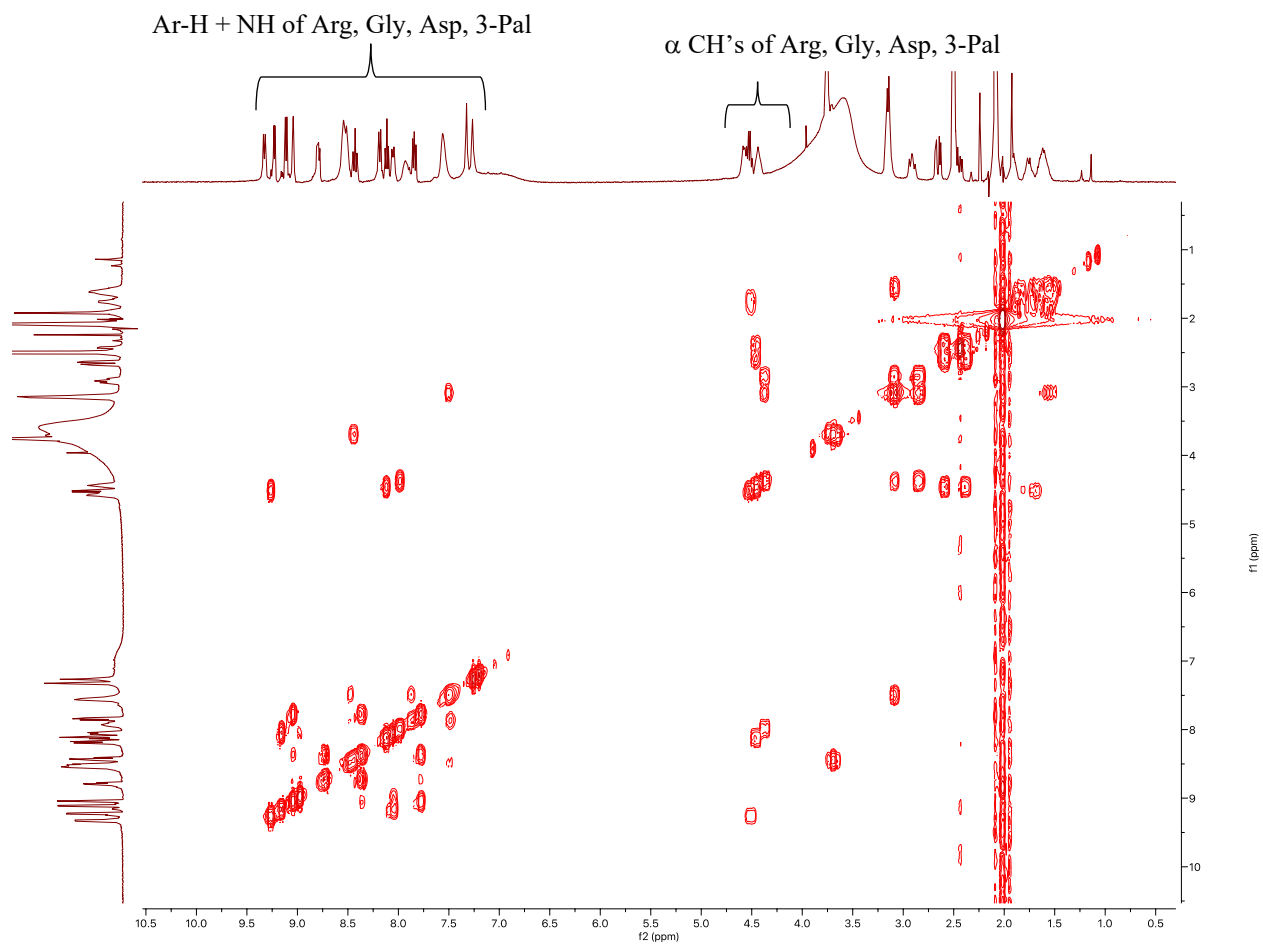
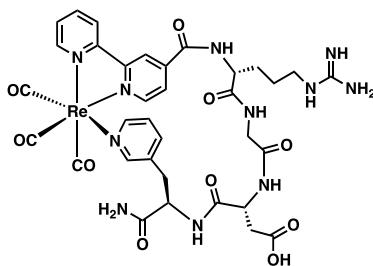
NOESY NMR spectra of  $\text{Re}(\text{CO})_3[\text{Bipyd-Ala-Ala-Ala-3Pal}]$  (**3.13**) in  $\text{DMSO-d}_6$  at 400 MHz



$^1\text{H}$  NMR spectra of  $\text{Re}(\text{CO})_3[\text{Bipyd-Arg-Gly-Asp-3Pal}]$  (**3.14**) in  $\text{DMSO-d}_6$  at 400 MHz

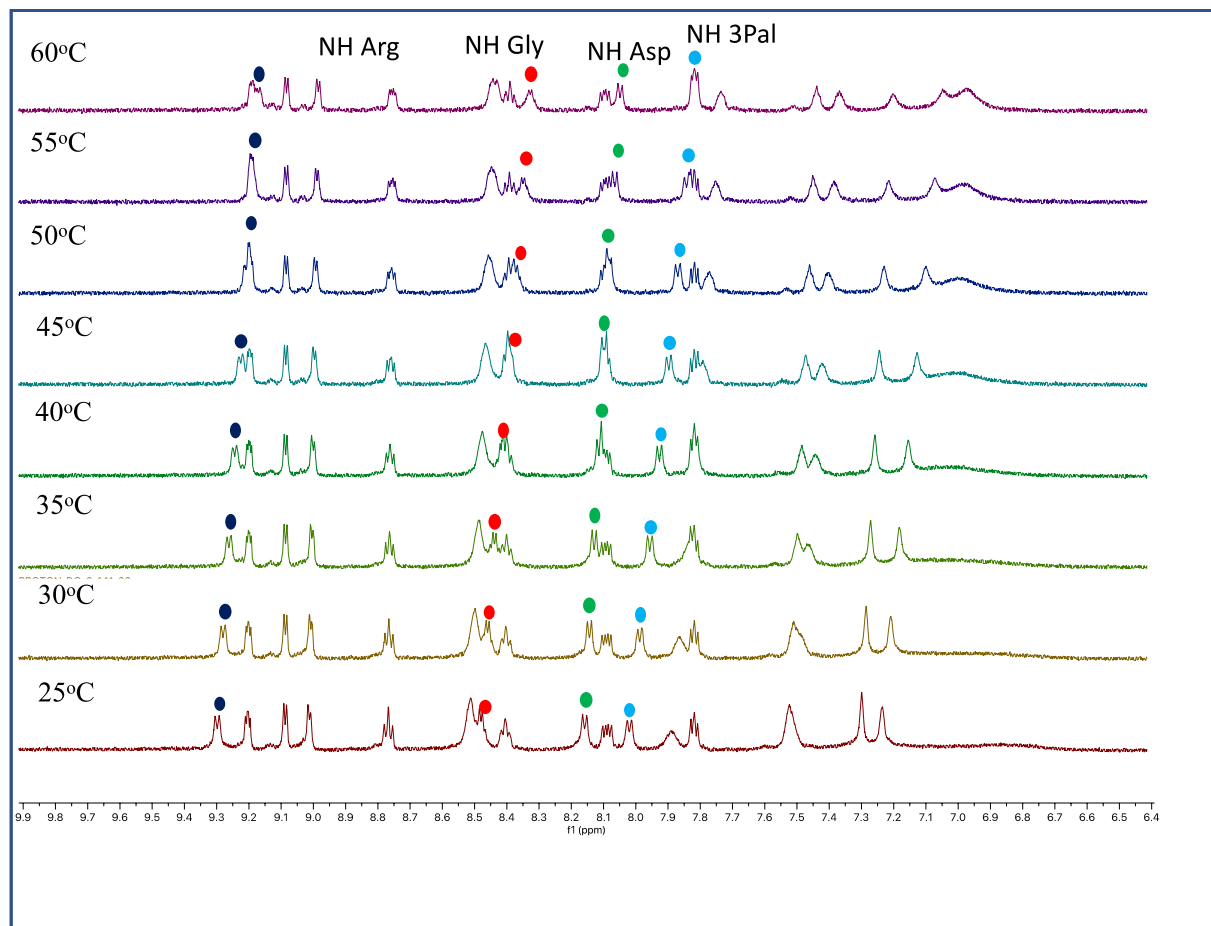


g-COSY NMR spectra of  $\text{Re}(\text{CO})_3[\text{Bipyd-Arg-Gly-Asp-3-Pal}]$  (**3.14**) in  $\text{DMSO-d}_6$  at 400 MHz

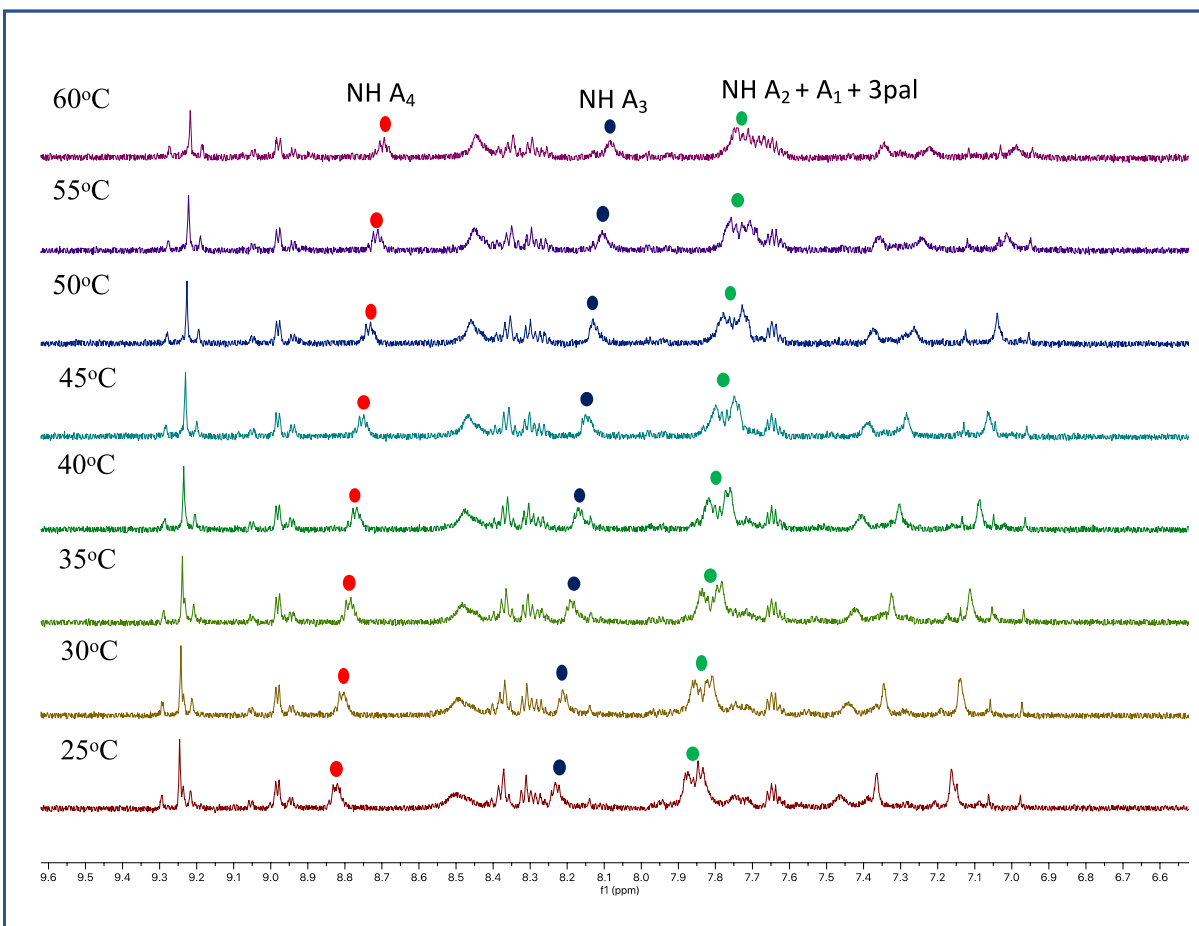


## Appendix C. Variable temperature NMR spectra

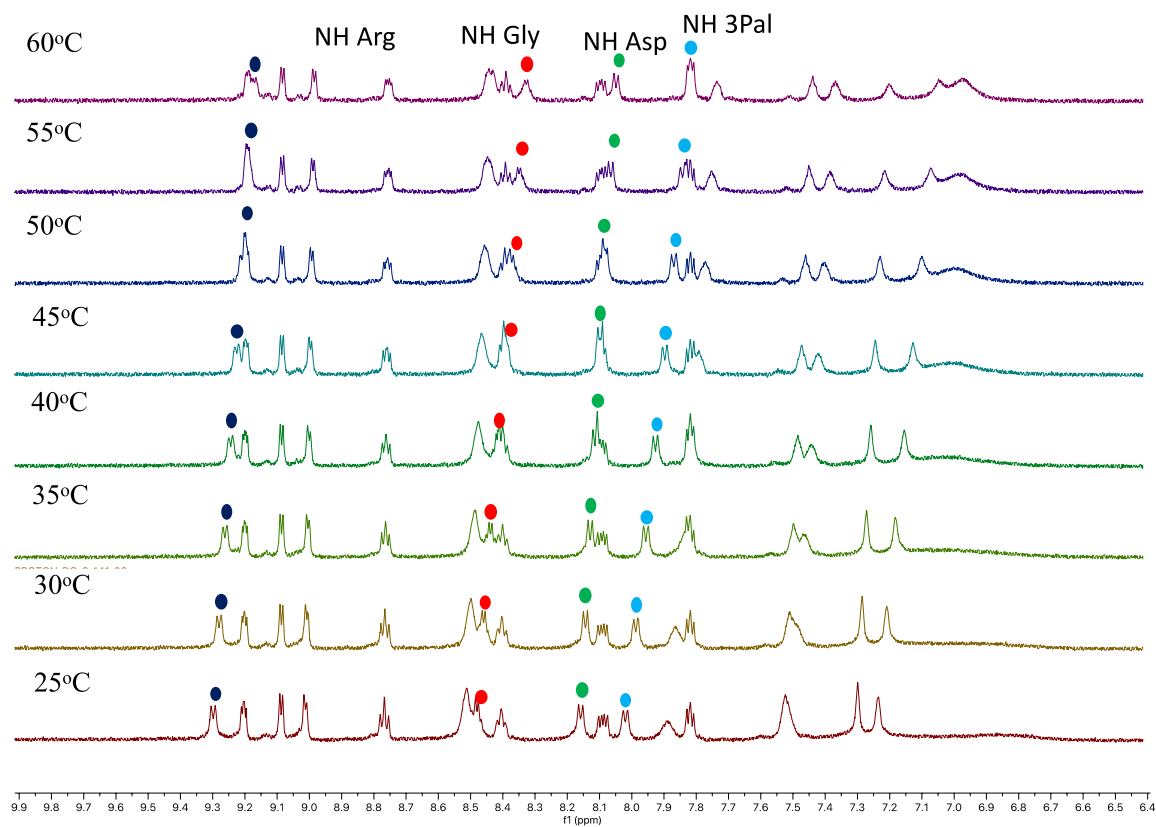
$\text{Re}(\text{CO})_3[\text{pyta-Arg-Gly-Asp-3pal}]$  (**3.9**) in  $\text{DMSO-d}_6$  at 600 MHz from 25°- 60°C



Re(CO)<sub>3</sub>[pyta-Ala-Ala-Ala-Ala-3pal] (**3.10**) in DMSO-d<sub>6</sub> at 600 MHz from 25°- 60°C



Re(CO)<sub>3</sub>[Bipyd-Arg-Gly-Asp-3pal] (3.14) in DMSO-d<sub>6</sub> at 600 MHz from 25°- 60°C





## Curriculum Vitae

- Name:** Dhvani Oza
- Post-secondary Education and Degrees:** K. J Somaiya college, University of Mumbai, Mumbai, Maharashtra, India  
2013-2016, BSc - chemistry
- K. J Somaiya college, University of Mumbai, Mumbai, Maharashtra, India  
2016-2018, MSc- chemistry
- University of Western Ontario, London, Ontario, Canada  
2018-2020, MSc- chemistry
- Honours and Awards:** Achievement in academics award, K. J Somaiya college, 2018
- Western Graduate Research Scholarship, Chemistry 09/2018 – 12/2020
- Related Work Experience** Teaching Assistant  
University of Western Ontario  
2018-2020
- Chemistry tutor (after school classes), India, 2015-2018
- Publications:** R. S Chauhan, **D. Oza**, S. Yadav, C. Dash, A. Slawin, Copper complexes of aryl Selenolate-based compounds: synthesis and catalytic activity in azide alkyne cycloaddition reaction, *New. J. Chem*, 2019, 43, 2381-2388.